A Hyperdiverse Ant Fauna from Dominican Amber

Gianpiero Fiorentino, Natalia Ladino, Daniela Mera-Rodríguez, Daniela Cubillos, Joshua Pablo Cavalcanti, Rodolfo S. Probst, Bonnie B. Blaimer, Gabriela P. Camacho, Fernando Fernández, Rodrigo M. Feitosa, Roberto J. Guerrero, John Lattke, John S. Lapolla, Ted R. Schultz, Jeffrey Sosa-Calvo, Evan P. Economo, Diyael Sosa, Santo Navarro, and Phillip Barden



Bulletin of the American Museum of Natural History

A HYPERDIVERSE ANT FAUNA FROM DOMINICAN AMBER

GIANPIERO FIORENTINO, NATALIA LADINO, DANIELA MERA-RODRÍGUEZ, DANIELA CUBILLOS, JOSHUA PABLO CAVALCANTI, RODOLFO S. PROBST, BONNIE B. BLAIMER, GABRIELA P. CAMACHO, FERNANDO FERNÁNDEZ, RODRIGO M. FEITOSA, ROBERTO J. GUERRERO, JOHN LATTKE, JOHN S. LaPOLLA, TED R. SCHULTZ, JEFFREY SOSA-CALVO, EVAN P. ECONOMO, DIYAEL SOSA, SANTO NAVARRO, AND PHILLIP BARDEN

BULLETIN OF THE AMERICAN MUSEUM OF NATURAL HISTORY
Number 486, 132 pp., 56 figures, 7 tables
Issued November 19, 2026

Copyright © American Museum of Natural History 2026 ISSN 0003-0090

CONTENTS

Author affiliations 4
Abstract 5
Introduction 5
Materials and methods 11
Results and discussion 13
Neotropical stability, disjunct distributions, and evidence for relict lineages 22
The untapped potential of fossil ants from the Neotropics 28
Systematic paleontology 28
Subfamily Amblyoponinae Forel, 1893 29
Fulakora Mann, 1919 29
†*Fulakora lata* Ladino, Lattke, Fiorentino, and Barden, sp. nov. 29
Prionopelta Mayr, 1866 33
†*Prionopelta ambigua* Ladino, Lattke, Barden, and Fiorentino, sp. nov. 33
Subfamily Dolichoderinae Forel, 1878 37
†*Chimerodous* Guerrero, Barden, and Fiorentino, gen. nov. 37
†*Chimerodous alpha* Guerrero, Barden, and Fiorentino, sp. nov. 38
†*Schismiscapus* Varela-Hernández et al., 2022 42
Subfamily Ectatomminae Emery, 1895 46
Poneracantha Emery, 1897 47
†*Poneracantha minima* Camacho, Lattke, Barden, and Fiorentino, sp. nov. 47
Subfamily Formicinae Latreille, 1802 50
Brachymyrmex Mayr, 1868 50
†*Brachymyrmex atrapada* Fernández, Sosa, Fiorentino, Barden, and Probst, sp. nov. 50
Camponotus Mayr, 1861 53
†*Camponotus matunai* LaPolla, Fiorentino, and Barden, sp. nov. 53
Subfamily Myrmicinae Lepeletier de Saint-Fargeau, 1835 56
Acromyrmex Mayr, 1865 56
†*Acromyrmex yucayequensis* Mera-Rodríguez, Sosa-Calvo, Fiorentino, Barden, and Schultz, sp. nov. 56
Cardiocondyla Emery, 1869 60
†*Cardiocondyla larimar* Fiorentino, Sosa, Navarro, and Barden, sp. nov. 60
Crematogaster Lund, 1831 63
†*Crematogaster diunota* Blaimer, Fiorentino, and Barden, sp. nov. 63
Eurhopalothrix Brown and Kempf, 1961 66
†*Eurhopalothrix electrina* Probst, Barden, and Fiorentino, sp. nov. 66
Kempfidris Fernández, Feitosa and Lattke, 2014 71
†*Kempfidris priminatus*, Fiorentino, Barden, Feitosa, and Fernández, sp. nov. 71
Mycetomoellerius Solomon, Rabeling, Sosa-Calvo, and Schultz, 2019 72
†*Mycetomoellerius yucahu* Mera-Rodríguez, Sosa-Calvo, Fiorentino, Barden and Schultz, sp. nov. 72
Paratrachymyrmex Solomon, Rabeling, Sosa-Calvo, and Schultz, 2019 77
†*Paratrachymyrmex primaevus* (Baroni Urbani, 1980a), comb. nov. 77
Pogonomyrmex Mayr, 1868 80
†*Pogonomyrmex tiempopogo* Barden and Fiorentino, sp. nov. 80

Rhopalothrix Mayr, 1870 83
†*Rhopalothrix macorixia* Probst, Barden, and Fiorentino, sp. nov. 83
Rogeria Emery, 1894 86
†*Rogeria primaeva* Feitosa, Barden, and Fiorentino, sp. nov. 86
Allomerus Mayr, 1878 89
†*Allomerus bi* Fiorentino, Barden, and Fernández, sp. nov. 89
Ponerinae Lepeletier de Saint-Fargeau, 1835 91
Brachyponera Emery, 1900 93
†*Brachyponera mamajuanis* Fiorentino, Cubillos, Fernández, and Lattke, sp. nov. 93
Leptogenys Roger, 1861 95
†*Leptogenys intacta* Cubillos, Cavalcanti, and Lattke, sp. nov. 95
Mayaponera Schmidt and Shattuck, 2014 99
†*Mayaponera bachata* Fiorentino, Cubillos, Fernández and Lattke, sp. nov. 99
†*Cayrapone* Cubillos, Fiorentino, and Lattke, gen. nov. 102
†*Cayrapone hupia* Cubillos, Fiorentino, and Lattke, sp. nov. 103
†*Kiskeyapone* Fiorentino, Cubillos, Barden, Fernández, and Lattke, gen. nov. 106
†*Kiskeyapone armilla* Fiorentino, Cubillos, Barden, Fernández, and Lattke, sp. nov. . . . 107
Pseudoponera Emery, 1900 111
†*Pseudoponera hatuey* Cubillos, Fernandez, Lattke, and Fiorentino, sp. nov. 111
†*Stenoponera* Lattke, Cubillos, Fernández, and Fiorentino, gen. nov. 115
†*Stenoponera petiolata* Lattke, Cubillos, Fernández, and Fiorentino, sp. nov. 115
Acknowledgments 118
References 118
Appendix 1. List of recorded ponerinae genera from the fossil record, ordered alphabetically . . . 127
Appendix 2. Fourier Transform Raman (FTR) spectroscopy 131

Online supplement https://doi.org/10.5281/zenodo.23482755

AUTHOR AFFILIATIONS

Gianpiero Fiorentino: Federated Department of Biological Sciences, New Jersey Institute of Technology, Newark, NJ.

Natalia Ladino: Departamento de Ecologia, Zoologia e Genética, Universidade Federal de Pelotas, Pelotas, RS, Brazil; Departamento de Zoologia, Universidade Federal do Paraná, Curitiba, PR, Brazil.

Daniela Mera-Rodríguez: Department of Integrative Taxonomy and Biodiversity of Insects, Institute of Biology, University of Hohenheim, Stuttgart, Germany; KomBioTa—Center for Biodiversity and Integrative Taxonomy, University of Hohenheim and State Museum of Natural History Stuttgart, Stuttgart, Germany; Social Insect Research Group, School of Life Sciences, Arizona State University, Tempe, AZ.

Daniela Cubillos: Departamento de Zoologia, Universidade Federal do Paraná, Curitiba, PR, Brazil.

Joshua Pablo Cavalcanti: Departamento de Zoologia, Universidade Federal do Paraná, Curitiba, PR, Brazil.

Rodolfo S. Probst: Department of Entomology and Nematology, University of California, Davis, CA; Science Research Initiative, College of Science, University of Utah, Salt Lake City, UT.

Bonnie B. Blaimer: Museum für Naturkunde, Leibniz Institute for Evolution and Biodiversity Science, Center for Integrative Biodiversity Discovery, Berlin, Germany.

Gabriela P. Camacho: Museu de Zoologia, Universidade de São Paulo, São Paulo, SP, Brazil.

Fernando Fernández: Instituto de Ciencias Naturales, Universidad Nacional de Colombia sede Bogotá, Bogotá D.C., Colombia.

Rodrigo M. Feitosa: Departamento de Zoologia, Universidade Federal do Paraná, Curitiba, PR, Brazil.

Roberto J. Guerrero: Universidad del Magdalena, Santa Marta, Colombia.

John Lattke: Departamento de Zoologia, Universidade Federal do Paraná, Curitiba, PR, Brazil.

John S. LaPolla: Department of Biological Sciences, Towson University, Towson, MD.

Ted R. Schultz: National Museum of Natural History, Smithsonian Institution, Washington, DC.

Jeffrey Sosa-Calvo: National Museum of Natural History, Smithsonian Institution, Washington, DC; Department of Biology, University of Central Florida, Orlando, FL.

Evan P. Economo: Department of Entomology, University of Maryland, College Park, MD; Biodiversity and Biocomplexity Unit, Okinawa Institute of Science and Technology Graduate University, Onna, Okinawa, Japan.

Diyael Sosa: Instituto de Investigaciones Botánicas y Zoológicas Prof. Rafael M. Moscoso, Universidad Autónoma de Santo Domingo, DR.

Santo Navarro: Instituto de Investigaciones Botánicas y Zoológicas Prof. Rafael M. Moscoso, Universidad Autónoma de Santo Domingo, DR.

Phillip Barden: Federated Department of Biological Sciences, New Jersey Institute of Technology, Newark, NJ; Division of Invertebrate Zoology, American Museum of Natural History, New York.

ABSTRACT

Neotropical ants are diverse and globally distinct. Although ants have occupied this region since the Lower Cretaceous, there are few windows into the history of this fauna. Ant fossils from Miocene Dominican amber, a Konservat-Lagerstätte on the island of Hispaniola, are an exception. The fossil assemblage preserved in Dominican amber is diverse, comprising 96 described species from 36 genera. Here we describe a further 23 species representing 22 genera previously unknown from this deposit. We also provide updated taxonomic placements for two additional species. The ant assemblage is remarkably modern—out of 59 genera, 50 persist in the Neotropics today—but it evidences a dynamic insular ecosystem. Fossil taxa are surprisingly distinct from the modern ant assemblage of Hispaniola and exhibit approximately 25% greater generic diversity. With 11 contemporary genera now locally extinct on the island, the fossil record also points to significant faunal turnover; a pattern affecting both specialist and generalist taxa. Nineteen of the genera reported here reinforce strong affinities with other Neotropical fossil and extant faunas, particularly the Miocene Chiapas amber assemblage. However, we also report three taxa with clear Old World biogeographic links, suggesting previously widespread distributions for several lineages now restricted to the Paleotropics.

INTRODUCTION

The ant diversity of the Neotropics is both globally distinct and exceptionally rich (Bolton, 2025). Of the nearly 14,500 known ant species (Fernández et al., 2021; Bolton, 2025), the Neotropics harbor 137 genera and approximately 3100 species, accounting for about 22% of global ant diversity (Fernández et al., 2021). Although portions of the region have been relatively well studied and sampled (Kass et al., 2022), the Neotropics remain a potential biodiversity hotspot for ants (Moreau and Bell, 2013), shaped in part by high levels of endemism (Economo et al., 2018; Raven et al., 2020; Kass et al., 2022). While the region contains a large share of the world's extant insect diversity, deep-time perspectives are limited by the scarcity of known and explored fossil deposits (LaPolla et al., 2013; Barden, 2017). Only six Neotropical deposits are known to yield fossil ants, and just two of these have produced more than one described ant species (Barden, 2017; Perrichot et al., 2019). A third deposit, the Crato Formation of Brazil, may also house a diverse paleo ant fauna, but further research is required (Brandão and Martins-Neto, 1989; Lepeco et al., 2025).

Miocene-aged amber from the Dominican Republic, on the island of Hispaniola, offers the only well-sampled window into Neotropical insect paleodiversity. This fossil resin deposit (Konservat-Lagerstätte) is renowned for its capacity for retaining biological inclusions with exceptional fidelity and has yielded over 1300 described arthropod inclusions. The age of Dominican amber has long been debated (Penney, 2010; Braga et al., 2012), but current consensus places it in the Miocene or Late Oligocene, between 25 and 15 million years ago (Iturralde-Vinent, 1996; Iturralde-Vinent and MacPhee, 2019).

The Caribbean is one of the most diverse regions in the Neotropics and has been extensively studied for its high levels of endemism and complex biogeography (Lubertazzi, 2019; Perez-Gelabert, 2020). Hispaniola, the second largest of the Greater Antilles, comprises Haiti and the Dominican Republic. Its extant ant fauna includes a mixture of island endemics, Neotropical natives, and introduced or invasive species. To date, 173 ant species are known from the island—152 native, 21 introduced—nearly half of all species are endemic (table 1; Lubertazzi, 2019; Prebus, 2021; LaPolla and Kallal, 2019; Fiorentino et al., 2025).

Much like Hispaniola's modern ant fauna, the fossil assemblage preserved in Dominican amber is diverse, comprising 96 described species across 36 genera prior to this monograph

TABLE 1

List of extant ant species recorded from Hispaniola. Species are noted by status. Asterisks denote undescribed species highlighted by Lubertazzi (2019). Abbreviations: **En,** endemic; **In,** Invasive; **Na,** native.

Subfamily	Species	Status
Amblyoponinae		
	Fulakora falcata	Na
Dolichoderinae		
	Bothriomyrmex enigmaticus	Na, En
	Dorymyrmex antillanum	Na
	Linepithema dispertitum	Na
	Linepithema humile	In
	Linepithema keiteli	Na, En
	Tapinoma litorale	Na
	Tapinoma melanocephalum	In
	Tapinoma opacum	Na, En
	Tapinoma rasenum	Na
Dorylinae		
	Cylindromyrmex darlingtoni	Na
	Syscia n. sp.*	Na, En
Ectatomminae		
	Gnamptogenys falcaria	Na, En
	Gnamptogenys schmitti	Na, En
	Holcoponera haytiana	Na, En
	Holcoponera striatula	Na
	Poneracantha insularis	Na, En
	Poneracantha lineolata	Na, En
	Poneracantha semiferox	Na, En
Formicinae		
	Acropyga dubitata	Na, En
	Acropyga fuhrmanni	Na, En
	Acropyga parvidens	Na, En
	Brachymyrmex australis	Na
	Brachymyrmex bruchi	Na
	Brachymyrmex cordemoyi	Na
	Brachymyrmex heeri	Na
	Brachymyrmex minutus	Na
	Brachymyrmex obscurior	Na
	Brachymyrmex termitophilus	Na
	Camponotus albistramineus	Na, En
	Camponotus altivagans	Na, En

TABLE 1 *continued*

Subfamily	Species	Status
	Camponotus augustei	Na, En
	Camponotus christophei	Na, En
	Camponotus claviscapus occultus	Na
	Camponotus fumidus fraterculus	Na, En
	Camponotus fumidus haytianus	Na, En
	Camponotus fumidus illitus	Na, En
	Camponotus fumidus imbecillus	Na, En
	Camponotus fumidus soulouquei	Na, En
	Camponotus lucayanus	Na
	Camponotus picipes plombyi	Na, En
	Camponotus ramulorum vernulus	Na, En
	Camponotus saussurei	Na, En
	Camponotus sexguttatus	Na
	Camponotus toussainti	Na, En
	Camponotus ustus	Na
	Myrmelachista gagates	Na, En
	Myrmelachista ramulorum	Na
	Nylanderia bibadia	Na, En
	Nylanderia bourbonica	Na
	Nylanderia caerula	Na, En
	Nylanderia disatra	Na, En
	Nylanderia esperanza	Na, En
	Nylanderia fulva	Na
	Nylanderia fuscaspecula	Na, En
	Nylanderia guatemalensis	In
	Nylanderia metacista	Na, En
	Nylanderia pini	Na, En
	Nylanderia pubens	Na
	Nylanderia steinheili	Na
	Nylanderia vividula	Na
	Zatania darlingtoni	Na, En
	Zatania gibberosa	Na
Myrmicinae		
	Aphaenogaster relicta	Na, En
	Aphaenogaster relicta epinotalis	Na, En
	Cardiocondyla emeryi	In
	Cardiocondyla minutior	In
	Cardiocondyla venustula	In

TABLE 1 *continued*

Subfamily	Species	Status
	Cephalotes argentiventris	Na, En
	Cephalotes auricomus	Na, En
	Cephalotes decoloratus	Na, En
	Cephalotes flavigaster	Na, En
	Cephalotes hamulus	Na, En
	Cephalotes unimaculatus	Na, En
	Cephalotes vinosus	Na, En
	Crematogaster dorada	Na, En
	Crematogaster russoi	Na, En
	Crematogaster steinheili	Na
	Cyphomyrmex minutus	Na
	Cyphomyrmex rimosus	Na
	Eurhopalothrix floridana	Na
	Monomorium bicolor	In
	Monomorium ebeninum	Na,
	Monomorium floricola	In
	Monomorium pharaonis	In
	Mycetomoellerius haytianus	Na, En
	Mycetomoellerius jamaicensis	Na
	Mycocepurus smithii	Na
	Paratrechina longicornis	In
	Pheidole darlingtoni	Na, En
	Pheidole drepanon	Na, En
	Pheidole flavens	Na
	Pheidole harlequina	Na, En
	Pheidole hispaniolae	Na, En
	Pheidole indica	In
	Pheidole jamaicensis	Na
	Pheidole jelskii	Na
	Pheidole megacephala	In
	Pheidole moerens	Na
	Pheidole noar	Na, En
	Pheidole subarmata	Na
	Pheidole susannae	In
	Pheidole terresi	Na, En
	Pogonomyrmex aterrimus	Na, En
	Pogonomyrmex saucius	Na, En
	Pogonomyrmex schmitti	Na, En

TABLE 1 *continued*

Subfamily	Species	Status
	Rogeria alzatei	Na
	Rogeria brunnea	Na
	Rogeria curvipubens	Na
	Rogeria leptonana	Na
	Solenopsis geminata	Na
	Solenopsis globularia	Na
	Solenopsis pollux	Na
	Solenopsis pygmae	Na
	Solenopsis succinea	Na
	Solenopsis terricola	Na
	Strumigenys economoi	Na, En
	Strumigenys eggersi	Na
	Strumigenys emmae	In
	Strumigenys gundlachi	Na
	Strumigenys lanuginosa	Na
	Strumigenys louisianae	Na
	Strumigenys membranifera	In
	Strumigenys nigrescens	Na
	Strumigenys rogeri	In
	Strumigenys silvestrii	In
	Strumigenys zemi	Na, En
	Temnothorax agavicola	Na, En
	Temnothorax bahoruco	Na, En
	Temnothorax balaclava	Na, En
	Temnothorax ciferrii	Na, En
	Temnothorax creolus	Na, En
	Temnothorax flavidulus	Na, En
	Temnothorax harlequina	Na, En
	Temnothorax hispaniolae	Na, En
	Temnothorax laticrus	Na, En
	Temnothorax sallei	Na, En
	Temnothorax wilsoni	Na, En
	Tetramorium bicarinatum	In
	Tetramorium caldarium	In
	Tetramorium lanuginosum	In
	Tetramorium lucayanum	In
	Tetramorium simillimum	In
	Trichomyrmex destructor	In

TABLE 1 *continued*

Subfamily	Species	Status
	Allomerus auropunctata	Na
Ponerinae		
	Anochetus haytianus	Na, En
	Anochetus longispinus	Na, En
	Anochetus mayri	Na
	Hypoponera inexorata	Na, En
	Hypoponera opaciceps	Na
	Hypoponera opacior	Na
	Hypoponera punctatissima	Na
	Leptogenys antillana	Na, En
	Leptogenys pubiceps	Na
	Odontomachus bauri	Na
	Odontomachus insularis	Na
	Odontomachus ruginodis	Na
	Platythyrea punctata	Na
	Platythyrea strenua	Na, En
	Pseudoponera stigma	Na
	Pseudoponera succedanea	Na
	Thaumatomyrmex n. sp.*	Na, En
Proceratiinae		
	Discothyrea testacea	Na
	Proceratium longiscapus	Na, En
	Proceratium taino	Na, En
Pseudomyrmecinae		
	Pseudomyrmex cubaensis	Na
	Pseudomyrmex haytianus	Na, En
	Pseudomyrmex simplex	Na
	Pseudomyrmex subater	Na

(table 2). These fossils are of evolutionary and biogeographic significance, offering key insights into lineage diversification and historical distributions (Sawh et al., 2023; Grimaldi and Engel, 2005; Barden, 2017). Many represent the earliest known occurrences of major ant lineages, including one subfamily, two tribes, and 41 genera (table 3).

Dominican amber also reveals a pattern of local extinction. Wilson (1985a), in the first comparative analysis of the fossil and extant Hispaniolan ants, documented this large-scale faunal turnover. He argued that the low dispersal ability of highly specialized taxa contributed to their extinction, noting that over a third of fossil genera known at the time were absent from the island's modern ant fauna (Barden, 2017; Fiorentino et al., 2023; Fiorentino et al., 2025; Wilson, 1985a). Since Wilson's (1985a) pioneering study, most subsequent work on Dominican amber ants has emphasized alpha taxonomy (Wilson, 1985b, 1985c, 1985d; Wilson, 1986; Vierbergen and Scheven, 1995; Lattke, 2002; Lattke, 2003; Casadei-Ferreira et al., 2019) and, to a lesser extent, the implications of these fossils for ant systematics (Ward, 1992; De Andrade and Baroni Urbani, 1999).

Dominican amber ants, together with other fossil taxa, have consistently revealed compelling examples of disjunct distribution patterns. Wilson (1985b) first noted this in *Pheidole* Westwood, *Paraponera* Smith, *Neivamyrmex* Borgmeier, and various Dolichoderines. This pattern was later explored by Baroni Urbani (1995), highlighting possible connections between extinct Dominican amber and modern Paleotropical ant faunas, particularly in Indomalaya, Oceania, and Australia. This pattern was underscored by the discovery of *Leptomyrmex neotropicus* (Baroni Urbani, 1980b; but see Boudinot et al., 2016) and several proceratiines (De Andrade, 1998c; De Andrade and Baroni Urbani, 2003), with affinities to Australian and African ants, respectively. Yet, even as some fossil taxa are closely related to extant paleotropical lineages, the Dominican amber assemblage as a whole exhibits its strongest affinities with modern Neotropical communities (Guénard et al., 2015). This Neotropical signal is particularly evident in *Cylindromyrmex* Mayr, *Neoponera* Emery, and *Odontomachus* Latreille (De Andrade, 1994; De Andrade, 2001; Fiorentino et al., 2023), among others (Baroni Urbani and De Andrade, 1994; De Andrade et al., 1999; Lattke, 2002, 2003; Baroni Urbani and De Andrade, 2007; Schultz, 2007).

Even after 40 years since the first monograph on Dominican amber ants, numerous taxa of historical, biogeographic, and ecological significance remain undescribed. Here, we describe and provide CT scan–based volumetric models of 23 new species and four new genera of ants from Dominican amber—an increase of roughly 70% in the generic diversity of this Neotropical Lagerstätte. With these contributions, the Dominican amber record now comprises 116 ant species assigned to 59 genera, including seven extinct genera (table 2). This number includes the previously known 96 species, the species described herein. We also provide a brief overview of the phylogenetic diversity of this fossil ant assemblage and discuss the broader importance of Neotropical fossils for understanding ant evolutionary history.

MATERIALS AND METHODS

Study material: We reviewed Dominican amber specimens deposited at the American Museum of Natural History (AMNH), New York, the Museum of Comparative Zoology (MCZ) Entomology Collection of Harvard University, Cambridge, MA, State Museum of Natural History Stuttgart (SMNS), Germany, and specimens housed at the New Jersey Institute of Technology, which were deposited at the Museo Nacional de Historia Natural "Prof. Eugenio de Jesús Marcano" (MNHN), Santo Domingo, Dominican Republic. All MCZ and MNHN specimens were purchased from the northern mines of the Santiago Province, Dominican Republic. AMNH specimens were also purchased directly from the northern

mines, with the exception of AMNH DR RP 359 and AMNH JVE 781, which were donations made to the American Museum of Natural History.

Assessing the provenance of amber specimens: There are multiple resiniferous deposits across the Dominican Republic that yield fossils and subfossils of varying age. In addition to deposits of Miocene amber (Iturralde-Vinent and MacPhee, 1996), there is at least one locality known to produce much younger copal, which can be up to tens of thousands of years old (Solórzano-Kraemer et al., 2020). There are also known instances of museum forgeries or misidentified material that have led to erroneous species descriptions (Grimaldi et al., 1994; Grimaldi, 2019; Sosiak et al., 2022). To assess the provenance of the specimens in this study, we developed two independent assays. First, we tested the solubility of the specimens using ethanol, following Currie (1997). Resin polymerizes progressively during its maturation process (Seyfullah et al., 2018). Amber is resin that has undergone extensive maturation and long-term polymerization and cross-linking over geological timescales (Bai et al., 2019; Saitta and Kaye, 2025). In contrast, subfossil copal and recent resins are much younger and have undergone less maturation. Consequently, subfossil copal and recent resins are generally more soluble in ethanol than amber, which is more chemically stable and highly polymerized (Currie, 1997). Ethanol exposure tests have previously been applied to Dominican resins (Heinrichs et al., 2013) and other fossils such as Triassic-age Italian amber (Roghi and Gianolla, 2006). For our test, we applied a single drop of 75% ethanol to each specimen and allowed it to remain in contact with the surface for 30 seconds before dabbing it away with a cotton ball. Solubility was then assessed based on whether the specimen surface became sticky and tacky, and whether any cotton fibers remained adhered to the surface. We performed this test on all amber specimens included in the present study, as well as two reference copal specimens from the Dominican Republic and one reference copal specimen from Colombia.

Our second assay assessed specimen maturity using Raman spectroscopy. The ratio of intensity between peaks at 1646 and 1450 cm^{-1} has been associated with specimen maturation (Edwards and Farwell, 1996). We assessed specimen maturity by calculating the ratio of maximum intensity at the values between ranges of 1543–1771 and 1400–1510 cm^{-1} (peak ratio), following Brody et al. (2001). We then compared our values with reported ratios for other amber and subfossil resin deposits. We obtained spectra for all type and reference copal specimens using a Thermo Scientific DXRxi Raman Microscope at the New Jersey Institute of Technology Otto H. York Center for Environmental Engineering and Science. The microscope was equipped with a 785 nm excitation laser set to 30 mW at 10× magnification and spectra were acquired for 0.1 seconds averaged across 60 replicates. Spectra were baseline corrected under a "modpolyfit" approach and normalized by total intensity in the R package ChemoSpec 6.2 (Hanson, 2025).

Light microscopy, microcomputed tomography scanning, and three-dimensional reconstruction: All amber pieces were trimmed and polished as close to the inclusion of interest as possible with a water-fed trim saw and water-fed grinder. We imaged all holotype specimens with Nikon SMZ25 stereomicroscopes equipped with Nikon DS-Ri2 and Digital Sight 10 cameras at the New Jersey Institute of Technology. All images are digitally stacked photomicrographic composites of several individual focal planes obtained with NIS Elements v6.1. We generated a microcomputed tomography (CT) scan of each type specimen using a Zeiss Xradia 510 Versa 3D X-ray microscope operated with the Zeiss Scout-and-Scan Control System software (v. 14.0.14829.38124) at the Okinawa Institute of Science and Technology Graduate University, Japan and a Zeiss Xradia 630 3D X-ray microscope operated with the Zeiss Scout-and-Scan Control System software (v. 14.0.14829.38124) at the American Museum of Natural History (AMNH). We performed the scans with varying beam intensity and magnification objectives con-

tingent on specimen size and density. We then segmented the resulting z-stack images using 3D Slicer v. 5.8.1. The final volume renderings were produced using MeshLab 2023.12.

Measurements and morphological terminology: We took measurements both directly on the amber specimens using light microscopy and corroborated measurements using the 3D models produced from CT scanning. We measured all specimens following Sosiak and Barden (2021; fig. 1A–C). We also took additional lineage specific measurements to help with taxonomic descriptions (table 4). Morphological terminology primarily follows Bolton (1994) for most body structures and Harris (1979) for sculpture, with the addition of lineage-specific terminology when required.

RESULTS AND DISCUSSION

Specimen provenance: We examined a total of 28 specimens: 25 putative Dominican amber specimens, two Dominican copal reference specimens, and one Colombian copal reference specimen. The copal specimens reacted positively to the ethanol solubility test, developing a tacky surface to which cotton fibers became affixed (table 5). In contrast, none of the putative Dominican amber specimens developed a tacky surface and showed no reaction to ethanol.

Raman peak ratios varied widely across putative Dominican amber specimens, ranging from 0.72 to 1.07 (table 5, appendix 2). Two specimens, AMNH 99 24 and AMNH DR 10 881, consistently exhibited ratios exceeding 1.00—values that are above a proposed cutoff to discern between copal and fossil resin (Brody et al., 2001). Sixteen of the 25 ratios fell below previously reported ranges for Dominican amber of between 0.91 to 1.00 (Brody et al., 2001). Our findings demonstrate a much broader potential range of peak values when compared to previous studies. This may be due to our large sampling size; Brody et al. (2001) examined only six Dominican amber specimens—and no Dominican copal—and previous investigations that established a putative cutoff ratio value of 1.0 included just one Dominican amber specimen and no copal from the Dominican Republic (Winkler et al., 1998, 2001; Tay et al., 1998). Notably, one reference Dominican copal specimen exhibited a ratio within the range previously reported for Dominican amber (0.94). While Raman spectroscopy has been proposed as a method to distinguish amber from copal and other resins (Edwards and Farwell, 1996; Rao et al., 2013), there are no systematic assessments of Dominican amber and copal, specifically. Our results suggest that previously reported peak ratios vary considerably beyond reliable ranges that can be used for establishing maturation in this case. Brody et al. (2001) posit that the burial environment may play a key role in the maturation process and that resin chemistry affects the utility of using peak ratios in this region. The broad range of ratios found here may be evidence of differences in the maturation process of Dominican amber or even differences in specimen storage within collections (Bisulca et al., 2012).

Ethanol reactivity as well as documentation for specimen acquisition from definitive amber mining sites suggests that the type material is Dominican amber. The material with more ambiguous acquisition information—two donated AMNH specimens—exhibited the same nonreactivity as the authenticated samples, suggesting that they too are Dominican amber. Our results also highlight the difficulties in distinguishing between Dominican amber and copal using Raman spectroscopy at present, in contrast to other fossil resin localities with more characteristic spectroscopic identities (e.g., the "Baltic Shoulder" of Wagner-Wysiecka, 2018). While Raman spectroscopic analyses remain inconclusive, we include our approach and spectroscopic data for all type material to facilitate future efforts to establish assays of specimen provenance. While the prospect of retroactively assessing some 1300 described Dominican amber type specimens is daunting, an accessible and rigorous assay for amber type material will greatly improve the utility of fossil insect taxa.

TABLE 2

List of ant species described from Dominican amber.
Species are noted by author. While all species are presumed extinct, dagger (†) denotes extinct genera.

Subfamily	Species	Author
Amblyoponinae		
	Fulakora lata	This study
	Prionopelta ambigua	This study
Dolichoderinae		
	Azteca alpha	Wilson, 1985
	Azteca eumeces	Wilson, 1985
	†*Chimerodous alpha*	This study
	Dolichoderus caribbaeus	Wilson, 1985
	Dolichoderus dibolius	Wilson, 1985
	Dolichoderus intermedius	Mackay, 1993
	Dolichoderus primitivus	Wilson, 1985
	Dolichoderus prolaminatus	Wilson, 1985
	Gracilidris humiloides	(initially *Iridomyrmex humiloides*) Wilson, 1985
	Leptomyrmex neotropicus	Baroni Urbani, 1980
	†*Schismiscapus caritatis*	(Initially *Technomyrmex caritatis*) Brandao et al., 1999.
	†*Schismiscapus hispaniolae*	(Initially *Iridomyrmex hispaniolae*) Wilson, 1985
	Tapinoma troche	Wilson, 1985
Dorylinae		
	Acanthostichus hispaniolicus	De Andrade, 1998
	Cylindromyrmex antillanus	De Andrade, 1998
	Cylindromyrmex electrinus	De Andrade, 1998
	Cylindromyrmex inopinatus	De Andrade, 2001
	Neivamyrmex ectopus	Wilson, 1985
Ectatomminae		
	Gnamptogenys casca	Lattke, 2002
	Gnamptogenys levinates	Baroni Urbani, 1980
	Gnamptogenys pristina	Baroni Urbani, 1980
	Poneracantha brunoi	Lattke, 2002
	Poneracantha minima	This study
Formicinae		
	Acropyga glaesaria	LaPolla, 2005
	Brachymyrmex atrapada	This study
	Camponotus matunai	This study
	Nylanderia vetula	LaPolla and Dlussky, 2010
	Zatania electra	LaPolla et al., 2012

TABLE 2 *continued*

Subfamily	Species	Author
Myrmicinae		
	Acanthognathus poinari	Baroni Urbani, 1994a
	Acromyrmex yucayequensis	This study
	Aphaenogaster amphioceanica	De Andrade, 1995
	Apterostigma electropilosum	Schultz, 2007
	Apterostigma eowilsoni	Schultz, 2007
	Basiceros enana	Fiorentino et al., 2025
	Cardiocondyla larimar	This study
	Cephalotes alveolatus	Vierbergen and Scheven, 1995
	Cephalotes bloosi	De Andrade and Baroni Urbani, 1999
	Cephalotes brevispineus	De Andrade and Baroni Urbani, 1999
	Cephalotes caribicus	De Andrade and Baroni Urbani, 1999
	Cephalotes dieteri	De Andrade and Baroni Urbani, 1999
	Cephalotes hispaniolicus	De Andrade and Baroni Urbani, 1999
	Cephalotes integerrimus	Vierbergen and Scheven, 1995
	Cephalotes jansei	Vierbergen and Scheven, 1995
	Cephalotes obscurus	Vierbergen and Scheven, 1995
	Cephalotes serratus	Vierbergen and Scheven, 1995
	Cephalotes squamosus	Vierbergen and Scheven, 1995
	Cephalotes sucinus	De Andrade and Baroni Urbani, 1999
	Crematogaster diunota	This study
	Cyphomyrmex taino	De Andrade, 2003
	Eurhopalothrix electrina	This study
	†*Ilemomyrmex caecus*	Wilson, 1985
	Kempfidris priminatus	This study
	Mycetomoellerius yucahu	This study
	Nesomyrmex caritatis	De Andrade and Wagensberg, 1999
	Nesomyrmex dominicanus	De Andrade and Wagensberg, 1999
	†*Oxyidris antillana*	Wilson, 1985
	Paratrachymyrmex primaevus	Baroni Urbani, 1980
	Pheidole anticua	Casadei-Ferreira et al., 2019
	Pheidole primigenia	Baroni Urbani, 1995
	Pheidole tethepa	Wilson, 1985
	Pogonomyrmex tiempopogo	This study
	Rhopalothrix macorixia	This study
	Rogeria primaeva	This study
	Solenopsis lamellata	Bouju et al., 2026
	Solenopsis merengue	Bouju et al., 2026

TABLE 2 *continued*

Subfamily	Species	Author
	Solenopsis picapica	Bouju et al., 2026
	Solenopsis pilonaria	Bouju et al., 2026
	Solenopsis viralata	Bouju et al., 2026
	Strumigenys electrina	Baroni Urbani and De Andrade, 1994
	Strumigenys pilosula	Baroni Urbani and De Andrade, 2007
	Strumigenys poinari	Baroni Urbani and De Andrade, 2007
	Strumigenys schleeorum	Baroni Urbani and De Andrade, 1994
	Temnothorax praecreolus	De Andrade, 1992
	Allomerus bi	This study
Paraponerinae		
	Paraponera dieteri	Baroni Urbani, 1994b
Ponerinae		
	Anochetus ambiguus	De Andrade, 1994
	Anochetus brevidentatus	Mackay, 1991
	Anochetus conisquamis	De Andrade, 1994
	Anochetus corayi	Baroni Urbani, 1980
	Anochetus dubius	De Andrade, 1994
	Anochetus exstinctus	De Andrade, 1994
	Anochetus intermedius	De Andrade, 1994
	Anochetus lucidus	De Andrade, 1994
	Brachyponera mamajuanis	This study
	Hypoponera electrocacica	Fiorentino et al., 2026
	†*Kiskeyapone armilla*	This study
	Leptogenys intacta	This study
	Mayaponera bachata	This study
	†*Cayrapone hupia*	This study
	Neoponera vejestoria	Fiorentino et al., 2023
	Odontomachus pseudobauri	De Andrade, 1994
	Odontomachus spinifer	De Andrade, 1994
	Platythyrea dentata	Lattke, 2003
	Platythyrea procera	Lattke, 2003
	Platythyrea pumilio	De Andrade, 2004
	Platythyrea scalpra	Lattke, 2003
	Pseudoponera hatuey	This study
	†*Stenoponera petiolata*	This study
Proceratiinae		
	Discothyrea gigas	De Andrade, 1998c
	Proceratium denticulatum	Lattke, 1990

TABLE 2 *continued*

Subfamily	Species	Author
	Proceratium dominicanum	Baroni Urbani and De Andrade, 2003
	Proceratium gibberum	Baroni Urbani and De Andrade, 2003
	Proceratium poinari	Baroni Urbani and De Andrade, 2003
Pseudomyrmecinae		
	Pseudomyrmex antiquus	Ward, 1992
	Pseudomyrmex avitus	Ward, 1992
	Pseudomyrmex baros	Ward, 1992
	Pseudomyrmex coruscus	Ward, 1992
	Pseudomyrmex macrops	Ward, 1992
	Pseudomyrmex nexilis	Ward, 1992
	Pseudomyrmex oryctus	Ward, 1992
	Pseudomyrmex prioris	Ward, 1992
	Pseudomyrmex succinus	Ward, 1992
	Pseudomyrmex thecolor	Ward, 1992
	Pseudomyrmex vicinus	Ward, 1992

The Dominican amber ants: The Dominican amber ant fauna now consists of 116 species across 59 genera and 10 subfamilies (table 2). The most diverse subfamily in the amber assemblage is the Myrmicinae with 48 species, accounting for approximately 40% of species. These are distributed among 25 genera, with 19 genera known from a single species and three genera with more than four species: *Cephalotes* (12 species), *Solenopsis* (five species), and *Strumigenys* (four species). The second and third most diverse subfamilies, Ponerinae (19% of species-level diversity) and Dolichoderinae (11%), show a similar distribution of species-level diversity. The Ponerinae consists of 23 species in 12 genera, and only two genera are known from more than four described species: *Anochetus* and *Platythyrea*. Dolichoderine taxa comprise 12 species in seven genera; a single genus, *Dolichoderus*, is represented by four species. The Pseudomyrmecinae (9%) are represented by 11 species in a single genus, *Pseudomyrmex*. The Dorylinae, Ectatomminae, Formicinae, and Proceratiinae each account for 4% of species diversity, while just two Amblyoponinae (2%) and one Paraponerinae (1%) species are known.

We highlight newly recorded taxa in the subfamily Ponerinae, expanding its known diversity from five to 11 genera, including three extinct and one Old World genera. Ponerine taxa comprise a diversity of fossil hunter ants across a broad range of worker sizes, from *Pseudoponera hatuey*, sp. nov. (WL 1.01) to *Kiskeyapone armilla*, sp. nov. (WL 3.97). Ant taxonomy is mostly based upon the worker caste; however, the case of *Leptogenys intacta*, sp. nov., known only from a single male specimen, underscores the potential for male specimens to inform the breadth of the predatory ant assemblage in fossil localities.

Most of the ant descriptions since Wilson (1985a) correspond to extant lineages, and we report five extinct genera. The extinct ponerines, Cayrapone, gen. nov., *Kiskeyapone*, gen. nov., and *Stenoponera*, gen nov., can be confidently placed within or near modern lineages, but they are also evidence of lost subfamilial diversity. This loss is not only taxic; it includes morphology and natu-

TABLE 3

Dominican amber species representing the oldest records of higher taxa
Species are listed by taxonomic rank.

Subfamily	Tribe	Species	Taxonomic Rank
Amblyoponinae			
	Amblyoponini		
		Fulakora lata	genus
		Prionopelta ambigua	genus
Dolichoderinae			
	Leptomyrmecini		
		Azteca alpha	genus
		Chimerodous alpha	genus
		Gracilidris humiloides	genus
		Leptomyrmex neotropicus	genus
Dorylinae	-		
		Acanthostichus hispaniolicus	genus
		Cylindromyrmex antillanus	genus
		Neivamyrmex ectopus	genus
Ectatomminae			
	Ectatommini		
		Poneracantha brunoi	genus
Formicinae			
	Plagiolepidini		
		Acropyga glaesaria	genus
	Myrmelachistini		tribe
		Brachymyrmex atrapada	genus
	Lasiini		
		Zatania electra	genus
Myrmicinae			
	Attini	*Acanthognathus poinari*	genus
		Acromyrmex yucayequensis	genus
		Apterostigma electropilosum	genus
		Basiceros enana	genus
		Eurhopalothrix electrina	genus
		Mycetomoellerius yucahu	genus

TABLE 3 *continued*

Subfamily	Tribe	Species	Taxonomic Rank
		Paratrachymyrmex primaevus	genus
		Rhopalothrix macorixia	genus
		Strumigenys electrina	genus
		Allomerus bi	genus
	Crematogastrini		
		Crematogaster diunota	genus
		Cardiocondyla larimar	genus
		Nesomyrmex caritatis	genus
		Oxyidris antillana	genus
		Temnothorax praecreolus	genus
	Solenopsidini		
		Kempfidris priminatus	genus
	-	*Rogeria primaeva*	genus
		Ilemomyrmex caecus	genus
Paraponerinae			Subfamily
	Paraponerini		tribe
		Paraponera dieteri	genus
Ponerinae			
	Ponerini		
		Brachyponera mamajuanis	genus
		Leptogenys intacta	genus
		Mayaponera bachata	genus
		†*Cayrapone hupia*	genus
		†*Kiskeyapone armilla*	genus
		Neoponera vejestoria	genus
		Pseudoponera hatuey	genus
		Stenoponera petiolata	genus

TABLE 4

Specimen measurements
All measurements taken from specimens, their associated description, and specific taxa from which it was measured.

Trait	Description of Measurement	Genus from which Measurement Taken
Head width (HW)	The maximum width of the head in full face view, excluding the eyes. (Maximum width is usually posterior to level of eyes. Lateral tubercles and projections are generally ignored.)	All
Head length (HL)	The length of the head capsule excluding the mandibles, measured in full face view in a straight line from the midpoint of the anterior clypeal margin to the mid-point of the posterior margin. In species where one or both of these margins is concave the measurement is taken from the midpoint of a transverse line that spans the apices of the projecting portions.	All
Eye length (EL)	Maximum diameter of compound eyes in lateral view	All
Eye height total (EHT)	Calculated as the sum of EHD + EHV	All
Eye height dorsal (EHD)	Vertical distance from the center point of the eye to the dorsal margin of the head, in lateral view	All
Eye height ventral (EHV)	Vertical distance from the center point of the eye to the ventral margin of the head, in lateral view	All
Eye length total (ELT)	Calculated as the sum of ELA + ELP	All
Eye length anterior (ELA)	Horizontal distance from the center point of the eye to the anterior margin of the head, in lateral view	All
Eye length posterior (ELP)	Horizontal distance from the center point of the eye to the posterior margin of the head, in lateral view	All
Mandible length profile (MLP)	Maximum distance from point of clypeal insertion to apicalmost tooth of mandible; measurement taken in anterolateral view of mandible	All
Scape length (SL)	Length of the antennal scape, excluding the basal condyle and its peduncle	All
Weber's length (WL)	Diagonal length of mesosoma in profile, from the midpoint of the anterior pronotal declivity to the posterior basal angle of the metapleuron	All
Procoxal length (PcL)	Length from articulation point with propleuron to the distal tip of the procoxa	All
Mesosoma height (MH)	Taken at a right angle to Weber's length from the ventral margin of propleuron to dorsal margin of pronotum	All
Pronotum width (PrW)	Measured at the widest point of the pronotum when viewed dorsally	All
Metafemur length (MfL)	Measured from articulation point with trochanter to distal tip of the metafemur	All
Ocellar width (OW)	Maximum width of median ocellus, in dorsal view	*Leptogenys*

TABLE 4 *continued*

Trait	Description of Measurement	Genus from which Measurement Taken
Ocellar eye space (OES)	Minimum distance from lateral ocellus to compound eye in dorsal view	*Leptogenys*
MeL (mesoscutum length)	Maximum length of mesoscutum in dorsal view	*Leptogenys*
MeW (mesoscutum width)	Maximum width of mesoscutum in dorsal view	*Leptogenys*
Scape lobe length (SLL)	Measured along same line as scape length, distance from furthest extension of basal lobe to point perpendicular to anterior sinus formed by neck and basal condyle of scape	*Eurhopalothrix, Rhopalothrix*
Pronotal length (PrL)	Maximum length of the pronotum (excluding the collar) in dorsal view.	*Prionopelta, Schismiscapus*
Propodeal spine length (SPL)	Propodeal spine length, measured from tip of propodeal spine to closest point on outer rim of propodeal spiracle, maximizing spine length in lateral view	*Acromyrmex, Crematogaster,*
Petiole width (PeW)	Midline width of the petiolar node in dorsal view	*Acromyrmex, Cardiocondyla, Kempfidris, Mycetomoellerius, Paratrachymyrmex*
Petiole height (PeH)	Maximum height of the petiole measured in lateral view, as the perpendicular distance from the dorsal surface of the petiolar node to the ventral margin of the petiolar node, immediately anterior to the subpetiolar process	*Poneracantha, Acromyrmex, Cardiocondyla, Kempfidris, Mycetomoellerius, Paratrachymyrmex, Leptogenys*
Petiole length (PeL)	Maximum length of the petiole in lateral view, measured from the anterior face to the posterior margin of the petiole	*Poneracantha, Acromyrmex, Cardiocondyla, Eurhopalothrix, Kempfidris, Mycetomoellerius, Paratrachymyrmex, Rhopalothrix, Mayaponera, Kiskeyapone, Pseudoponera, Leptogenys*
Postpetiole width (PpeW)	Midline width of the postpetiole node in dorsal view.	*Acromyrmex, Cardiocondyla, Kempfidris, Mycetomoellerius, Paratrachymyrmex*
Postpetiole height (PpeH)	Maximum height of the postpetiole measured in lateral view	*Acromyrmex, Mycetomoellerius, Paratrachymyrmex*
Postpetiole length (PpeL)	Maximum length of the postpetiole in lateral view, measured from the anterior face to the posterior margin of the postpetiole	*Acromyrmex, Cardiocondyla, Eurhopalothrix, Kempfidris, Mycetomoellerius, Paratrachymyrmex, Rhopalothrix*
First gastral tergite length (T1L)	Length of first gastral (third abdominal) tergite in dorsal view	*Prionopelta, Schismiscapus*
Gaster length (GL)	Maximum length of gaster (abdominal segments III to VII) in lateral view, excluding sting.	*Poneracantha, Acromyrmex, Cardiocondyla, Crematogaster, Eurhopalothrix, Kempfidris, Mycetomoellerius, Paratrachymyrmex, Rhopalothrix, Mayaponera, Kiskeyapone, Pseudoponera, Leptogenys*

TABLE 4 *continued*

Trait	Description of Measurement	Genus from which Measurement Taken
Total length (TL)	Calculated as the sum of HL + WL + PetL + T1L, or HL + ML + WL + PeL + GL, or HL + ML + WL + PeL + PpeL + GL.	*Poneracantha, Acromyrmex, Cardiocondyla, Crematogaster, Eurhopalothrix, Kempfidris, Mycetomoellerius, Paratrachymyrmex, Rhopalothrix, Mayaponera, Kiskeyapone, Pseudoponera, Leptogenys*
Cephalic index (CI)	Calculated as: HW/HL	*Eurhopalothrix, Rhopalothrix, Mayaponera, Pseudoponera*
Ocular index (OI)	Calculated as: EL/HW	*Mayaponera*
Scape index (SI)	Calculated as: SL/HW	*Crematogaster, Mayaponera, Pseudoponera*
Scape lobe index (SLI)	Calculated as: 100*SLL/SL	*Eurhopalothrix, Rhopalothrix*
Propodeal spine length (SPI)	Calculated as SPI/WL	*Crematogaster*

ral history, particularly with *Stenoponera*. Within the Dolichoderinae, *Chimerodous*, gen. nov., likely belongs to the Leptomyrmecini, and our report includes new records for *Schismiscapus* (Varela-Hernandez et al., 2022), previously known only from a single species in Chiapas amber. The transfer of *S. hispaniolae* and *S. caritatis* from *Technomyrmex* to *Schismiscapus* marks the first record of an extinct genus found in both Chiapas and Dominican amber.

The current composition of Dominican amber ants is now nearly twice the genus-level diversity described by Wilson (1985a). While the taxonomic scale has increased, descriptions over the last four decades and herein have affirmed some of Wilson's observations. The great majority of fossil species belong to contemporary lineages. We also confirm the presence of genera previously proposed by Wilson (1985a), with *Crematogaster*, *Rogeria*, *Prionopelta*, *Camponotus*, *Solenopsis* (Bouju et al., 2026), and *Pachycondyla* (*Trachymesopus* now *Pseudoponera*). Though this monograph increases the number of species from Dominican amber by ~25%, these 116 species are just a small portion of the diversity that must have existed on the island of Hispaniola during the Miocene.

Neotropical Stability, Disjunct Distributions, and Evidence for Relict Lineages

Wilson's (1985a) initial review of the Dominican paleomyrmecological fauna proposed strong affinities between this fossil assemblage and the modern Neotropical ant fauna. The presence of genera such as *Neivamyrmex*, *Paraponera*, *Gnamptogenys*, and *Pseudomyrmex*—all of which are currently restricted to the tropical and warm temperate regions of the New World—supported this hypothesis. Yet, the discovery of *Pheidole tethepa*, with spinescence known only from Old World *Pheidole* lineages, led Wilson to suggest potential convergent evolution while casting doubt on its generic placement within *Pheidole*, given its aberrant morphology (Wilson, 1985b). Subsequent discoveries of *Leptomyrmex* and another spinescent *Pheidole* in Dominican amber (Baroni Urbani and Wilson, 1987; Baroni Urbani, 1995) further hinted at some potential Old World affinities. Although Guénard et al. (2015) supported Wilson's initial hypothesis of Neotropical affinities, a genus-level analysis of regional fossil and extant assemblages suggested that similarities to Old World genera or species groups—such as *Leptomyrmex neotropicus* and *Pheidole*

TABLE 5

Results of ethanol assays and Raman spectroscopic analyses of Dominican amber specimens
Results correspond to lowest peak ratio (see appendix 2). Specimens are noted by peak ratio, solubility results, designation and locality. * denotes northern mines of the Santiago Province, Dominican Republic. ** denotes donated material with unverified locality, but likely same as *.

Specimen	Peak Ratio	Ethanol Results	Designation	Locality
Colombian copal	1.039	tacky	copal	Santander, Colombia
AMNH Dominican copal #1	0.937	tacky	copal	Likely Cotui, Dominican Republic
AMNH Dominican copal #2	0. 913	tacky	copal	Likely Cotui, Dominican Republic
MNHNSD FOS 18.117	0.764	nonreactive	putative amber	*
AMNH_99_24	1.068	nonreactive	putative amber	*
AMNH_10_240	0.722	nonreactive	putative amber	*
AMNH_10_165	0.908	nonreactive	putative amber	*
MNHNSD FOS 18.120	0.777	nonreactive	putative amber	*
MNHNSD FOS 18.121	0.769	nonreactive	putative amber	*
MNHNSD FOS 18.122	0.911	nonreactive	putative amber	*
AMNH-DR-99-416	0.696	nonreactive	putative amber	*
AMNH-DR-14-278	0.883	nonreactive	putative amber	*
MNHNSD FOS 18.123	0.851	nonreactive	putative amber	*
AMNH-DR-14-907	0.766	nonreactive	putative amber	*
AMNH-DR-14-519	0.734	nonreactive	putative amber	*
AMNH-DR-15-48	0.961	nonreactive	putative amber	*
AMNH_DR_RP_359	0.764	nonreactive	putative amber	**
PALE-44317	0.792	nonreactive	putative amber	*
AMNH_DR_14_935	0.923	nonreactive	putative amber	*
MNHNSD FOS 18.124	0.777	nonreactive	putative amber	*
AMNH-11735C	0.823	nonreactive	putative amber	*
AMNH_DR_14_945	0.936	nonreactive	putative amber	*
AMNH_10-239	0.769	nonreactive	putative amber	*
AMNH_DR_14_930	0.820	nonreactive	putative amber	*
AMNH_DR_14_51	0.911	nonreactive	putative amber	*
AMNH_JVE_781	0.928	nonreactive	putative amber	**
AMNH_DR_14_881	1.059	nonreactive	putative amber	*
AMNH_DR_14_897	0.832	nonreactive	putative amber	*

TABLE 6

List of ant genera described from Dominican amber, ordered alphabetically by subfamily
Species are noted by contemporary distribution, current status, and number of species described.
Abbreviations: **Afr,** African; **Aus,** Australasian; **Ext,** Extinct; **Im,** Indo-Malayan; **In,** Invasive; **Nea,** Nearctic; **Neo,** Neotropical; **Pal,** Palearctic.

Subfamily	Genus	Contemporary Distribution	Locally Extinct	Species (no.)
Amblyoponinae				2
	Fulakora	Aus, Neo		1
	Prionopelta	Afr, Aus, Im, Neo	Ex	1
Dolichoderinae				12
	Azteca	Neo	Ex	2
	Chimerodous	Fossil	Ex	1
	Dolichoderus	Aus, Im, Nea, Neo, Pal	Ex	5
	Gracilidris	Neo	Ex	1
	Leptomyrmex	Aus, Neo	Ex	1
	†*Schismiscapus*	Fossil	Ex	2
	Tapinoma	Afr, Aus, Im, Nea, Neo, Pal		1
Dorylinae				5
	Acanthostichus	Nea, Neo	Ex	1
	Cylindromyrmex	Neo		3
	Neivamyrmex	Nea, Neo	Ex	1
Ectatomminae				5
	Gnamptogenys	Nea, Neo		4
	Poneracantha	Neo		1
Formicinae				5
	Acropyga	Afr, Aus, Im, Nea, Neo, Pal		1
	Brachymyrmex	Nea, Neo		1
	Camponotus	Afr, Aus, Im, Nea, Neo, Pal		1
	Nylanderia	Afr, Aus, Im, Nea, Neo		1
	Zatania	Neo		1
Myrmicinae				48
	Acanthognathus	Neo	Ex	1
	Acromyrmex	Nea, Neo	Ex	1
	Aphaenogaster	Afr, Aus, Im, Nea, Neo, Pal		1
	Apterostigma	Neo	Ex	2

TABLE 6 *continued*

Subfamily	Genus	Contemporary Distribution	Locally Extinct	Species (no.)
	Basiceros	Neo	Ex	1
	Cardiocondyla	Afr, Aus, Im, Pal	In	1
	Cephalotes	Nea, Neo		12
	Crematogaster	Afr, Aus, Im, Nea, Neo, Pal		1
	Cyphomyrmex	Neo		1
	Eurhopalothrix	Aus, Im, Neo		1
	†*Ilemomyrmex*	Fossil	Ex	1
	Kempfidris	Neo	Ex	1
	Mycetomoellerius	Nea, Neo		1
	Nesomyrmex	Afr, Nea, Neo	Ex	2
	†*Oxyidris*	Fossil	Ex	1
	Paratrachymyrmex	Neo	Ex	1
	Pheidole	Afr, Aus, Im, Nea, Neo, Pal		3
	Pogonomyrmex	Neo, Nea		1
	Rhopalothrix	Neo	Ex	1
	Rogeria	Aus, Nea, Neo		1
	Solenopsis	Afr, Aus, Im, Nea, Neo, Pal		6
	Strumigenys	Afr, Aus, Im, Nea, Neo, Pal		4
	Temnothorax	Afr, Im, Nea, Neo, Pal		1
	Allomerus	Neo		1
Paraponerinae				1
	Paraponera	Neo	Ex	1
Ponerinae				23
	Anochetus	Afr, Aus, Im, Neo		8
	Brachyponera	Afr, Aus, Im	Ex	1
	Hypoponera	Afr, Aus, Im, Nea, Neo		1
	Leptogenys	Afr, Aus, Im, Nea, Neo		1
	Mayaponera	Neo	Ex	1
	†*Cayrapone*	Fossil	Ex	1
	†*Kiskeyapone*	Fossil	Ex	1
	Neoponera	Neo	Ex	1
	Odontomachus	Afr, Aus, Im, Nea, Neo		2
	Platythyrea	Afr, Aus, Im, Neo		4
	Pseudoponera	Aus, Neo		1
	†*Stenoponera*	Fossil	Ex	1

TABLE 6 *continued*

Subfamily	Genus	Contemporary Distribution	Locally Extinct	Species (no.)
Proceratiinae				5
	Discothyrea	Afr, Aus, Im, Nea, Neo		1
	Proceratium	Afr, Aus, Im, Nea, Neo, Pal		4
Pseudomyrmecinae				11
	Pseudomyrmex	Nea, Neo		11

primigenia—likely reflect modern relictual distributions or previously unrecognized cases of morphological convergence (Baroni Urbani, 1995; Casadei-Ferreira et. al., 2019). Subsequent reconstruction of the biogeographic history of *Leptomyrmex* provided further support for the relictual distribution hypothesis; *Leptomyrmex* indeed originated in the Neotropics and subsequently radiated into Australasia across Antarctica during the Eocene (Boudinot et al., 2016; Barden et al., 2017). On the other hand, recent molecular phylogenies of *Pheidole* have shown that four extant Old World lineages have evolved prominent pronotal spines independently (Sarnat et al., 2017), providing further support for Wilson's hypothesis of convergent evolution of pronotal spinescence in the Neotropics.

The Dominican paleomyrmecological fauna exhibits a clear affinity with the assemblage of Miocene-age Chiapas amber, the only other somewhat well-sampled amber deposit from the Neotropics (Varela-Hernández et al., 2024). Of the nine known genera in Chiapas amber, six are found in Dominican amber. Of the remaining three, two are extinct endemics known only from Chiapas amber. The discovery of *Schismiscapus* in Dominican amber underscores the biogeographic links between these deposits. The taxonomic history of *Schismiscapus hispaniolae* and *S. caritatis* is complex—these species were first described as *Iridomyrmex* (Wilson, 1985c), then transferred to *Linepithema* (Shattuck, 1992a), and penultimately placed within *Technomyrmex* (Brandão et al., 1999). Other genus-level commonalities include a mixture of exclusively Neotropical and widely distributed taxa: *Aphaenogaster*, *Cephalotes*, *Cyphomyrmex*, *Discothyrea*, and *Odontomachus* (De Andrade, 1995, 1998b, 2003; De Andrade and Baroni Urbani, 1999; França and Gomes, 2025). Within the cosmopolitan genus *Pheidole*, a spinescent species was recently discovered from Chiapas amber, and the spines allow for putative placement near the spinescent *Pheidole primigenia* of Dominican amber (Varela-Hernández and Riquelme, 2024).

Though fewer, genera with no known modern Neotropical lineages play a significant role in understanding modern biogeographical patterns. Nine of the 59 genera preserved in Dominican amber do not correspond to modern Neotropical lineages and include seven now-extinct genera—†*Chimerodous*, †*Ilemomyrmex*, †*Oxyidris*, †*Kiskeyapone*, †*Cayrapone*, †*Schimiscapus*, and †*Stenoponera*—and, most notably, two definitively Old World lineages: *Brachyponera* and *Cardiocondyla* (table 6). *Cardiocondyla larimar*, a species belonging to the now cosmopolitan invasive genus *Cardiocondyla*, can be confidently placed within the modern *C. wroughtonii* species complex. Excluding the invasive species *C. obscurior*, the current distribution of this complex is restricted to the Indomalayan and Afrotropical bioregions. The discovery of *C. larimar* in amber, along with the modern invasion of Hispaniola by *C. obscurior* and *C. emeryi*, provides a protracted illustration of Wilson's invasion-extinction hypothesis, underscoring the stochastic forces shaping island fauna composition.

TABLE 7

Number of fossil and extant species in each subfamily present on the Island of Hispaniola

Of the 59 genera known from the fossil record, 50 belong to lineages at least partially distributed in the Neotropics at present, while 23 of the genera belong to lineages known only from the Neotropics.

Subfamily	Fossil Species	Extant Species
Amblyoponinae	2	1
Dolichoderinae	13	9
Dorylinae	5	2
Ectatomminae	5	7
Formicinae	5	47
Myrmicinae	48	82
Paraponerinae	1	0
Ponerinae	23	18
Proceratiinae	5	3
Pseudomyrmecinae	11	4

Modern *Brachyponera* have an Afrotropical, Indomalayan, and Australasian distribution, which they share with six of the 12 known Dominican Ponerinae genera. Yet the lack of revisions and phylogenetic treatments for many of these genera precludes a confident placement for some fossil species, making further biogeographical inference difficult. What remains certain is the large diversity of ponerine hunter ants in the Dominican fossil ant assemblage and the presence of genera without modern Neotropical congeners. These taxa hint at a large-scale extinction of Ponerine ants since the formation of these fossils (Fiorentino et al., 2023; Varela-Hernández et al., 2024).

Connections to diversity within the Eastern Hemisphere extend beyond the genus level. Species within the Proceratiinae appear to have clear links to Afrotropical and Indomalayan species groups. De Andrade (1998b) noted this affinity in *Discothyrea*, where *D. gigas* is considered closely related to Afrotropical *Discothyrea*. Similarly, the *Proceratium* species from Dominican amber—*P. denticulatum* and *P. gibberum*—can be placed within the *Proceratium stictum* group (Baroni Urbani and De Andrade, 2003). This group is comprised of species primarily distributed in the Indomalayan and Australasian bioregions, with only two relictual species in Central America. A similar pattern may be observed in *Fulakora*, whose modern congeners are restricted to the New World and Australasia (Ward and Fisher, 2016). Likewise, some fossil *Platythyrea* species—despite a contemporary pantropical distribution of the genus—have been hypothesized to share affinities with the Indomalayan *P. clypeata* complex (Kugler, 1977; Lattke, 2003; De Andrade, 2004). However, these relationships remain speculative (Lattke 2003; De Andrade, 2004). Indeed, many ant species found in Dominican amber belong to genera with disjunct New World and Old World distributions, a pattern reminiscent of that observed in *Leptomyrmex* (Barden et al., 2017). However, the lack of comprehensive phylogenetic studies for most of these groups limits our ability to draw definitive comparisons between fossil and extant taxa.

A dynamic insular fauna: The most conventional interpretation of the Dominican amber fauna is its apparent similarity to the modern Dominican fauna. This has historically been a key takeaway in assessments of the deposit. Yet, as more discoveries emerge, it is increasingly clear that these two assemblages are remarkably distinct. Most of the genera present in the fossil record have modern congeners. Yet, early evidence of now locally extinct subfamilies—such as Paraponerinae (Wilson, 1986; Baroni Urbani, 1994a) and those that have experienced a dramatic decline in diversity, like Dolichoderinae and Dorylinae (Wilson, 1985c, 1985d; Baroni Urbani and Wilson, 1987), point to bigger structural differences. Our findings support a broader pattern of local extinction, given the 11 genera that no longer occur on Hispaniola (table 7). Wilson previously observed this trend and proposed that highly specialized genera might be more prone to local extinction due to lower dispersal ability. However, many of the extinct

taxa identified in our study belong to less specialized, even generalist genera such as *Pseudoponera* and *Allomerus*, as well as genera with broad Old World distributions like *Brachyponera* and *Cardiocondyla*. Conversely, several highly specialized genera discovered since Wilson's hypothesis—including *Eurhopalothrix*, *Proceratium*, *Discothyrea*, *Pogonomyrmex*, and *Fulakora*— are present across time intervals. While this does not entirely refute the specialist extinction hypothesis, community-level analyses are likely to yield new insight into these insular extinction patterns.

In addition to highlighting extinction, our results also point to long-term persistence. Several genera previously believed to be recent colonizers of the Greater Antilles—such as *Camponotus* and *Allomerus* (Longino and Fernández, 2007; Ward et al., 2025)—are now confirmed to have been present in the early Miocene, indicating deeper temporal roots in the region. Taken together, the 24 new fossil genera reported, along with the absence of many of these genera in the modern ant assemblage, highlight a widespread pattern of decline in diversity, previously observed in the arboreal ant assemblage (Ward, 1992). The contrast between fossil and modern faunas highlights long-term shifts in colonization and extinction. Despite the fossil record's lower overall species richness—due in part to most genera being represented by single species—it exhibits 23% more generic diversity than the modern assemblage. This may be a conservative estimate, as previous studies have shown that amber preservation is subject to resin-capture biases that can obscure the true diversity of ancient insect communities (Solórzano Kraemer et al., 2015; Solórzano Kraemer et al., 2018). Arboreal taxa tend to be overrepresented in amber, while forest-floor-dwelling insects are often undersampled. Our findings may help reevaluate this bias, given the high number of typically ground-nesting taxa recovered (e.g., *Allomerus*, *Rogeria*, *Brachyponera*) and even potentially cryptobiotic genera such as *Rhopalothrix*, *Fulakora*, and *Prionopelta*.

The Untapped Potential of Fossil Ants from the Neotropics

Fossils play a key role in biological studies, particularly in evolutionary and systematics research. However, most paleoentomological understanding relates to deposits in North America, Asia, and Europe, partly because these regions have been much more extensively explored compared to tropical—and especially Neotropical—deposits (Barden, 2017; LaPolla et al., 2013; Bolton, 2025). Fewer than one fifth (15 out of 84) of all known ant-yielding fossil deposits come from the Global South (Bolton, 2026). The comparative underrepresentation of Neotropical fossils has a range of drivers; these include limited specimen access for local researchers, resource asymmetry across continents, and historical regional exploitation (Monarrez et al., 2022; Cisneros et al., 2022; Brache, 2025; Nakamura et al., 2025). Currently, 97% of fossil occurrence data is contributed by researchers based in North America and Western Europe (Raja et al., 2022)—fossil ant species descriptions are also greatest in these regions (Barden, 2017). Nevertheless, when Neotropical deposits have been explored, they have yielded impactful discoveries that have shaped modern views on ant evolution (Laza, 1982; De Andrade and Baroni Urbani, 1999; Barden, 2017; Sawh et al., 2023; Fiorentino et al., 2025). A key example is the recent discovery of *Vulcanidris cratensis* Lepeco et al., 2025, a Cretaceous hell ant from the Crato Formation of Brazil (Lepeco et al., 2025). *Vulcanidris cratensis* represents the only known Neotropical member of the Haidomyrmecinae and is the oldest ant discovered. At present, amber from the Dominican Republic represents one of the few Lagerstätten from the Western Hemisphere, let alone the Neotropics. Our report of 23 new species represents the largest exploration of Dominican ant fossils since Wilson's initial review in his series in Psyche, highlighting the richness yet to be explored in this and other Neotropical deposits. This work also underscores an opportunity to foster paleoentomological research in the Neotropics through thoughtful collaboration and consideration across hemispheres (Herrera and Maharaj, 2025).

SYSTEMATIC PALEONTOLOGY

Order Hymenoptera Linnaeus, 1758

Family Formicidae Latreille, 1809

Subfamily Amblyoponinae Forel, 1893

The fossil record of Amblyoponinae spans species within the extinct genus *Casaleia* Pagliano and Scaramozzino as well as the extant genera *Myopopone* Roger and *Stigmatomma* Roger (Bolton, 2026). Pagliano and Scaramozzino (1990) provided the genus name *Casaleia*, which includes the Eastern Hemisphere imprint fossil species *Casaleia eocenica* Dlussky and Wedmann, 2012, and *Casaleia orientalis* Dlussky et al., 2015, from the Eocene, together with *Casaleia inversa* (Dlussky, 1981) and *Casaleia longiventris* (Heer, 1849) from the Miocene. *Myopopone sinensis* Zhang, 1989, is known from a rock imprint fossil of Miocene age, while *Stigmatomma electrinum* (Dlussky, 2009) and *Stigmatomma groehni* (Dlussky, 2009) are preserved in Eocene Baltic amber.

Fulakora Mann, 1919

†***Fulakora lata*** Ladino, Lattke, Fiorentino, and Barden, sp. nov.

Figures 2, 3

ZooBank LSID: urn:lsid:zoobank.org:act:2FDB06A9-7E5A-4FC6-9240-5A1A7EEB7D4F

Diagnosis (queen): Mandible with two separate rows of nonbasally fused teeth. Inner margins of frontal lobes spaced about one lobe-width apart. Genal tooth absent. Broadest portion of head located at level of posterior margin of clypeus. Scape not reaching eye midlength. Anterior petiolar margin straight. Subpetiolar process with fenestra. In profile, posterior margin of subpetiolar process with a small, pointed projection protruding backward.

Holotype queen measurements (in mm): HW 1.23, HL 1.57, EL 0.32, EHT 1.05, EHD 0.56, EHV 0.49, ELT 1.63, ELA 1.06, ELP 0.57,

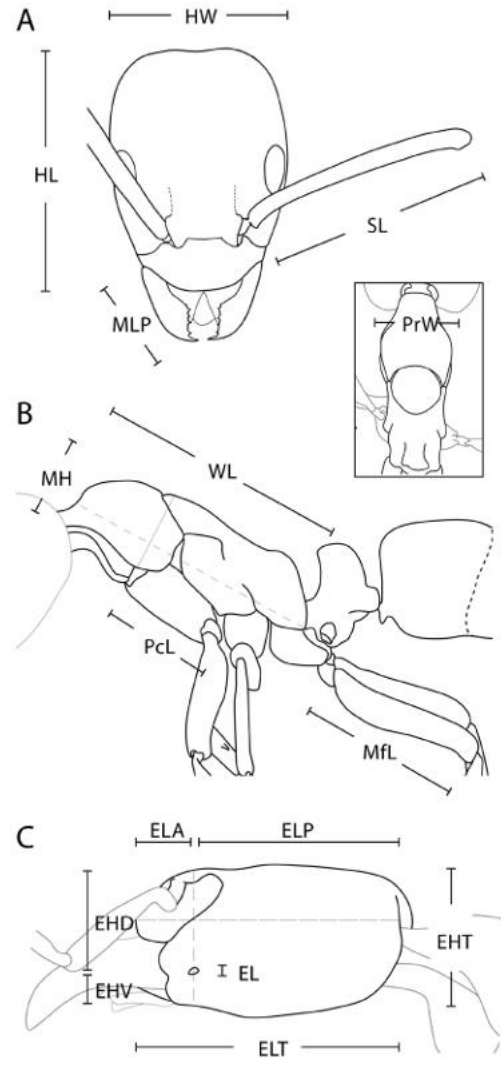


FIGURE 1. Summary of morphological measurements taken from all specimens. **A.** Head in full-face view. **B.** Lateral view of the body. **C.** Head in profile view. **Inset.** Dorsal view of the mesosoma. Based on Sosiak and Barden, 2021. Abbreviations: **EHD,** eye height dorsal; **EHT,** eye height total; **EHV,** eye height ventral; **EL**, eye length; **ELA,** eye length anterior; **ELP,** eye length posterior; **ELT,** eye length total; **HL,** head length; **HW,** Head width; **MfL,** metafemur length; **MH,** mesosoma height; **MLP,** mandible length in profile; **PcL,** procoxa length; **PrW,** Pronotum width; **SL,** scape length; **WL,** weber's length. See table 4 for full measurement descriptions and additional measurements taken from each species.

MLP 1.27, SL 0.83, WL 2.28, PcL 0.58, MH 0.93, PrW 0.84, MfL 1.19.

DESCRIPTION (queen). Head: mandible, clypeus, frontal lobes, and antennae lighter than rest of body. In full-face view, head longer than broad, diverging anteriorly at level of posterior clypeal margin. Posterior corner convex. Mandible long, linear, curved inward toward tip. Inner surface with two separate rows of nonbasally fused teeth. Apical tooth longest and robust, followed by two small denticles (see Comments), remaining teeth conspicuous, one tooth followed by second one, first pair of teeth, and then three pairs of teeth. Small diastema present between three basal-most pairs of teeth, but not less than between inconspicuous teeth; largest diastema between last individual tooth and first pair, followed by the space between individual teeth. Genal tooth absent. Frontal lobes separated by a distance approximately equivalent to width of each lobe. Antenna 12-segmented. Antennal scape not reaching eye midlength. Flagellomeres slightly but gradually thicker toward apex, first flagellomere the longest. Ocelli present. Postgenal bridge complete.

Mesosoma: Profile of mesosoma uniformly convex. Alate, wings folded over the body, details obscured within the inclusion. Notopropodeal sulcus well marked. In profile, dorsal surface of propodeum and its declivity not clearly distinct. In dorsal view, lateral margins of mesosoma slightly convex, midportion widest.

Metasoma: Anterior margin of petiole straight in profile. Anteroventral portion of petiolar tergite projected as a small lateral carina, visible from dorsal and lateral views. Subpetiolar process broad, lobed, directed forward, with a posteroventral angle acute protruding from the straight posterior margin. Fenestra present. Prora present.

Sculpturing and setae: Body with at least two types of pilosity (see Comments), pubescence, and long, flexible, straight setae. Mandible and clypeus with long, flexible, straight setae and a longitudinal elevation of the integument in the outer surface. Clypeus with at least six (and up to seven or eight) short, straight acute setae ("chaetae" of Jacintho et al., 2025; "dentiform clypeal setae" of Keller, 2011) projecting downward, not arising from tuberclelike processes but from the flat cuticle (char. 2 of Keller, 2011). Tarsi pubescent. Lateral surfaces of mesosoma and metasoma apparently smooth.

Etymology: The specific name *lata* refers to the broadest portion of head, at the level of the posterior clypeal margin, from the feminine form of the Latin adjective *latus* meaning "wide" or "broad".

Type material: Holotype. AMNH_DR_99-24 queen, deposited in the American Museum of Natural History (figs. 2, 3). Preserved within a 13 mm by 10 mm section of dark red amber with internal bubbles along the body of the inclusion. Synclusions include a small staphylinid beetle (Pselaphinae), and a fungus gnat (Mycetophilidae).

Horizon and locality: Early Miocene, Burdigalian (ca. 16 Ma; Iturralde-Vinent and MacPhee, 1996); in amber from the northern mines of the Santiago Province, Dominican Republic.

Comments: The fossil species described here shares more morphological features with *Fulakora* than with *Stigmatomma*, including the nonbasally fused arrangement of teeth along the midlength of the mandible (fig. 3), and the fenestra of the subpetiolar process (fig. 2; see Ward and Fisher, 2016: 691 on distinguishing both genera). It also exhibits the expected queen modifications for Formicidae, in terms of a robust mesosoma adapted to flight, an enlarged gaster, and ocelli.

Fulakora lata differs from an undescribed Dominican fossil with code CASENT0906275-AMNH DR 14-385, informally associated with the genus, by at least the following combination of features: its smaller size (a difference of nearly 1.5 mm in WL); a head that is distinctly longer than wide, with the greatest width at the level of the posterior clypeal margin; an anterior petiolar margin that is straight rather than concave in profile, a subpetiolar process with a discontinuous posterior margin forming a small, posteriorly directed pointed projection; and a more prominent prora. Future physical access to this undescribed fossil will undoubtedly

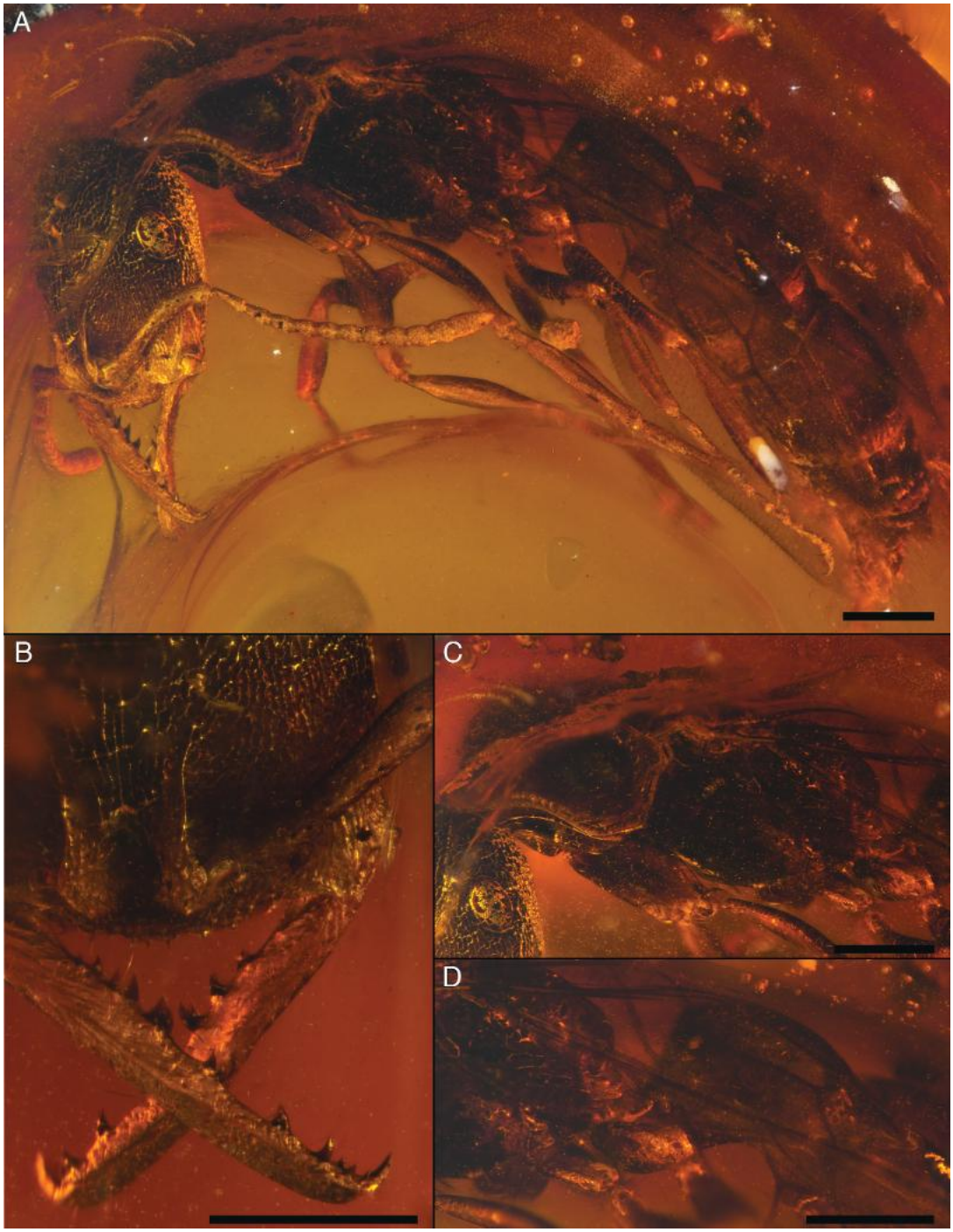


FIGURE 2. Photomicrographs of *Fulakora lata*, sp. nov. (holotype queen, AMNH_DR_99-24). **A.** Lateral view of body. **B.** Head in anterior face view. **C.** Mesosoma in lateral view. **D.** Propodeum and petiole in lateral view. Scale bars = 0.5 mm.

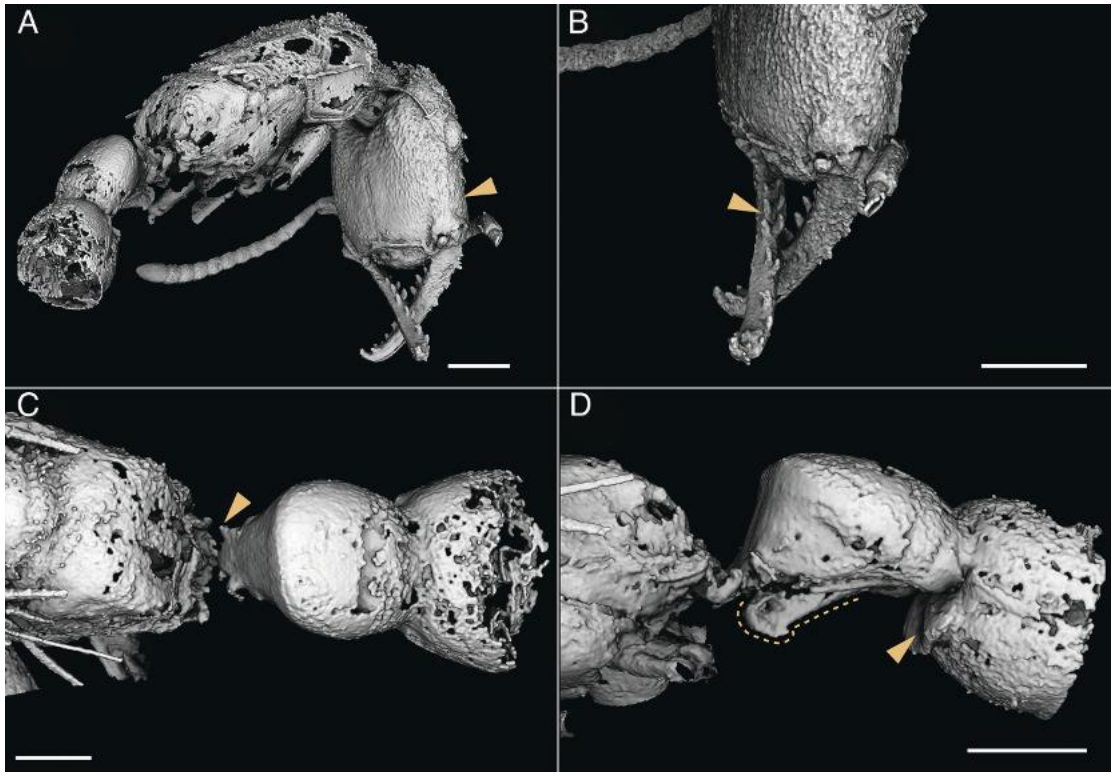


FIGURE 3. Volume renderings of *Fulakora lata*, sp. nov. **A.** Head and body from a posterior view, arrow indicating the head sculpturing at the ventral surface. **B.** Mandibles in lateral view, arrow indicating the two separate rows of teeth. **C.** Lateral carina in the anteroventral portion of the petiolar tergite indicated by the arrow. **D.** Shape of subpetiolar process and diagnostic characters indicated by a discontinuous line, prora indicated by the arrow. Scale bars = 0.5 mm.

provide further insight into the taxonomy of Dominican amber *Fulakora*.

This species also differs from any Australasian extant species of the genus, or for the species occurring in the Caribbean Islands: *Fulakora bierigi* (Santschi, 1930) (Cuba), *Fulakora falcata* (Lattke, 1991) (Greater and Lesser Antilles) and *Fulakora lurilabes* (Lattke, 1991) (Lesser Antilles). It may be distinguished from these species by the following: the mandible width, more uniform along its entire length and not noticeably wider toward the middle; clypeal setae that arise from the flat surface of the anterior clypeal margin (not from tuberclelike processes); the absence of genal teeth; and a distinct distance between the frontal lobes.

Jacintho et al. (2025) provided an identification key for the species of *Fulakora* in the Neotropics. Using this key, the specimen described here meets most of the characteristics leading to *Fulakora mystriops* (Brown, 1960), though it should be noted the metatarsal claws cannot be observed in the inclusion. Nevertheless, when compared to the holotype of *F. mystriops* (ANTWEB1008500), there are subtle differences suggesting the fossil may represent a different species. The lateral margins of the head of *F. lata* are more strongly divergent anteriorly, at the level of the posterior clypeal margin, compared with the widest point in *F. mystriops*, which occurs midway between the anterior margin of the eye and the posterior clypeal margin. Also,

the head of *F. lata* shows a more pronounced disparity between its length and width (no less than 0.2 mm). Furthermore, in lateral view, *F. mystriops* possesses a concave anterior petiolar margin and a subpetiolar process that lacks a posterior projection, both features that contrast with the diagnosis of *F. lata*. These features are also useful to separate the species from the known queens of extant species or *Fulakora* workers described in the Americas. Unfortunately, the state of preservation of *F. lata* obscures most features related to pilosity and body sculpture, as well as the left half of the ant, all pretarsal claws, the gaster, and the entire dorsal surface of the mesosoma and metasoma (fig. 2A). All these characters are important for understanding its differences from *F. mystriops*. Most of the features described here were recovered from the volume rendering (fig. 3), which showed asymmetry of the head in full face view. The cephalic capsule is the body region that concentrates the main number of diagnostic traits. The following ambiguous features are included here and not in the description since they are most susceptible to misinterpretation: the queen appears to have a reddish to dark brown color, lighter on the anterior half of the dorsal surface of head, excluding the mandibles; the posterior portion may have a color similar to the rest of the body; the head appears to have reticulated sculpture on the dorsal surface that contrasts with the longitudinally striated sculpture on the outermost portions of the ventral surface (fig. 3A), and with the mandible somewhat wrinkled; eight antennal pits on the scape that could correspond to the insertion of setae are present and similar pits are noticeable in the third and fourth flagellomeres.

Prionopelta Mayr, 1866

†***Prionopelta ambigua*** Ladino, Lattke, Barden, and Fiorentino, sp. nov.

Figures 4, 5

ZooBank LSID: urn:lsid:zoobank.org:act:1BCF27C6-A326-433A-AB30-6E16DF1C6449

Diagnosis (queen): Median tooth of mandible shorter than basal tooth. Anterior clypeal margin broadly convex. Twelve antennomeres. HL<0.60, T1L<0.24mm. Subpetiolar process with margins subparallel rendering a broad lobe; posterior margin concave, anteroventral angle obtuse, posteroventral angle right-angled.

Holotype queen measurements (in mm): HL 0.55 HW 0.39, EL 0.12, EHT 0.29, EHD 0.24, EHV 0.15, ELT 0.54, ELA 0.32, ELP 0.22, MLP 0.20, SL 0.27, WL 0.65, PcL 0.23, MH 0.22, PrW 0.29, PrL 0.21, T1L 0.22, MfL 0.28.

DESCRIPTION (queen). Head: longer than wide. Lateral margins slightly convex to almost straight. Posterior margin straight. Mandible short, tridentate. Apical tooth longest, followed by small diastema, median tooth, conspicuous diastema and basal tooth. Basal margin straight to slightly convex. Anterior clypeal margin broadly convex. Genal tooth minute. Antenna 12-segmented with well-defined 4-segmented club. Three well-developed ocelli, similar in size, arranged as an equilateral triangle.

Mesosoma: in profile, pronotum at lower level from rest of mesosoma. In dorsal view, posterior margin of propodeum straight. notopropodeal sulcus well marked. In profile, dorsal margin of propodeum and declivity distinguishable. Distance between bulla of metapleural gland and propodeal spiracle corresponds to one spiracle diameter. Distance between dorsal profile of propodeum and propodeal spiracle is 2× the spiracle diameter.

Wings: visible venation appears consistent with the description provided by Yoshimura and Fisher (2012: 17). In the forewing, veins C, Sc+R, Rs, and 2r-rs are well marked; the stigma is distinct and dark. Discernible venation in the hindwing includes the veins Sc+R, M,+Cu, and 1rs-m.

Metasoma: anterior margin of petiole straight in profile. Subpetiolar process with subparallel margins, anteroventral angle obtuse; posteroventral angle right-angled, rendering process lobed. Posterior margin of subpetiolar process concave.

Sculpturing and setae: mandible, clypeus, and legs lacking any noticeable sculpturing (see

comments for details on cephalic sculpturing). Shallow sculpturing associated with setae insertions on mesosoma and metasoma more conspicuous on dorsal surface, suggesting smooth integument. In lateral view, postero-inferior portion of propodeum shallowly striate. Body with three kinds of pilosity: pubescence, short setae, and long setae, more conspicuous in the dorsal surface, and erect, or subdecumbent. Mandible with long, flexible, curved setae. Anterior clypeal margin with 12 distinguishable acute setae ("tooth-like stout setae" of Ladino and Feitosa, 2020; "dentiform clypeal setae" of Keller, 2011), exposed and directed laterally. Clypeal disc with well-differentiated setae arranged as pairs on anterior portion, two medially and one posteriorly, near junction of frontal lobes. Antenna and legs pubescent. In profile, subpetiolar process with at least two curved flexible setae directed posteriorly.

Etymology: The name refers to its morphological similarity to other extant Neotropical species, none of which are recorded in the Dominican Republic; also, to the difficulties encountered when describing its cephalic sculpturing. Feminine adjective from the Latin *ambiguus*, meaning "doubtful, open to various interpretations."

Type material: Holotype. MNHNSD FOS 18.117 queen, deposited in the Museo Nacional de Historia Natural "Prof. Eugenio de Jesús Marcano," Santo Domingo, Dominican Republic (figs. 4, 5). Preserved within a 25 mm by 20 mm section of transparent yellow amber with internal cracks and bubbles along the body of the inclusion. Synclusions include three possible male *Prionopelta*, a dung midge (Scatopsidae), a springtail (Collembola), and a micro Hymenoptera (Mymaridae).

Horizon and locality: Early Miocene, Burdigalian (ca. 16 Ma; Iturralde-Vinent and MacPhee, 1996); in amber from the Northern mines of the Santiago Province, Dominican Republic.

Comments: *Prionopelta* was not included among the species-level studies of ants of Dominican amber by Wilson (1985a, 1985b, 1985c, 1985d). However, he later provided a synopsis of the West Indian ants that included a brief account of fossil specimens, with mentions of the genus (Wilson, 1988). Wilson cited *Prionopelta* as a genus displaying traits indicative of accidental events that allow a taxon to colonize islands (a "sweepstake" origin), noting it is a dominant element of South and Central America, which extended into the Antilles. Later, in his table 9-2, the author established categories based on the presence of ant genera in amber and their geographical retreat since that period. There, *Prionopelta* was listed as "*Now extinct in the Greater Antilles*, *but present elsewhere in the Neotropical region.*" The final reference to the genus in this publication highlights an idea derived from the study of fossil and modern ant species found in Hispaniola. Wilson investigated biological traits of living species within the same genus to identify which might have led to the extinction or survival of its members on the island and conducted analysis using G-tests of independence. Unlike the weak evidence found for *Dolichoderus* and *Paraponera*, a statistically significant relationship was identified between extinction and specialization in prey choice or nesting site for *Cylindromyrmex*, *Neivamyrmex*, *Octostruma*, and *Prionopelta*. Therefore, *Prionopelta* is pointed among the specialized ant genera that either went extinct on Hispaniola or have eluded discovery in contemporary ecosystems. Later studies have supported the interpretation of local extinction of the genus in the Greater Antilles, suggesting an introduction of *P. antillana* or its northward spread from South America to the Lesser Antilles (e.g., Jaffe and Lattke, 1994; Brown, 1960; Ladino and Feitosa, 2020). However, verifying which factors influence generic survival requires additional work to distinguish correlation from causation. Currently, literature supporting the presence of *Prionopelta* in the Greater Antilles is limited to the record of *P. antillana* in Cuba originally published by Fontenla (1997), and subsequently cited by Fontenla and Alfonso-Simonetti (2018) and Ferrer and Cobas (2022); the inclusions studied by Wilson; and this formal description of *Prionopelta ambigua.*

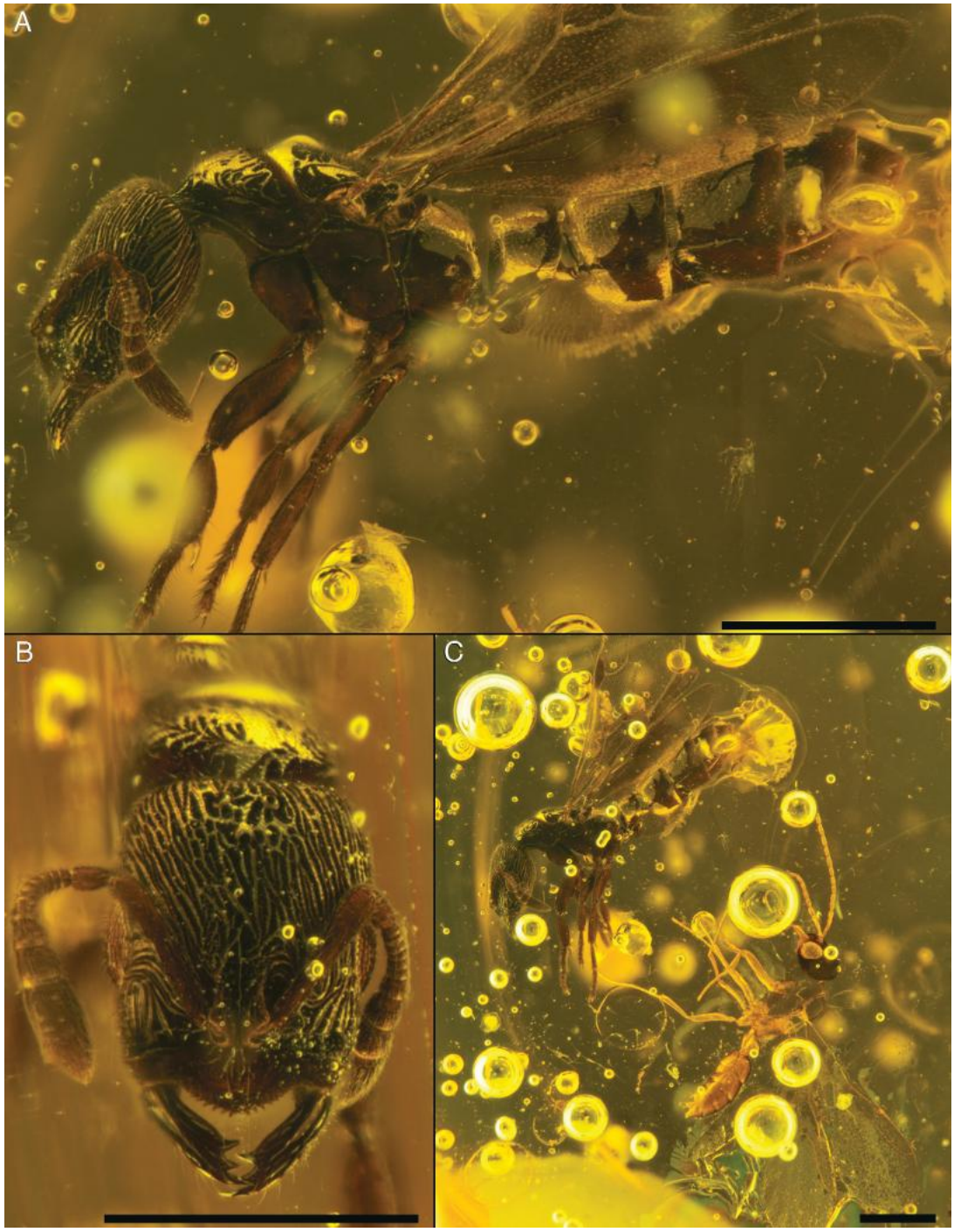


FIGURE 4. Photomicrographs of *Prionopelta ambigua*, sp. nov. (holotype queen, MNHNSD FOS 18.117). **A.** Body in lateral view. **B.** Head in full-face view. **C.** Lateral view of queen holotype and putative conspecific male specimen. Scale bars = 0.5 mm.

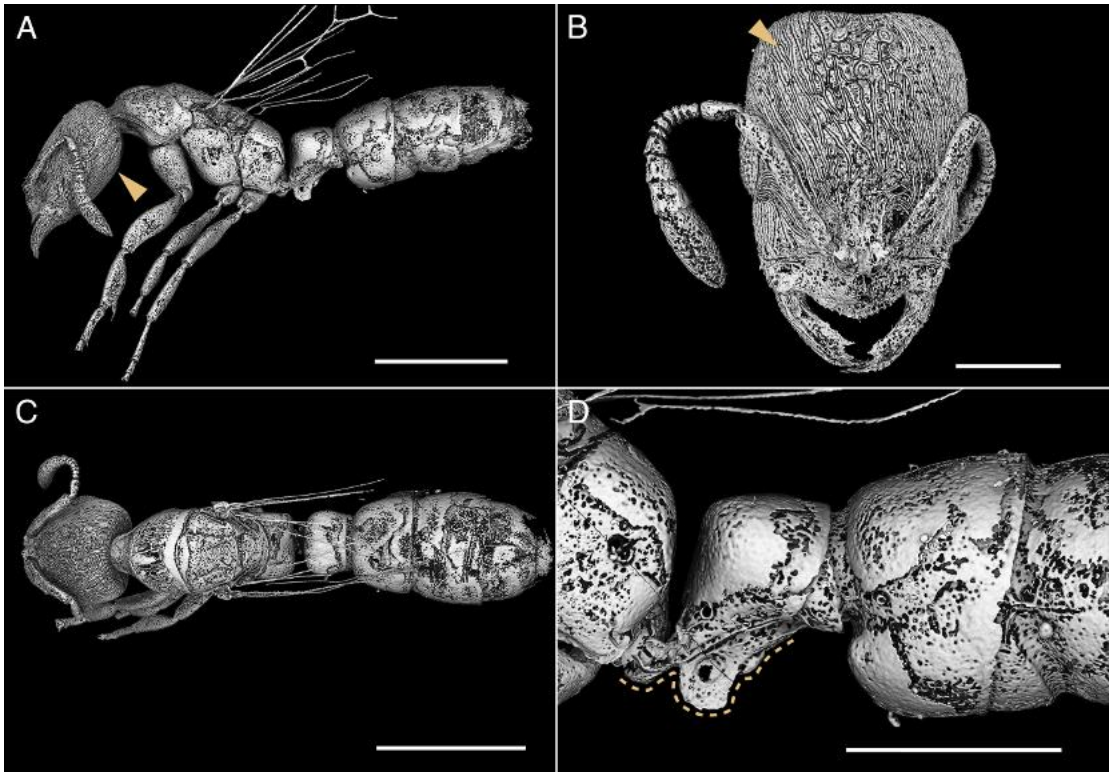


FIGURE 5. Volume renderings of *P. ambigua*, sp. nov. **A.** Body in lateral view, arrow indicates head sculpturing. **B.** Head in full-face view. Arrow indicates head sculpturing. **C.** Body in dorsal view, **D.** Detail of subpetiolar process. The dashed line outlines the shape of the subpetiolar process. Scale bars: A, B, D = 0.5 mm; C = 0.2 mm.

The holotype shares morphological features of the extant Neotropical fauna (fig. 4), exhibiting the expected queen modifications described in Ladino and Feitosa (2020). *Prionopelta ambigua* has 12 antennomeres, which in the Neotropics, leads to five species: *Prionopelta amabilis* Borgmeier, 1949, *Prionopelta antillana* Forel, 1909, *Prionopelta dubia* Ladino and Feitosa, 2020, *Prionopelta minuta* Ladino and Feitosa, 2020 and *Prionopelta modesta* Forel, 1909. It is easily distinguished from *P. minuta* and *P. modesta*, but *P. ambigua* exhibits a combination of traits found in the *P. amabilis*, *P. antillana* and *P. dubia* complex, particularly the former two. Accurate interpretation of the cephalic sculpturing is perhaps the most challenging aspect of this fossil. The integument could be described as mainly costate, conspicuous at the dorso-lateral and ventral surface, oriented diagonally, asymmetrical, with frons presenting a confused-rugulose sculpturing near ocelli; both are novel features in the genus. This seems to be supported by structural differences between the empty space and the cuticle recovered from volume renderings (fig. 5). However, these differences could be an artifact of the fossilization process. Similar patterns are present on the anterolateral portion of the pronotum, contrasting with the punctulate sculpture of the same sclerite, and on the entire dorsal surface of the mesosoma and metasoma, which is more consistent with the morphology of extant species (fig. 4). Some factors influenced this description, aiming to improve nomenclatural stability: (i) the representation of the genus in the Greater Antilles (ii) *P. ambigua* does not fully conform to the diagnostic characteristics of other species within the taxo-

nomic complex in the Neotropics, and (iii) further information regarding queen morphology and additional specimens from Dominican amber is needed to assess affinities with extant species.

Subfamily Dolichoderinae Forel, 1878

The Dolichoderinae are well represented in the fossil record with 22 genera and 142 valid species (Bolton, 2026). Several of these genera may correspond to stem group dolichoderines (e.g., *Eotapinoma* Dlussky), given the more than 30 million years between the divergence of Aneuretinae and crown group dolichoderines (Ward et al., 2010). The oldest Dolichoderinae genera are *Chronomyrmex* McKellar et al., and *Eotapinoma* Dlussky, both from the Late Cretaceous, 78–79 Ma (Campanian Grassy Lake amber of southern Alberta, Canada; McKellar et al., 2013), while *Schismiscapus* Varela-Hernández, Riquelme and Guerrero, known from the Miocene (Chiapas amber) would be the youngest extinct genus described (Varela-Hernández et al., 2022). Most of these genera are described from inclusions in amber of different ages, ranging from 24 to 79 million years, although some lineages are also known from fossil impressions, mainly found in the Eocene deposits (e.g., *Emplastus* Donisthorpe; *Protazteca* Carpenter).

Some extant dolichoderine genera are first recorded in Middle Eocene deposits (Wilson, 1985e; Dlussky and Rasnitsyn, 2002), but the diversity of this subfamily increases considerably from the Late Eocene (Radchenko, 2023). Shifts in Dolichoderinae diversity in the Neotropics are still unknown due to the lack of fossil deposits before the late Oligocene. Most of the known Neotropical fossil ant fauna is more recent, between Chiapas, Dominican, and Peruvian amber. Amber deposits from Chiapas have increased the known diversity of extinct dolichoderine ants with the notable discovery of genera with no previous fossil record (e.g., *Forelius chenpauch* Varela-Hernández et al., 2023), as well as extinct genera (*Schismiscapus* Varela-Hernández et al., 2022). Likewise, amber deposits in Peru (amber from the Pebas Formation, late Middle Miocene, ~12 Ma) expose the first extinct species in the genus *Tapinoma* for South America (Perrichot et al., 2019). Neotropical dolichoderine fossils illustrate disjunct distribution patterns, as is the case of *Leptomyrmex* Mayr (Boudinot et al., 2016), and most interestingly, cases of extinct genera such as *Schismiscapus* or *Chimerodous* gen. nov.

†***Chimerodous*** Guerrero, Barden, and Fiorentino, gen. nov.

Figures 6–8

ZooBank LSID: urn:lsid:zoobank.org:act:00B25635-681D-4C39-880A-06A4993E25B0

Type species: †*Chimerodous alpha*, sp. nov.

Diagnosis (worker): Mandible combining teeth and denticles along its masticatory margin as follows, apical tooth conspicuous, four teeth decreasing in size from the subapical tooth toward the basal margin, spaces between these teeth (=diastema) filled with very fine sawlike denticles; basal margin apparently smooth, without denticles of any kind, along entire surface, barely differentiated from the masticatory margin by its last denticles (figs 6, 7), hypostomal bridge forming a conspicuous U-shaped notch (fig 8B); in dorsal view, central region of clypeus raised; anterior margin of clypeus, strongly convex, with the anteromedial margin projecting in front of the anterolateral margins; compound eye long, placed slightly dorsad from lateral margin, ocular middistance just anterad of midlength of lateral cephalic margin; scape long, extending beyond the posterior cephalic margin at about ⅓ of its length; dorsal face of the propodeum is almost half the length of the declivitous face; propodeal spiracle with a protruding rim, situated in the middle length of the margin that meets the lateral face with the declivitous; scale petiolar completely absent; first gastral segment projecting anteriorly and concealing petiole in dorsal view.

Etymology: *Chimerodous* is a name derived from the combination of two words of Greek origin, Chimera (= χίμαιρα) referring to the combi-

nation of morphological features that are present in other previously described genera of dolichoderine ants but are exhibited together in this new genus; -odous (= οδούς) referring specifically to the remarkable combination of teeth and denticles on the masticatory margin of the mandible.

†***Chimerodous alpha*** Guerrero, Barden, and Fiorentino, sp. nov.

ZooBankLSID: urn:lsid:zoobank.org:act:EFC4D266-5CC8-413A-AEC3-1FA6527A2429

Type material: Holotype. AMNH DR 10-165 worker, deposited in the American Museum of Natural History.

Diagnosis (worker): See diagnosis for the genus.

Holotype worker measurements (in mm): HW 0.50, HL 0.68, EL 0.14, EHD 0.07, EHV 0.23, ELA 0.25, ELP 0.30, MLP 0.23, SL 0.62, WL 0.65, PcL 0.23, MH 0.24, PrW 0.32, MfL 0.64.

DESCRIPTION (worker). Head: ovoid, with convex lateral margins, more convex toward the middle length of the eyes, straight and slightly divergent anteriorly; margins posterior to eyes curving strongly toward rounded posterolateral corners and continuing into posterior cephalic margin, the latter with a smooth and narrow mesal concavity. Mandible subtriangular, divergent apically, very narrow toward the base; external margin strongly curved toward the apex, but straight from the middle posterior ⅔; masticatory margin straight, armed with teeth and denticles as defined for the genus; mandibular basal margin as the diagnosis of the genus. Palp formula 6:4, first maxillary palp small, half the length of second maxillary palp, 2nd–5th maxillary palps 3× longer than wide, 6th maxillary palp 2× longer than the length of any of the four preceding palps. Clypeus 2× wider than high, strongly convex anteriorly; anteromedial margin lacking medial notch, concavity or depression of any kind; dorsum of clypeus bulging toward the median region; posterior margin straight, truncate, barely extending past the base of the antennal insertions. In ventral view, hypostomal bridge forming a conspicuous U-shaped notch (fig 8B). Anterior tentorial pit nearer the antennal socket than mandibular insertion. Frontal lobes weakly developed, no completely covering antennal condyle ; frontal carinae straight and parallel to each other, extending little beyond the anterior surface of the antennal sockets cavities Antenna 12-segmented; antennal scape long (SI ~92), notably extending beyond posterior cephalic margin (see diagnosis of genus); antennal scapes slightly curved basally outward, with margins parallel from base to apex; pedicel and remaining flagellomeres rectangular, almost 2× longer than wide (fig. 7). Compound eye oval, slightly longer than wide, located almost equidistant anteroposteriorly.

Mesosoma: in lateral view, promesonotum convex anteriorly; mesonotum straight falling into a slope forming a short posterior face that continues into the dorsal face of the straight propodeum, the latter below the promesonotum; the posterior most part of propodeum presenting a rounded posterodorsal elevation curved slightly anteriorly; declivitous face of propodeum beginning at the apex of the elevation, approximately 1.8× longer than the dorsal face of propodeum; notopropodeal sulcus reduced to a suture at midventral level, but absent toward the dorsal face, forming an uninterrupted surface between the mesonotum and the propodeum. In dorsal view, promesonotal groove impressed, extending laterally, separating the two sclerites; pronotum rounded anteriorly; mesonotum pear-shaped, almost 2× longer than wide, converging posteriorly, anterior face rounded, while posterior one straight. Propodeal spiracle circular, with a rim rising from the body surface.

Metasoma: petiolar scale is completely absent, with the posterior surface extended along the length, sloping slightly downward to form an angle with the ventral surface, with no anterior surface. Gaster with four visible tergites, with the profile strongly convex anteriorly and straight posteriorly; ventral profile convex throughout.; first tergite projecting anteriorly and concealing the petiole in dorsal view and with indentation for the reception of the petiole.

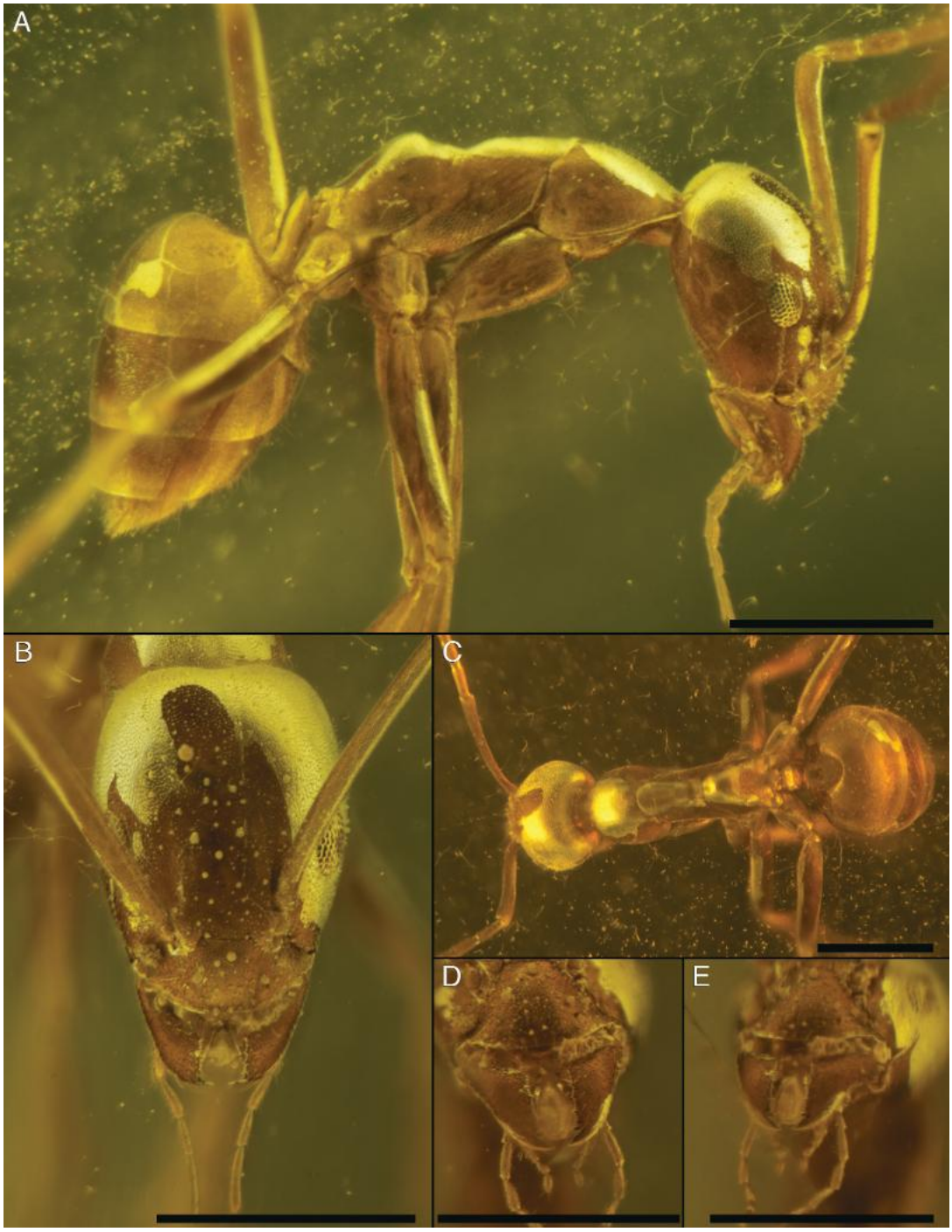


FIGURE 6. Photomicrographs of *Chimerodous alpha*, gen. nov. and sp. nov. (holotype worker, AMNH DR 10-165). **A.** Lateral view of body. **B.** Head in full-face view. **C.** Dorsal view of head, mesosoma, and metasoma. **D, E.** Alternate frontal and ventrolateral views of mandibles, clypeus, and palps. Scale bars = 0.5 mm.

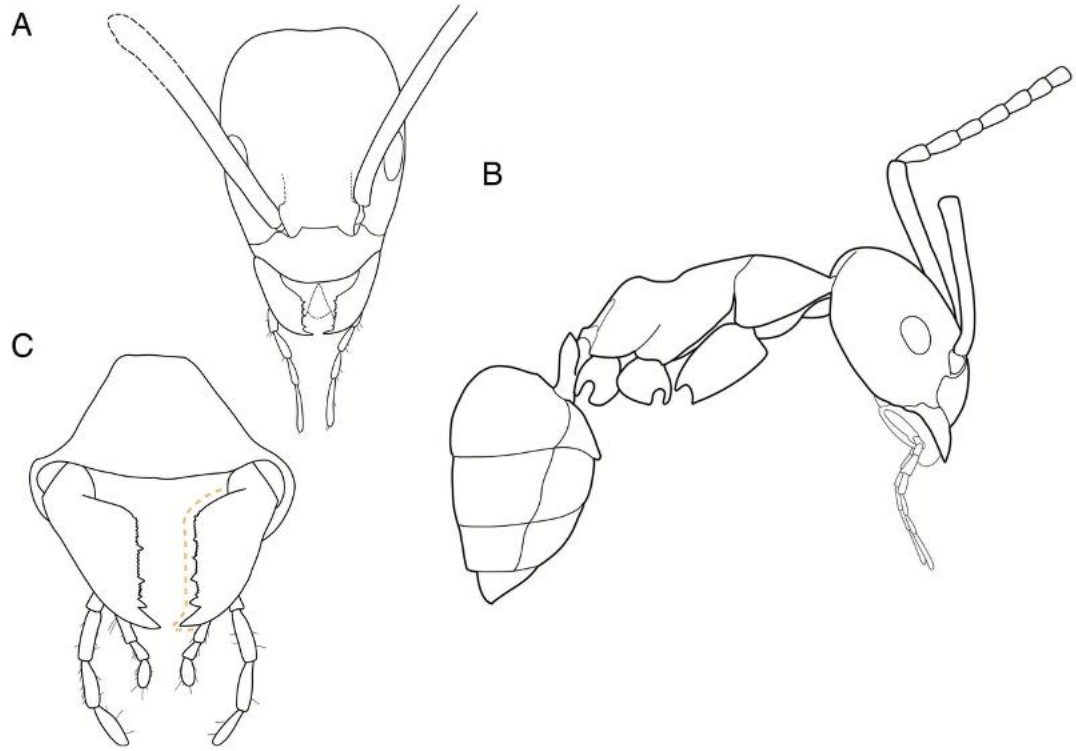


FIGURE 7. Line drawings of *Chimerodous alpha* worker. **A.** Head in full-face view. **B.** Lateral view of the body. **C.** Detail of the mouthparts, highlighting the masticatory margin with the pattern of teeth and denticles (thick black line); the clypeal plate is shown above the mandibles, while maxillary and labial palps are behind them.

Sculpturing and setae: body surface glabrous. Head and dorsum of pronotum punctulate over entire surface (fig. 6). In lateral view, mesosoma with imbricated sculpturing on the surface, very visible on the mesonotal katepisternum and metapleural region; gaster completely imbricated on its surface. Dorsal surface of mandible with scattered long hairs. Dorsum of clypeal plate with two long, forward-directed hairs well above anterolateral margin of clypeus. Head, scape, and dorsum of pronotum with very short, decumbent pilosity. 1st–3rd gastral tergites apparently glabrous, 4th gastral tergite with short pilosity; gastral sternites with long, erect hairs. Legs unsculptured and glabrous.

Etymology: The specific epithet "alpha" is a Greek word that refers to something that is first, so it is used here to mean that this is the first species described in the genus *Chimerodous*.

Type material: Holotype. AMNH DR 10-165 worker, deposited in the American Museum of Natural History. (figs. 6–8). Preserved within a 28 mm by 10 mm section of transparent yellow amber with few internal cracks and bubbles. Synclusions include fragments of an unidentifiable dipteran.

Horizon and locality: Early Miocene, Burdigalian (ca. 16 Ma; Iturralde-Vinent and MacPhee, 1996); in amber from the Northern mines of the Santiago Province, Dominican Republic.

Comments: *Chimerodous*, gen. nov., is proposed based on the combination of several traits that may be independently shared with several genera of extant or extinct dolichoderine ants. In this sense, the definition of *Chimerodous* as proposed here, suggests that this genus apparently presents a series of homoplastic traits, which make it difficult to infer a possible phylogenetic

placement of this taxon within the subfamily Dolichoderinae. Although the above is true for most traits (i.e., several homoplastic traits), a feature of the propodeal spiracle is a possible apomorphy. The spiracle has a protruding rim and is situated in the middle length of the margin between the lateral and declivitous faces of the propodeum. This character has not been recorded in any of the other known dolichoderine genera (see Shattuck, 1992b).

Chimerodous could be closely related to *Tapinoma* and *Technomyrmex*, considering the absence of the petiole scale. But other features separate this taxon from those genera: the masticatory margin of the mandible is more like *Linepithema*, the basal margin of the mandible is differentiated and smooth in *Chimerodous* and not undifferentiated and denticulate as in *Tapinoma* and *Technomyrmex*, and the anteromedial clypeal margin is completely entire in *Chimerodous* instead of notched or shallowly concave in *Tapinoma* and *Technomyrmex*. The absence of a petiolar scale could be convergent, as previously reported within the Tapinomini (Ward et al., 2010). Detailed comparisons with the genus *Bothriomyrmex* Emery (another genus with Neotropical distribution) are not made, but the palpal formula allows separating them from each other.

On the other hand, *Chimerodous* resembles ants of the genus *Linepithema* by the pattern of teeth and denticles on the masticatory margin of the mandible. This pattern is very similar (mandible with dentition consisting of an elongate apical tooth and a smaller subapical tooth followed by a series of 3–4 small teeth alternating with denticles sensu Wild (2007), but the small teeth of *Linepithema* are similar in size, whereas in *Chimerodous* the four small teeth, posterad the subapical tooth, decreasing in size toward the basal margin. Despite the similarity in teeth and denticles on the masticatory margin of the mandible between both genera, notable differences in the shape of the clypeus (anteromedial clypeal margin with a broad, shallow concavity on *Linepithema* instead of an anteromedial clypeal margin entire on *Chimerodous*) and petiole (petiolar scale present on *Linepithema* while there is no petiolar scale in *Chimerodous*) do not support the relationship of this new taxon within *Linepithema*. *Chimerodous* and *Gracilidris* could be closely related based on the similarity in head shape, the anterior margin of the clypeus projecting forward in a strong convexity, the length of the scape exceeding the posterior cephalic vertex, and the relative position of the eyes in the head capsule. However, the absence of a petiolar scale in the first genus contrasts strongly with the tall dorsal scale with apex narrowed and distinctly curved posterad present in *Gracilidris* (Wild and Cuezzo, 2006). Other Neotropical genera of the Tribe Leptomyrmecini Emery are not compared here, but in any case, the petiolar scale is conspicuous in variable development and the pattern of dentition on the masticatory margin of the mandible is contrasting. Despite the notable morphological differences of *Chimerodous* with other Neotropical Leptomyrmecini genera, this ant presents a U-shaped notch in the hypostomal bridge as in the genera *Leptomyrmex* and *Schismischapus*, offering insights into its possible phylogenetic affinity with these genera within the tribe.

Although of uncertain position within the subfamily Dolichoderinae, *Chimerodous* can be separated from other dolichoderine genera by considering together the dentition of the masticatory margin, U-shaped notch in the hypostomal bridge, and the distinctive configuration of the petiole scale, traits that are distributed separately across dolichoderine lineages. It is necessary to explore more pieces of Dominican amber that allow identifying more specimens and gather more information on the stability of these traits and their taxonomic and phylogenetic utility. Likewise, it is necessary to expand the explorations and comparisons with the dolichoderine ant fauna of Chiapas (Mexico) and Peruvian amber to evaluate a possible wider distribution of *Chimerodous*.

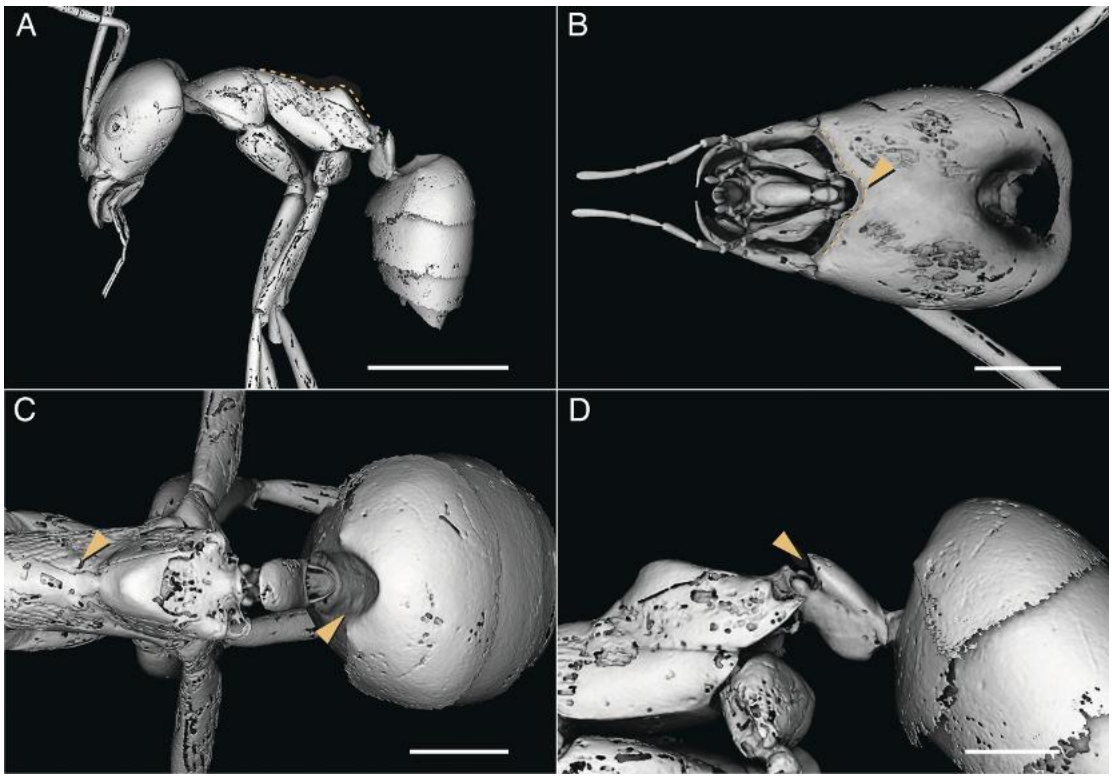


FIGURE 8. Volume renderings of *Chimerodous alpha*, sp. nov. **A.** Body in lateral view. **B.** Head in ventral view showing the hypostomal bridge forming a U-shaped notch, indicated with the dashed line. **C.** Posterior half of body in dorsal view. Arrow indicates dorsally projecting metathoracic spiracle and deep groove in first gastral tergite. **D.** Propodeum and petiole in profile view. Arrow indicates reduced petiolar scale. Scale bars: A = 0.5 mm; B–D = 0.2 mm.

Schismiscapus Varela-Hernández et al., 2022

Figures 9–11

Diagnosis (worker): The diagnosis of the genus *Schismiscapus* is modified to include some fossil Dolichoderinae species that match the diagnostic traits proposed by Varela-Hernández et al. (2023): hypostomal bridge forming a U-shaped notch without any denticle; base of scape strongly flattened; mesosoma long, narrow and sinuous; metanotal spiracles protruding, tubuliform, directed backward; strong constriction, like a waist, at center of mesonotum; mesonotal sternum with anterolateral depression of variable depth; mesonotum and propodeum separated by a wide and deep depression; propodeum with distinct anterior, dorsal and declivitous faces; trochanter of foreleg large, as long as maximum length of compound eye; legs long and slender; compound eyes positioned anteriorly on head; conspicuous petiolar peduncle extending well behind the petiole scale in a long tube that joins with the gaster.

Taxonomic changes:

†*Schismiscapus caritatis* (Brandão and Baroni Urbani, 1999), comb. nov.

†*Technomyrmex caritatis* Brandão and Baroni Urbani, 1999: 416, figs. 1, 4–6 (w) Dominican Republic (Dominican Amber, Miocene).

Type material: Holotype. AMNH DR 10-187 worker, deposited in the American Museum of Natural History. (fig. 9). Preserved within a

round 12 mm by 9 mm section of darkened red amber. Synclusions include three other *S. caritatis* workers.

Horizon and locality: Early Miocene, Burdigalian (ca. 16 Ma; Iturralde-Vinent and MacPhee, 1996); in amber from the Northern mines of the Santiago Province, Dominican Republic.

Examined material: Dominican amber; Dominican Republic, Santiago Province, Northern mines. Miocene—16 Ma. MNHNSD FOS 18.119.

Holotype worker measurements (in mm): HW 0.40, HL 0.55, EL 0.12, EHD 0.24, EHV 0.15, ELA 0.32, ELP 0.23, MLP 0.20, SL 0.27, WL 0.71, PcL 0.23, MH 0.22, PrW 0.29, MfL 0.28, PrL 0.21, T1L 0.22

Schismiscapus hispaniolae (Wilson, 1985c) comb. nov.

†*Iridomyrmex hispaniolae* Wilson, 1985c: 32, fig. 10 (w.) Dominican Republic (Dominican Amber, Miocene).

†*Technomyrmex hispaniolae* (Wilson, 1985c). Combination in *Linepithema*: Shattuck, 1992a: 16.

†*Technomyrmex hispaniolae* (Wilson, 1985c). Combination in *Technomyrmex*: Brandão et al., 1999: 414.

Holotype worker measurements (in mm): HW 0.88, HL 0.90, EL 0.21, EHT 0.56, EHD 0.10, EHV 0.46, ELT 0.93, ELA 0.43, ELP 0.50, MLP 0.45, SL 1.11, WL 1.27, PcL 0.49, MH 0.42, PrW 0.50, MfL 1.25.

Type material: Holotype. AMNH DR 10-240 worker, deposited in the American Museum of Natural History (figs. 10, 11). Preserved within a 13 mm by 6 mm section of darkened red amber. No synclusions.

Horizon and locality: Early Miocene, Burdigalian (ca. 16 Ma; Iturralde-Vinent and MacPhee, 1996); in amber from the Northern mines of the Santiago Province, Dominican Republic.

Additional examined material: Dominican amber; Dominican Republic, Santiago Province, northern mines. Miocene: 16 Ma. MNHNSD FOS 18.118, MNHNSD FOS 18.119.

Comments: The type specimens of *Technomyrmex hispaniolae* and *Technomyrmex caritatis*, as well as several workers of these two species from other Dominican amber deposits, do not present the fifth gastral tergite dorsally, thus do not match the diagnosis of the genus *Technomyrmex* Mayr (Shattuck, 1992a; Bolton, 2007). The presence of only four gastral tergites in dorsal view in the workers of both species provides justification for excluding these two species from the genus *Technomyrmex*. The morphologies of both species, however, do not fall within those of known modern extant genera but do fall within those of the extinct genus *Schismiscapus* Varela-Hernández et al. 2022. On this basis, we propose new taxonomic combinations *Schismiscapus hispaniolae*, comb. nov., and *Schismiscapus caritatis* (Brandão and Baroni, 1999), comb. nov.

Varela-Hernández et al. (2022) proposed the genus *Schismiscapus* based on a combination of eight morphological traits. Some of these traits are retained here, but others are excluded or modified, since two species of Dominican amber ants, previously described in the genus *Technomyrmex*, match many of the diagnostic traits of *Schismiscapus*. The specimens studied here present features that are treated as putative synapomorphies, such as a strongly flattened base of antennal scape, but in no case notched as in *S. exstinctus*, medial hypostomal bridge with a U-shaped notch, strong constriction at center of mesonotum, mesonotal sternum with anterolateral depression, and posteriorly projecting petiolar peduncle. Among these features, the U-shaped hypostomal bridge is a plesiomorphic trait, shared with ants of the genus *Leptomyrmex* Mayr, 1862, supporting a close phylogenetic relationship between both genera (Varela-Hernández et al., 2022). If *Schismiscapus* and *Leptomyrmex* are sister taxa, then other traits such as the elongated scapes exceeding the posterior cephalic margin by more than half their length, as well as the elongated and slender mesosoma, should be considered as shared characteristics from a common ancestor that lived in the Neotropical region more than 46 my ago (Boudinot et al., 2016).

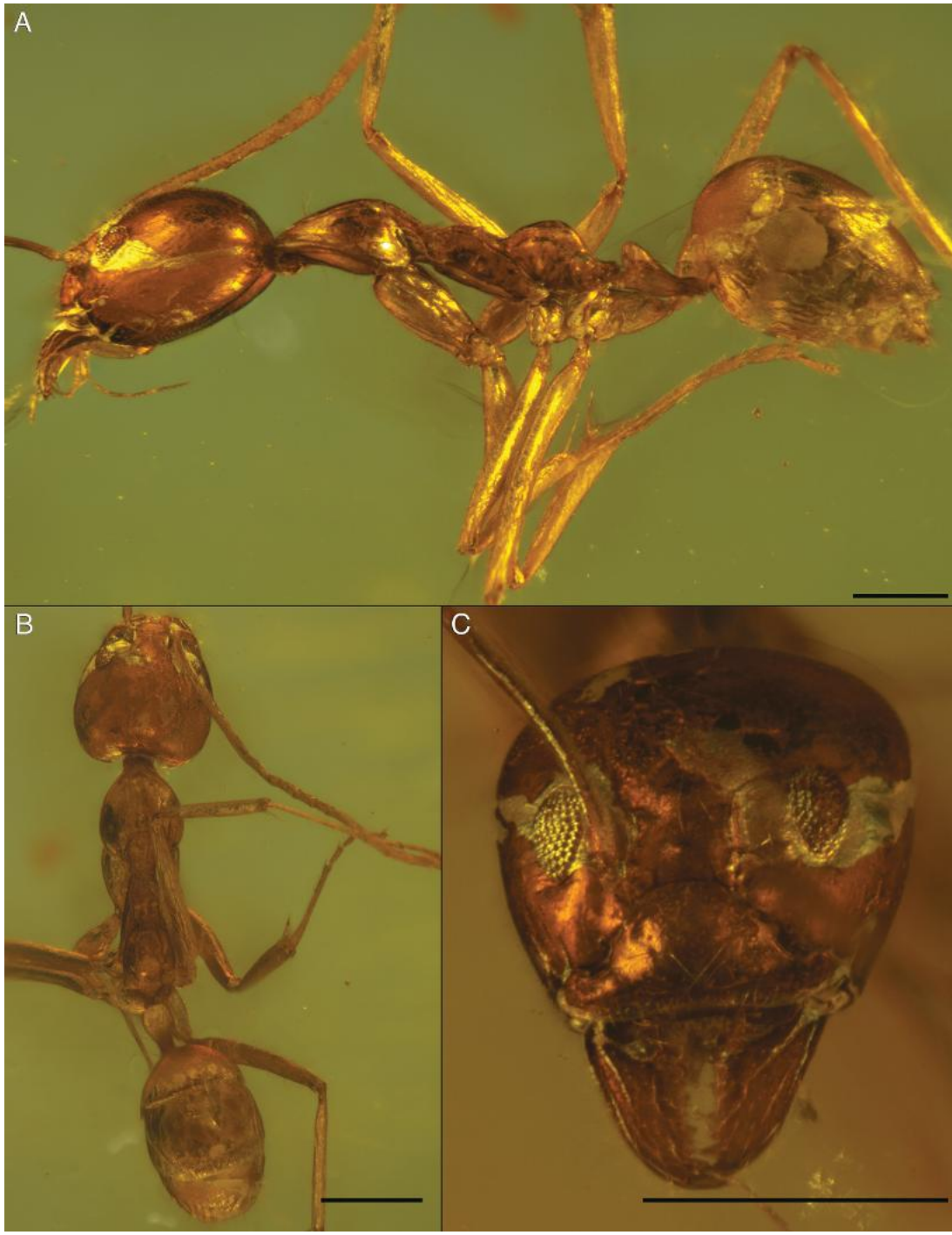


FIGURE 9. Photomicrographs of *Schismiscapus caritatis*, comb. nov. (Brandão and Baroni Urbani, 1999; worker specimen MNHNSD FOS 18.119). **A.** Lateral view of body **B.** Dorsal view of specimen. **C.** Frontal view of head. Scale bars = 0.5 mm.

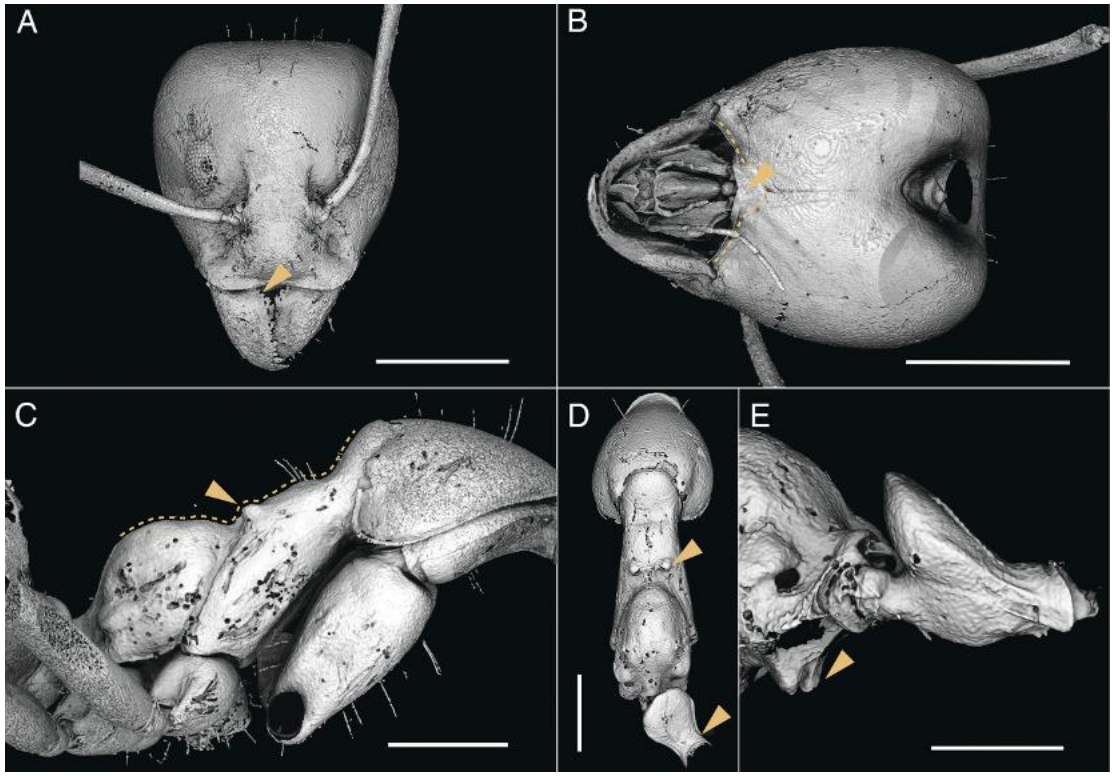


FIGURE 10. Volume renderings of *Schismiscapus hispaniolae*, sp. nov. **A.** Head in dorsal view; arrow indicates the serrated masticatory margin. **B.** Head in ventral view; dashed line indicates the U-shaped hypostomal bridge. Arrow points to the anterior lamella filling that bridge. **C.** Lateral view of the mesosoma; the dashed line shows the sinuous profile of the mesosoma and arrow indicates the protruding metanotal spiracle. **D.** Mesosoma in dorsal view; arrows indicate projected metathoracic spiracles and posterior petiolar peduncle. **E.** Profile of the propodeum and petiolar scale. Scale bars: A, B = 0.5 mm; C, D = 0.25 mm.

The genus *Schismiscapus*, as defined here, shares some putatively homoplastic traits with Neotropical genera of other dolichoderine tribes (Ward et al., 2010). The tuberculiform metanotal spiracles, projecting posteriorly, are also found in the two Neotropical *Technomyrmex* species (Fernández and Guerrero, 2008) and some *Dolichoderus* of the *attelaboides* group (Mackay, 1993). A mesonotum and propodeum separated by a wide and deep depression, as well as propodeum with distinct anterior, dorsal and declivitous faces are traits also found in some species of *Linepithema* Mayr, 1866 such as *L. angulatum* (Emery, 1894) or *L. dispertitum* (Forel, 1885) (see Wild, 2007). Long and slender legs are typical of ants with running habits, such as *Dorymyrmex* Mayr, 1866 (Cuezzo and Guerrero, 2012), some *Iridomyrmex* Mayr, 1862 (e.g., *I. agilis* Forel, 1907), and macro-*Leptomyrmex* ants (Lucky and Ward, 2010), including †*Leptomyrmex neotropicus*. Despite these shared traits, ants of the genus *Schismiscapus* can be unambiguously differentiated from other dolichoderine tribes by the configuration of the petiolar peduncle.

Some morphological differences are notable among the three species of the genus *Schismiscapus*. The base of the scape is flattened in all three species, but the notch at the base is only

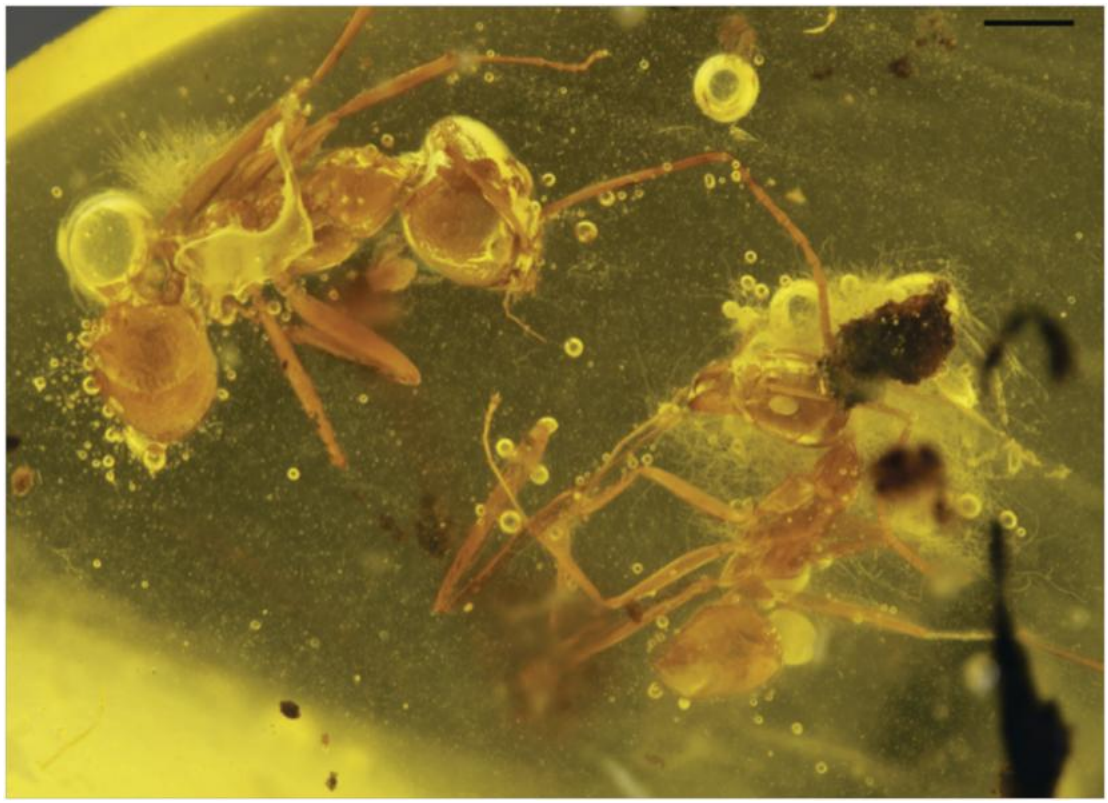


FIGURE 11. Polymorphism in *Schismicapus hispaniolae* workers (paratype workers MNHNSD FOS 18.118). Note the differences in width and head shape between the two workers. Major worker (left) and minor worker (right) are in different positions relative to each other. Scale bar = 0.5 mm.

present in *Schismiscapus exstinctus*. The shape of the propodeum is also similar among the species, with three well-differentiated faces, but in none of the Dominican amber species does the dorsal face present a shallow mesal depression like that in *S. exstinctus*. The length of the petiolar peduncle is variable, with the posterior extension much longer in *S. exstinctus*, while in *S. caritatis* and *S. hispaniolae* this extension is as long as the height of the petiolar scale. The ants of *Schismiscapus exstinctus* and *S. caritatis* have a thin and slender mesosoma, with the mesonotal dorsum longitudinally carinate (fig. 10), whereas in *S. hispaniolae* the mesosoma is thick and compact, without any carinulae on the dorsum. The anterolateral depression of the mesonotal sternites is strongly impressed in *S. exstinctus* and *S. caritatis*, forming a concavity that is deeper and wider in the first species, while in *S. hispaniolae*, this notch is barely impressed. Interestingly, *S. hispaniolae* also exhibits apparent polymorphism (fig. 11, MNHNSD FOS 18.118): robust major workers exhibit broad, heart-shaped heads, apparently wider than long, while slender minor workers possess heads that are longer than wide.

Ectatomminae Emery, 1895

The fossil record of Ectatomminae is moderately well represented and spans from the Late Cretaceous to the Miocene, encompassing a range of compression and amber-preserved specimens. The oldest putative representative is

†*Canapone* Dlussky, recovered from Canadian amber and dated to approximately 79 Ma (Late Cretaceous) (Grimaldi et al., 1997; Moreau et al., 2006). However, its placement within *Ectatomminae* remains controversial (Dlussky, 1999). A more confidently placed fossil, †*Pseudoectatomma* Dlussky and Wedmann, was recovered from the Middle Eocene Messel Formation in Germany (ca. 47 Ma). Preserved as a compression fossil, it has been accepted as a definitive member of the subfamily (Dlussky and Wedmann, 2012; Mertz and Renne, 2005). Additional Eocene records include several amber inclusions from Baltic deposits, such as †*Electroponera* Wheeler and †*Gnamptogenys* Roger species (e.g., †*G. europaea*, †*G. rohdendorfi*), although the affinity of some of these taxa with *Ectatomminae* is disputed. Notably, †*Electroponera* has been considered unrelated to the subfamily (Wheeler, 1915; Moreau et al., 2006), and †*G. rohdendorfi*, described only from a male, is difficult to compare with extant taxa (Dlussky, 2009). Oligocene records include †*Ectatomma gracile* Emery, 1891, from Sicilian amber (ca. 33.9–28.1 Ma), although its generic assignment has been questioned (Moreau et al., 2006), with some authors treating it as incertae sedis (Bolton, 1994). The Miocene provides more robust records, primarily from Dominican amber, including multiple *Gnamptogenys* species (†*G. brunoi*, †*G. casca*, †*G. levinates*) and †*Ectatomma* sp. specimens morphologically close to *E. tuberculatum* (Lattke, 2002; Baroni Urbani, 1995; Moreau et al., 2006). These fossils represent a taxonomically and geographically diverse assemblage, albeit fragmentary and often affected by uncertainty regarding taxonomic placement. Importantly, molecular divergence-time analyses are congruent with this fossil evidence: a recent phylogenomic study by Borowiec et al. (2025) estimated the crown age of Ectatomminae at approximately 81 Ma (95% HPD: 64–96 Ma), placing the origin of the extant subfamily in the Late Cretaceous. Together, fossil and molecular data indicate that crown Ectatomminae lineages were already established by the Eocene, with probable stem-group representatives extending back into the Late Cretaceous.

Poneracantha Emery, 1897

†*Poneracantha minima* Camacho, Lattke, Barden, and Fiorentino, sp. nov.

Figures 12, 13

ZooBank LSID: urn:lsid:zoobank.org:act:53D59D35-0E98-42B2-A594-1EFB99669665

Diagnosis (queen): Small size (TL 3.72 mm). Propodeal spiracle directed posterodorsally, separated from the declivitous margin by a length longer than its width. Anterolateral lobe of petiole well developed, fitting into convexity of posterior margin of propodeum. Anterolateral margin of third abdominal tergite projecting laterally as low, but distinct crest.

Holotype queen measurements (in mm): HW 0.83, HL 0.91, EL 0.25, EHT 0.56, EHD 0.25, EHV 0.31, ELT 0.78, ELA 0.46, ELP 0.32, MLP 0.73, SL 0.78, WL 1.48, PcL 0.54, MH 0.62, PrW 0.77, MfL 0.93, PeH 0.34, PeL 0.36, GL 1.18, TL 3.72.

DESCRIPTION (queen). Head: in full-face view, head subquadrate, almost as long as wide; posterior head margin concave. Mandible subtriangular; masticatory margin serrate, without prominent preapical teeth; apical tooth robust, possibly crossing with opposing tooth when mandibles closed; external margin with a strong concavity proximally, giving mandible a curved shape; midpoint of mandible wider than the basal width. Anterior clypeal margin broadly concave; lateral corners of anterior clypeal lamella blunt. Frontal lobes not expanded, barely covering antennal insertions. Scapes seem to slightly surpass vertexal margin in frontal view; flagellomeres slightly but gradually larger and wider toward apex. Ocelli present. Color apparently dark reddish-brown.

Mesosoma: Promesonotal suture well marked. Profile of mesosomal dorsal margin



FIGURE 12. Photomicrographs of *Poneracantha minima*, sp. nov. (holotype queen, MNHNSD FOS 18.120). **A.** Lateral view of body. **B.** Head in full-face view. **C.** Dorsal view of head and mesosoma. Scale bars = 0.5 mm.

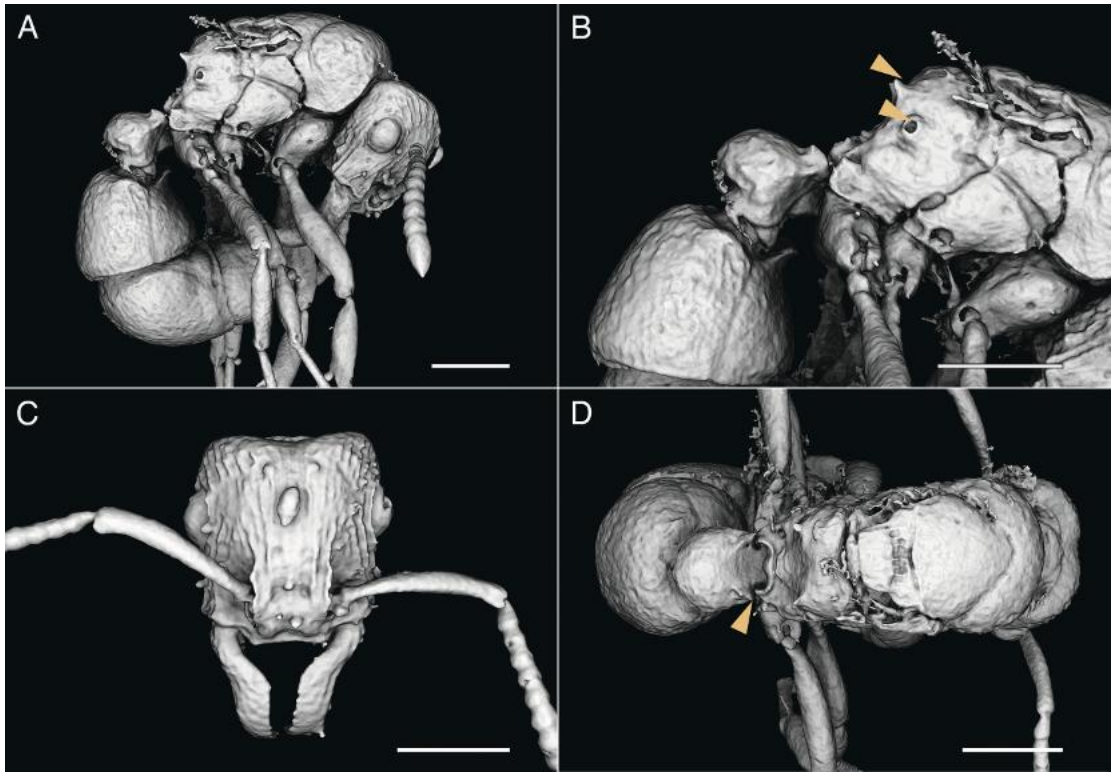


FIGURE 13. Volume renderings of *Poneracantha minima*, sp. nov (holotype queen, MNHNSD FOS 18.120). **A.** Body in lateral view. **B.** Close-up view of the propodeum and petiole in lateral view, arrow indicates the propodeal spine and spiracle. **C.** Head in full-face view. **D.** Dorsal view, arrow indicates the anterolateral toothlike projections of the petiolar node. Scale bars A–D = 0.5 mm.

slightly and uniformly convex. Vestiges of wings present; wing venation not visible. Notopropodeal sulcus well marked by wide costulae. Dorsal margin of propodeum convex and narrow. Petiolar spiracle round, opening directed posterodorsally; spiracle opening as wide as length of propodeal tooth, and separated from declivitous margin by length longer than its width. Propodeal tooth acute, with wide base, pointed posteriorly. Metacoxal tooth distinctive and acute, almost as long as propodeal tooth. Propodeal lobe extending posteriorly, forming convexity on posterior margin of propodeum.

Metasoma: Petiole not pedunculate. Anterior margin of petiolar node in lateral view, forming continuous convexity with dorsal margin, posterior margin straight. Node with anterolateral distinctive toothlike projection that seems to fit into convexity of posterior margin of propodeum. Subpetiolar process not distinguishable. In dorsal view, anterolateral margin of third abdominal tergite projecting laterally as low but distinct lobe. Prora large and visible laterally. fourth abdominal segment strongly curved.

Sculpturing and setae: Head, mesosoma, and metasoma with wide and coarse longitudinal costulae, with slightly irregular margins. Body predominantly covered by thin, long and medium, erect and suberect hairs. Scape longitudinally rugulose and covered by many decumbent hairs and some medium suberect hairs.

Etymology: The name refers to its small size compared to other extant Neotropical species,

including the other species recorded for the Dominican Republic. From the Latin *minimus* meaning "smallest."

Type material: Holotype. MNHNSD FOS 18.120 alate queen, deposited in the Museo Nacional de Historia Natural "Prof. Eugenio de Jesús Marcano," Santo Domingo, Dominican Republic (figs. 12, 13). Preserved within a 15 mm section of darkened yellow amber with internal cracks and bubbles around the inclusions. Synclusions include an alate Myrmicinae male and a small mite (Mesostigmata).

Horizon and locality: Early Miocene, Burdigalian (ca. 16 Ma; Iturralde-Vinent and MacPhee, 1996); in amber from the Northern mines of the Santiago Province, Dominican Republic.

Comments: This species is smaller than most of the extant species of the genus, comparable in size only to *Poneracantha brunoi*, another fossil described from Dominican amber by Lattke (2002). It can be easily distinguished from *P. brunoi* by the position of the petiolar spiracle (proximal to the declivity margin in *P. brunoi*) and the absence of a posterior platform on the petiolar node. In some *Poneracantha*, the anterolateral petiolar lobe is not as well developed, but we could not examine a broad sample of species. The bluntly angular lateral crest on the third abdominal tergite is not shared with any other congeneric.

Subfamily Formicinae Latreille, 1802

The fossil record of Formicinae is extensive and spans from the Late Cretaceous to the Pliocene, with occurrences across all continents and preservation in both amber and compression deposits (Bolton, 2026; Barden, 2017). The oldest definitive representative dates to approximately 92 Ma, recovered from Cretaceous deposits in North America. Subsequent records become more abundant in the Paleocene (Russia) and Eocene, where Baltic amber, along with deposits from Canada, China, England, and the United States, have yielded a remarkable diversity of species (LaPolla et al., 2013; Barden, 2017). Currently, 202 fossil Formicinae species are described (Bolton, 2026), including one tribe and 36 genera exclusively known from fossils. However, many of these may be dubious and are currently treated as incertae sedis in Formicinae (Ward et al., 2016, Bolton, 2026; Ward et al., 2025). Additional fossils are known from the Oligocene of Italy and Mexico, as well as Miocene deposits in Croatia and Germany, extending into the Pliocene with material from Willershausen, Germany (ca. 2 Ma). Formicines are most abundant across much of the European formations (LaPolla and Greenwalt, 2015; Barden, 2017), making up to 41% of the ant composition of Bol'shaya Svetlovodnaya, Russian Far East deposit (Khalaim, 2008; Dlussky et al., 2015) and as much as half of the ant records of the Messel Formation in Germany (Dlussky and Wedmann, 2012). Neotropical fossils are comparatively scarcer, with †*Elektroformica azquil* from Chiapas amber representing the only extinct genus described to date (Varela-Hernández and Riquelme, 2024). There are just three previously described species known from Dominican amber: *Acropyga glaesaria* (LaPolla, 2005), *Nylanderia vetula* (LaPolla and Dlussky, 2010), and *Zatania electra* (LaPolla et al., 2012). Those descriptions, as well as those provided herein, likely represent a substantial underestimate of historical formicine diversity.

Brachymyrmex Mayr, 1868

†***Brachymyrmex atrapada*** Fernandez, Sosa, Fiorentino, Barden, and Probst, sp. nov.

Figures 14, 15

ZooBank LSID: urn:lsid:zoobank.org:act:32237F82-9BC3-44AB-A9F1-48BF0DA5F151

Diagnosis (worker): Head slightly wider than long in full-face view, eyes positioned anteriorly on head, antennae with nine segments, dorsum of propodeum strongly convex and much shorter than propodeal slope; propodeal slope slightly convex, meeting dorsum of propodeum at approximately a 70° angle; absence of erect hairs on the mesosoma, deep notopropodeal sulcus, and gaster with scattered hairs.

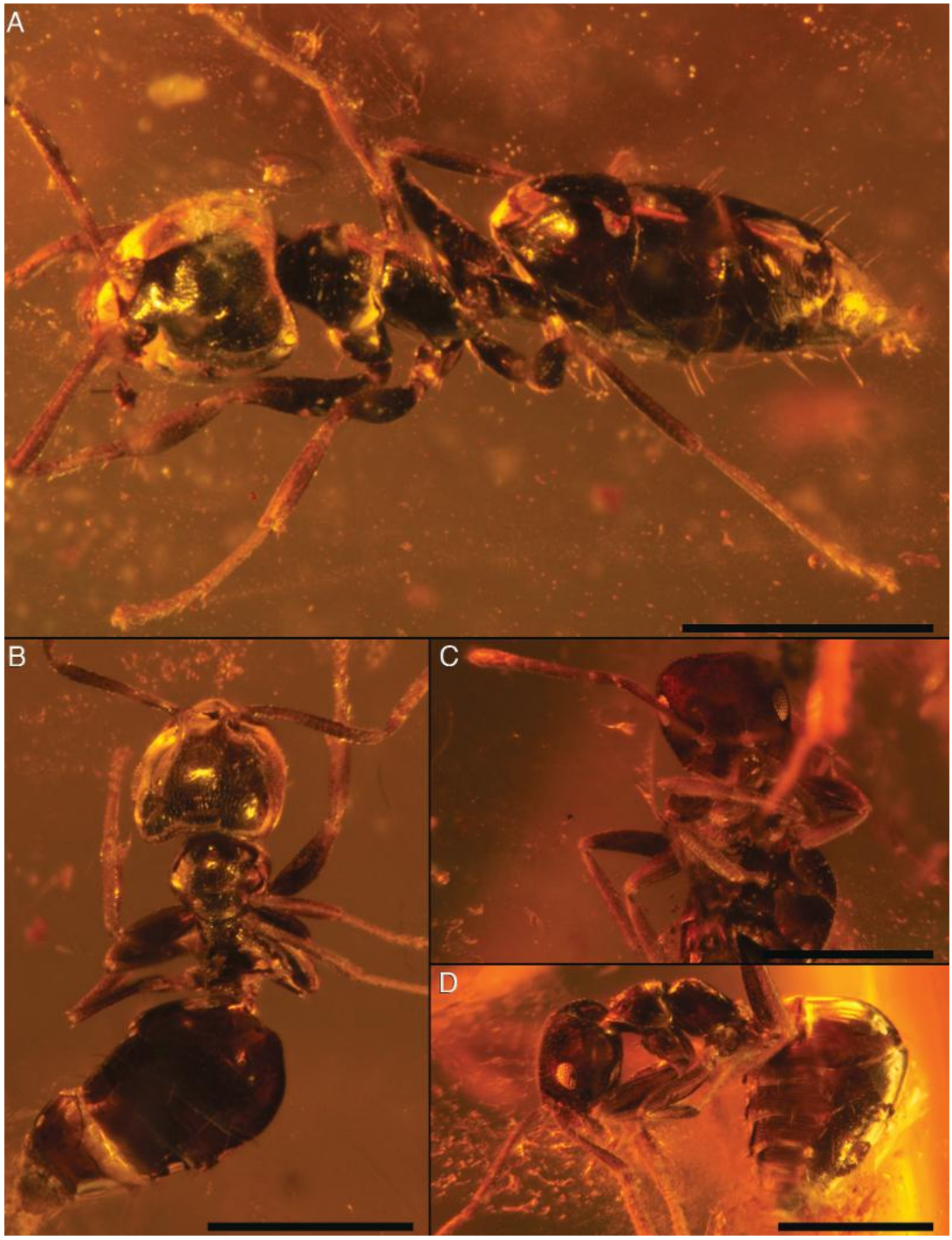


FIGURE 14. Photomicrographs of *Brachymyrmex atrapada*, sp. nov. (holotype worker, MNHNSD FOS 18.121). **A.** Lateral view of body. **B.** Dorsal view of specimen. **C.** Frontal view of head, ventral view of metasoma. **D.** Alternate lateral view of synclusion worker. Scale bars = 0.5 mm.

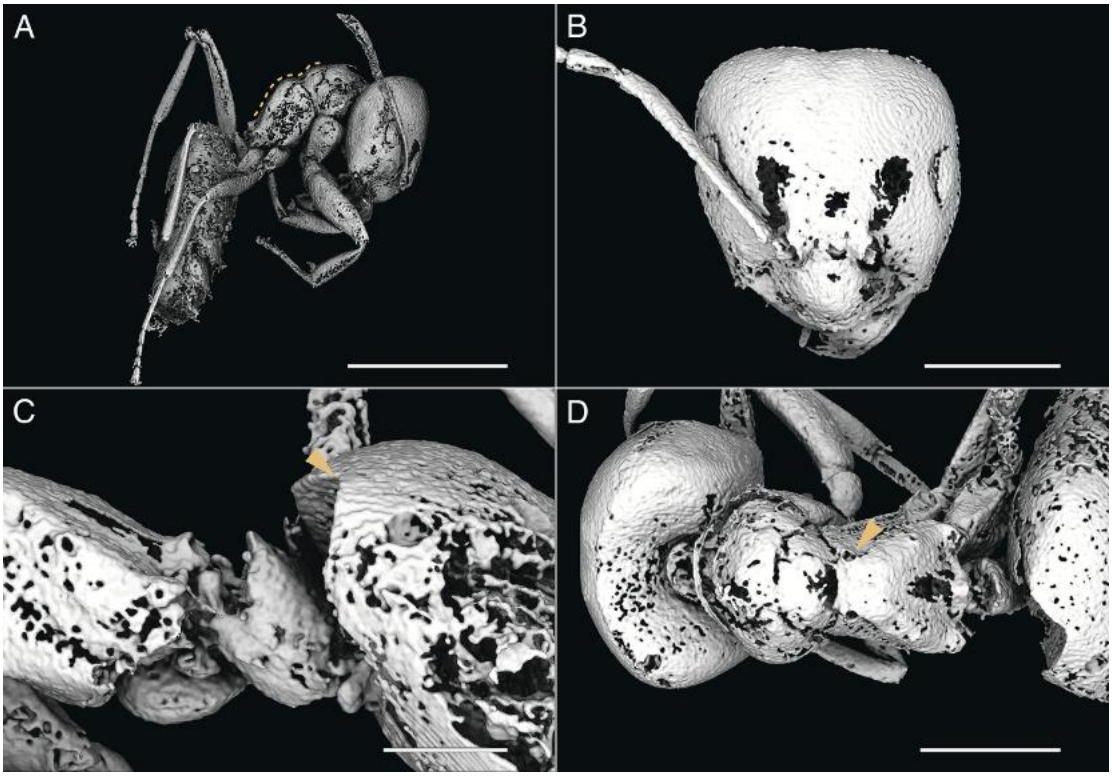


FIGURE 15. Volume renderings of *Brachymyrmex atrapada*, sp. nov. **A.** Body in lateral view; dashed line indicates mesosoma outline. **B.** Head in full-face view. **C.** Close-up view of the propodeum and petiole in lateral view. Arrow indicates methathoracic spiracles. **D.** Dorsal view, arrow indicating metathoracic spiracles. Scale bars: A = 0.5 mm; B, D = 0.2 mm; C = 0.1 mm.

Holotype worker measurements (in mm): HW 0.41, HL 0.39, EL 0.09, EHT 0.24, EHD 0.10, EHV 0.15, ELT 0.37, ELA 0.18, ELP 0.19, MLP 0.14, SL 0.31, WL 0.46, PcL 0.18, MH 0.18, PrW 0.26, MfL 0.36.

DESCRIPTION (worker). Head: Slightly wider than long in full-face view; posterior cephalic margin slightly concave. Head wider at eye level, narrowing anterad. Dorsum of head with dense appressed hairs; smooth and shining. Clypeus with rounded anterior margin. Toruli surpassing posterior clypeal margin in oblique anterodorsal view. Scapes surpass posterior cephalic margin by length less than maximal diameter of eye, and with appressed hairs. Ocelli absent. Eyes positioned anteriorly on head, with 9 or 10 ommatidia along maximal diameter.

Mesosoma: Mesonotum inflated and bulging dorsally above pronotum in lateral view. Notopropodeal sulcus deeply impressed; metathoracic spiracles large and in dorsolateral position, slightly protruding, not touching the propodeal suture, separated from posterior margin of mesonotum by more than one spiracular diameter. Dorsum of propodeum strongly convex and much shorter than propodeal slope. Propodeal slope slightly convex, meeting dorsum of propodeum at approximately a 70° angle. In dorsal view, mesosoma is hourglass shaped, being narrower at the level of the metanotal sulcus. Propodeal spiracle circular and positioned on posterior propodeal margin, projecting slightly laterally; slightly posteriorly of middle of propodeal slope. Mesosoma lacking any distinct erect hairs. Legs with appressed hairs.

Metasoma: Petiole wedge shaped with a relatively conspicuous node, inclined forward. Gaster with sparse appressed pubescence and several scattered long erect hairs.

Sculpturing and setae: Body mostly smooth and shining, except for the dorsum of the mesosoma, which is slightly rugulose-punctate. Body uniformly reddish brown to dark brown, but with slightly lighter antenna and tarsi.

Etymology: The specific epithet *atrapada* is a participial adjective in feminine form, derived from the Spanish word *atrapar*, meaning "to trap" or "to catch." It refers to the fossilized condition of the specimen, preserved in amber and permanently confined in time, a biological state of entrapment and stasis.

Type material: Holotype. MNHNSD FOS 18.121 alate queen, deposited in the Museo Nacional de Historia Natural "Prof. Eugenio de Jesús Marcano," Santo Domingo, Dominican Republic (figs. 14, 15). Preserved within a 22 mm section of darkened yellow amber with internal cracks and bubbles around the inclusions. Synclusions include 20–30 *B. atrapada* workers, a mantis, a dung midge (Scatopsidae), and fragments of a spider (unidentifiable).

Horizon and locality: Early Miocene, Burdigalian (ca. 16 Ma; Iturralde-Vinent and MacPhee, 1996); in amber from the northern mines of the Santiago Province, Dominican Republic.

Comments: The absence of erect hairs on the mesosoma, together with the deep notopropodeal sulcus, appear to be unique characters in this genus. *B. bicolor*, *B. depilis*, *and B. feitosai* all share the lack of erect hairs on the mesosoma (Ortiz-Sepulveda et al., 2019); however, *B. bicolor* and *B. depilis* lack the deep notopropodeal sulcus, while *B. feitosai* can easily be distinguished by its tumuliform metathoracic spiracles (Ortiz and Fernández, 2014, Ortiz-Sepulveda et al., 2019). Several species have at least a pair of erect hairs on the pronotum or between propodeal spiracles. There are several species of *Brachymyrmex* that have a deep or well-marked notopropodeal sulcus, but they can be separated from the new species by other attributes, in *B. gaucho* Santschi erect hairs are present on the antennal scape (absent in *B. atrapada*, sp. nov.), in *B. musculus* Forel the profile of the mesosoma is almost continuous (discontinuous in *B. atrapada*), in *B. coactus* Mayr, *B. tristis* Mayr and *B. degener* Emery erect hairs are present on the promesonotum (absent in *B. atrapada*), and in *B. gagates* Wheeler the mesonotum is almost circular in dorsal view (transverse in *B. atrapada*; Ortiz-Sepulveda et al., 2019). The erect hairs in *Brachymyrmex* are relatively easy to see, or, if they are broken, they can be seen as piliferous pits, so we can be reasonably certain they are absent in the new species. There are no previous fossil records of *Brachymyrmex* or its sister genus *Myrmelachista*. The absence of *Brachymyrmex* in amber is likely explained by its small size and leaf-litter habits, whereas *Myrmelachista*—a regular inhabitant of tree branches and vegetation—would be expected to appear in amber inclusions. Because Myrmelachistini represents the earliest-diverging lineage of Formicinae (Ward et al., 2016), and given the ecological association of *Myrmelachista* with arboreal habitats favorable for resin entrapment, its presence in the fossil record is to be expected.

Camponotus Mayr, 1861

†***Camponotus matunai*** LaPolla, Fiorentino, and Barden, sp. nov.

Figures 16, 17

ZooBankLSID:urn:lsid:zoobank.org:act:F57976CC-A5A7-4953-9900-8A1E2B9732CC

Diagnosis (worker): Large species (TL 14.22); mandible with six well-defined teeth; head cordate with anterior medial margin of clypeus coming to a small point.

Holotype worker measurements (in mm): HW 3.49, HL 3.76, EL 0.86, EHT 2.68, EHD 0.94, EHV 1.74, ELT 3.57, ELA 2.32, ELP 1.25, MLP 1.53, SL 2.54, WL 4.61, PcL 1.86, MH 1.20, PrW 1.80, MfL 4.29.

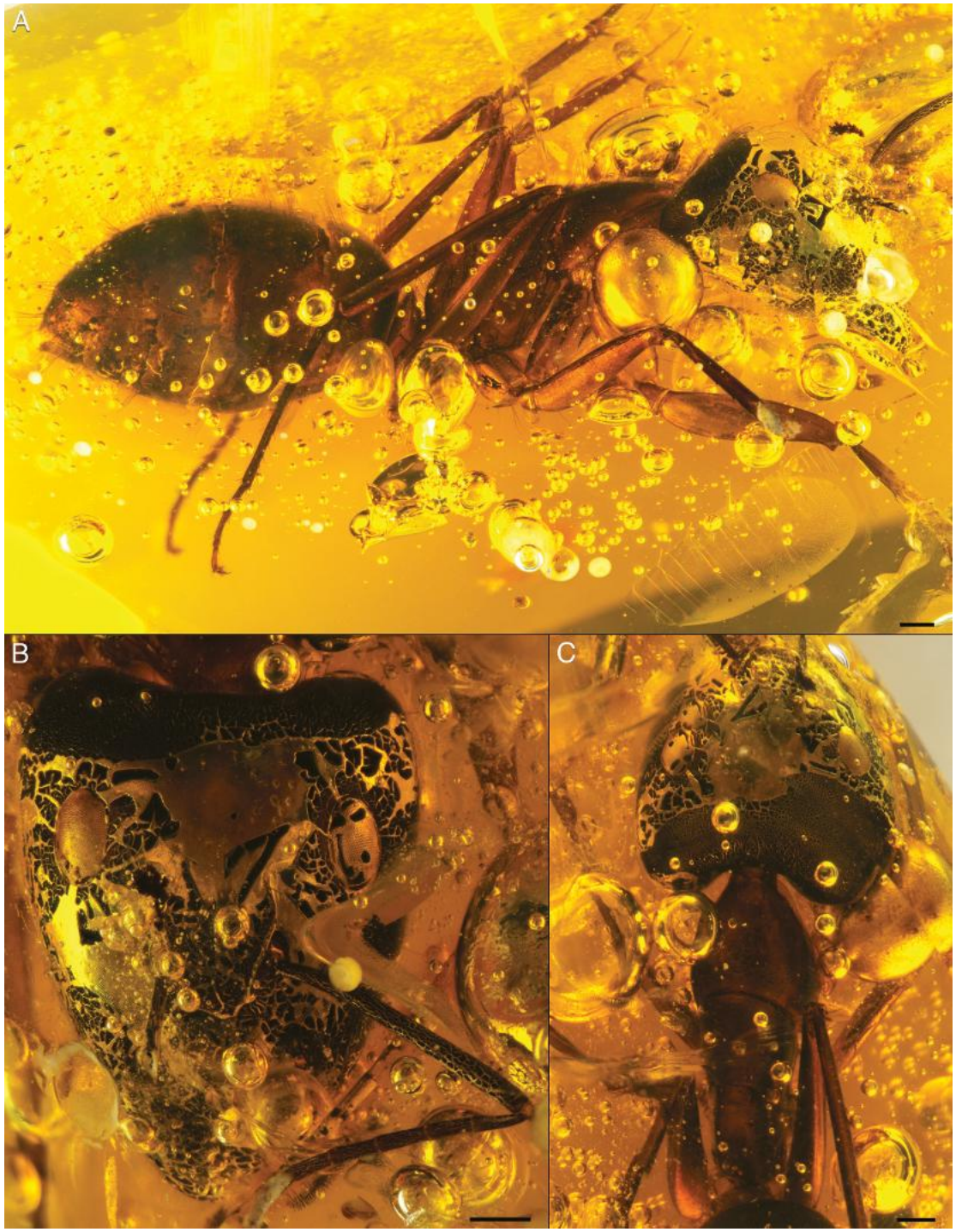


FIGURE 16. Photomicrographs of *Camponotus matunai*, sp. nov. (holotype worker, MNHNSD FOS 18.122). **A.** Lateral view of body. **B.** Frontal view of head. **C.** Dorsal view of head, mesosoma. Scale bars = 0.5 mm.

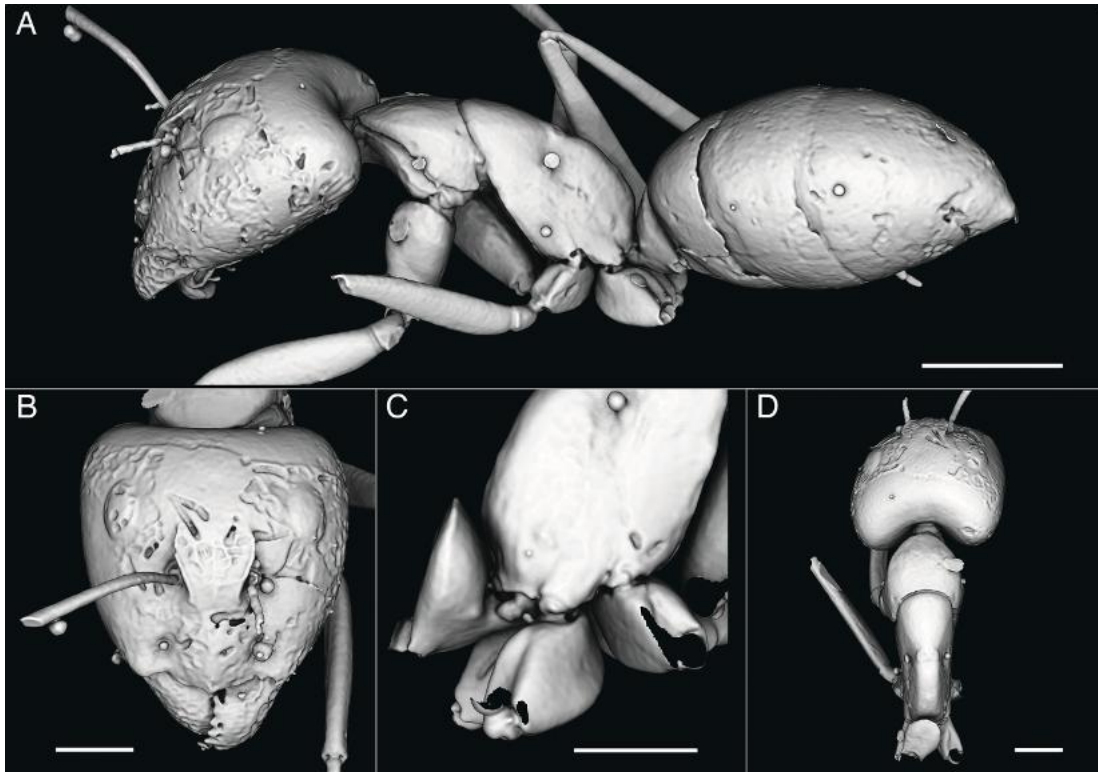


FIGURE 17. Volume renderings of *Camponotus matunai*, sp. nov. (holotype worker MNHNSD FOS 18.122). **A.** Body in lateral view. **B.** Head in full-face view, **C.** Close-up view of the propodeum and petiole in lateral view, **D.** Dorsal view of mesosoma. Scale bars: A = 2 mm; B–D = 1 mm.

DESCRIPTION (worker). Head: Cordate, anterior portion distinctly narrower than posterior; clypeus subquadrate, slightly longer than wide, slightly convex medially; medial anterior margin with small point; mandible subtriangular and robust with 6 well-defined teeth (masticatory margin length 1.17); apical tooth longer than others; frontal carina well developed extending to just posterad of anterior margin of eye; torulus and antennal base exposed; scape reaches medial posterior margin, slightly fails to reach posterolateral corners; eye slightly convex, placed well posterior to midline of head length; posterior margin concave medially with well-developed posterolateral corners.

Mesosoma: Pronotal profile slightly convex, gently curved from anterior margin toward mesonotum; promesonotal suture well developed and distinctly impressed; mesonotum slightly convex; notopropodeal sulcus indistinct with only slight impression; dorsal face much shorter than declivitous face of propodeum; declivitous margin convex in profile with steep slope. In dorsal view, metanotal suture broad, with two concave indentations, propodeum uniformly narrow. Propodeal spiracles oval shaped, posterior facing, positioned near metapleuron.

Metasoma: Petiole robustly cuneate in dorsal/lateral view; node anterior face slightly convex rising steeply toward summit; posterior face relatively straight; petiolar peduncle short.

Sculpturing and setae: Long suberect to erect macrosetae scattered across entire body; greatest number of macrosetae on pronotum and mesonotum; on head macrosetae just off midline and along posterior margin; on gaster macrose-

tae greater along segmental margins; all leg segments with scattered macrosetae; head appears to be covered in fine pubescence (although anterior portion of head is hard to see if pubescence is present); mesosomal notum also appears to have layer of fine pubescence; gaster with fine pubescence as well, but seemingly more scattered than on head and mesonotal dorsum.

Etymology: The species epithet *matunai* is derived from the Taíno language, meaning "heart." This is in reference to the large heart-shaped head of this soldier ant.

Type material: Holotype. MNHNSD FOS 18.122 alate queen, deposited in the Museo Nacional de Historia Natural "Prof. Eugenio de Jesús Marcano," Santo Domingo, Dominican Republic (figs. 16, 17). Preserved within a 35 mm section of darkened yellow amber with internal bubbles and debris around the inclusions. Synclusions include a midge, a springtail, and a cockroach nymph.

Horizon and locality: Early Miocene, Burdigalian (ca. 16 Ma; Iturralde-Vinent and MacPhee, 1996); in amber from the Northern mines of the Santiago Province, Dominican Republic.

Comments: This very large species has a distinctly cordate (heart-shaped) head. Based on the posterior margin being concave medially and its large size, it seems reasonable to consider the only known specimen of this species to be a soldier. This head morphology, along with the mesosoma in profile arched and a tall petiolar scale, possibly places this species near the *Tanaemyrmex* subgenus. *C. matunai* is strikingly similar to *C. picipes* complex yet is much larger than any modern *C. picipes* (WL 4.6 mm vs. 2.9 mm in *C. picipes plombyi*). The eye position in *C. matunai* is more forward facing and central, as opposed to more lateral in *C. picipes*, and the head shape is almost triangular in *C. matunai*, while it is less wide posteriorly in *C. picipes.* However, some of these variations may be found in the *C. picipes* complex.

Myrmicinae Lepeletier de Saint-Fargeau, 1835

The fossil record for the subfamily Myrmicinae is by far the most extensive, both in diversity and global distribution. With 42 genera and ~215 species, Myrmicinae account for nearly 24% of all known ant fossils. The earliest putative myrmicine fossil belongs to †*Afromyrma petrosa* Dlussky et al., 2004, from Orapa, Botswana. The fossil appears in the Late Cretaceous, though this assignment remains uncertain (Barden, 2017). Unambiguous representatives are known from the early Eocene, especially in the Ypresian stage (~50–55 Ma) from Oise (France), Cambay (India), and Fushun (China) ambers (LaPolla et al., 2013). By this time, much of the subfamily's tribal-level diversity had been established (Ward et al., 2016). Fossils from the Oligocene and Miocene, including the rich assemblages of Mexican and Dominican ambers (~20–16 Ma), further demonstrate the early establishment of modern Neotropical communities (Wilson, 1985a; Baroni Urbani, 1995). Genera such as *Pheidole*, *Cephalotes*, and *Solenopsis* occur in forms strikingly similar to their living relatives, reflecting both morphological conservatism and long-term ecological success. Overall, the fossil history of Myrmicinae suggests a rapid early diversification and a major role in Cenozoic ecosystems, paralleling the global expansion of angiosperm-dominated habitats (LaPolla et al., 2013).

Acromyrmex Mayr, 1865

†***Acromyrmex yucayequensis*** Mera-Rodríguez, Sosa-Calvo, Fiorentino, Barden, and Schultz, sp. nov.

Figures 18, 19

ZooBank LSID: urn:lsid:zoobank.org:act:88E25419-E3E2-4647-9C08-007D0D18D283

Diagnosis (worker): Integument conspicuously spiny, tuberculate, and carinate. Supraocular spines and lateral pronotal spines bifid. At least one pair of vertexal spines longer than half the length of spines on posterior corners of head. Spines on posterior ventral margin of head (postgena) long and acute, similar in length to longest vertexal spines. Preocular carina with a small anterior denticle. Clypeus with extremely



FIGURE 18. Photomicrographs of *Acromyrmex yucayequensis*, sp. nov. (Holotype worker, AMNH-DR-99-416). **A.** Lateral view of body. **B.** Frontal view of head. **C.** Dorsal view of head, mesosoma. Scale bars = 0.5 mm.

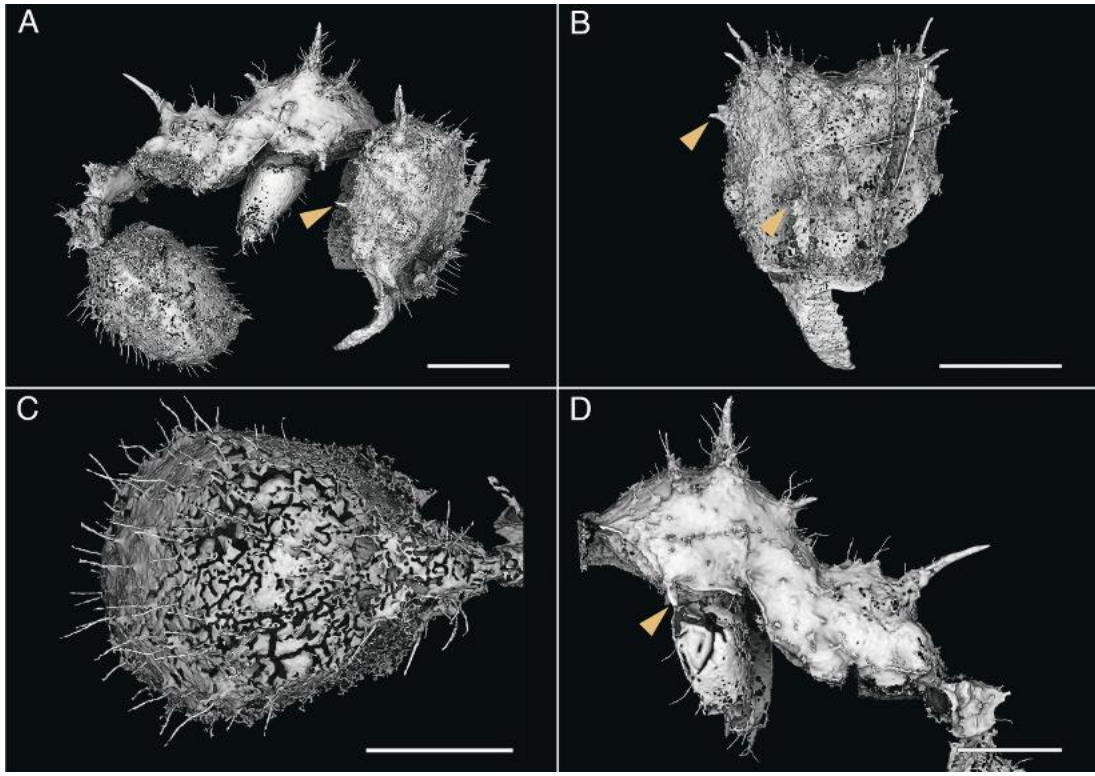


FIGURE 19. Volume renderings of *Acromyrmex yucayequensis*, sp. nov. **A.** Body in lateral view, arrow indicates postgenal spine. **B.** Head in full-face view, arrow indicates supraoccular spine and the frontal lobe, **C.** Close-up view of the first tergite of gaster in dorsal view, arrow indicates tubercle on first tergite of gaster, dashed line outlines the four rows of tubercles on first gastral tergite. **D.** Close-up of mesosoma in lateral view. Arrow indicates spinelike projection of the inferior margin of the pronotum. Scale bars: A, B, D = 0.5 mm; C = 0.2 mm.

long flagelliform setae, almost half the length of the mandible. Median pronotal spines present. Anterior mesonotal spines conspicuously long and thick, about 3× the length of lateral pronotal spines. Dorsopropodeal ridges present and with small denticles. Gastral tubercles not organized in longitudinal rows. Long, thick, flagelliform setae present on head, antennal scapes, mesosoma, metasoma, gastral tubercles, and legs.

Holotype worker measurements (in mm): HW 0.86, HL 1.38, EL 0.20, EHT 0.83, EHD 0.45, EHV 0.38, ELT 0.98, ELA 0.36, ELP 0.62, MLP 0.76, SL 1.18, WL 1.67, PcL 0.63, MH 0.49, PrW 0.39, MfL 1.83, SPL 0.44, PeW 0.07, PeH 0.15, PeL 0.22, PpeW 0.2, PpeH 0.24, PpeL 0.32, GL 1.01, TL 5.37.

Description (worker). Head: Head longer than wide. Lateral margins parallel anterior to supraocular spines, narrowing toward cephalic corners. Posterior cephalic (vertexal) margin deeply emarginate. Posterior corners of head with extremely long and acute spines (0.23 mm), similar in length to longest axis of eyes. Posterior cephalic margin interrupted by numerous acute spines. At least one pair of vertexal spines long (0.13 mm), longer than half the length of spines on posterior corners of head. Supraocular spines present, long (0.11 mm) and bifid (i.e., consisting of two conjoined spines), approximately half the length of spines on posterior corners of head, interrupting lateral margin of head when seen in full-face view. Postgenal

spines (i.e., spines on posterior ventral margin of head) long (0.11 mm) and acute, similar in length to longest vertexal spines. Antennal scape uniformly thick from base to apex, without basal lobe. Antennal scape long, surpassing posterior margin of head by more than one third of its length. Antennae apparently with 11 segments; note that the type specimen has 10 segments, but the antennae on this specimen are incomplete. Eyes convex, slightly interrupting the contour of lateral cephalic margin. Anterior margin of clypeal apron concave medially. Clypeus with extremely long flagelliform setae, almost half the length of the mandible. Preocular carina with small anterior denticle. Lateral margins of frontal lobes subparallel, ending posteriorly in spines that project dorsad (i.e., perpendicular to head). Mandibles triangular, with outer margin sinuate. Masticatory margin of mandible with nine teeth, apical tooth distinctly larger, followed by medium-sized teeth interspersed with smaller denticles. Dorsum of mandible striate from outer to masticatory margin.

Mesosoma: Promesonotal suture ill defined laterally, absent dorsally. Median pronotal spines present, short (0.07 mm), distinct and separated. Lateral pronotal spines short (0.12 mm), slightly longer than median pronotal spines, and bifid, each connected by a short carina to a tubercle. Anterior mesonotal spines conspicuously long and thick, 3× the length of lateral pronotal spines (0.35 mm). Inferior pronotal spines present and blunt. Inferior margin of pronotum carinate and with posterior spinelike projection. Posterior mesonotal spines present, acute, directed posteriorly. Posterior to posterior mesonotal spines, a third pair of tubercles is present on the mesonotum. Dorsopropodeal lateral ridges present, each with three small denticles increasing in size posteriorly. Propodeal spines present, long (0.44 mm) and sharply pointed, directed posteriorly, slightly longer than anterior mesonotal spines.

Metasoma: Petiole sessile, without a distinct peduncle; uniformly wide, longer than wide. Dorsum of petiole with a pair of spiniform tubercles. Subpetiolar (anterior) process absent, sternum not superficially convex or lobed. Postpetiole slightly longer than its maximum width. Dorsum of postpetiolar node with two pairs of spiniform tubercles. Subpostpetiolar process lobed. First gastral tergite with several spinelike tubercles of various sizes; largest tubercles occur on anterior median half of first gastral tergite, gradually decreasing in size toward posterior half of first gastral tergite. Gastral tubercles not organized in longitudinal rows.

Sculpturing and setae: Integumental sculpturing extremely spiny, tuberculate, and carinate. Long, thick, flagelliform setae present on head, antennal scapes, mesosoma, metasoma, gaster tubercles, and legs. Head and metasoma are more densely covered with these setae, while setae on mesosoma are more sparsely distributed.

Etymology: Derived from the Taíno word *yucayeque*, meaning "agricultural community." The species name refers to the collective fungus-growing behavior of the leaf-cutting ants.

Type material: Holotype. AMNH-99-416 worker, deposited in the American Museum of Natural History (figs. 18, 19). Preserved within an 8 mm by 5 mm section of transparent yellow amber treated with translucent epoxy. No synclusions.

Horizon and locality: Early Miocene, Burdigalian (ca. 16 Ma; Iturralde-Vinent and MacPhee, 1996); in amber from the northern mines of the Santiago Province, Dominican Republic.

Comments: The worker of *A. yucayequensis*, sp. nov., is similar in morphology to the extant species *Acromyrmex aspersus*, as they both have anterior mesonotal spines conspicuously longer and thicker than lateral pronotal spines, as well as median pronotal spines present and slightly shorter than lateral pronotal spines. In addition, some workers of *A. aspersus* also have supraocular tubercles and lateral pronotal spines spiniform and bifid. However, *A. yucayequensis* is uniquely different from *A. aspersus* because *A. yucayequensis* has long postgenal spines (i.e., spines on the posterior ventral margin of the head), which are reduced to tiny denticles in *A. aspersus*. Additionally,

A. yucayequensis bears clypeal setae longer than half the length of the mandibles, whereas in *A. aspersus* these setae do not reach half the mandibular length. Moreover, at least one pair of vertexal spines are longer than half the length of spines on posterior corners of head in *A. yucayequensis*, whereas in *A. aspersus* vertexal spines are shorter. Finally, *A. yucayequensis* has dorsopropodeal ridges with three pairs of angulate denticles, whereas *A. aspersus* has a maximum of one pair.

Cardiocondyla Emery, 1869

†***Cardiocondyla larimar*** Fiorentino, Sosa, Navarro, and Barden, sp. nov.

Figures 20, 21

ZooBankLSID:urn:lsid:zoobank.org:act:2FB78D49-1433-4101-BB7A-5DDF52412173

Diagnosis (worker): Frons deeply impressed, wide, narrowing posteriorly, frontal carinae sinous, converging frontad; frontal triangle forming a conspicuous inverted V-shape; mesosoma in dorsal view trapezoidal in shape, with concave lateral margins; petiole wide and high, in lateral view with a long peduncle, petiolar node with concave anterior margin, a strongly convex dorsum leading to a rounded posterior face; postpetiolar sternite with anterolaterally rounded lobiform protrusions on each side, the surface of the sternite thus appearing deeply concave in frontal view, in ventral view protrusions are connected by a concave carinae forming a small well. Most of the body covered by foveolae and punctations, first gastral tergite microreticulate, giving a matte appearance.

Holotype worker measurements (in mm): HW 0.33, HL 0.45, EL 0.11, EHT 0.25, EHD 0.12, EHV 0.13, ELT 0.44, ELA 0.19, ELP 0.25, MLP 0.21, SL 0.31, WL 0.45, PcL 0.15, MH 0.19, PrW 0.22, MfL 0.30, PeW 0.117, PeH 0.149, PeL 0.19, PpeW 0.211, PpeL 0.147, GL 0.497, TL 1.729.

Description (worker): Head: Subquadrate, moderately long; posterior margin in full-face view laterally rounded and medially concave; mandible triangular, with five teeth, apical tooth enlarged, decreasing in size from apex to base; clypeus prominently extended forward, medially emarginate, completely covering basal margin of mandible; frons deeply impressed, wide, narrowing posteriorly, frontal carinae sinous, converging frontad; frontal triangle forming a conspicuous inverted V-shape; antennae 12-segmented, antennal scapes not surpassing posterior margin of head, 3-segmented antennal club; eyes situated slightly anteriorly, with 12 ommatidia in largest diameter, bean-shaped, notably protruding from lateral head margin in full-face view.

Mesosoma: Lateral outline of promesonotum straight to slightly sinuous; in dorsal view promesonotum with humeral corners slightly rounded, in trapezoidal shape, with concave lateral margins, promesonotal suture inconspicuous in dorsal view, but deeply impressed in lateral view; in lateral view, mesonotum without a distinct posterior face, notopropodeal sulcus deeply impressed dorsally, clearly separating dorsal face of mesonotum from the propodeum. Dorsal face of propodeum short and convex, propodeal declivity flat, sloping at ~45°; in dorsal view, lateral margins of propodeum strongly convex posterior to notopropodeal sulcus; in lateral view, propodeal spines slightly curved, in lateral view directed upward (~45°), in dorsal view diverging, posteriorly forming a slight carinae leading into a unidentate propodeal lobe; propodeal spiracle circular, small, posterior facing, situated behind base of propodeal spines.

Metasoma: Petiole wide and high, in lateral view with a long peduncle, petiolar node with concave anterior margin, a strongly convex dorsum leading to a rounded posterior face, petiole in dorsal view with a semiglobular node, slightly wider than long. Postpetiole moderately wide and very high, in dorsal view much wider than long, anterior margin straight and posterior mar-

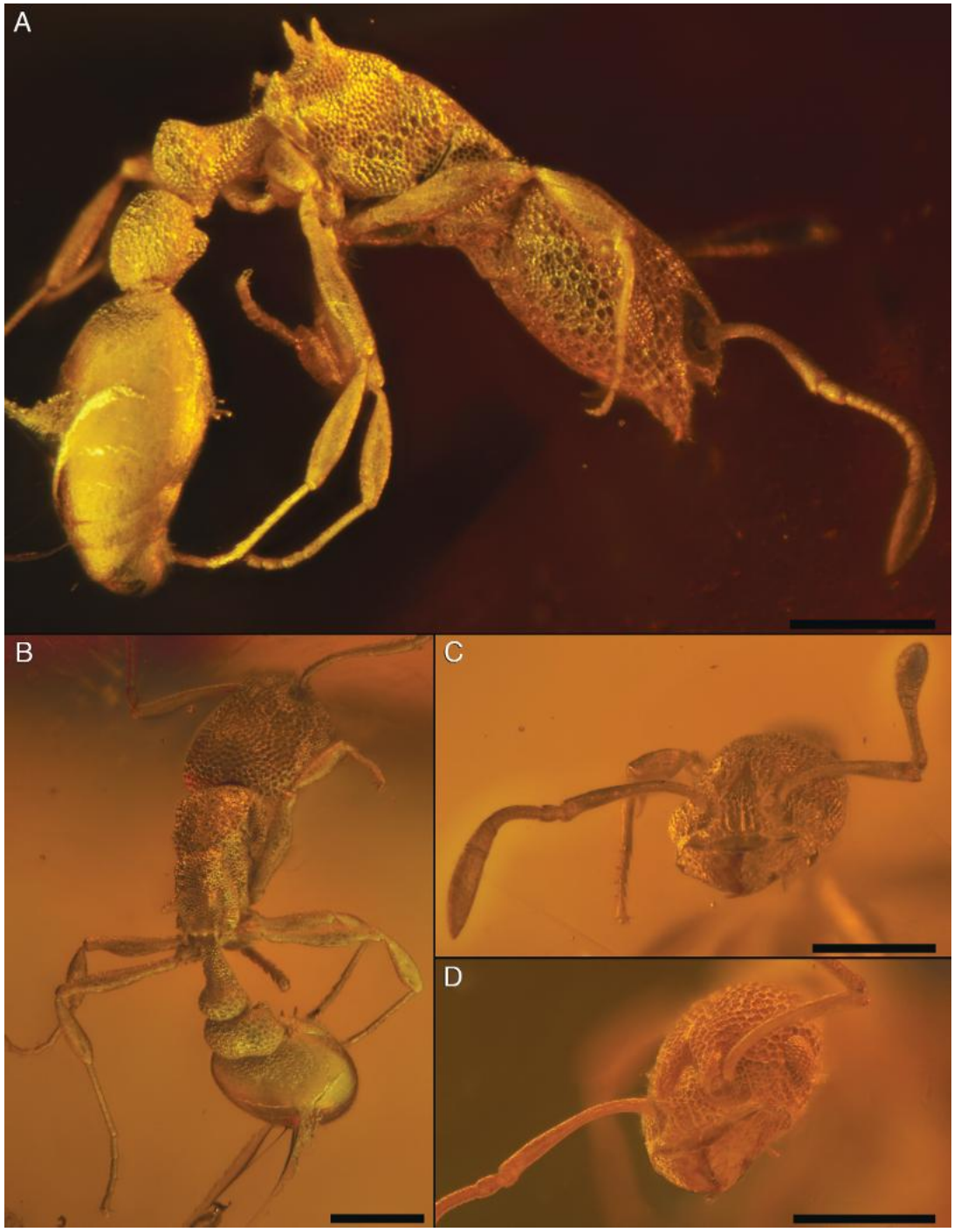


FIGURE 20. Photomicrographs of *Cardiocondyla larimar*, sp. nov. (holotype worker, AMNH-DR-14-278). **A.** Lateral view of body. **B.** Dorsolateral view of specimen. **C, D.** Alternate anterior and anterolateral views of head. Scale bars = 0.25 mm.

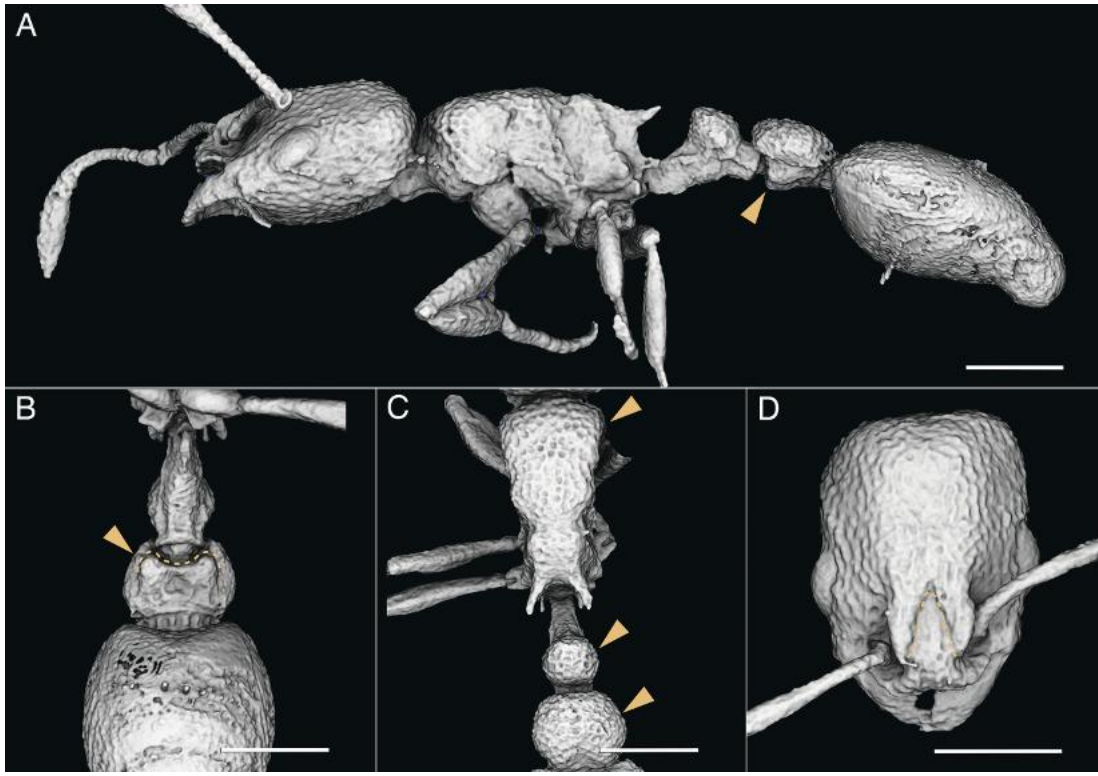


FIGURE 21. Volume renderings of *Cardiocondyla larimar*, sp. nov. **A.** Body in lateral view. Arrow indicates postpetiolar protrusion. **B.** Close-up of petiole, postpetiole, and gaster in ventral view. Arrow indicates postpetiolar protrusions and dashed line outlines the shape of the protrusion, **C.** Dorsal view of mesosoma. Arrows indicate the sculpturing on the humeral angle, petiolar node, and postpetiolar node. **D.** Head in full-face view; dashed line outlines the frontal triangle. Scale bars = 0.2 mm.

gin slightly convex; postpetiolar sternite with anterolaterally rounded lobiform protrusions on each side, the surface of the sternite thus appearing deeply concave in frontal view, in ventral view protrusions are connected by a concave carina forming a small well.

Sculpturing and setae: Whole surface of dorsal head with irregularly sized circular foveolae that show a flat central tubercle; the interspaces between foveolae on vertex smaller than foveolar diameter and coarse. Microsculpture on dorsum of mesosoma similar to that of head, with stronger size irregularity between foveolae; lateral mesosoma interspaces between foveolae punctate. Petiole and postpetiole laterally finely punctate, dorsally foveate. Basal part of first gastral tergite microreticulate and matte in appearance. Body appears to be uniformly reddish in color.

Etymology: The specific epithet *larimar* makes reference to the striking foveate and punctations found all over the body in patterns resembling those found in the Larimar, a silicate mineral pectolite found only on the island of Hispaniola.

Type material: Holotype. AMNH DR 14-278 worker, deposited in American Museum of Natural History (figs. 20, 21). Preserved within 16 mm section of dark red amber. Synclusions include an *Azteca alpha* worker.

Horizon and locality: Early Miocene, Burdigalian (ca. 16 Ma; Iturralde-Vinent and MacPhee, 1996); in amber from the Northern mines of the Santiago Province, Dominican Republic.

Comments: *Cardiocondyla larimar*, sp. nov., represents the third fossil *Cardiocondyla* (Wang et al, 2021; Radchenko and Khomych, 2025), and, more remarkably, the first Neotropical species of this, until now, Old World genus. Modern distributions range from the Palearctic and Afrotropical to Southeast Asia and Oceania (Seifert, 2002, 2023, 2024), with tramp species belonging to the genus present in the Americas (Seifert, 2002). *C. larimar* possesses mostly modern traits and can be very easily attributable to the *C. wroughtonii* species complex because of the bilobate postpetiolar sternite (Seifert, 2024). However, *C. larimar* can be distinguished from modern *C. wroughtonii* complex species by the combination of a conspicuous frontal triangle forming an inverted V-shape and the petiole morphology. While the frontal triangle is present to a lesser degree in some modern *C. wroughtonii* complex species, such as *C. wroughtonii* and *C. allonivalis*, in neither is the triangle as projected posterad or as conspicuous. The anterior face of the petiolar node in *C. larimar* is straight and meets the peduncle at an almost sharp right angle, as opposed to being slightly curved and meeting the peduncle at much more obtuse angles in the rest of the *C. wroughtonii* species complex.

Cardiocondyla larimar is one of four distinct genera with affinities to Old World fauna found on the island of Hispaniola. It is present in the Caribbean today, although as an invasive species. The species representing the other Old World fauna—*Bothriomyrmex*, *Leptomyrmex and Brachyponera*—are clearly distinguishable from their modern congeners (Barden et al., 2017; Prebus and Lubertazzi, 2016; herein). This is not the case with *C. larimar*, as it can be comfortably placed within a modern species complex.

Crematogaster Lund, 1831

†***Crematogaster diunota*** Blaimer, Fiorentino, and Barden, sp. nov.

Figures 22, 23

ZooBankLSID:urn:lsid:zoobank.org:act:9D579C30-6C8D-4E4A-AA76-ABEA98CD6C22

Diagnosis (worker): With the following diagnostic characters of the subgenus *C.* (*Orthocrema*) (Blaimer, 2012): Petiole in dorsal view ovo-rectangular, with dorsoposterior lateral denticles bearing erect setae. Postpetiole globular with faint median impression. Occipital carina sharp and distinct. Propodeal spiracle subcircular. Antennae 11-segmented with a two-segmented club. Posterior head margin rounded.

Holotype worker measurements (in mm): HW 0.49, HL 0.51, EL 0.11, EHT 0.35, EHD 0.14, EHV 0.21, ELT 0.51, ELA 0.29, ELP 0.21, MLP 0.26, SL 0.42, WL 0.57, PcL 0.20, MH 0.26, PrW 0.31, MfL 0.47, SPI 0.19, GL 0.75, TL 2.35, SI 0.86.

DESCRIPTION (worker): Head: Very small (HW 0.49, WL 0.57) relative to other *Crematogaster* species. Head square, with posterior margin in full-face view laterally rounded; occipital carina well pronounced. Mandibles triangular, with four teeth, apical tooth enlarged; palp formula 5, 3; clypeus moderately convex; frontal carinae short. Antennae 11-segmented, with scapes of medium length (SI 0.86), just reaching posterior margin of head; two-segmented apical club present. Eyes with ~10 ommatidia in the largest diameter, rounded, emarginate and notably protruding from lateral head margin in full-face view; midline of eyes situated well above midline of head in full-face view.

Mesosoma: Lateral outline of promesonotum moderately convex; in dorsal view, promesonotum of rounded trapezoidal shape, promesonotal suture absent; in dorsolateral view, promesonotum laterally subangular, posterolaterally marginate, and notopropodeal sulcus bordered by raised ridges; mesonotum without a distinct pos-

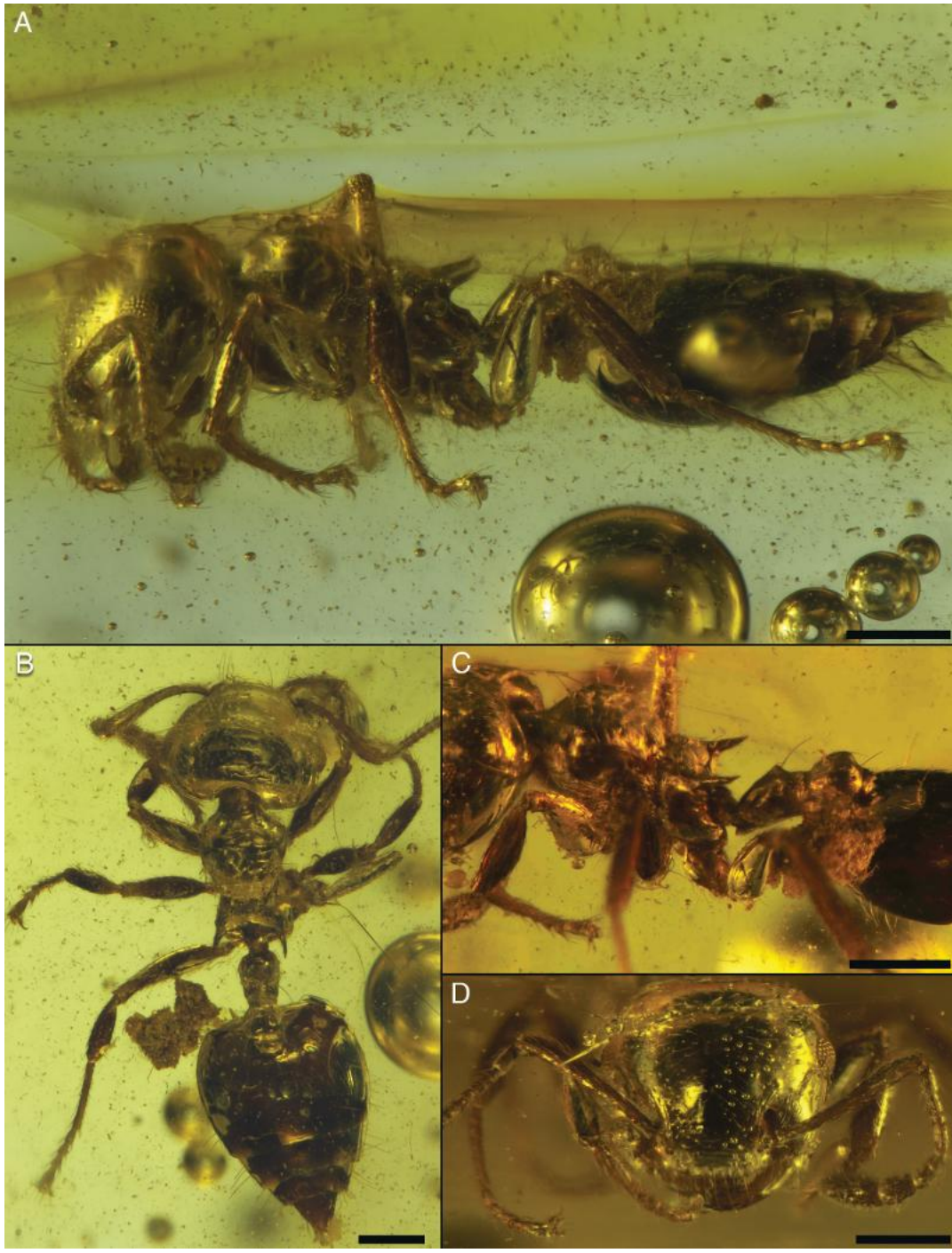


FIGURE 22. Photomicrographs of *Crematogaster diunota*, sp. nov. (holotype worker, MNHNSD FOS 18.123). **A.** Lateral view of body. **B.** Dorsal view of specimen. **C.** Dorsolateral view of head, mesosoma, and metasoma. **D.** Frontal full-face view of head. Scale bars = 0.25 mm.

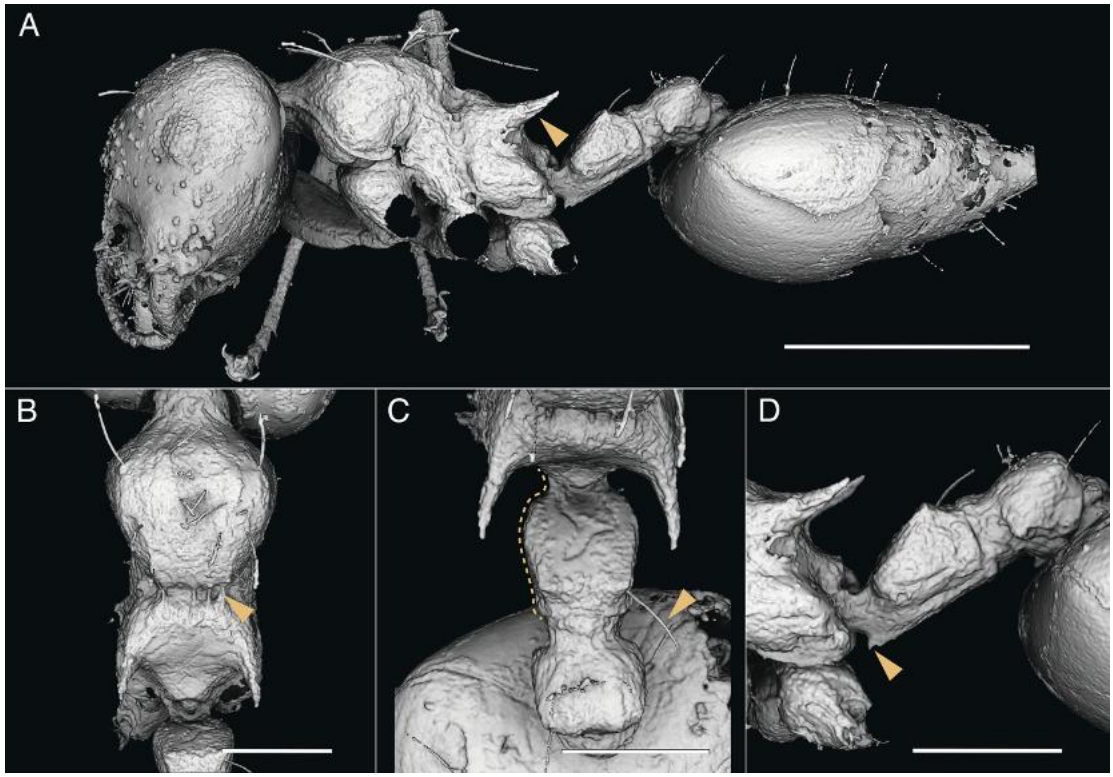


FIGURE 23. Volume renderings of *Crematogaster diunota*, sp. nov (holotype worker, MNHNSD FOS 18.123). **A.** Body in lateral view. Arrow indicates the propodeal spine. **B.** Close-up of mesosoma in dorsal view. Arrow indicates the sculpturing of the notopropodeal sulcus. **C.** Close-up of propodeum, petiole, and postpetiole in dorsal view; dashed line outlines the shape of the petiole and petiolar peduncle. Arrow indicates erect hair on petiolar node. **D.** Close-up of petiole in lateral view. Arrow indicates the subpetiolar tooth. Scale bars: A = 0.5 mm; B–D = 0.2 mm.

terior face, sloping continuously toward propodeum; notopropodeal sulcus bordered by carinae. Dorsal face of propodeum short and convex; propodeal declivity flat, sloping at ~45°; propodeal spines of medium length (SPI 0.19), straight, in lateral view directed upward (~45°), in dorsal view almost parallel and not diverging; propodeal spiracle subcircular, located at base of propodeal spine.

Metasoma: Petiole in dorsal view ovo-rectangular, slightly wider than long, with weakly carinate dorsolateral margins and small posterolateral denticles; subpetiolar process developed as a sharp, projecting tooth. Postpetiole globular, posteriorly with a faint median impression; subpostpetiolar process developed as a small, acute tooth.

Sculpturing and setae: Sculpture only partially visible, appearing as follows. Head sculpture aciculate; mesosoma with promesonotum dorsally aciculate; propodeum with dorsal face carinulate, posterior declivous face smooth and shining; gaster shining. Pilosity likely incomplete, affected by preservation. Face with five visible long erect setae, and abundant short, subdecumbent pubescence; clypeus with six long setae projecting over mandibles. Pronotum with three (likely originally four paired) long erect humeral setae, and four paired long erect setae at lateral border of mesonotum; five suberect setae present dorsally on metanotum. Petiole with a single long, erect seta on right posterolateral denticle, setae on left denticle missing but likely

originally present. Postpetiole laterally left with one long, erect dorsoposterior seta, right dorsoposterior seta missing but likely originally present. Abdominal tergites and sternites 4–7 with fairly abundant long erect pilosity (>20 setae). Abundant short, subdecumbent hairs on trochanter, femur, tibia, and tarsi. Body coloration likely affected by preservation, appearing brown.

Etymology: From Latin *diu nota* meaning "long known," referring to the long time the genus was known from Miocene amber before formal description of a species.

Type material: Holotype. MNHNSD FOS 18.123 worker, deposited in the Museo Nacional de Historia Natural "Prof. Eugenio de Jesús Marcano," Santo Domingo, Dominican Republic (figs. 22, 23). Preserved within a round 20 mm by 13 mm section of yellow amber with internal bubbles and debris around the inclusions. Synclusions include two conspecific workers and a small beetle.

Horizon and locality: Early Miocene, Burdigalian (ca. 16 Ma; Iturralde-Vinent and MacPhee, 1996); in amber from the northern mines of the Santiago Province, Dominican Republic.

Comments: This is the first fossil *Crematogaster* species described from Miocene amber, although the presence of the genus in Dominican amber had already been noted by Wilson (1985a), and a potential male *Crematogaster* specimen in Chiapas amber was mentioned by Brown (1973). The following combination of characters will be important to distinguish the species from other undescribed contemporary fossil *C.* (*Orthocrema*) species: antennae with scapes just reaching posterior head margin (SI 0.86); propodeal spines straight, medium length (SPI 0.19); petiole with subpetiolar process developed as sharp, projecting tooth; pilosity with long erect setae on head, mesosoma, and metasoma as described below.

Due to the transfer of previously described fossils from Rovno and Sicilian amber and Kishenehn shale from *Crematogaster* to *Incertogaster* (Boudinot et al., 2024), the newly described *Crematogaster diunota* is also currently the only described fossil member of the genus. *Crematogaster diunota* appears morphologically close to the extant Caribbean species *C. steinheili*, but has longer, flexuous erect pilosity on face, meso- and metasoma than the latter species.

Eurhopalothrix Brown and Kempf, 1961

†***Eurhopalothrix electrina*** Probst, Barden, and Fiorentino, sp. nov.

Figures 24, 25

ZooBank LSID: urn:lsid:zoobank.org:act:F4EBF973-1D5F-41B1-A087-7A4195F37755

Diagnosis (worker): Comparatively large species (TL 3.04, HL 0.60, WL 0.80). Labrum approximately 2× broader than long, anterior margin bilobed; apex of labral lobes with two distinct setae. Mandibles with a single row of 10 to 12 triangular teeth; head pilosity sparse and decumbent, frons with two rows of specialized spatulate setae. Promesonotum with two dorsal pairs of clavate setae anteriorly and one pair of thick spatulate setae posteriorly; propodeal spine long and sharp.

Holotype worker measurements (in mm): HW 0.56, HL 0.60, EL 0.09, EHT 0.40, EHD 0.08, EHV 0.32, ELT 0.65, ELA 0.38, ELP 0.27, MLP 0.34, SL 0.51, SLL 0.46, WL 0.80, PcL 0.26, MH 0.36, PrW 0.40, MfL 0.66, PeL 0.41, PpeL 0.24, GL 0.99, TL 3.04, CI 93, SLI 91.

DESCRIPTION (worker): Head: Subtrapezoidal, posterolateral sides diverging posteriorly to a subround angle, vertexal margin weakly concave medially; cervical margin carinate, carina rounded. Head surface evenly divided into anterior and posterior portions by broad antennal fossa. Labrum much broader than long, anterolateral gibbosities of basal portion developed ventrally directed projections, apical portion very short, flexed dorsally, anterior margin bilobed; apex of labrum with two distinct setae. Compound eyes relatively small. Mandibles triangular; in full-face view, apex strongly convex, basal angle right, followed by masticatory margin with a single row of 12 triangular teeth, apical teeth larger than basal teeth; in lateral view, mandibular apex slightly curved ventrally. Anterior

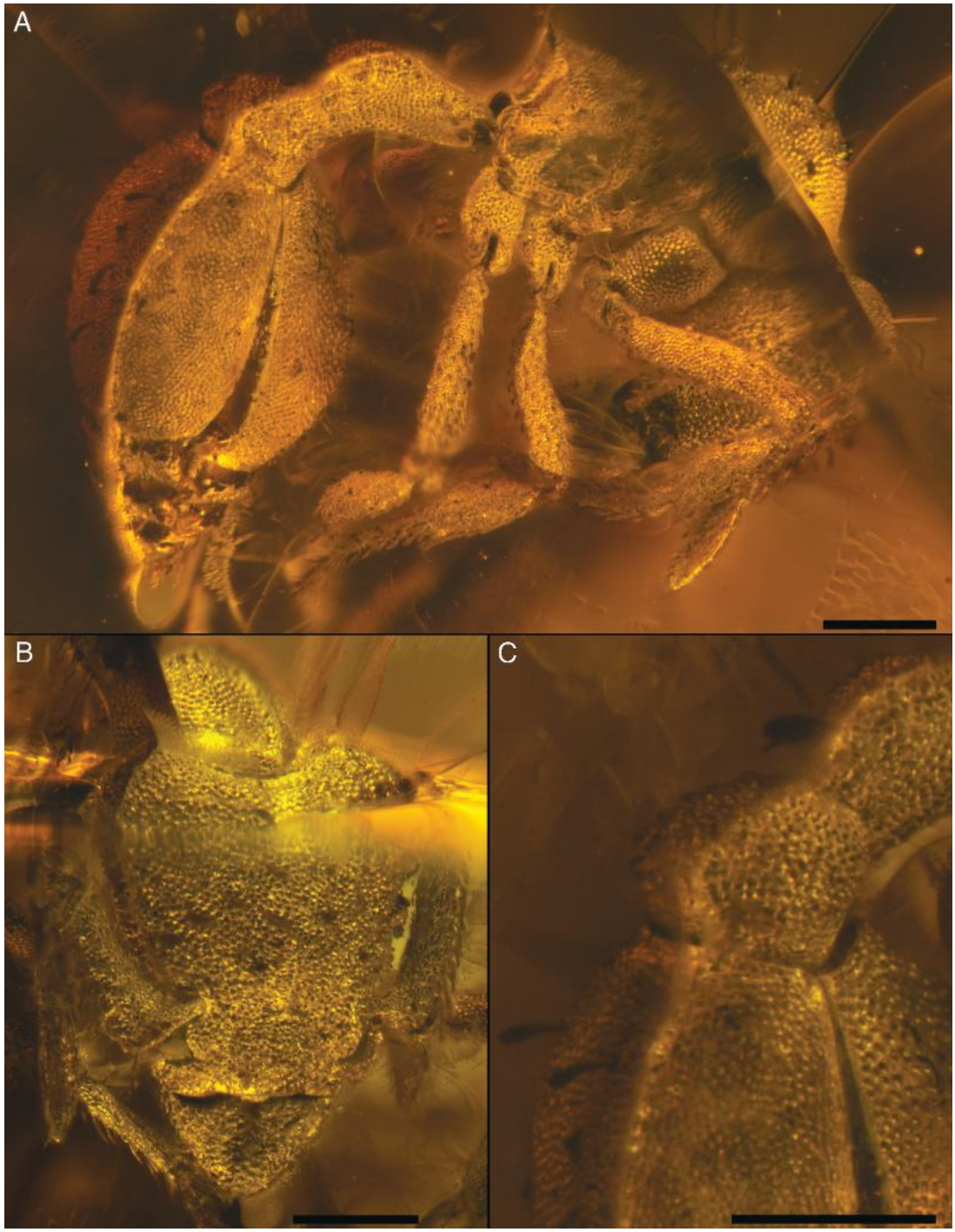


FIGURE 24. Photomicrographs of *Eurhopalothrix electrina*, sp. nov. (holotype worker, AMNH DR 14-907). **A.** Lateral view of body. **B.** Frontal full-face view of head and pronotum. **C.** Enlarged lateral view of petiole, postpetiole, and first gastral segments. Scale bars = 0.25 mm.

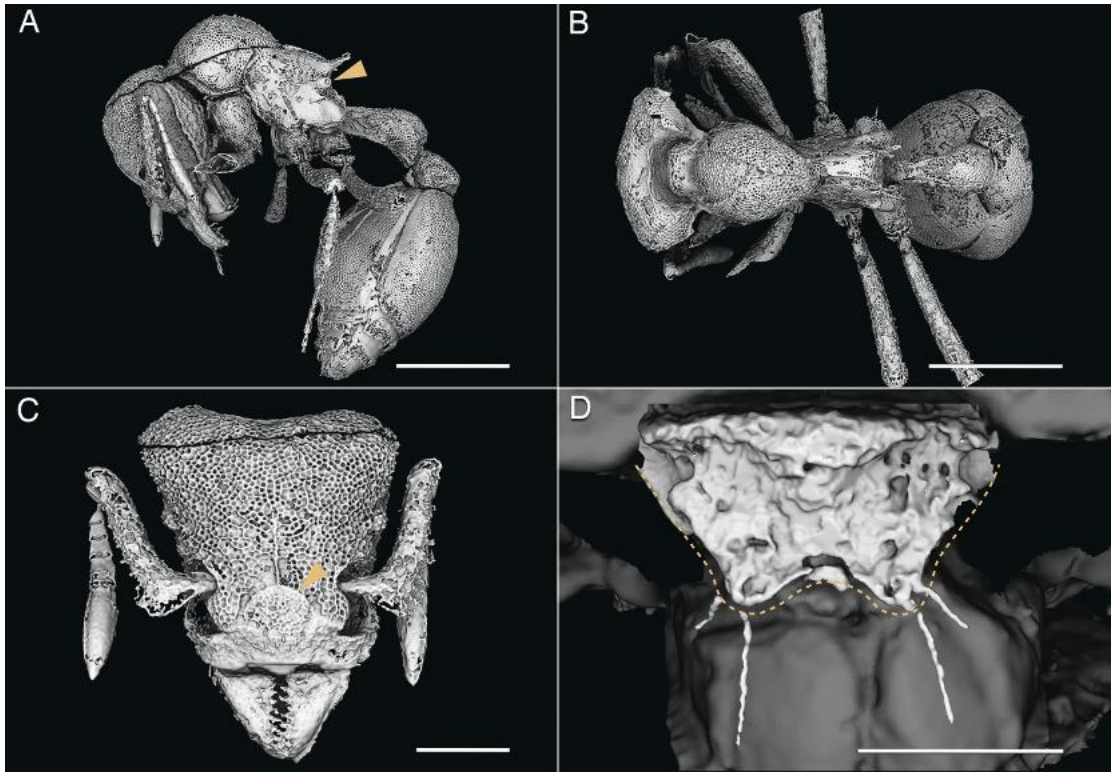


FIGURE 25. Volume renderings of *Eurhopalothrix electrina*, sp. nov. **A.** Body in lateral view. Arrow indicates the protruding propodeal spiracle. **B.** Body in dorsal view. **C.** Head in full-face view. Arrow indicates the antennal fossa and connecting ridge, **D.** Close-up of labrum, dashed line outlines the labrum shape. Scale bars: A = 0.5 mm; B, C = 0.2 mm; D = 0.1 mm.

clypeal margin gently concave medially, lamellate. Antennae seven-segmented, apical funicular joint slightly shorter than the rest of the funiculus. Scape with strongly developed basal lobe; scrobe deep, sharply delimited ventrally and less so dorsally, sitting below broad antennal fossa.

Mesosoma: In profile with pronotum strongly convex, evenly curved; promesonotal suture weakly impressed; mesonotum profile flat, noticeably below pronotum and in same plane as dorsal face of propodeum. Notopropodeal sulcus broad. Dorsal and posterior faces of propodeum distinct, posterior face sloping posteriorly, dorsal and posterior faces of propodeum subequal in length; area between basal and declivous face meeting at acute propodeal spine. Propodeal spiracle large, directed posteriorly.

Metasoma: Petiole broad, node convex, indistinct from petiolar peduncle, postpetiole short and broadly connected to gaster. Petiolar peduncle connected to anterior face of node at rounded obtuse angle; posterior face of node elongate; ventral margin with large, blunt subpetiolar process followed by an irregular keel.

Sculpturing and setae: Head sculpture on anterior and posterior portions foveate; occiput foveolate; ventral surface punctate. Mandibular surface rugose and punctate. Clypeal surface coarse, followed by translucent flange. Entire mesosoma minutely foveolate. Petiole, postpetiole, and gaster densely foveolate. Frons with two rows of specialized setae, the anterior row composed of eight clavate hairs forming an arch, second row composed of four hairs on the middle

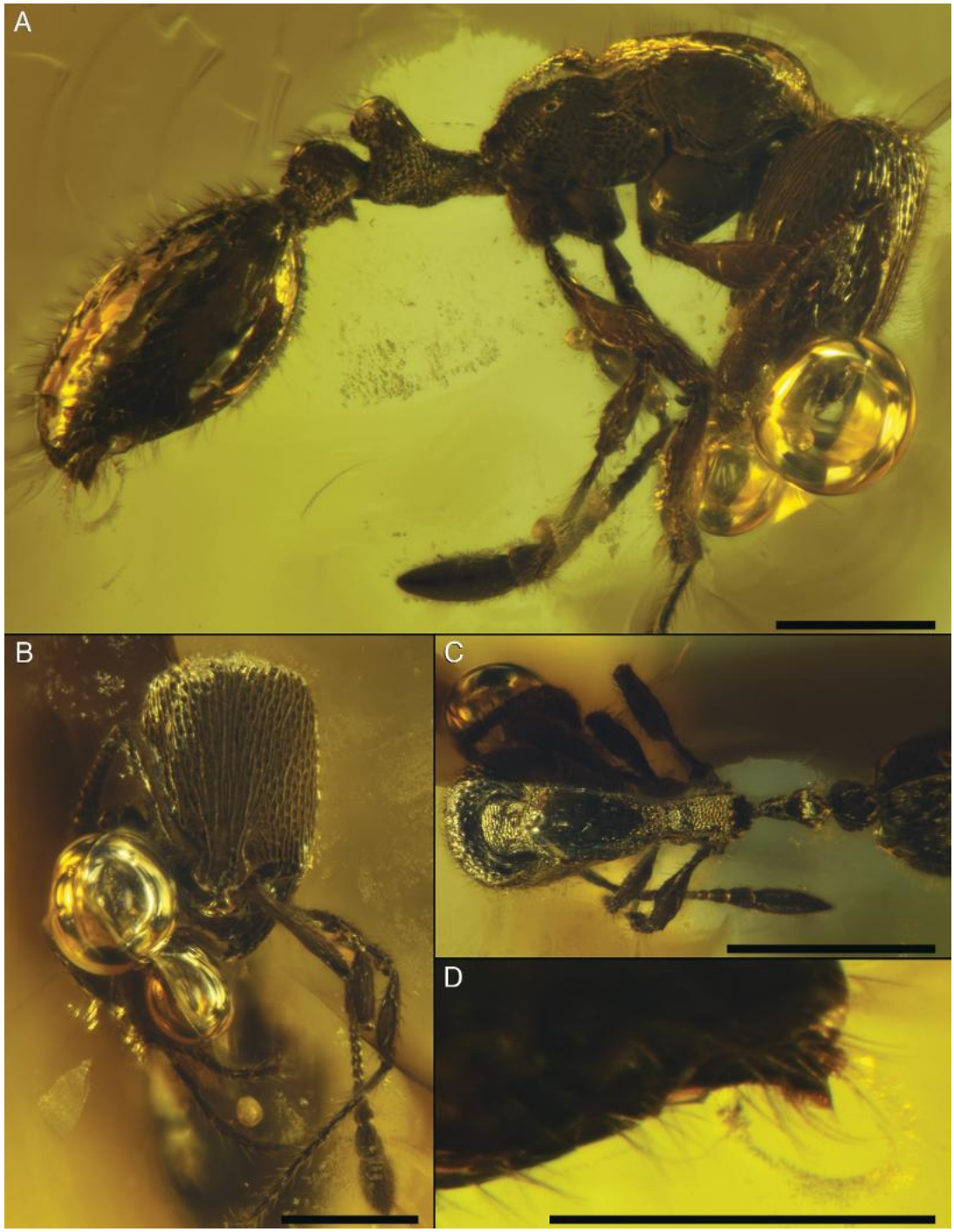


FIGURE 26. Photomicrographs of *Kempfidris priminatus*, sp. nov. (holotype worker, AMNH-DR-14-519). **A.** Lateral view of specimen. **B.** Frontal face on view of head. **C.** Dorsal view of specimen. **D.** Enlarged lateral view of pygidium on terminal abdominal segments. Scale bars = 0.25 mm.

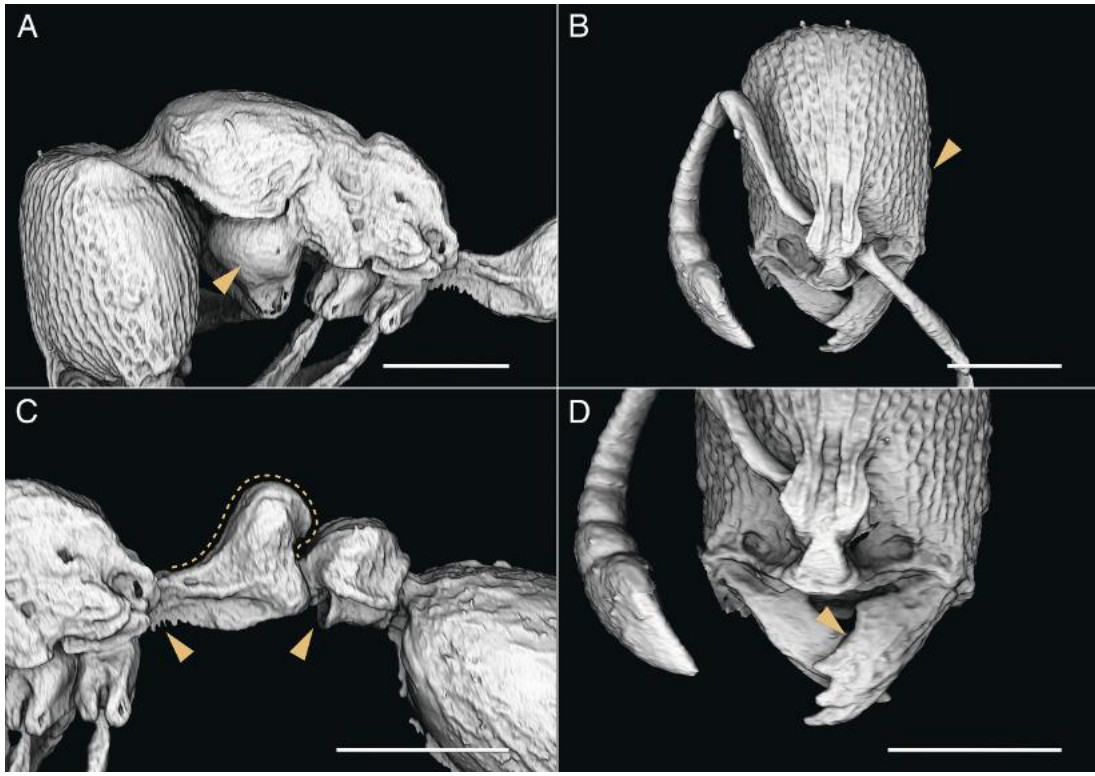


FIGURE 27. Volume renderings of *Kempfidris priminatus*, sp. nov. **A.** Mesosoma in lateral view. Arrow indicates the swollen procoxae. **B.** Head in full-face view. Arrow indicates the reduced eye. **C.** Close-up of petiole and postpetiole in lateral view. Arrows indicate the subpetiolar and subpostpetiolar processes, dashed line outlines the petiolar node. **D.** Close-up of mandibles. Arrow indicates the mandibular diastema. Scale bars = 0.2 mm.

of vertex. Dorsal surface of scape with abundant subdecumbent hairs; ~9 projecting spatulate setae on external margin of scape. Sparse pilosity on frons and clypeus surface; promesonotal dorsum with hairs similar to those on face, also sparse. Two pairs of clavate setae on the laterodorsal margin of pronotum; one pair of spatulate setae on posterior margin of mesonotum. Legs with sparse, spatulate, subdecumbent setae on mesofemur and anterior face of metafemur, somewhat sparser on other surfaces; tibiae apically covered by larger spatulate setae. Petiole and postpetiole lacking any projecting spatulate setae; first gastral tergite with four or five pairs of spatulate suberect setae.

Etymology: The specific epithet *electrina* is a Latin feminine adjective meaning "of amber."

Type material: Holotype. AMNH_DR_14_907 worker, deposited in the American Museum of Natural History (figs. 24, 25). Preserved within a 10 mm by 10 mm section of transparent, yellow amber with internal cracks along the body of the inclusion. No synclusions.

Horizon and locality: Early Miocene, Burdigalian (ca. 16 Ma; Iturralde-Vinent and MacPhee, 1996); in amber from the northern mines of the Santiago Province, Dominican Republic.

Comments: This species shares similarities, based on overall head and body morphologies and pilosity patterns, with other New World *Eurhopalothrix* taxa (e.g., *E. schmidti* and *E. megalops* from Costa Rica and *E. guadeloupensis* from Guadeloupe). The labrum of *E. electrina* is very similar in shape to the Cuban *Eurhopalo-*

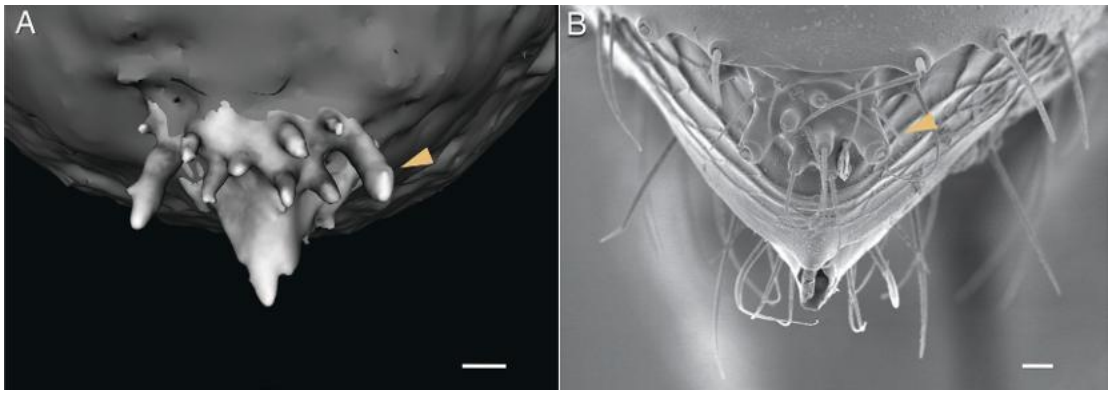


FIGURE 28. Volume rendering of the gaster of **A.** *Kempfidris priminatus* compared with **B.** SEM image of the gaster of *Kempfidris inusualis* (Fernández et al., 2014). Arrows indicate the micropegs in both *K. priminatus* and *K. inusualis*. Based on a microcomputed tomography scan, showing details of the micropegs of the pygidium, an autapomorphy for the genus. Scale bar = 10 μm.

thrix species, *E. mabuya*, hinting at a potential case of an ancestral radiation of the genus in the Caribbean. The configuration of clavate setae on the frons is reminiscent of those found in *E. vulcan*, although the number of setae in the two rows is distinct. The most distinguishing trait in *E. electrina* is its petiole, lacking a distinct node. This trait is similar to that of *E. chapmani*, an extant taxon found in the Philippines. However, the petiolar node is even less pronounced in *E. electrina*, appearing as a continuous convexity throughout the entirety of the petiolar tergite. Only one extant species is known from Hispaniola, *E. floridana*, though it is not endemic to the island (Longino, 2013).

Kempfidris Fernández, Feitosa and Lattke, 2014

†***Kempfidris priminatus*** Fiorentino, Barden, Feitosa, and Fernandez, sp. nov.

Figures 26–28

ZooBank LSID: urn:lsid:zoobank.org:act:F766FB5F-91B1-490E-972C-6FBA8751892A

Diagnosis (worker): Head considerably longer than wide, antenna 12-segmented with well-defined three-segmented club, mandible with four teeth and a conspicuous diastema between the basal and third teeth. In dorsal view, propodeum about half of the maximum pronotal width, widening posteriorly. Procoxae very large, many times the size of midcoxae. Petiole pedunculated, petiolar peduncle clearly narrowing anterad; petiolar node higher than long and rounded dorsally, with a nearly straight anterior margin and posterior margin concave, sloping posteriorly over the postpetiole. Pygidium with eight conspicuous micropegs organized as two large lateral and six smaller micropegs between them.

Holotype worker measurements (in mm): HW 0.33, HL 0.44, EL 0.04, EHT 0.22, EHD 0.12, EHV 0.10, ELT 0.37, ELA 0.17, ELP 0.20, MLP 0.23, SL 0.28, WL 0.53, PcL 0.18, MH 0.19, PrW 0.20, MfL 0.30, PeW 0.09, PeH 0.19, PeL 0.18, PpeW 0.12, PpeL 0.12, GL 0.53, TL 1.8.

DESCRIPTION (worker). Head: Considerably longer than wide. Antenna 12-segmented with well-defined 3-segmented club. Scape short, failing to reach the vertexal border by 3× its maximum width. Apical antennomere conspicuously large, as long as the two preceding ones combined. Eye reduced, with six ommatidia. Frontal carina short; antennal scrobe absent. Frontal lobe small and close. Mandible with four teeth, organized as a basal tooth, followed by a conspicuous diastema, a large second tooth and well-defined subapical

and apical teeth (fig. 27D). Clypeus strongly projected anteromedially.

Mesosoma: Promesonotum convex in lateral view. Promesonotum wider anteriad, narrowing posteriad. Promesonotal suture not well defined. Notopropodeal sulcus well marked and very deep. Bulla of metapleural gland large. Dorsal face of propodeum strongly elevated anteriorly, forming a rounded projection, and strongly sloping posteriorly, posterior face of propodeum straight. Propodeal lobes absent. In dorsal view, propodeum about half the maximum pronotal width, widening posteriorly. Procoxae very large, at least 3× the size of midcoxae.

Metasoma: Petiole pedunculated, petiolar peduncle clearly narrowing anterad; petiolar node higher than long and rounded dorsally, with a nearly straight anterior margin and posterior margin concave, sloping posteriorly over the postpetiole. Postpetiole rounded and wide (fig. 27C); postpetiolar sternum formed as a wide anterior-facing projection in the shape of a shovel. Pygidium with eight conspicuous micropegs organized as two large lateral and six smaller micropegs between them (fig. 28A).

Sculpturing and setae: Head surface with coarse longitudinal striae, mixed laterally with coarse foveae; dorsum of mesosoma mostly smooth, with slight reticulation, sides of mesosoma, petiole and postpetiole reticulated, dorsum of propodeum with coarse foveae. Short erect hairs sparsely distributed on head and mesosoma; metasoma more densely covered by longer and suberect pilosity.

Etymology: From the Latin *primus*, "first," and *natus*, "born," refers to the old known species in the genus *Kempfidris*.

Type material: Holotype. AMNH-DR-14-519 worker, deposited in the American Museum of Natural History (figs. 26–28). Preserved within a 20 mm × 20 mm section of transparent, yellow amber with internal cracks along the body of the inclusion. Synclusions include two different parasitoid wasps (Platygastridae), a *Gracilidris* sp. ant worker, and a *Proplebia* bee.

Horizon and locality: Early Miocene, Burdigalian (ca. 16 Ma; Iturralde-Vinent and MacPhee, 1996); in amber from the northern mines of the Santiago Province, Dominican Republic.

Comments: This is the second species of the so far monotypic *Kempfidris*, also representing a significant expansion in time and distribution, as the first fossil record for the genus. At first glance, the worker has a series of unique characteristics that could make it difficult to assign it to any known genus, such as the enlarged procoxae, the posterior narrowing of the promesonotum, the deep notopropodeal sulcus, the narrow propodeum dorsal view, and posteriorly sloping petiolar node. However, these attributes can be accommodated within the diagnosis of *Kempfidris*, even with features as disparate as the enormous procoxae. No other known ant (at least in the New World) possesses this characteristic. On the other hand, the sculpture of the head in frontal view, reduced eyes, the overall shape of petiole and postpetiole and the processes of the pygidium strongly resemble the diagnostic characters of *Kempfidris inusualis*. In *K. inusualis*, the last segment of the metasoma has a series of tubules or micropegs, probably associated with exocrine glands, a unique feature within all known ants (Fernández et al., 2014). *K. inusualis* is known from the Amazon basin in Colombia, Ecuador, and Brazil, and for isolated populations in the Brazilian Atlantic Forest (Bahia). Due to its small size, it is rarely collected and is usually identified as other morphologically similar genera, such as *Monomorium*.

Mycetomoellerius Solomon et al., 2019

†***Mycetomoellerius yucahu*** Mera-Rodríguez, Sosa-Calvo, Fiorentino, Barden, and Schultz, sp. nov.

Figures 29, 30

ZooBank LSID: urn:lsid:zoobank.org:act:17C23BFF-87ED-42BD-95A5-089CC500556E

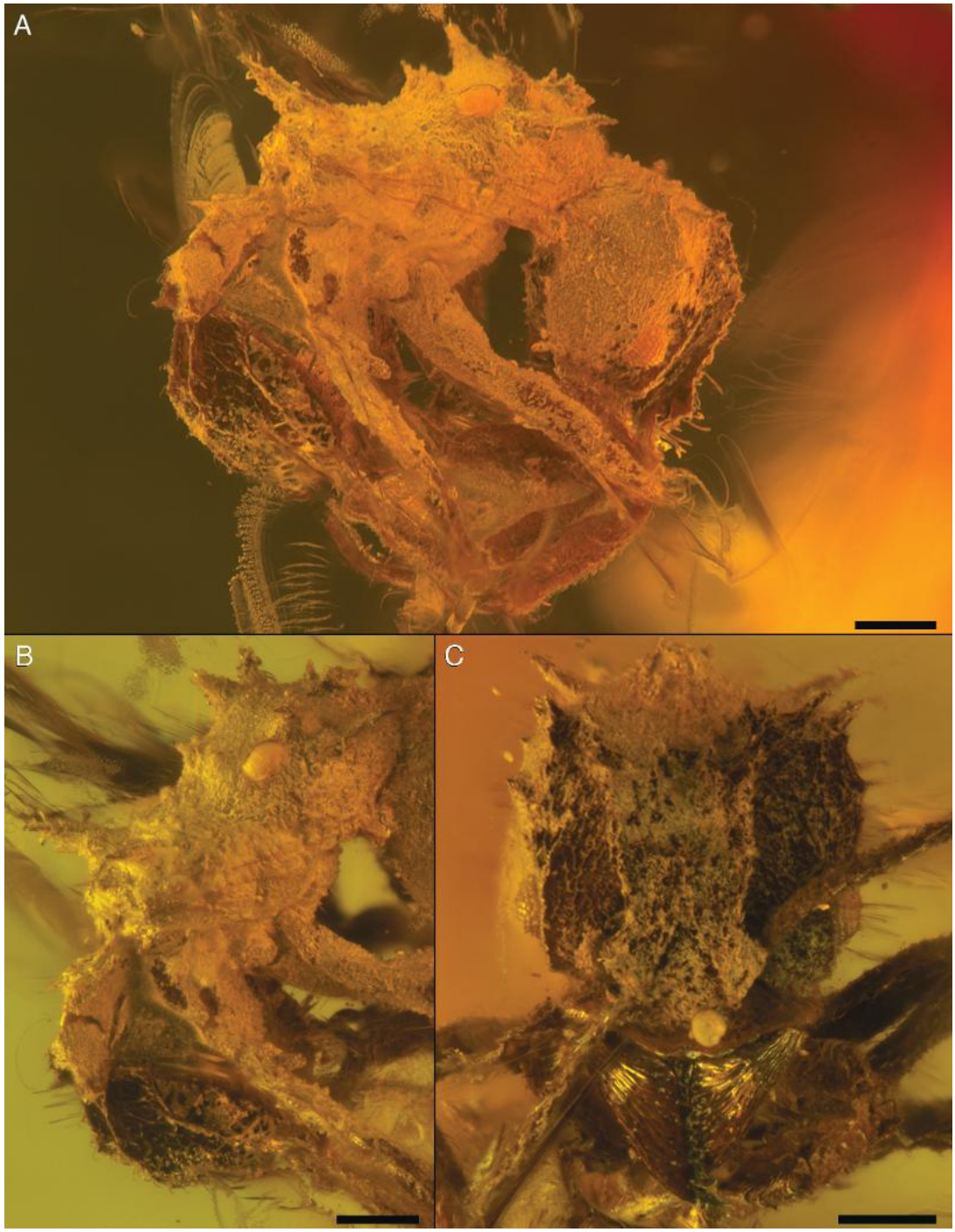


FIGURE 29. Photomicrographs of *Mycetomoellerius yucahu*, sp. nov. (holotype worker, AMNH-DR-15-48). **A.** Lateral view of specimen. **B.** Dorsolateral view of mesosoma, petiole, and postpetiole. **C.** Frontal face-on view of head. Scale bars = 0.25 mm.

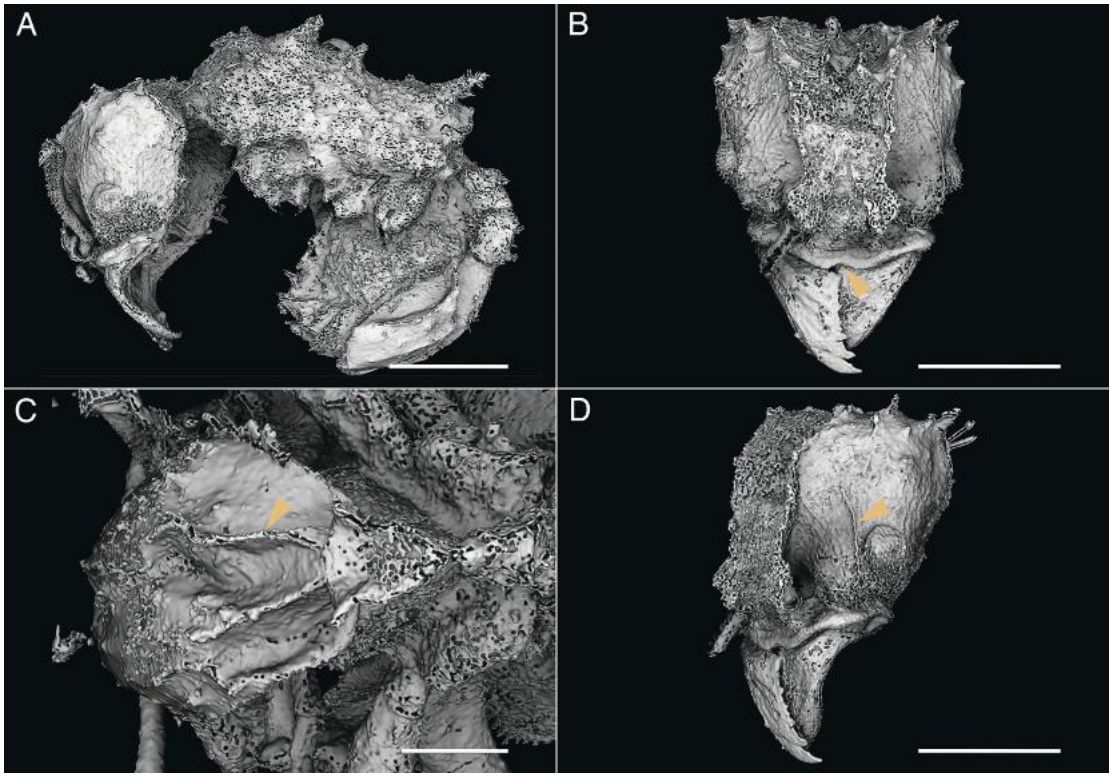


FIGURE 30. Volume renderings of *Mycetomoellerius yucahu*, sp. nov. **A.** Body in lateral view. **B.** Head in full-face view. Arrow indicates the medial clypeal apron. **C.** Close-up of first tergite of gaster in dorsal view. Arrow indicates the conspicuous medial depression. **D.** Head in side view centering the preocular carinae. Arrow indicates the preocular carinae. Scale bars: A, B, D = 0.5 mm; C = 0.2 mm.

Diagnosis (worker): Posterior margin of head concave, with shallow median impression. Cephalic corners angulate, prolonged into spines. Preocular carinae bend weakly mesad above the eyes before fading from view. Frontal carinae strongly developed, extending to the posterior margin of the head to form a carinate scrobe. Posterior cephalic corner ending in spines. Supraocular tubercle conspicuous. Dorsum of mandible striate from outer to masticatory margin. Median pronotal spines present and apparently fused. Propodeal spines long, directed posteriorly, and longer than distance between their bases. Posterior margin of postpetiole straight in dorsal view (i.e., postpetiole in lateral view without posteromedial impression). First gastral tergite with conspicuous median impression and a few tubercles. Lateral and median ridges conspicuous, bearing small denticles.

Holotype worker measurements (in mm): HW 0.88, HL 0.84, EL 0.17, EHT 0.67, EHD 0.34, EHV 0.34, ELT 0.83, ELA 0.28, ELP 0.55, MLP 0.58, SL 0.68, WL 1.10, PcL 0.42, MH 0.48, PrW 0.50, MfL 1.18, PeW 0.16, PeH 0.198, PeL 0.32, PpeW 0.17, PpeH 0..22, PpeL 0.276, GL 0.89, TL 1.69.

DESCRIPTION (worker): Head. Subquadrate, slightly longer than wide. Lateral margins of head diverging above level of eyes, then narrowing toward cephalic corners. Posterior margin of head concave, with shallow median impression. Posterior and lateral margins of head tuberculate, with largest tubercles on cephalic corners. Cephalic

corners angulate, prolonged into spines. Frontal carinae diverge from vertexal carinae at level of supraocular tooth. Both the frontal and vertexal carinae continue to the posterior cephalic margin and end in small denticulate tubercles. Preocular carinae bend weakly mesad above the eyes before fading from view. Frontal carinae strongly developed, extending to the posterior margin of the head to form a carinate scrobe. Posterior cephalic corner ending in spines. Supraocular tubercle conspicuous. Eye convex, interrupting contour of lateral cephalic margin. Frontal lobe triangular, posterior margin approximately half the length of medial margin; angle between lateral and posterior margins obtuse, and angle between lateral and medial margins acute (as defined in Ješovnik and Schultz, 2017). Anterior margin of clypeal apron medially concave. Antennal scape uniformly thick from base to apex, without a basal lobe, and barely surpassing posterior margin of head. Antenna 11-segmented. Mandibles triangular, with outer margins sinuate, and masticatory margin with nine teeth. Apical and preapical teeth distinctly larger followed by a series of six small teeth. Dorsum of mandible striate from outer to masticatory margin. Mandibles with long setae that extend from outer to masticatory margin.

Mesosoma: promesonotal suture not well defined. Median pronotal spines present and apparently fused. Lateral pronotal spines present, blunt at the tip and projecting horizontally, not vertically. Inferior pronotal corner developed into a spatulate tooth. Mesosomal spines large and aculeate, bearing tubercles and curved setae. Anterior mesonotal spines present and blunt at tips. Anterior mesonotal spines project vertically and are subequal in length but thicker at the base compared to lateral pronotal spines. Posterior mesonotal spines present. Dorsopropodeal ridge reduced to two small denticles. Propodeal spines long, directed posteriorly and longer than distance between their bases.

Metasoma: Petiole sessile; longer than wide, with a pair of sharply pointed tubercles. Postpetiole longer than wide. Dorsum of postpetiolar node with two rows of dentate tubercles, increasing in size posteriorly. Postpetiole in lateral view without posteromedial impression; in dorsal view, posterior margin straight. Postpetiolar node with two lateral carinae, each bearing a row of teeth, increasing in size posteriorly. First gastral tergite with conspicuous median impression and a few tubercles. Lateral and median ridges conspicuous, bearing small denticles.

Sculpturing and setae: Head and mesosoma tuberculate, some tubercles with short, curved setae. Metasoma with conspicuous lateral and median ridges bearing small denticles. Head with standing setae.

Etymology: From the Taino word *Yúcahu* or *Yocahu*. In Taino mythology, Yúcahu refers to the principle "zemi," or deity, of agriculture as well as the "zemi" of peace and tranquility. Here, the name is in reference to the agricultural behaviour of the fungus-growing ants.

Type material: Holotype. AMNH-DR-15-48 worker, deposited in the American Museum of Natural History (figs. 29–30). Preserved within a 12 mm by 7 mm section of transparent yellow amber. Synclusions include a small mite (Mesostigmata).

Horizon and locality: Early Miocene, Burdigalian (ca. 16 Ma; Iturralde-Vinent and MacPhee, 1996); in amber from the Northern mines of the Santiago Province, Dominican Republic.

Comments: We assign this species to the genus *Mycetomoellerius* Solomon et al. (2019) based on the combination of the following traits: presence of an antennal scrobe formed by the frontal and preocular carinae; posterior margin of the head with a strong median impression; conspicuous supraocular tubercles; the posterior margin of the postpetiole straight in dorsal view; propodeal spines long; and first gastral tergite with very strong pairs of lateral and median carinae as in, e.g., *M. isthmicus* (Solomon et al., 2019; Dos Santos et al., 2025).

While *M. yucahu* shares several diagnostic traits with other *Mycetomoellerius* species, it can be distinguished from most of them by the strongly striate mandibles, a trait uncommon in the genus,



FIGURE 31. Photomicrographs of *Paratrachymyrmex primaevus*, comb. nov. (worker, DR_RP_359). **A.** Dorsolateral view of specimen. **B.** Frontal, lateral view of head. Scale bars = 0.5 mm.

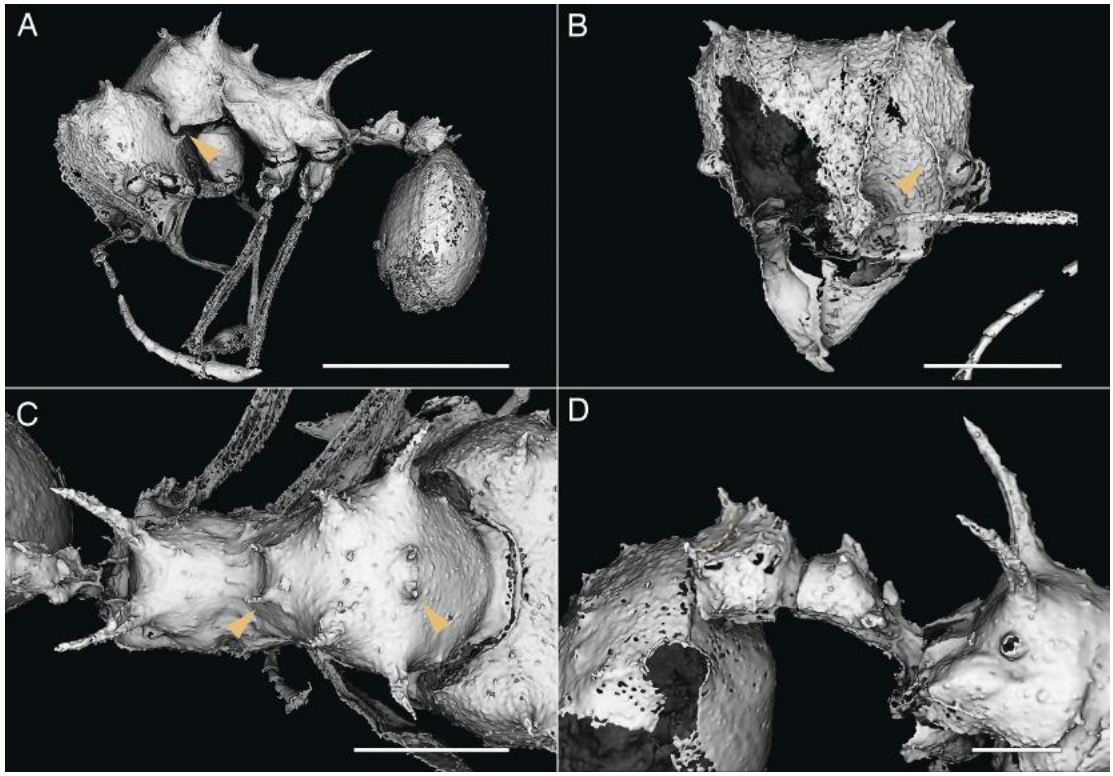


FIGURE 32. Volume renderings of *Paratrachymyrmex primaevus* comb. nov. **A.** Body in lateral view. Arrow indicates the lateral pronotal spines. **B.** Head in full-face view. Arrow indicating preocular carinae. **C.** Mesosoma in dorsal view. Arrows indicate the anterior pronotal spines and the posterior mesonotal spines. **D.** Close-up of petiole and postpetiole in lateral view; dashed line outlines the convex posterior margin of postpetiole. Scale bars: A = 1 mm, B, C = 0.5 mm; D = 0.2 mm.

where mandibles are typically smooth and shiny. The mandibles of *M. yucahu* are distinctly striate from base to apex, resembling those of *M. iheringi*. However, *M. yucahu* can be further separated from *M. iheringi* by other morphological differences. For instance, *M. yucahu* has convex eyes, while *M. iheringi* has flat eyes. Additionally, the gaster in *M. iheringi* does not present conspicuous lateral and median ridges seen in *M. yucahu*. Other species in *Mycetomoellerius*, such as *M. atlanticus* and *M. isthmicus* also present conspicuous lateral and median ridges. However, they differ from *M. yucahu* in that *M. atlanticus* has smooth mandibles, and *M. isthmicus* has median pronotal spines absent.

Paratrachymyrmex Solomon et al., 2019

†*Paratrachymyrmex primaevus*
(Baroni Urbani, 1980b), comb. nov.

Figures 31, 32

Diagnosis (worker): Midposterior margin of head moderately concave. Preocular carinae slightly curved mesad above eye, traversing approximately one third the distance between eye and frontal carinae. Dorsum of mandible striate from outer to masticatory margin. Ventral margin of head (i.e., postgena) with acute well-defined tooth. Median pronotal spines present,

separated, not fused at base. Mesosomal spines long, spinelike, bearing tubercles and several setae. Propodeal spines long and sharply pointed. Petiolar peduncle long. Dorsum of postpetiole with posteromedial impression in lateral view. In dorsal view, posterior margin of the postpetiole convex; in lateral view, carina forming the posterior margin of postpetiole overhanging the gaster. First gastral tergite with inconspicuous and short lateral ridges and median ridges absent.

Worker measurements (in mm): HW 1.03, HL 0.86, EL 0.13, EHT 0.84, EHD 0.46, EHV 0.38, ELT 0.88, ELA 0.34, ELP 0.54, MLP 0.62, SL 0.91, WL 1.16, PcL 0.37, MH 0.50, PrW 0.60, MfL 1.15, PeW 0.07, PeH 0.13, PeL 0.35, PpeW 0.21, PpeH 0.21, PpeL 0.23, GL 0.76, TL 3.87.

REDESCRIPTION (worker). Head: Subquadrate, slightly wider than long. Lateral margin of head diverging above eyes, interrupted by a conspicuous supraocular tooth, narrowing toward cephalic corners. Midposterior (vertexal) margin of head moderately concave. Posterior and lateral margin of head tuberculate, with largest tubercules on cephalic corners. Cephalic corners slightly rounded, convex. Frontal carinae reaching posterior margin of head. Preocular carinae slightly curved mesad above eye, traversing approximately one third the distance between eye and frontal carinae. Eye convex, interrupting contour of lateral cephalic margin in full-face view. Frontal lobe subtriangular and rounded, prolonged anteriorly. Antennal scape uniformly thick from base to apex, without basal lobe. Antennal scape long, surpassing cephalic margin by approximately one third of its length. Antenna with 11 segments. Mandible triangular, with outer margin sinuate, and nine teeth in its masticatory margin. Apical and preapical teeth distinctly larger followed by six medium to small teeth. Dorsum of mandible striate from outer to masticatory margin. Clypeal apron notched medially. Ventral margin of head (i.e., postgena) with acute well-defined tooth.

Mesosoma: Promesonotal suture absent. Median pronotal spines present, separated, not fused at base. Lateral pronotal spines present, acute, projecting laterally. Anterior mesonotal spines present, acute, projecting upward. Inferior pronotal tubercle forming a rounded tooth. Mesosomal spines large, spinelike, bearing tubercles and several setae. Anterior mesonotal spines shorter and thicker at base compared to lateral pronotal spines. Posterior mesonotal spines present. Dorsopropodeal ridge reduced to two small denticles. Propodeal spines present, long, sharply pointed, directed posteriorly.

Metasoma: Petiolar peduncle long, in this way differing from extant species of higher fungus-growing ants, which have a short petiolar peduncle or sessile petiole. Petiolar node longer than wide. Dorsum of the petiolar node with a pair or dentate tubercles. Subpetiolar process absent, sternum not superficially convex or dentate. Postpetiole subquadrate. Dorsum of the postpetiolar node with at least two pairs of teeth. Dorsum of postpetiole with posteromedial impression in lateral view. In dorsal view, posterior margin of the postpetiole convex, in lateral view, carina forming the posterior margin of postpetiole overhanging the gaster. Subpospetiolar process absent. First gastral tergite with a few small denticles. First gastral tergite with inconspicuous and short lateral ridges and median ridges absent.

Sculpturing and setae: Body tuberculate, tubercles small with short, curved setae.

Material examined: AMNH-DR-RP-359 worker, deposited in the American Museum of Natural History (figs. 31, 32). Preserved within a 40 mm by 35 mm section of transparent yellow amber. Synclusions include a small spider (Salticidae), *Schismiscapus*, *Pheidole*, Oribatidae, 9 conspecific *Paratrachymyrmex*, plant debris, and nest debris. AMNH DR-14-1135, AMNH DR-16-330, and AMNH DR-10-248, also deposited in the American Museum of Natural History. Do-377-K-1 holotype worker, Do-377-K-2-3-5+6+10-11-13 paratype workers, deposited in the State Museum of Natural History Stuttgart (SMNS), Germany.

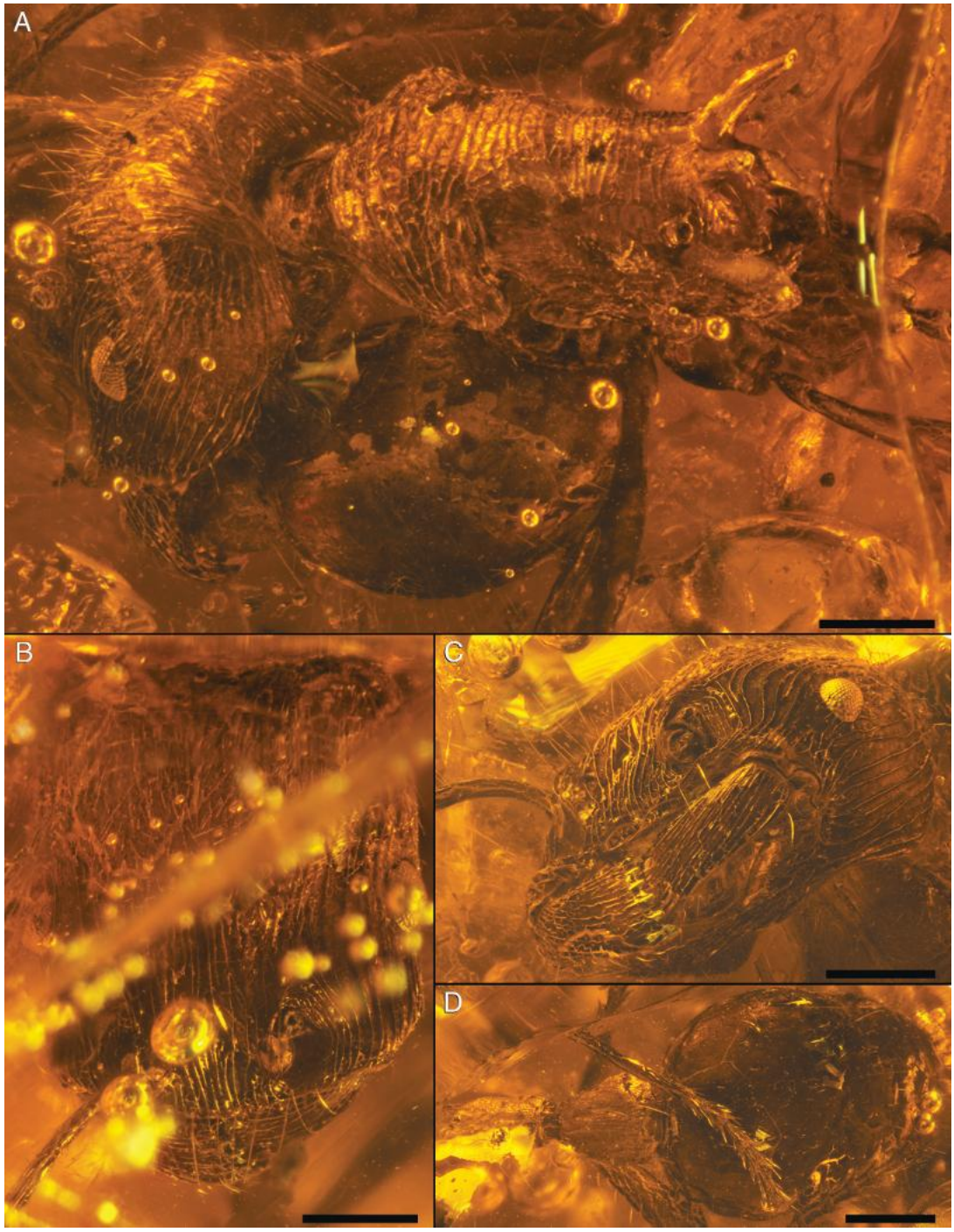


FIGURE 33. Photomicrographs of *Pogonomyrmex tiempopogo*, sp. nov. (holotype worker, PALE-44317). **A.** Dorsolateral view of specimen, excluding metasoma. **B.** Frontal full-face view of head. **C.** Anterolateral view of head. **D.** Dorsal view of petiole, postpetiole, and gaster. Scale bars = 0.5 mm.

Horizon and locality: Early Miocene, Burdigalian (ca. 16 Ma; Iturralde-Vinent and MacPhee, 1996); in amber from the northern mines of the Santiago Province, Dominican Republic.

Comments: We transfer this species, formerly assigned to *Mycetomoellerius* Solomon et al. (2019) into the genus *Paratrachymyrmex* Solomon et al. based largely on character states defined in both Solomon et al. (2019) and Dos Santos et al. (2025), including: preocular carina weakly developed, faintly curving mesad above the eye; median pronotal spines separated and distinct; posterior margin of postpetiole in dorsal view convex, not emarginate; dorsum of mandibles striate. The species differs from other members of the genus, however, in having a moderately well-developed supraocular tooth and very long propodeal spines. *Paratrachymyrmex diversus*, *P. intermedius*, and *P. mandibularis* have moderately well-developed propodeal spines, but none as long as those in *P. primaevus*. *Paratrachymyrmex primaevus* shares with most species of *Trachymyrmex* the presence of a faint pair of abbreviated lateral carinae and the absence of median carinae on the first gastral tergite, a trait also found in *Paratrachymyrmex* species such as *P. intermedius*. *Paratrachymyrmex primaevus* has a long petiolar peduncle, a character more commonly observed in lower than in higher fungus-growing ant genera. In addition, *P. primaveus* has an acute well-defined tooth on the ventral margin of head (i.e., postgena), a trait uncommon in *Paratrachymyrmex*, *Trachymyrmex*, and *Mycetomoellerius*, but common in leaf-cutting ant genera like *Acromyrmex* and *Atta*.

Pogonomyrmex Mayr, 1868

Pogonomyrmex tiempopogo Barden and Fiorentino, sp. nov.

Figures 33, 34

ZooBank LSID: urn:lsid:zoobank.org:act:45F114B6-54AE-4442-8A07-FF79F091AE91

Diagnosis (workers): Head elongate with widely spaced longitudinal rugosity, lacking robust psammophore. Dorsum of mesosoma with transverse rugosity while mesopleuron and metapleuron with longitudinal rugosity. Pronotum and mesopleuron with ventrally distending flanges that partially obscure procoxa in lateral view. Propodeal spine enormous and slightly flattened dorsally. Petiole elongate with peduncle comprising half its length.

Holotype worker measurements (in mm): HW 1.81, HL 1.98, EL 0.34, EHT 1.28, EHD 0.63, EHV 0.66, ELT 1.77, ELA 0.74, ELP 1.04, MLP 0.99, SL 1.59, WL 2.63, PcL 0.97, MH 0.82, PrW 1.16, MfL 1.99.

DESCRIPTION (worker). Head: Slightly longer than wide in frontal view, vertex mildly concave; lateral margins flat, widening slightly near clypeus; posterior margin flattened and posteroanterior length approximately 1.5× dorsoventral depth in lateral view. Occipital foramen deeply impressed and boomerang shaped, 2× to 3× wider than long at beginning of elevational declivity. Eyes situated at posteroanterior midline in frontal view and positioned dorsad in lateral view approximately ⅔ along the dorsoventral axis; eyes bulging, extending beyond lateral margins of head by approximately one half their maximal width. In frontal view, frontal carinae originate distant from, but along the axis of, the anterior margin of the eyes at angle ~30° away from anteroposterior midline of head; cuticle deeply impressed beneath frontal carinae; cuticle impression is free from fine sculpturing and rugosity, oval shaped, and extends to the anterior clypeal margins. Antennal sockets with demarcated toruli along anterior and lateral margins. Basal margin of scape with ringlike flange; scape bow shaped, this curvature extending approximately 50% its length. Mandibles triangular, masticatory margin oblique, comprising two distinct margins with four apically positioned and two basally positioned teeth, respectively.

Mesosoma: Anterior margin of pronotum bilobed in dorsal view, dorsal margin of mesosoma without interruption between sclerites; conspicuous circular flange present at posteroventral margin of pronotum, this cuticle flattened and laterally

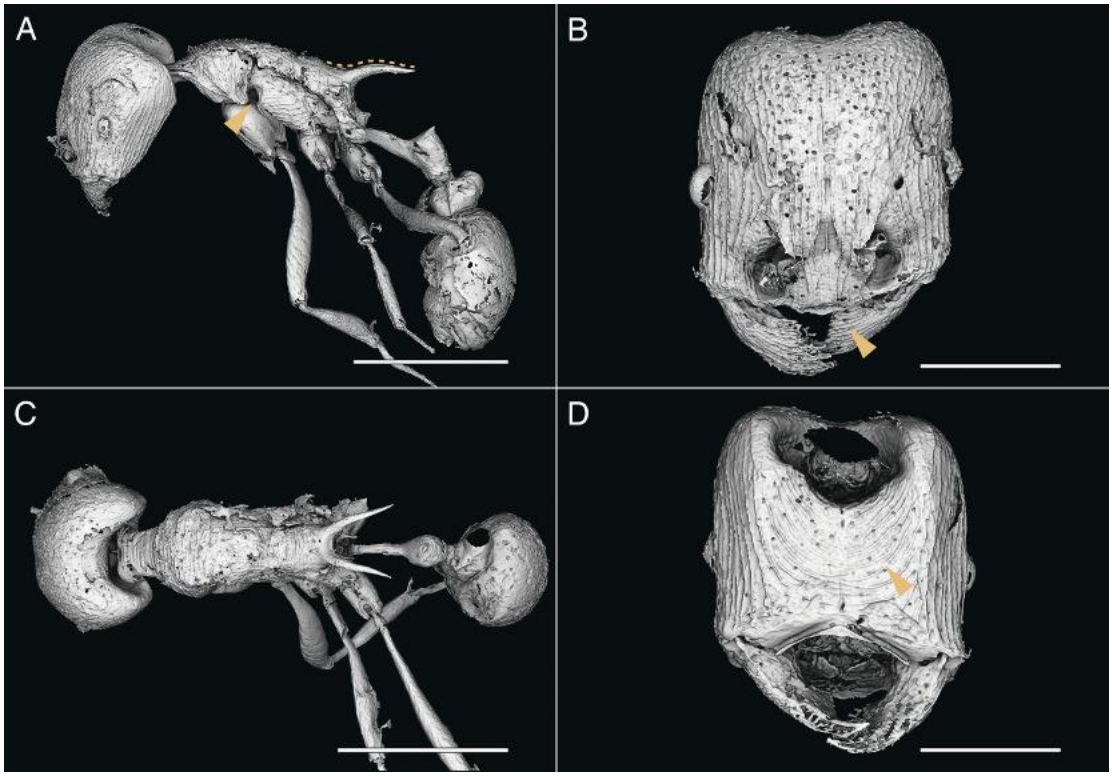


FIGURE 34. Volume renderings of *Pogonomyrmex tiempopogo*, sp. nov. **A.** Body in lateral view. Arrow indicates flanges forming a socket above the procoxae; dashed line outlines the shape of the propodeal spine. **B.** Head in full-face view. Arrow indicates the sculpturing of the mandible. **C.** Body in dorsal view. **D.** Head in ventral view. Arrow indicates the sculpturing on the postgenal bridge. Scale bars: A, C = 2 mm; B, D = 1 mm.

expanded over procoxa, similar subrectangular flange on mesopleuron, these two flanges form a kind of a socket around procoxa. Deep sutures present between propleuron and mesopleuron, with less conspicuous sutures between the mesopleuron and propodeum. Propodeum with elongate, slightly recurved spine approximately equidistant to length of propodeum in lateral view; gaping and posterior-facing propodeal spiracle present just below spine. Propodeal flange above petiole: posterodorsally pointed. Procoxae elongate, approximately 2× longer than wide; profemur and protibial distally swollen, width approximately 2× wider above terminus. Metatibial spur finely pectinate; tarsomeres densely setose.

Metasoma: First petiole segment with elongate peduncle comprising ~½ of length, petiole node face gradually increasing in elevation in lateral view with distinct dorsal point followed by slight slope comprising gradually declivitous dorsal petiole margin. Postpetiole bell-shaped with deep tergosternal suture; ventral margin of postpetiole slightly ventrad to ventral petiole margin, maximal dorsal margins of petiole and postpetiole approximately coequal.

Sculpturing and setae: Cuticle of head capsule conspicuously rugose, longitudinally along dorsal margin and in concentric pattern along hypostoma; spacing between rugose channels is greatest near lateral margins of the head, channel width between compound eyes and antennal carinae is approximately 2× the width of medial head rugosity and sinuous. Mandibles longitudinally rugose. Hypostoma slightly impressed medially.

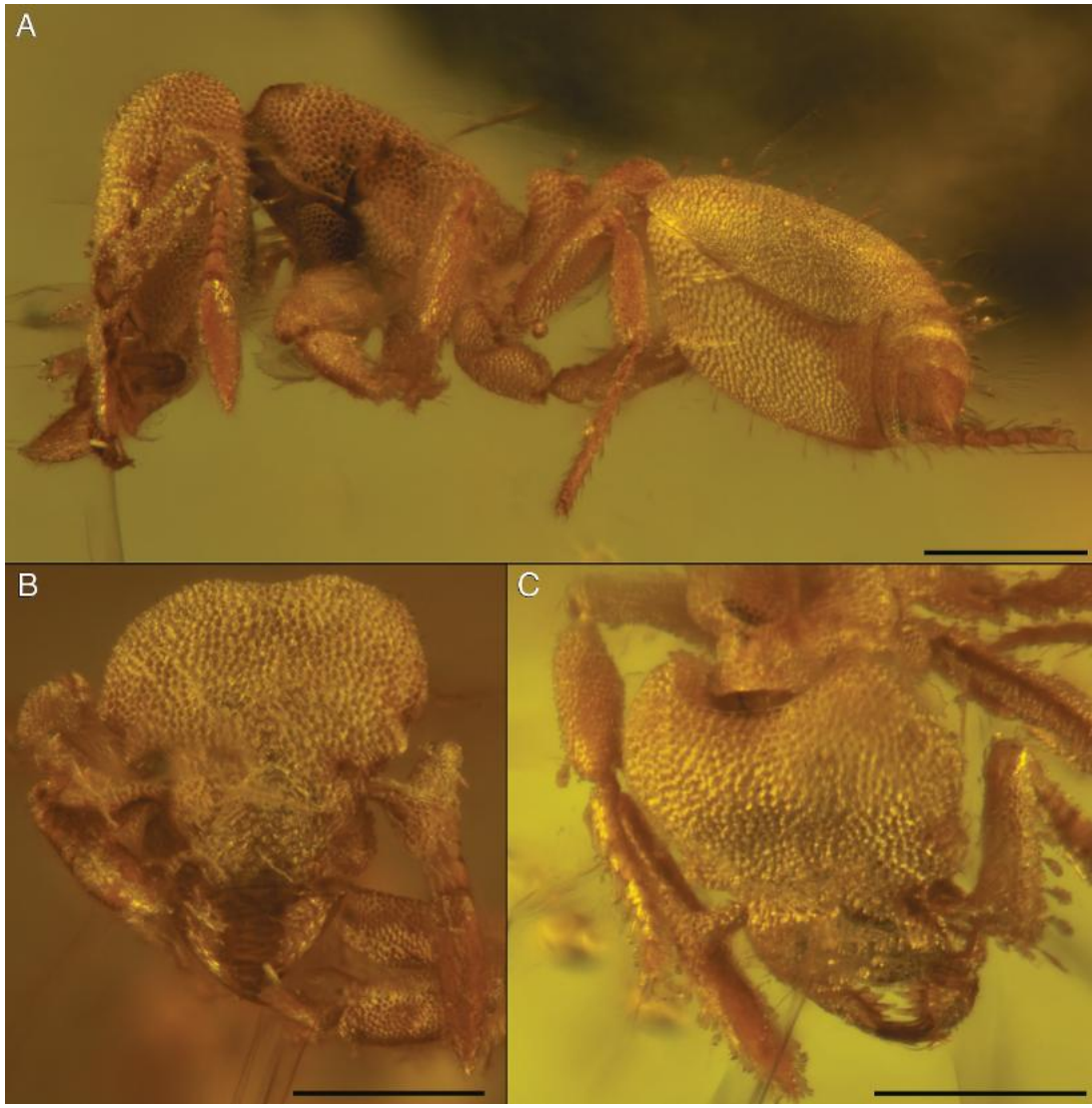


FIGURE 35. Photomicrographs of *Rhopalothrix macorixia*, sp. nov. (holotype worker, AMNH_DR_14_935). **A.** Lateral view of specimen. **B.** Frontal full-face view of head. **C.** Dorsolateral view of head. Scale bars = 0.25 mm.

Psammophore comprises sparse, fine setae with a maximum length of ~0.4mm. Mesosoma with latitudinal rugosity present along pronotum and dorsal margins of sclerites; mesopleuron and metapleuron with longitudinal rugosity. Dorsal margin of postpetiole with two elongate pairs of widely spaced longitudinal setae. Gaster glabrous, posterior margins of abdominal tergites three, four, and five with sparse setae.

ETYMOLOGY: From the Spanish *tiempo*, meaning "time" and "pogo" from the Greek noun *pogon* (πώγων), meaning "beard," referring to the generic name *Pogonomyrmex* and its discovery in the fossil record.

TYPE MATERIAL: Holotype. PALE-44137 worker, deposited in the Museum of Comparative Zoology at Harvard University in Cambridge, MA (figs. 33, 34). Preserved within a 20 mm by 15 mm

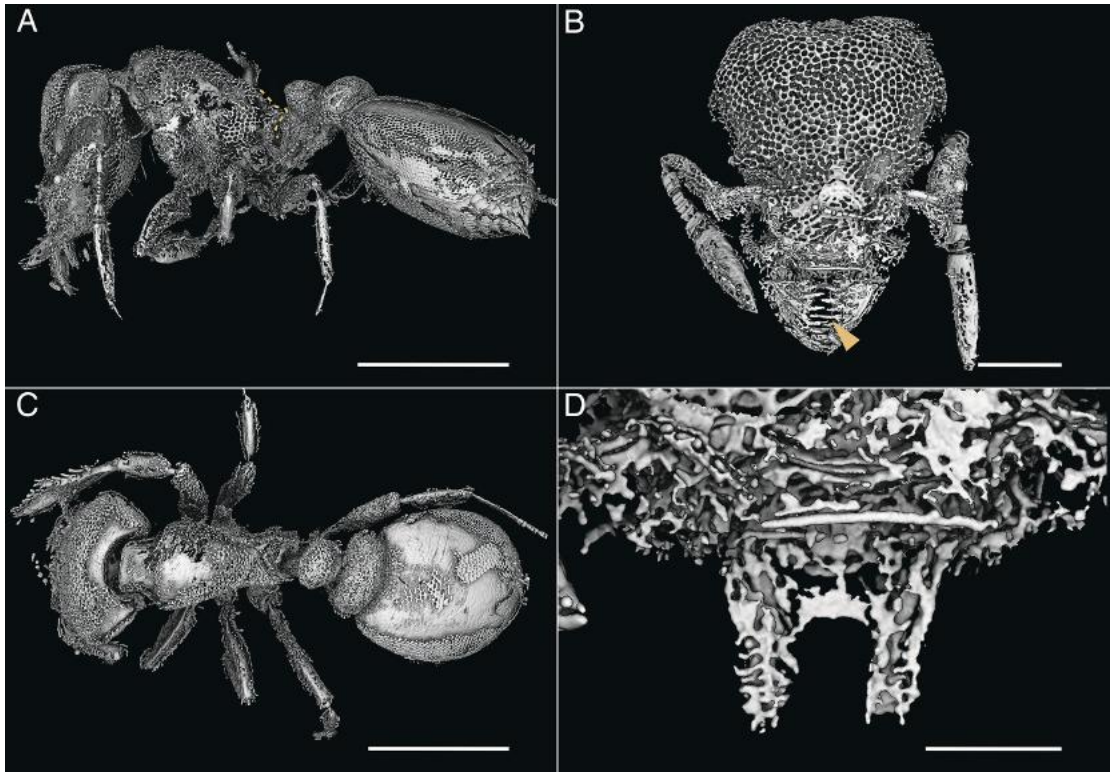


FIGURE 36. Volume renderings of *Rhopalothrix macorixia*, sp. nov. **A.** Body in lateral view. **B.** Head in full-face view. Arrow indicates masticatory margin, **C.** Body in dorsal view. **D.** Head in ventral view. Scale bars: A, C = 0.5 mm, B = 0.2 mm, D = 0.1 mm.

section of transparent yellow amber with internal cracks, bubbles and debris along the body of the inclusion. Synclusions include three partial conspecific *P. tiempopogo* ants.

Horizon and locality: Early Miocene, Burdigalian (ca. 16 Ma); in amber from the Northern mines of the Santiago Province, the Dominican Republic.

Comments: P*ogonomyrmex tiempopogo* is most readily distinguishable from other species by its enlarged propodeal spine. This spine is approximately as long as the propodeum itself, reminiscent of some species in the genus *Vombisidris*. There are three extant *Pogonomyrmex* species on Hispaniola—*P. aterrimus*, *P. saucius*, and *P. schmitti* (Johnson and Cover, 2015)—*P. tiempopogo* may represent a distinct lineage on the basis of its distinct mesosomal sculpturing and distending flanges on the pronotum and mesopleuron. These flanges, which partially obscure the procoxa, are similar to those found in *P. striatinodus* from Brazil (Fernández and Palacio, 1997).

Rhopalothrix Mayr, 1870

†***Rhopalothrix macorixia*** Probst, Barden, and Fiorentino, sp. nov.

Figures 35, 36

ZooBank LSID: urn:lsid:zoobank.org:act:504EA902-8767-47F9-9E78-FFE9FBE4728A

Diagnosis (worker): Comparatively small species (TL 1.77 mm). Mandible subtriangular, with a single row of teeth; apical fork devel-

oped. Pilosity of face sparse and decumbent, head lacking specialized setae. Eyes minute. Mesosoma lacking specialized setae, apart from a single erect pair near the notopropodeal sulcus. Propodeal spines translucent, lamellate.

Holotype worker measurements (in mm): HW 0.56, HL 0.63, EL 0.03, EHT 0.27, EHD 0.08, EHV 0.19, ELT 0.55, ELA 0.29, ELP 0.27, MLP 0.26, SL 0.19, SLL 0.08, WL 0.60, PcL 0.18, MH 0.22, PrW 0.32, MfL 0.36, PeL 0.18, PpeL 0.11, GL 0.51, TL 1.77, CI 97.6, SLI 44.

Description (worker): Head: Trapezoidal, vertexal margin medially concave. Occipital carina rounded; occiput carinate. Mandibles subtriangular, dorsal surface convex; masticatory margin with a single row of about seven slender teeth, middle tooth largest; intercalary teeth prominent, some about half as long as apical tooth; apical fork conspicuous. Labrum as long as broad, trapezoidal, distal margin bilobed; lobes bluntly triangular, inner margins shallowly sloping to broad median cleft. Antennal scapes with conspicuous basal lobe; antennal scrobe broad, delimited uniformly with raised carina, sitting below deep antennal fossa. Eyes minute.

Mesosoma: Promesonotum slightly convex; arcuate promesonotal groove lacking dorsal impression, notopropodeal sulcus weakly impressed. Propodeum with dorsal face longer than posterior, both faces distinct, meeting at right angle in infradental lamella; propodeal spiracle small.

Metasoma: Petiole with short neck, node convex with posterior face elongate; postpetiole short and broad.

Sculpturing and setae: Body densely foveolate. Ventral surface of head punctate. Clypeus coarse. Mandible surface punctate. Specialized erect setae present on first gastral tergite, uniformly covering entire tergite, at least posterior half with abundant seta. Dorsal surface of scape with sparse subdecumbent pilosity; erect spatulate setae on external margin of scape; sparse pilosity on clypeus and face. Specialized spatulate setae sparse (broad, flat, and rounded tip), with a single pair of erect setae near matenotal groove and on petiolar node; first gastral tergite with eight or nine rows of spatulate setae, more abundant at posterior half. Legs with sparse subdecumbent setae.

Etymology: *Rhopalothrix macorixia*, sp. nov., is named in homage to the Macorix people, an indigenous group that historically inhabited the island of Hispaniola. The Macorix were semisedentary, with a lifestyle deeply connected to the land, also alluding to the ecological environment in which this species was found. *Rhopalothrix* are typically associated with the leaf-litter substrate, but the individual described here may have wandered into the vegetation and was ultimately preserved in tree resin. The epithet ties this species to a broader understanding of both its natural habitat and the way in which the Macorix people's seminomadic, yet grounded, way of life parallels the ant's movement through the environment.

Type material: *Holotype*. AMNH_DR_14_935 worker, deposited in the American Museum of Natural History (figs. 35, 36). Preserved within an 8 mm × 9 mm section of transparent, yellow amber. No synclusions.

Horizon and locality: Early Miocene, Burdigalian (ca. 16 Ma); in amber from the northern mines of the Santiago Province, the Dominican Republic.

Comments: *Rhopalothrix macorixia* shares similarities in overall morphology with other species described from Central America, such as *R. therion* (Longino and Boudinot, 2013) and *R. subspatulata* (Longino and Boudinot, 2013). However, the mandible structure is distinctly not falcate, instead being subtriangular, making them much more similar to the mandibles of the recently described *Rhopalothrix amati* (Guerrero et al., 2024). Another key differentiator is that many described *Rhopalothrix* have dense head pilosity of spatulate setae, and this fossil lacks these. *Rhopalothrix macorixia* can be distinguished from all other *Rhopalothrix* valid species by its distinctive pilosity, size, and sculpture. Moreover, eye size is small (EL 00.3/

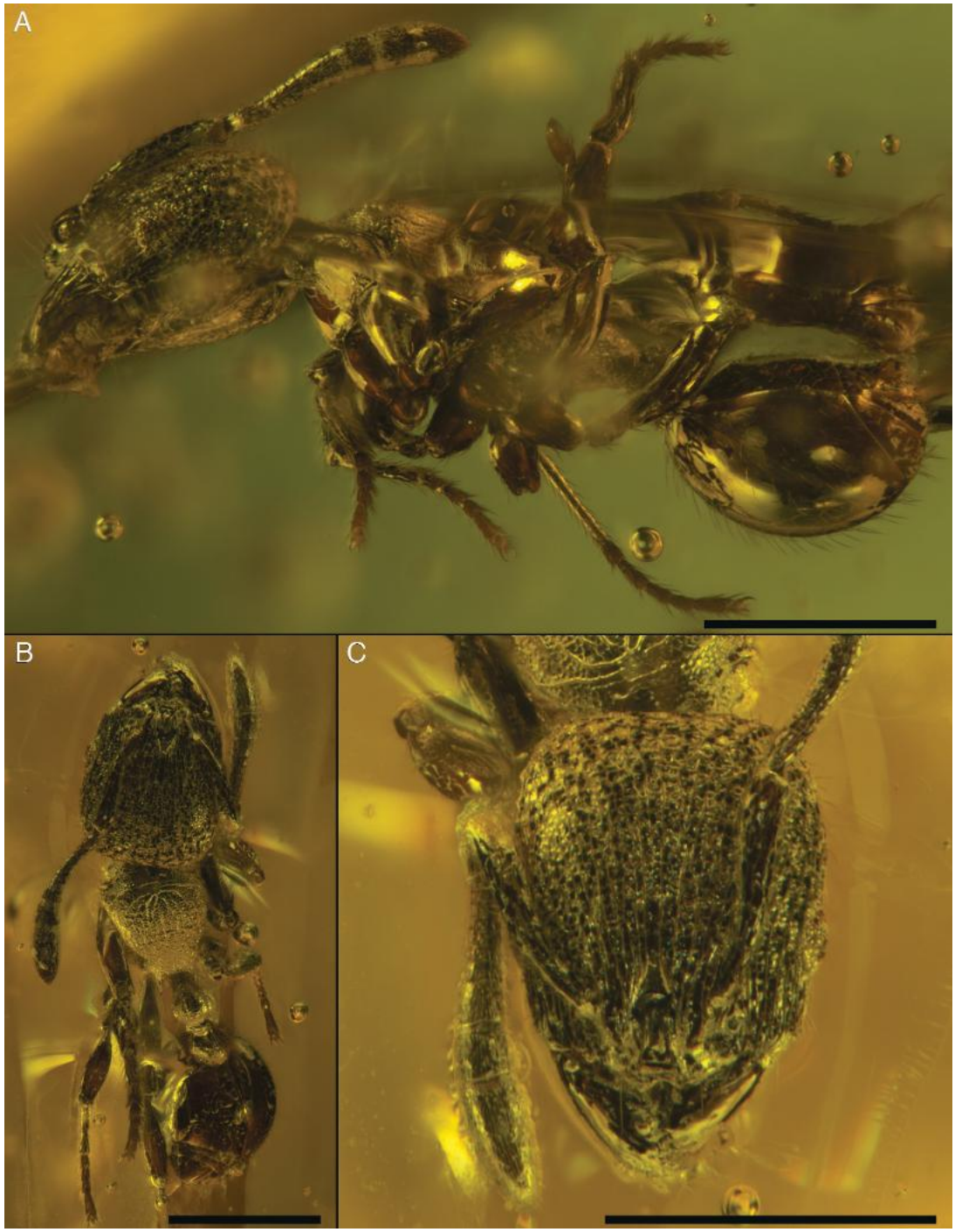


FIGURE 37. Photomicrographs of *Rogeria primaeva*, sp. nov. (holotype worker, MNHNSD FOS 18.124). **A.** Lateral view of specimen. **B.** Dorsal view of specimen; note that gaster is inverted. **C.** Frontal view of head. Scale bars = 0.5 mm.

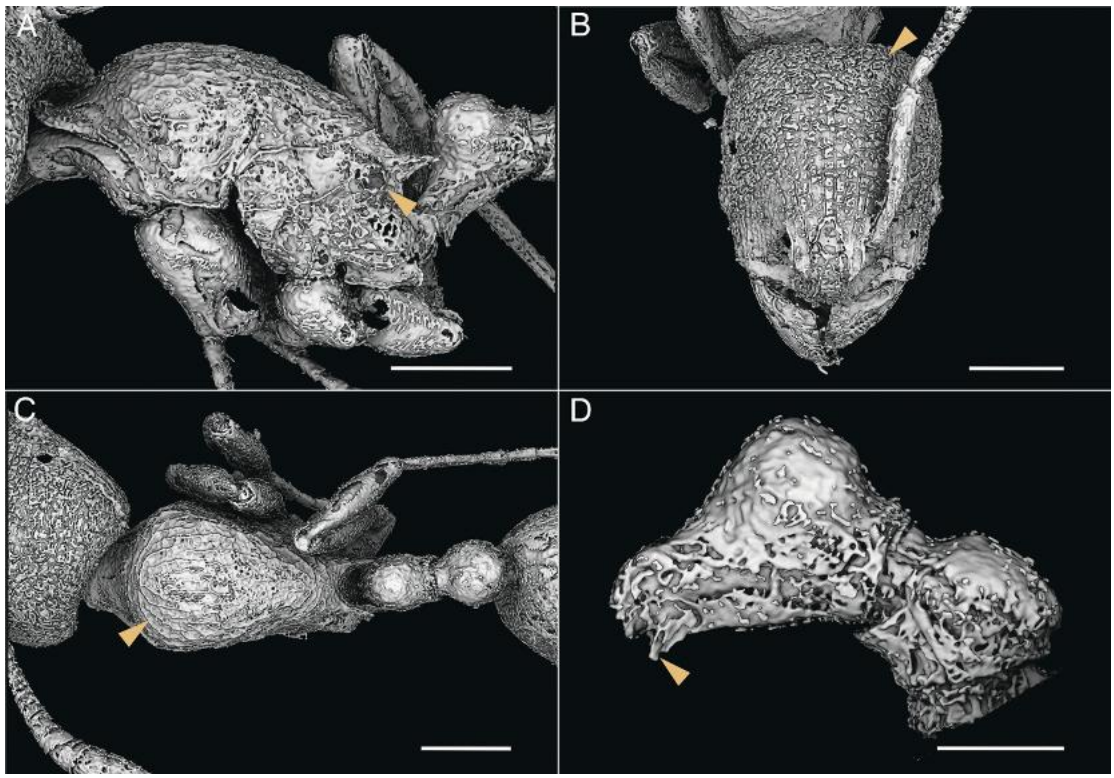


FIGURE 38. Volume renderings of *Rogeria primaeva*, sp. nov. MNHNSD FOS 18.124). **A.** Mesosoma in lateral view. Arrow indicates the propodeal spiracle. **B.** Head in full-face view. Arrow indicates the sculpturing on the head. **C.** Body in dorsal view. Arrow indicates the sculpturing on the pronotum. **D.** Close-up of petiole and postpetiole in lateral view. Arrow indicates the subpetiolar projection. Scale bars: A–C = 0.2 mm, D = 0.1 mm.

HL 0.63 = 0.048) when compared to, for example, *R. subspatulata*.

Rogeria Emery, 1894

†***Rogeria primaeva*** Feitosa, Barden, and Fiorentino, sp. nov.

Figures 37, 38

ZooBankLSID:urn:lsid:zoobank.org:act:0C2794CE-F055-4ED1-B3A9-DD7EF75DFBD1

Diagnosis (worker): Anterior margin of the clypeus medially concave. Eye well developed, with about 20 ommatidia. Dorsal profile of the mesosoma continuous, slightly inclined posteriorly toward the propodeal spine. Propodeal spine comparatively short. Subpetiolar process spiniform anteriorly. Petiolar node dorsally rounded, with the anterior face faintly ascending from the dorsal margin of the peduncle, without forming a conspicuous angle with the latter. Postpetiole somewhat elongate; postpetiolar node dorsally rounded and abruptly truncated posteriorly, so that its highest point is located posterior to its midlength in lateral view. Sculpturing predominantly areolate-rugose on the dorsum of the head, with intervals bearing areolate microsculpture. Irregular longitudinal rugae on the dorsum and sides of the promesonotum, metapleura, and mesopleura, with microareolate intervals. Petiole and

postpetiole microareolate, with the central disc predominantly smooth in dorsal view. Dorsum of the head, mesosoma, and gaster densely covered by long and suberect hairs.

Holotype worker measurements (in mm): HW 0.46, HL 0.56, EL 0.09, EHT 0.29, EHD 0.13, EHV 0.16, ELT 0.55, ELA 0.25, ELP 0.31, MLP 0.28, SL 0.36, WL 0.62, PcL 0.22, MH 0.29, PrW 0.34, MfL 0.46.

DESCRIPTION (worker): Head: Subrectangular, longer than wide, with subparallel lateral margins. Vertexal margin straight. Mandible subtriangular, masticatory margin apparently with five teeth. Anterior margin of the clypeus medially concave. Frontal carina short, not reaching the anterior margin of the eye. Antennal scrobe absent. Antenna 12-segmented with a well-defined three-segmented club. Scape short, failing to reach the vertexal border by at least 3× its maximum width. Eye elliptical and well developed, with about 20 ommatidia.

Mesosoma: Dorsal profile of the mesosoma continuous, slightly sloping posteriorly toward the propodeal spine. In dorsal view, humeral corners convex and lateral margins of promesonotum converging posteriorly toward the propodeum. Notopropodeal sulcus obsolete. Propodeum set slightly below the level of the promesonotum. Propodeal spine comparatively short and slightly curved ventrally at the apex. Opening of the propodeal spiracle large and rounded. Propodeal lobe subtriangular.

Metasoma: In lateral view, petiolar peduncle minimally shorter than the length of the petiolar node; subpetiolar process long, forming a ridge below the peduncle with a spiniform anterior projection; in dorsal view, petiolar node as long as wide; in lateral view, petiolar node dorsally rounded, with the anterior face faintly ascending from the dorsal margin of the peduncle, without forming a conspicuous angle with the latter. In lateral view, postpetiole somewhat elongate; postpetiolar node dorsally rounded and abruptly truncate posteriorly, so that its highest point is located posterior to its midlength in lateral view; anteroventral angle of the sternum not projected; in dorsal view, postpetiole rounded.

Sculpturing and setae: Mandible smooth and shining, except for spaced piligerous punctures. Central disc of clypeus mostly smooth, with a pair of median carinulae; lateral portions longitudinally striated. Frontal lobe, frons, and malar area longitudinally covered by subparallel rugae; cephalic surface with areolate-rugose sculpturing, and intervals microareolate. Frontal face of the pronotum microareolate with weak transverse rugae; dorsum and sides of the promesonotum with irregular longitudinal rugae and intervals with areolate microsculpture. Petiole and postpetiole microareolate, with the central disc predominantly smooth in dorsal view. Mandible and scape with decumbent hairs and appressed pubescence. Anterior margin of clypeus with equally spaced hairs, gradually increasing in size from the lateral to the central portion. Dorsum of the head, mesosoma, and gaster densely covered by long and suberect hairs.

Etymology: From the Latin *primus*, meaning "first" or "foremost"; and *aeva*, plural of the word *aevum*, which means "age," or "a long period of time." "Primaeva" can be interpreted as of "the first ages" or "belonging to the earliest time."

Type material: Holotype. MNHNSD FOS 18.124 worker, deposited in the Museo Nacional de Historia Natural "Prof. Eugenio de Jesús Marcano," Santo Domingo, Dominican Republic (figs. 37, 38). Preserved within a round 20 mm section of yellow amber with internal bubbles and debris around the inclusions. Synclusions include a micro hymenoptera.

Horizon and locality: Early Miocene, Burdigalian (ca. 16 Ma; Iturralde-Vinent and MacPhee, 1996); in amber from the northern mines of the Santiago Province, Dominican Republic.

Comments: The combination of antennae with 12 antennomeres and a three-segmented club, scape not reaching the vertexal margin, absence of antennal scrobes, compact mesosoma with a vestigial metanotal suture, and terminal

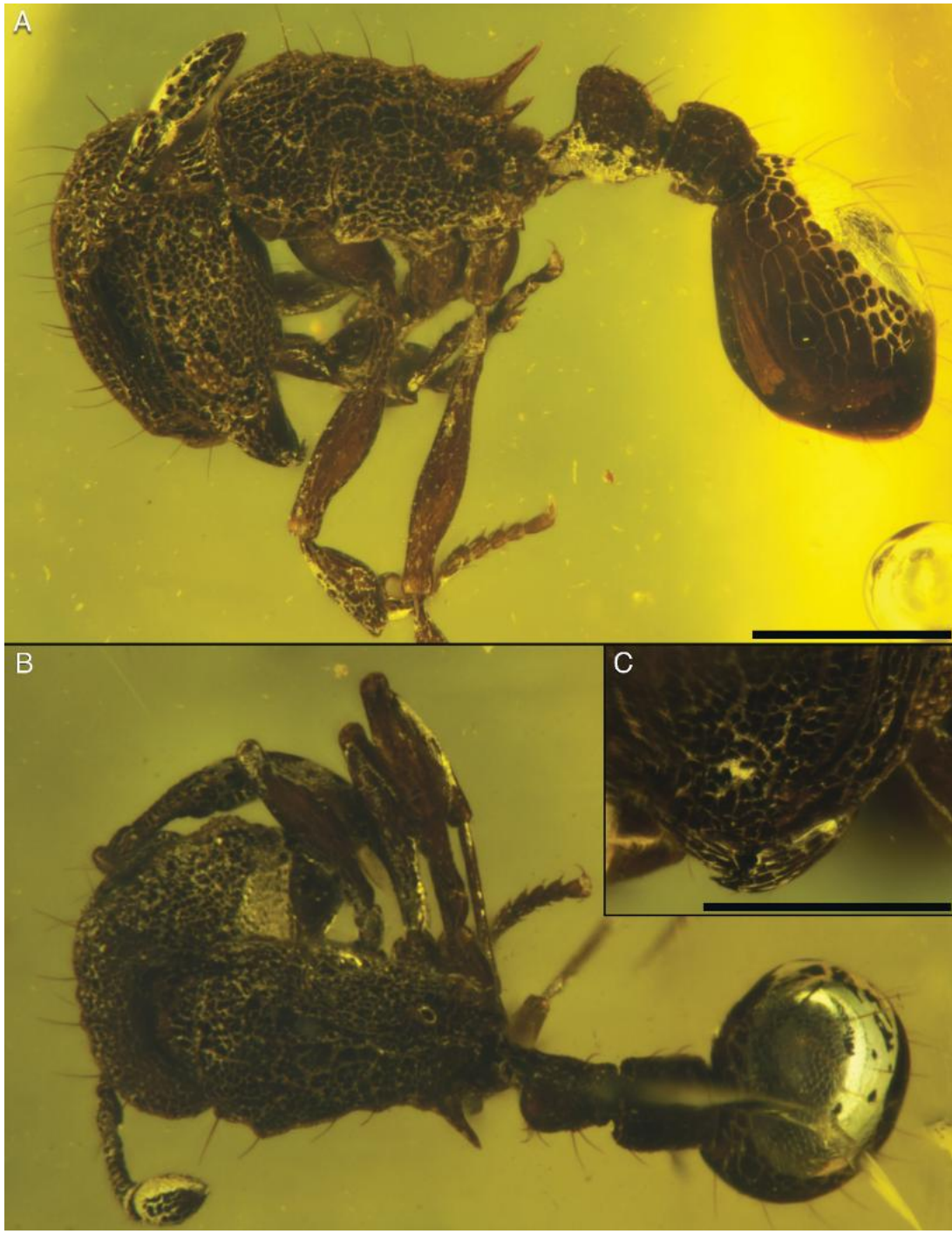


FIGURE 39. Photomicrographs of *Allomerus bi*, sp. nov. (holotype worker, AMNH-11735C). **A.** Lateral view of specimen. **B.** Dorsal view of specimen; note that gaster is inverted. **C.** Enlarged full-face view of mandibles and anteriormost region of head. Scale bars = 0.25 mm.

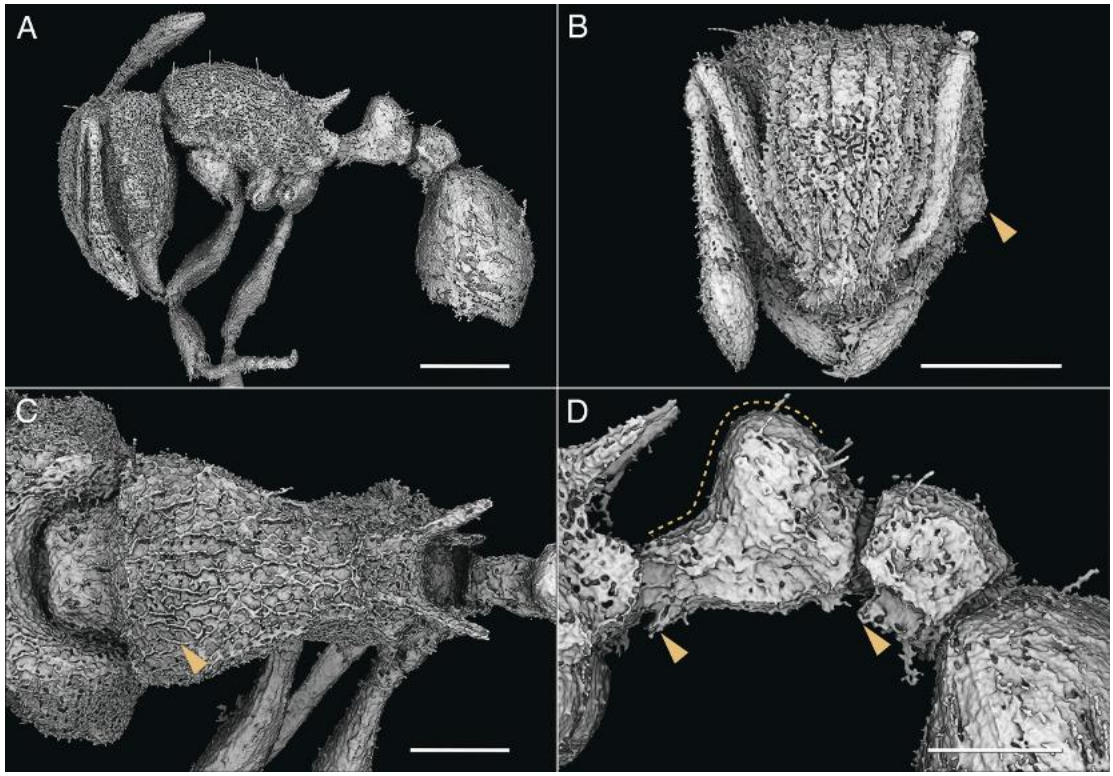


FIGURE 40. Volume renderings of *Allomerus bi*, sp. nov. (holotype worker, AMNH-11735C). **A.** Mesosoma in lateral view. **B.** Head in full-face view. Arrow indicates the eye. **C.** Mesosoma in dorsal view, arrow indicates the sculpturing on the pronotum. **D.** Close-up of petiole and postpetiole in lateral view. Arrows indicate subpetiolar and subpostpetiolar teeth; dashed line outlines petiolar node. Scale bars: A–C = 0.2 mm, D = 0.1 mm.

segments of the gaster ventrally directed confidently allows the inclusion of *Rogeria primaeva* in this genus. Species of the genus are cryptic inhabitants of leaf litter and decaying wood on the forest floor in tropical forests of the Neotropics and Australasia. *Rogeria primaeva* represents the first known individual from the fossil record. The sculpturing pattern, with fine, predominantly longitudinal and irregular rugae, together with the low profile of the postpetiolar node, morphologically aligns this species with a group of living species restricted to the Caribbean and Venezuela, comprising *R. brunnea* Santschi, 1930, *R. carinata* Kugler, 1994, and *R. unguispina* Kugler, 1994. Among these, *R. primaeva* is morphologically closer to *R. brunnea*, which is endemic to the island of Cuba, and from which it can be distinguished by the concave anterior margin of the clypeus (as opposed to convex in *R. brunnea*), significantly larger eyes (about 20 ommatidia) compared to the reduced eyes in *R. brunnea*, and long, dense pilosity versus short, sparse pilosity in the Cuban species (Kugler, 1994).

Allomerus Forel, 1893

†***Allomerus bi*** Fiorentino, Barden, and Fernandez, sp. nov.

Figures 39, 40

ZooBankLSID:urn:lsid:zoobank.org:act:70B1E7B5-70B1-40A4-B028-B386C850372A

Diagnosis (worker): Head and mesosoma covered in rough, irregular, coarse striae. Deep and pronounced antennal scrobes. Eyes notably protruding, situated anteriorly with nine ommatidia in the largest diameter. Petiolar peduncle short followed by a tall anteriorly convex node.

Holotype worker measurements (in mm): HW 0.38, HL 0.38, EL 0.08, EHT 0.21, EHD 0.11, EHV 0.10, ELT 0.37, ELA 0.13, ELP 0.24, MLP 0.17, SL 0.30, WL 0.41, PcL 0.14, MH 0.22, PrW 0.24, MfL 0.31.

DESCRIPTION (worker). Head: Subquadrate, longer than wide; posterior margin in full-face view laterally rounded and medially concave; mandibles triangular, with about five teeth, no denticles; Median anterior clypeal margin convex. Anteclypeus present; antennae 12 segmented, scapes not surpassing posterior margin of head, two-segmented antennal club, antennal scrobes deep and pronounced; eyes situated anteriorly, located close to mandibular base, with nine ommatidia in the largest diameter, semicircle shaped, notably protruding from lateral head margin in full-face view; front carinae extend to near the posterior margin of the head, parallel above the eyes.

Mesosoma: Lateral outline of promesonotum gently convex; in dorsal view promesonotum with humeral corners slightly rounded, in trapezoidal shape, with straight lateral margins, promesonotal suture inconspicuous in dorsal view, slightly impressed in lateral view; in lateral view, mesonotum without a distinct posterior face, notopropodeal sulcus deeply impressed absent. Dorsal face of propodeum short with parallel sides; propodeal spines curved, extend outward in a U-shape, the length of each spine greater than the distance between the spines; in lateral view directed upward (~45°), in dorsal view diverging, posteriorly forming a slight carinae leading into a rounded propodeal lobe; propodeal spiracle circular, small, posterior facing, situated behind base of propodeal spines.

Metasoma: In lateral view, petiole peduncular, petiolar node with straight to concave anterior margin, a strongly convex dorsum leading to a rounded posterior face, petiole in dorsal view with a semiglobular node, about as wide as long; petiolar sternite produced as an anteriorly projecting tooth; Postpetiole about as long as high, in dorsal view slightly wider than long, anterior margin straight and posterior margin slightly convex; postpetiolar sternite with small anterolaterally rounded protrusions on each side, in ventral view protrusions are connected by a concave carinae forming a small well.

Sculpturing and setae: Head and mesosoma covered with rough, irregular, coarse striae; area between striae covered with rough aerolate-rugulose sculpturing. Erect hairs on the vertex, mesosoma, petiole, postpetiole, and gaster.

Etymology: From the Taino word *bi*, meaning "small." In reference to the ants particularly small size (1.5 mm).

Type material: Holotype. AMNH-11735C worker, deposited in the American Museum of Natural History. Preserved within a 4 mm section of yellow amber. No synclusions.

Additional material: Paratype MNHNSD FOS 18.125 deposited in the Museo Nacional de Historia Natural "Prof. Eugenio de Jesús Marcano," Santo Domingo, Dominican Republic (figs. 39, 40). No synclusions.

Horizon and locality: Early Miocene, Burdigalian (ca. 16 Ma; Iturralde-Vinent and MacPhee, 1996); in amber from the Northern mines of the Santiago Province, Dominican Republic.

Comments: This is the first fossil record of *Allomerus*, a genus with 10 living species in the Neotropical region (Longino and Fernández, 2007). This species does not have unique features that distinguish it from other *Allomerus*, so its separation is due more to exclusion from the known species. *Allomerus auropunctatus*, the most common species of the genus, is separated from the new species by the angulate anterodorsal margin of the petiole, a unique feature in the group (Longino and Fernández, 2007). The strongly projected clypeus in *A. scrobifera* and the long petiole peduncle in *A. iheringi* easily separate these species from *A. bi*. In *W. sulcati-*

ceps and *A. williamsoni* the petiole node is more square, the promesonotum taller and the propodeal spines more modest. In *W. lutzi*, the node is thicker and flatter dorsally, the propodeal spines are thin, and the mesosoma profile is more continuous in lateral view. *Allomerus affinis* (known from Brazil), *A. rochai* (wide distribution), and *A. sigmoidea* most resemble *A. bi* in their lateral profiles. However, the deep antennal scrobes, the crude sculpture of sinuous wrinkles on the head and dorsum of the mesosoma, and the short petiolar peduncle followed by the tall anteriorly convex node separate this species from the others in the genus.

Ponerinae Lepeletier de Saint-Fargeau, 1835

This publication raises the number of ponerine genera in the fossil record from 25 to 32. Sixteen genera are presently known only from fossils. There are 98 described fossil species, a small fraction of the presently known 1290 ponerine species (Bolton, 2025). The oldest described putative ponerine fossils are known from Turonian aged deposits of mudstone in Botswana, with an approximate age of 89–83.5 Ma (Dlussky et al., 2004). These ants, placed in the genus *Afropone*, are represented by compression fossils that lack much morphological detail, but they arguably resemble Ponerinae more than any other known ants. Archibald et al. (2006) disagree, contending that the morphology is neither ponerine nor myrmeciine, suggesting they might represent an unknown lineage. Another potentially older ponerine fossil is represented by a specimen found in amber from Myanmar of approximately 99 Ma (Zheng et al., 2018). The ant was illustrated as an example of the discovery of a new Late Cretaceous fauna, but was not described, and even though the published image suggests a ponerine, it lacks detail. The age of the specimen is well after the estimated Early Cretaceous origin of crown Ponerinae (Doré et al., 2025). The earliest nonequivocal Ponerine fossil is a *Platythyrea* species found in Early Eocene (55–52 Ma) amber from Oise, France (Aria et al., 2011).

The usual lack of detail in compression and impression fossils, especially the latter, may hinder generic placement or even subfamily placement, depending on the degree of conservation and the overall habitus of the ant. Most ponerine fossils are preserved in these fossilization modes; only 38 species are described from amber. Even though amber usually implies much better conservation, it is not free of uncertainty as fissures, debris, bubbles, and other artifacts may also hinder observation. Very distinct morphology, such as that of *Odontomachus* (Wappler et al., 2014) or *Odontoponera* (Perrichot, 2022), facilitates genus recognition, but more generalized ponerines, such as *Pachycondyla*, *Ponera*, *Hypoponera*, *Mesoponera*, and other superficially similar taxa are problematic. They share an overall morphological appearance that is frequent among ponerines and thus defy genus placement when conservation is poor, which is the usual case. The informal name *Ponerites* was used for them, until Dlussky and Rasnitsyn (2002) proposed using this name as a formal morphogenus. A recent diagnosis of *Ponerites* can be consulted in Antropov et al. (2014). The implications are that these taxa share a superficial resemblance, with no pretense of monophyly. *Pachycondyla* is an interesting case study of such taxonomic uncertainties that span time and geography. There are 18 valid fossil species that span from the Eocene to the Miocene, from deposits in Europe, North America and Asia. The 17 extant species are all from the Americas, except for three Southeast Asian species and one African species, all represented by males. Recent revisions of Ponerinae (Schmidt and Shattuck, 2014) and *Pachycondyla* (Marcineiro and Lattke, 2024) question the assignment of the non–New World species to *Pachycondyla*. Many fossils need to be restudied for a better understanding of their identity, either because of poor conservation, superficial description, or a



FIGURE 41. Photomicrographs of *Brachyponera mamajuanis*, sp. nov. (holotype worker, AMNH-DR_14_945). **A.** Lateral view of specimen. **B.** Dorsal view of specimen. **C.** Frontal face on view of head and pronotum. Scale bars = 0.5 mm.

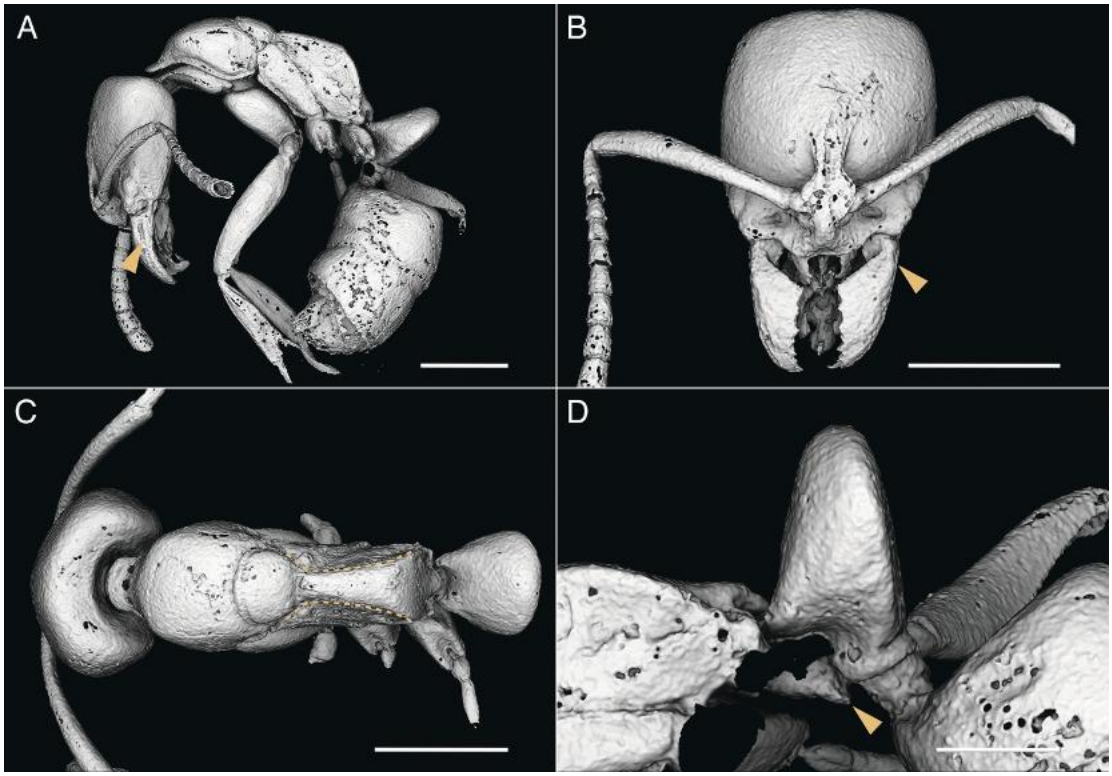


FIGURE 42. Volume renderings of *Brachyponera mamajuanis*, sp. nov**. A.** Mesosoma in lateral view. Arrow indicates basal groove of mandible. **B.** Head in full-face view. Arrow indicates basal groove of mandible. **C.** Body in dorsal view; dashed lines outline the propodeum. **D.** Close-up of petiole in lateral view. Arrow indicates the subpetiolar process. Scale bars: A–C = 0.5 mm, D = 0.2 mm.

combination of both. A good number are destined to remain *incertae sedis*. The genus *Anochetus* harbors the highest number of fossil species, with eight known from the Dominican Amber (Baroni Urbani, 1980b; De Andrade, 1994; MacKay, 1991) and one from Indonesian amber (Ngô-Muller et al., 2021).

Most fossil ponerine species (44) are from the Eocene, with Miocene fossils trailing closely with 38 species. European deposits have contributed the most fossil species (47), followed by 22 species from Dominican Amber. Asian fossils come in third, with 15 species (appendix 1). The results of this study clearly indicate that there are many surprises waiting for us from the amber deposits from the Dominican Republic.

Brachyponera Emery, 1900

†***Brachyponera mamajuanis*** Fiorentino, Cubillos, Fernandez, and Lattke, sp. nov.

Figures 41, 42

ZooBank LSID: urn:lsid:zoobank.org:act:5888C209-637D-4459-B2B4-29C7A0EE4141

Diagnosis (worker): Head subquadrate, slightly longer than wide, scape surpassing vertexal border by about two maximum scape diameters, mandible broadly triangular with seven well-defined teeth, basal groove deeply impressed, extending along mandibular lateral edge midway through to apex. Compound eye small, located close to mandibular base, ante-

rior clypeal margin protruding, with medial concavity. Promesonotal suture well developed, promesonotal convexity attenuated. Propodeum unarmed, dorsal margin of propodeum in lateral view straight and sloping downward, meeting declivitous margin at a rounded angle that continues to propodeal lobe. Metasternal process forming two broadly triangular, bluntly pointed projections. Metatibia with two apical spurs. Tarsal claws simple, arolium absent. Petiolar node in dorsal view trapezoidal, anterior face rounded and posterior face straight, wider than long. Subpetiolar process relatively large with paired posteroventral teeth. Prora absent.

Holotype worker measurements (in mm): HW 0.71, HL 0.78, EL 0.12, EHT 0.42, EHD 0.22, EHV 0.20, ELT 0.84, ELA 0.22, ELP 0.62, MLP 0.55, SL 0.69, WL 1.20, PcL 0.49, MH 0.39, PrW 0.47, MfL 0.85.

DESCRIPTION (worker): Head: Subquadrate in dorsal view, slightly longer than wide; scape does not surpass vertexal border. Antennal scape arched, from basal margin to apex; scape rounded in from base to apex. Medial torular lobe broad, flat, outer margin distinctly convex, not fully concealing bulbous in cephalic dorsal view. Bulbous neck bent; anterior tentorial pit inconspicuous. Anterior clypeal margin protruding, with medial concavity. Clypeus with abundant long erect setae. Clypeal discal area smooth, lacking carinae. Supraclypeal area inconspicuous. Median clypeal line shallowly impressed. Clypeus forming evenly convex margin with frons in cephalic lateral view. Mandible triangular, relatively long and robust, with convex dorsal surface; masticatory margin with large apical tooth followed by six distinct teeth of varying size. Basal sulcus deeply impressed, extending along mandibular lateral edge midway through to apex. Mandible surface with abundant appressed setae and long erect setae along masticatory margin. Palpal formula 4, 3. Eye in profile located close to mandibular base, round, relatively large, with seven or eight ommatidia along longest axis.

Mesosoma: In dorsal view pronotum rounded, without humeral angle; promesonotal suture well marked, mesonotum broadly oval, notopropodeal sulcus well impressed, abruptly narrows anteriorly, greatly widening posterad to declivity; dorsum rounded, curving onto lateral face. Mesosomal dorsal margin in lateral view: pronotum distinctly convex, dome shaped; mesonotum convex, mesonotal-propodeal margin straight, notopropodeal sulcus well marked; propodeum slightly lower than promesonotum. Anapleural sulcus absent, ventral katepisternal margin with carina, mesometapleural suture well marked; propodeal spiracle round, posterior facing, located midway between propodeal declivity and metapleural gland. Propodeum unarmed, dorsal margin of propodeum straight and sloping downward, meeting declivitous margin at rounded angle that continues to propodeal lobes; declivity laterally carinate. Metasternal process forming two broadly triangular, bluntly pointed projections. Mesotibia lacking "traction setae" on external face; two apical metatibial spurs present.

Metasoma: Petiole much higher than long in lateral view, sessile, anterior node margin slightly straight, posterior node margin straight. Petiolar node in dorsal view trapezoidal, anterior face rounded and posterior face straight, wider than long. Subpetiolar process relatively large, with paired posteroventral teeth. Anterior margin of abdominal tergite 3 in lateral view mostly vertical, joining flat to weakly convex dorsal margin through convexity. Prora absent. Cinctus weakly developed.

Sculpturing and setae: Dorsum of mandible, head, mesosoma, and gaster punctulate, mesopleuron and metapleuron smooth and shining, Mesosoma with sparse erect setae. Body covered with short pubescence mixed with sparse, short erect hairs; erect hairs absent on propodeal dorsum and petiole. Antenna and legs without erect hairs.

Etymology: The specific epithet *mamajuanis* refers to *Mamajuana*, a traditional Dominican alcoholic beverage made by mixing rum with medicinal herbs and spices.

Type material: Holotype. AMNH-DR_14_945 worker, deposited in the American

Museum of Natural History (figs. 41, 42). Preserved within a 14 mm by 10 mm section of light red amber. No synclusions.

Horizon and locality: Early Miocene, Burdigalian (ca. 16 Ma; Iturralde-Vinent and MacPhee, 1996); in amber from the northern mines of the Santiago Province, Dominican Republic.

Comments: *Brachyponera mamajuanis*, sp. nov., can be comfortably placed within *Brachyponera* by the mixture of characters such as mandibles with a basal groove, small eyes located near the mandibular insertions, deep notopropodeal sulcus, propodeum at a lower elevation than the promesonotum and usually strongly narrowed dorsally, propodeal spiracle small and round, prora not externally visible, and metatibiae with two spurs. The overall morphology, particularly the head, mesosomal and petiolar morphology, match that of modern Indomalayan *Brachyponera*, such as *B. luteipes* (Mayr, 1862) and *B. jerdonii* (Forel, 1900), except for a noticeably lower propodeum in modern species. *B. mamajuanis* can be easily distinguished by its short antennal scapes that do not surpass the vertexal margin, small eyes, with only seven or eight ommatidia along the longest diameter, a conspicuous basal mandibular groove and the attenuated convexity of the promesonotum. This is the first record of *Brachyponera* in the Americas. All other known species (19 species) are found in the Afrotropics (*B. senaarensis*) and the Indomalayan and Australasian regions (Antmaps, 2025).

Leptogenys Roger, 1861

†***Leptogenys intacta*** Cubillos, Cavalcanti, and Lattke, sp. nov.

Figures 43, 44

ZooBank LSID: urn:lsid:zoobank.org:act:690C7510-03DF-453A-BD5B-4EE5251AA83B

Diagnosis (male): Clypeus strongly convex in lateral view. Ocellus strongly convex, interocellar space equal to ocellar width; distance between eye and lateral ocellus less than ocellar width. Vertex subtrapezoidal, with posterior margin narrowest. Third antennomere conspicuously longer than others, 3× longer than pedicel. Dorsoposterior margin of propodeum in lateral view straight, not concave.

Holotype male measurements (in mm): HW 0.87, HL 1.29, EL 0.71, EHD 0.28, EHV 0.41, ELA 0.35, ELP 0.54, MLP 0,19, SL 0.45, WL 2.57, PcL 0.79, MH 0.62, OW 0.17, OES 0.09, MeL 1.08, MeW 0.88, PrW 0.86, MfL 1.38, PeH 0.61, PeL 0.65, GL 2.62, TL 6.48.

DESCRIPTION (male): Head: Longer than wide in full-face view. Clypeus strongly convex in lateral view; anterior margin sinuous, with two weak convexities in frontal view, posterior margin convex. Frons triangular. Compound eye large and convex, occupying entire lateral cephalic margin, inner margin slightly emarginate anteriorly. Ocelli large and convex; interocellar space equal to ocellar width; distance between eye and lateral ocellus less than ocellar width. Vertex trapezoidal in full-face view, posterior portion narrowest. Occipital carina well developed on posterior cephalic margin, extending ventrally (fig. 43B). Mandibles spatulate and short, not reaching medial point of anterior margin of clypeus in frontal view, width of mandible uniform, less than width of scape. Edentate, apex truncate in frontal view; external margin convex in ventral view, dorsum smooth. Apical labial palpomere distinctly elongate with blunt tip, reaching more than half the length of mandible. Antennae filiform, elongated with 13 segments; scape short, wider than other segments, not reaching posterior eye margin; pedicel longer than wide, its length approaching one-third length of scape; third antennomere conspicuously longer than others, length longer than scape and pedicel combined (fig. 43A).

Mesosoma: Pronotum subtrapezoidal in dorsal view, wider than long, lateral margin anteriorly with slight concavity forming neck, diverging into broad convexity posteriorly; longer than high in lateral view, with dorsoposterior lobe. Promesonotal margin in lateral view

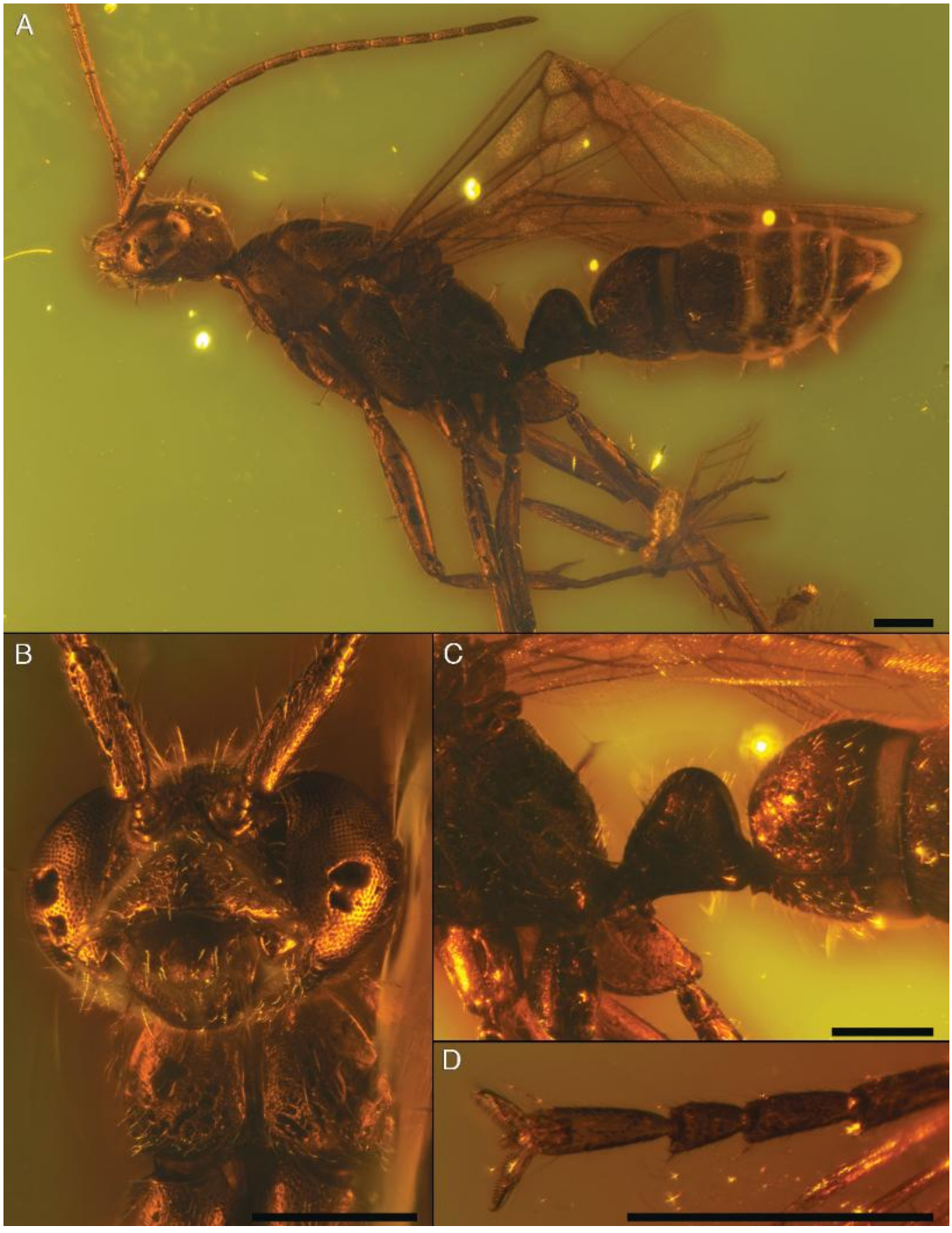


FIGURE 43. Photomicrographs of *Leptogenys intacta*, sp. nov. (holotype male, AMNH_10-239). **A.** Lateral view of specimen. **B.** Frontal view of head, ventral view of procoxae. **C.** Lateral view of propodeum, petiole, and first gastral segment. **D.** Enlarged view of foreleg tarsomeres and pretarsal claw. Scale bars = 0.5 mm.

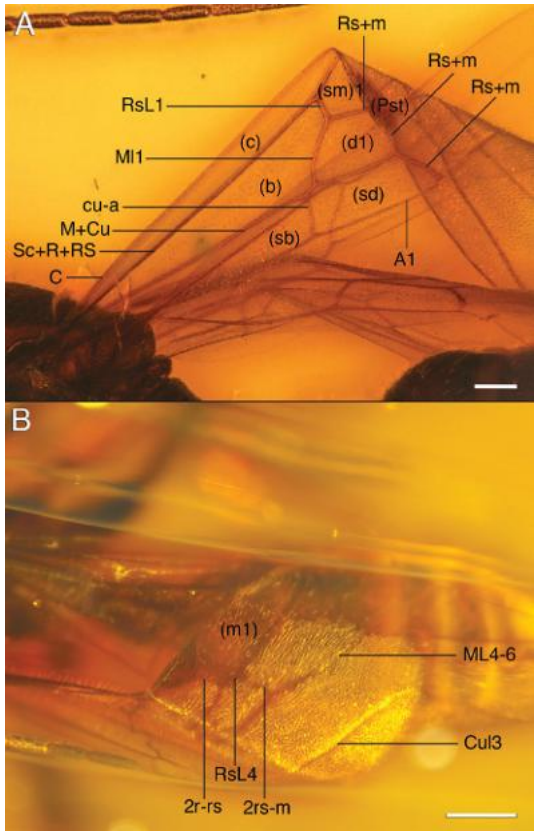


FIGURE 44. Photomicrographs of *Leptogenys intacta*, sp. nov. (Holotype, AMNH-DR-10-239). **A.** Anterior half of forewing, **B.** Portion posterior to Pterostigma of forewing. Scale bars: A = 0.25 mm; B = 0.5 mm.

forming two convexities differentiated by pronounced promesonotal suture. Mesoscutum anteriorly convex in dorsal view, longer than wide; broad convexity in lateral view. Notauli scrobiculate, converging on posterior portion of mesoscutum. Parapsidal line extends less than half mesoscutal length. Scutoscutellar sulcus scrobiculate. Mesoscutellum subtrapezoidal in dorsal view, posterior margin convex; dorsal margin convex in lateral view. Mesopleuron with anterodorsal lobe; anapleural sulcus weakly scrobiculate. Katepisternum with ventroposterior margin slightly convex, gradually curving posteriorly. Metascutellum strongly convex in lateral view. Propodeum longer than high in lateral view, with dorsal margin apparently straight, forming obtuse angle with posterior margin; propodeal spiracle apparently slit shaped (fig. 43A, C). Tarsal claws pectinate, arolium well developed (fig. 43D).

Wings: Surface with visible pubescence. Pterostigma dark and distinct from rest of surface. Anterior wing with well-developed C vein and lighter pigmentation than Sc+R+Rs. RsL1 straight, almost forming right angle at intersection with Sc+R+Rs, its length about half length of Rs+M. M+Cu does not reach Ml1, distance between them one-third length of vein cu-a. Ml1 slightly curved, forming obtuse angle with Rs+M. Vein m-cu appears straight and forms obtuse angle with Cu1. RsL4 is more than half length of 2r-rs. Cell d1 appears subpentagonal with unequal sides. Cell sd forms acute angle at junction of vein Cu and A1. Posterior wing not clearly visible (fig. 44A, B).

Metasoma: Petiole almost as long as high. Petiolar node subtriangular in lateral view, anterodorsal margin inclined posteriorly, strongly convex dorsally, node highest posteriorly. Posterior nodal face slightly concave. Subpetiolar process in lateral view subtrapezoidal, posterior margin highest, slightly rounded ventral margin. Prora present, longer than high, straight anterior margin, rounded tip, concave posterior margin in lateral view. Abdominal tergite III with anterior margin shorter than height of petiolar node, curving toward dorsal margin at two-thirds height of petiolar node. Gaster with cinctus strongly developed (fig. 44A, C).

Sculpturing and setae: Antenna densely punctate. Katepisternum apparently with oblique striae. Head with dense pilosity, erect and suberect long hairs on frontal area and decumbent and subdecumbent hairs on vertex, gena, and postgena. Clypeus with sparse erect and suberect hairs. Short erect hairs present on all antennomeres, additional pubescence on scape. Mesosomal dorsum with abundant erect and suberect hairs, and small decumbent and subdecumbent hairs on pleura. Legs with abundant, small decumbent and subdecum-

bent hairs. Petiolar node with sparse erect hairs. Subpetiolar process with suberect hairs on tip, inclined posteriorly on ventral margin. Gaster with suberect hairs on terga and sterna, and with visible pubescence.

Etymology: The specific epithet *intacta*, from Latin, is an adjective meaning "intact," feminine in form to modify *-genys* (γένυς) of the genus, which means "jaw." It refers to the good state of preservation of the specimen on the amber.

Type material: Holotype. AMNH_DR-10-239 male, deposited in the American Museum of Natural History (figs. 43, 44). Preserved within a 9 mm × 12 mm section of transparent, yellow amber with internal cracks along the body of the inclusion. Synclusions include a hemipteran, a dipteran and an unidentified insect, all of them entangled in the legs of the male *Leptogenys*.

Horizon and locality: Early Miocene, Burdigalian (ca. 16 Ma; Iturralde-Vinent and MacPhee, 1996); in amber from the northern mines of the Santiago Province, Dominican Republic.

Comments: The head, mandible, mesosomal dorsum, petiole and gaster exhibit a microsculpture that could not be observed in detail in the photographs or through stereomicroscopy. The anepisternum appears to have reticulated sculpture, although this may be an artifact of specimen desiccation rather than actual cuticular formation. In other parts, such as areas of the lateral surface of the pronotum, propodeum, petiolar node, and gaster, a similar "sculpture" to that of the anepisternum is also observed, lacking a defined pattern, further supporting the idea that it is a consequence of the fossilization process. In the forewing the Ml2 vein is not visible because the wing was folded, obscuring that section; however, based on the direction of adjacent veins such as Rs+M and 1m-cu, it can be inferred that the Ml2 vein is present and forms an obtuse angle with the Rs+M vein. It is not possible to observe the hind wing in detail.

Males of *Leptogenys* are easily distinguished from all other Ponerinae by the presence of a pectinate tarsal claw (Boudinot, 2019). In the Neotropical region, males of eight species have been described, with those belonging to the *unistimulosa* species group the most thoroughly reviewed by Tozetto et al. (2022). *Leptogenys intacta*, sp. nov., has the third antennomere longer than the adjacent ones, a scape 3× longer than the pedicel, and the subpentagonal discal cell with a curved Ml1 vein and a shorter Ml2 vein relative to the other veins surrounding the cell. These characteristics are shared with some species of the *arcuata* group, such as *L. arcuata* Roger, 1861 (recorded on Caribbean islands), and *L. donisthorpei* Mann, 1922, as well as with members of the *unistimulosa* group, including *L. bohlsi* Emery, 1896, *L. paraensis* Lattke, 2011, *L. pubiceps* Emery, 1890 (recorded in the Dominican Republic) and *L. unistimulosa* Roger, 1863. In contrast, males of other groups present in Central America, such as *L. manni* Wheeler, 1923, and *L. peninsularis* Mann, 1926, from the *elongata* group, possess a third antennomere similar in size to adjacent segments, a scape twice as long as the pedicel, and a subrectangular discal cell, with a straight Ml1 vein and an absent Ml2 vein.

Some characteristics are shared between workers and males in *Leptogenys*, such as the flagellomere proportions, some sculptural patterns, and frequently, trends in petiole shape. Even though the proportions may vary, the overall petiole shape in lateral view remains relatively constant between workers and males. Other *Leptogenys* groups in Central America have elongated subquadrate or subtriangular petioles and a predominantly smooth and shining sculpture in most species, differing from *L. intacta* sp. nov. Thus, based on morphological characters, the *unistimulosa* and *arcuata* species groups may be the most closely related to *L. intacta* sp. nov.

Leptogenys intacta represents the first *Leptogenys* fossil discovered in the Americas and preserved in amber, as well as the second known fossil record of the genus worldwide. Zhang (1989) described the first fossil species of the

genus, *L. lacerata* Zh-ang, 1989, from the Miocene Shanwang Formation in Shandong Province, northeastern China. *Leptogenys lacerata* was described from a winged queen, with the description provided in Mandarin. Additionally, the publication includes a generalized illustration of the specimen, underscoring the need for future examination of the fossil using new technological tools to reassess its morphology and confirm its classification within *Leptogenys*.

Mayaponera Schmidt and Shattuck, 2014

†***Mayaponera bachata*** Fiorentino, Cubillos, Fernández, and Lattke, sp. nov.

Figures 45, 46

ZooBankLSID: urn:lsid:zoobank.org:act:68BDF306-7813-46E2-B020-705FF66FFE9B

Diagnosis (worker): Head rectangular and elongate in frontal view, scape surpassing posterior margin by three diameters. Eyes flat and anteriorly placed on head, notopropodeal sulcus well impressed, propodeal spiracle round, propodeal dorsal surface anteriorly narrow; mesotibia without lateral traction setae and with single apical spur, metatibial apex with 2 spurs. Node scalelike, subpetiolar process with posterior point, fenestra absent.

Holotype worker measurements (in mm): HW 0.53, HL 0.81, EL 0.13, EHT 0.41, EHD 0.27, EHV 0.14, ELT 0.87, ELA 0.22, ELP 0.65, MLP 0.46, SL 0.78, WL 1.07, PcL 0.45, MH 0.39, PrW 0.37, MfL 0.68, PeL 0.41, GL 1.1, TL 3.1 mm, CI 0.67, OI 0.16, SI 1.38. Notes: HL taken posteriorly from perpendicular cord tangent to most posterior points of head. SL selected from lateral image of head.

DESCRIPTION (worker): Head: Elongate in dorsal view, widest posterior to eye and anterior to cephalic midlength, lateral margin broadly convex, posterior margin with median concavity. Antenna with 12 articles, scape surpassing vertex by three apical diameters; flagellum gradually widening apicad. Frontal carinae closely joined, lateral margin of carina convex, part of scape bulbous and lateral torulus visible in cephalic dorsal view. Eye small, length less than 20% of lateral cephalic length, eye weakly convex, almost flat, ovoid shaped in perpendicular view; anteriorly placed on head, separated from mandibular base by a little less than eye length. Clypeal anterior margin with broad, median projection, medially concave; anteromedially elevated, overhanging anterior margin; clypeal dorsal margin mostly very convex and overhanging mandible in lateral cephalic view. Anterior tentorial pit distinct. Mandible triangular, masticatory margin jagged, with seven or eight large teeth, each separated by small denticle, basal angle with two denticles. Mandible without basal groove or pit, neither with sulcus along lateral border. Anterior margin of labrum with median triangular cleft.

Mesosoma: Mesosomal dorsal margin in lateral view with pronotum mostly convex with weakly concave anterior margin, promesonotal suture distinct; mesonotum distinct, broadly convex; notopropodeal sulcus well impressed; propodeal margin mostly broadly convex with sharper convexity along transition of declivitous and dorsal margins. Pronotal humeral area rounded, lacking ridge or angle; mesonotum broadly oval shaped in dorsal view, wider than long. Propodeal dorsal face flattened and narrow, anterior width less than one half mesonotal width, gradually widening posterad, posterolateral margin concave; declivity separated from lateral face by sharp margin, cross section of declivitous face concave. Propodeal spiracle round, directed obliquely posteriorly, located at midheight, between the meta- and mesocoxae; metathoracic spiracular sclerite oval, dorsally convex. Mesometapleural suture distinctly impressed, forming narrow ridge along mesopleural margin; ventral and anterior margins of mesopleuron with sulcus and ridge, ridge thickest anteriorly, sulcus scrobiculate along anteroventral margin; anapleural sulcus absent. Metasternal process formed by two acicular, ventrally directed projections, their tips apparently broken. Mesotibia with single apical spur; metatibia with two apical spurs, arolium appear to be present on mesotarsal claw. All tarsi are mostly incomplete.



FIGURE 45. Photomicrographs of *Mayaponera bachata* sp. nov. (holotype worker, AMNH_DR_14_930). **A.** Lateral view of specimen. **B.** Frontal view of head. **C.** Lateral view of propodeum and petiole. **D.** Enlarged tibial spur. Scale bars: A–C = 0.5 mm; D = 0.25 mm.

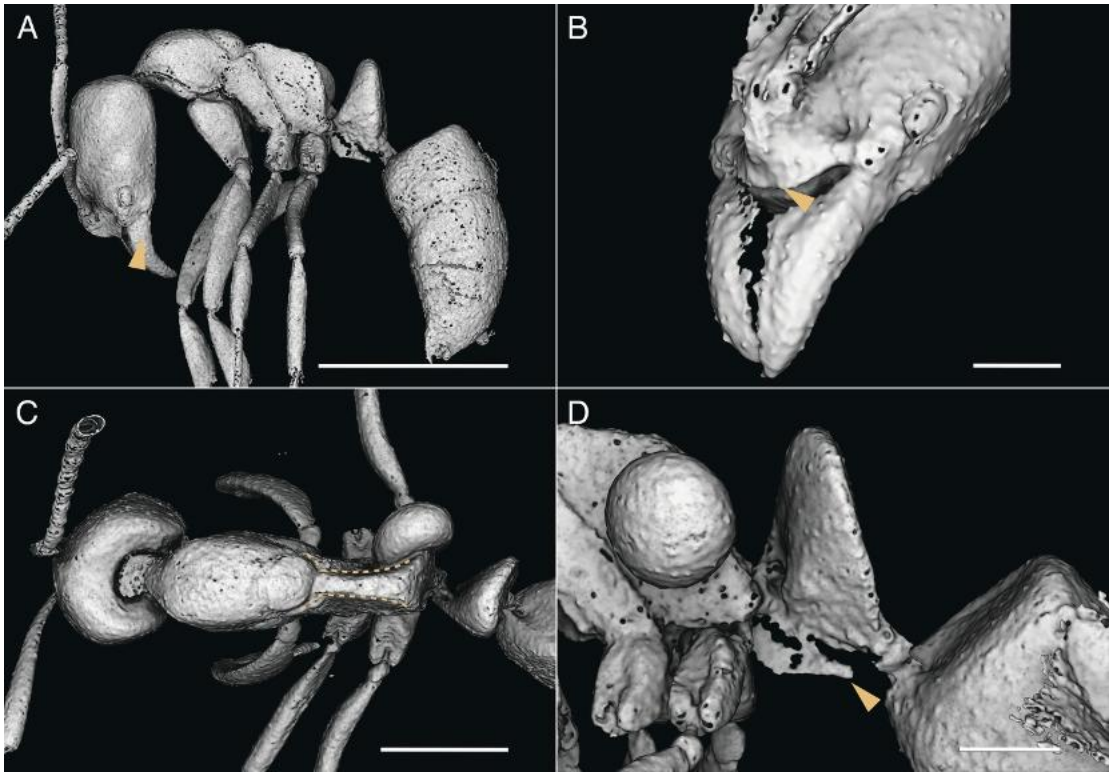


FIGURE 46. Volume renderings of *Mayaponera bachata*, sp. nov. **A.** Mesosoma in lateral view. Arrow indicates lack of basal groove on mandible. **B.** Close-up of head in side view, highlighting the clypeus, arrow indicates clypeal apron. **C.** Body in dorsal view; dashed line outlines propodeum. **D.** Close-up of petiole in lateral view. Arrow indicates posterior facing subpetiolar projection. Scale bars: A = 1 mm; B, D = 0.2 mm; C = 0.5 mm.

Metasoma: Petiole sessile, node shaped as a slender triangle in lateral view, anterior and posterior margins relatively straight, summit strongly convex; subpetiolar process well developed, anterior margin in lateral view convex, ventral margin weakly sinuous with irregularities formed by transverse costulae, posteriorly projecting as sharp point. Fenestra absent. Helcium situated ventrally on anterior face of abdominal tergite 3, prora indistinct or not visible. Anterior margin of abdominal tergite 3 vertical in lateral view, forming a right angle with dorsal margin; cinctus weakly constricted. Gaster weakly arched; dorsal margin broadly convex in lateral view, ventral margin relatively straight. Pygidium without stout setae or spines.

Sculpturing and setae: Mesosoma, node, and gaster with sparse, long, erect and arched hairs, hairs more abundant toward gastral tip; head with sparse erect hairs. Clypeus with approximately 10 long, anteriorly directed hairs distributed along anterior clypeal region. Body mostly without strong sculptural features: lateral clypeus with longitudinal fine striae, cephalic dorsum with punctulate areas.

Etymology: The specific epithet *bachata* (believed to be of African origin and common in the patois of the Dominican Republic) initially referred to a party, revelry, and lively gathering among friends, but today it refers to a danceable musical expression, the result of a fusion of rhythmic bolero with other Afro-Caribbean genres. Bachata is considered by the

Dominican people to be a vernacular cultural expression.

Type material: Holotype. AMNH_DR_14_930 worker, deposited in the American Museum of Natural History (figs. 45, 46). Preserved within an 18 mm by 9 mm section of light red amber. No synclusions.

Horizon and locality: Early Miocene, Burdigalian (ca. 16 Ma; Iturralde-Vinent and MacPhee, 1996); in amber from the northern mines of the Santiago Province, Dominican Republic.

Comments: This ant has a rather generalized ponerine morphology that lacks an apomorphy that could clearly hint at its identity. Using the identification keys to ponerine genera for different biogeographical regions in the following publications (Bolton and Fisher, 2016; Schmidt and Shattuck, 2014; Fernández and Guerrero, 2019; Esteves and Fisher, 2021; Feitosa and Dias, 2024) we are led to genera close to the Ponera group or *Hypoponera*. Considering the genera with rounded propodeal spiracles, the following comparisons rule out most of these genera. The lack of a fenestra eliminates *Ponera* and the lack of stout setae on the mesotibial dorsal edge rule out *Wadeura* and *Cryptopone*. It is not a *Hypoponera* nor a *Ponera* because these bear a single spur on the metatibial apex.

This specimen has an inconspicuous prora, a trait shared with *Brachyponera*, *Mayaponera*, and *Rasopone*. The subpetiolar process in *M. bachata* has a posterior projecting point. Though this feature is more prominent in *Rasopone*, the point in *Rasopone* is defined by a deep horizontal groove (Longino and Branstetter, 2020), while in *M. bachata* it is part of a concavity. The propodeal dorsum in *Rasopone* is not anteriorly strongly constricted, but of uniform width and usually curving on the lateral face. *Brachyponera* has a pit at the lateral mandibular base and a propodeal dorsum that is markedly lower than the promesonotum when seen in lateral view.

We favor recognizing this ant as a *Mayaponera* because it bears the combination of traits considered diagnostic for the genus as defined by Schmidt and Shattuck (2014), but also by Bolton and Fisher (2016). The mesosoma of *M. bachata*, sp. nov., resembles *Mayaponera constricta* (Mayr, 1884), though it lacks the strongly convex mesonotum. This new species can be distinguished from all modern *Mayaponera* by a combination of strongly projecting clypeus that is medially concave and mandible with seven or eight large teeth, each separated by small denticle, basal angle with two denticles. According to Doré et al. (2025), *Mayaponera* belongs to the *Pachycondyla* species group, which likely originated in the Neotropics with an estimated stem age of 81.5 million years (supplementary table S8). Additionally, *Mayaponera* itself is estimated to be approximately 40 million years old, with a probable origin in the Eocene (figs. S5 in the online supplement). Since *M. bachata* is the first described fossil for the genus, it can be included in future studies to achieve a more precise time calibration.

†***Cayrapone*** Cubillos, Fiorentino, and Lattke, gen. nov.

Figures 47, 48

ZooBank LSID: urn:lsid:zoobank.org:act:214C7649-EC8D-4758-B03F-C6DA84483DB8

Type species: *Cayrapone hupia* Cubillos, Fiorentino, and Lattke, sp. nov.

Diagnosis (worker): mandible with six prominent, triangular teeth, and diastema approximately the basal width of each tooth. Clypeus with anterior medial projection. Mesonotum elevated, dorsal margin forming an obtuse angle interrupting the dorsal mesosomal profile. Propodeum in lateral view, about high as long, with a flat dorsal margin forming a right angle with the posterior margin. Propodeal spiracle elliptical. Subpetiolar process with small, rounded anterior fenestra, and angular ventroposterior margin. Prora conspicuous, projecting anteriorly.

Etymology: The name *Cayrapone* is derived from the following combination: *Cayra*, from the Taíno language of the Indigenous peoples of the part of Caribbean, Cay (island) + *Ra* ("birth-

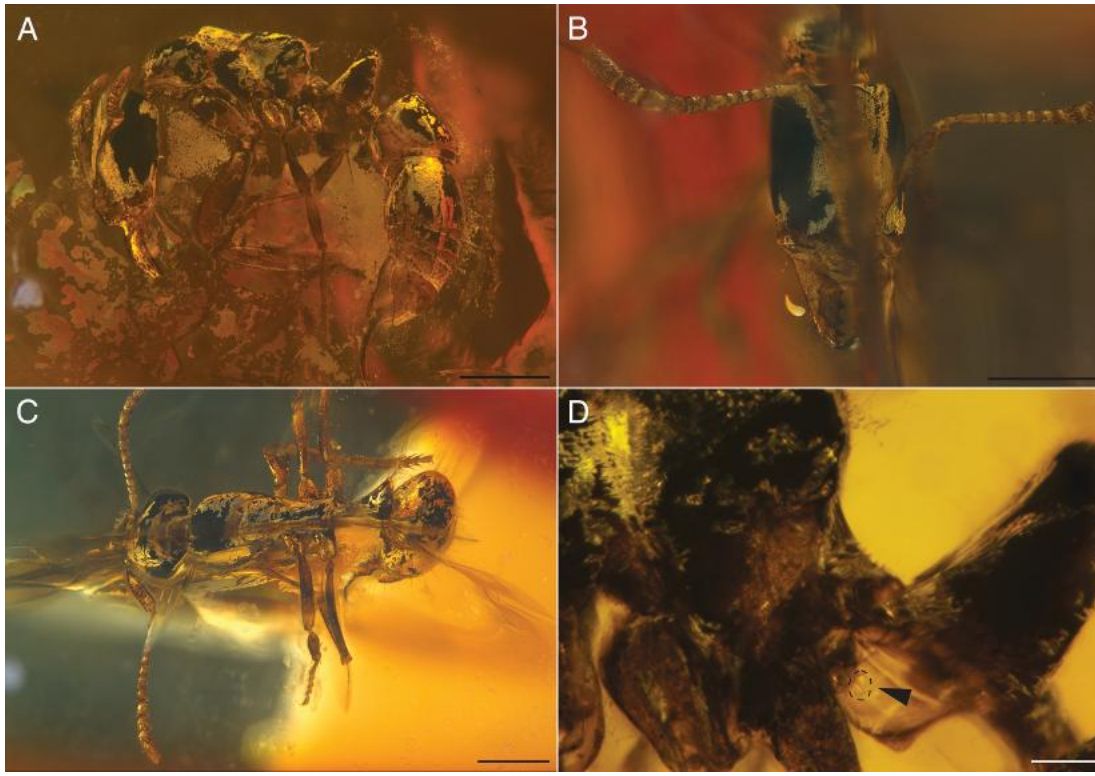


FIGURE 47. Photomicrographs of *Cayrapone hupia*, sp. nov. (holotype worker, AMNH_DR_14_51). **A.** Lateral view of specimen; note top left corner of amber matrix has been artificially filled in to maximize image size. **B.** Frontal face on view of head. **C.** Dorsal view of specimen. **D.** Profile view of propodeum and petiole. Arrow indicates an anterior-facing fenestra on subpetiolar process. Dashed line outlines the anterior-facing fenestra. Scale bars A–C = 0.5 mm; D = 0.1 mm.

place, origin"), thus referring to an ant genus "born on the island" or "originating from the island." The suffix -pone refers to the type genus of this subfamily, Ponera.

Cayrapone hupia Cubillos, Fiorentino, and Lattke, sp. nov.

ZooBank LSID: urn:lsid:zoobank.org:act:AF544248-1FB9-4E3E-B9E8-D1976A8FCE16

Diagnosis (worker): See diagnosis for the genus.

Holotype worker measurements (in mm): HW 0.81, HL 0.88, EL 0.05, EHT 0.39, EHD 0.29, EHV 0.09, ELT 0.81, ELA 0.21, ELP 0.60, MLP 0.45, SL 0.59, WL 1.11, PcL 0.34, MH 0.38, PrW 0.40, MfL 0.62.

DESCRIPTION (worker): Head: Subrectangular in full-face view, longer than wide, lateral margin nearly straight. Clypeus with transverse elevation separating anterior from posterior portion, anterior margin apparently converging into convex lobe with a conspicuous medial projection (fig. 48B). Frontal lobe small, laterally convex, apparently covers antennal insertion. Compound eye small, length shorter than the basal width of the scape, positioned near the basal margin mandible. Vertex rectangular. Posterior cephalic margin straight. Mandible triangular, elongated, length approaching more than half the length of the head. Masticatory margin

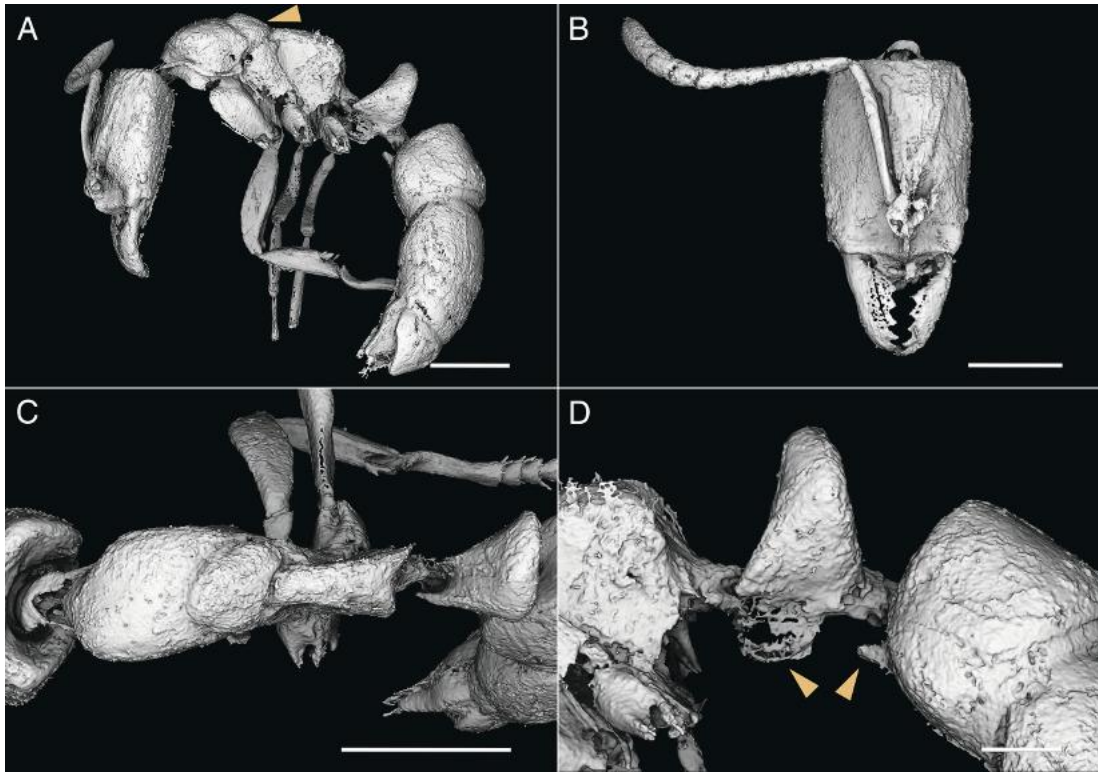


FIGURE 48. Volume renderings of *Cayrapone hupia*, sp. nov. **A.** Mesosoma in lateral view. Arrow indicates the elevated mesonotum. **B.** Head in frontal view. **C.** Mesosoma in dorsal view. **D.** Close-up of petiole in lateral view. Arrows indicate the subpetiolar process and prora. Scale bars: A–C = 0.5 mm; D = 0.2 mm.

with six teeth and diastema well defined, approximately the same width as the basal width of each tooth. Scape reaching to vertex margin. Pedicel twice the length of the basal flagellomere. Flagellomeres gradually increase in size; apical flagellomere conspicuously longer than the others.

Mesosoma: Pronotum wider than long in dorsal view, anterolateral margin convex; in lateral view, dorsal margin almost straight, posterior margin weakly concave. Propleuron in lateral view with ventral margin convex. Mesonotum elevated in lateral view, interrupting the mesosoma profile; dorsal margin with the highest point anteriorly, forming an obtuse angle with the posterior portion; length about ¾ of the dorsal length of the propodeum. Mesometapleural suture well developed, metapleural-propodeal suture apparently vestigial, notopropodeal sulcus shallow. Propodeum narrower than mesonotum in dorsal view, lateral margin subparallel diverging posteriorly; in lateral view, almost as high as long, with a flat dorsal margin forming a right angle with the posterior margin; posterior face apparently concave. Propodeal spiracle elliptical. Metatibia with two spurs near the apex.

Metasoma: Petiolar node subtriangular in lateral view, higher than long, anterior margin slightly concave, rounded dorsal margin, posterior margin straight. Subpetiolar process in lateral view longer than high, ventral margin convex, ventral posterior margin angled; small, rounded anterior fenestra occupies less than half of subpetiolar process. Gaster with well-developed constriction; abdominal segment III in lateral view with anterior margin straight, dorsal margin

almost straight, anterodorsal margin forming a right angle. Prora well developed, in lateral view projecting anteriorly, broader at the base, with a rounded tip.

Sculpturing and setae: Head finely punctate; mesosoma and metasoma surfaces may have the same sculpturing, though not clearly visible due to bubbles in the amber. Flagellomere with apparent pubescence. Dorsum of the head without hairs or pubescence; rest of the body with sparse long and erect hairs. Tarsi with long, thick lateral hairs.

Etymology: The specific epithet derives from the Taíno word *hupia* (also *opia*, *opi'a*, *op'a*, *operi'to*), meaning "spirit of a person who has died." The species name refers to the extinction of the genus in the Caribbean and the New World.

Type material: Holotype. AMNH_DR-14-51 worker, deposited in the American Museum of Natural History (figs. 47, 48). Preserved within an 11 mm × 5 mm section of transparent, yellow amber with internal cracks along the body of the inclusion. No synclusions.

Horizon and locality: Early Miocene, Burdigalian (ca. 16 Ma; Iturralde-Vinent and MacPhee, 1996); in amber from the northern mines of the Santiago Province, Dominican Republic.

Comments: Several ponerine genera lack apomorphies that allow them to be clearly differentiated from other groups, and in many cases their recognition requires a combination of multiple characters, as proposed by Schmidt and Shattuck (2014). The genera morphologically closest to specimen AMNH DR-14-51 include *Brachyponera*, *Cryptopone*, *Mayaponera*, *Mesoponera*, *Neoponera*, *Ponera*, and *Pseudoponera*. However, this specimen differs from *Brachyponera* by having mandibles without a basal pit or groove; from *Cryptopone* by the mesotibia without traction setae; from *Mayaponera* by propodeal spiracle nonrounded and having a well-developed prora. It differs from *Neoponera* by the absence of a stridulitrum on the pretergite of abdominal segment 4 and the reduced arolia; and from *Pseudoponera* by having a mandible without a basal groove, an oval shaped propodeal spiracle instead of slit shaped and subpetiolar process produced as large keel with posterior facing projection and anterior fenestra as opposed to being produced as an anterior facing rounded lobe lacking any fenestra. Furthermore, in the specimen, the head and mandibles are more elongated.

In addition to these characters, the combination of an angled clypeus in lateral view, small and closely approximated frontal lobes, small and anteriorly positioned compound eyes, triangular and elongate mandibles with well-developed teeth, dorsally narrowed propodeum, metatibia with two spurs, and a weakly sculptured body suggest closer similarity with the genus *Mesoponera*. Fisher et al. (2025) divided *Mesoponera* into four different lineages, two of which bear the closest overall resemblance to the fossil: *Mesoponera* and *Xiphopelta* Forel (1913). *Xiphopelta* has a median clypeal denticle that may be present in the fossil but may also be caused by desiccation. The subpetiolar process of the fossil is rounded, lacking the posteriorly projecting angle of *Xiphopelta*. Examining AntWeb images of 12 of the 14 valid species of *Xiphopelta* species, and of six of the seven valid species of *Mesoponera*, the following traits can be compared. The mandibles in most *Xiphopelta* and *Mesoponera* appear relatively slenderer than those of the fossil, with more than 10 fine teeth, compared to the six broadly, triangular teeth of the fossil. The constriction between abdominal segments III and IV in *Xiphopelta* and *Mesoponera* is absent or weakly developed, contrasting with the distinct girdling in the fossil. The prora in the fossil seems to project anteriorly more than in the other two genera, with a greater space separating it from the helcium in lateral view. Most of the Antweb images do not permit a detailed study of the prora shape, but a few suggest the prora may be more rounded with a concave dorsal surface. *Mesoponera* is now defined as a group of six valid species found in Asia, Australasia, and the Seychelles. *Xiphopelta* is found in the Afrotropical region (Fisher et al., 2025). Doré et al. (2025) postulate the diversification of these two lineages less than 20 Ma, a time when the world's geography

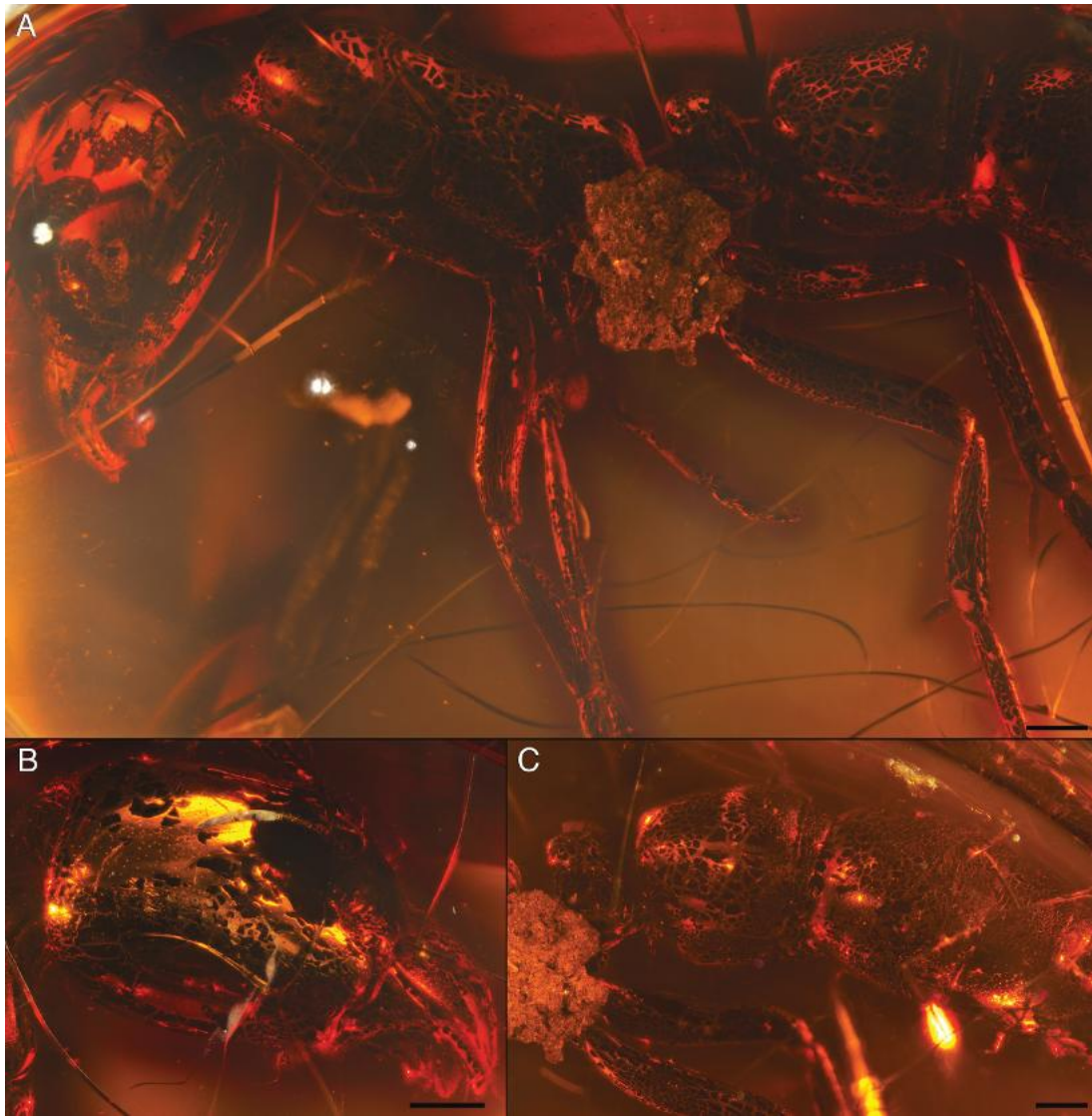


FIGURE 49. Photomicrographs of †*Kiskeyapone armilla*, gen. and sp. nov. (holotype worker, AMNH_JVE_781). **A.** Lateral view of specimen. **B.** Lateral view of head. **C.** Lateral view of petiole and gaster. Scale bars = 0.5 mm.

was already quite similar to the present. Despite the general morphological similarities between *Mesoponera*, *Xiphopelta*, and the fossil, there are significant differences that impede forcing the fossil into either of these two genera. This specimen is thus regarded as representing a new genus.

†*Kiskeyapone* Fiorentino, Cubillos, Barden, Fernandez, and Lattke, gen. nov.

Figures 49–51

ZooBankLSID:urn:lsid:zoobank.org:act:E59FCAB8-E717-44C9-ABDD-1B7F775F45737

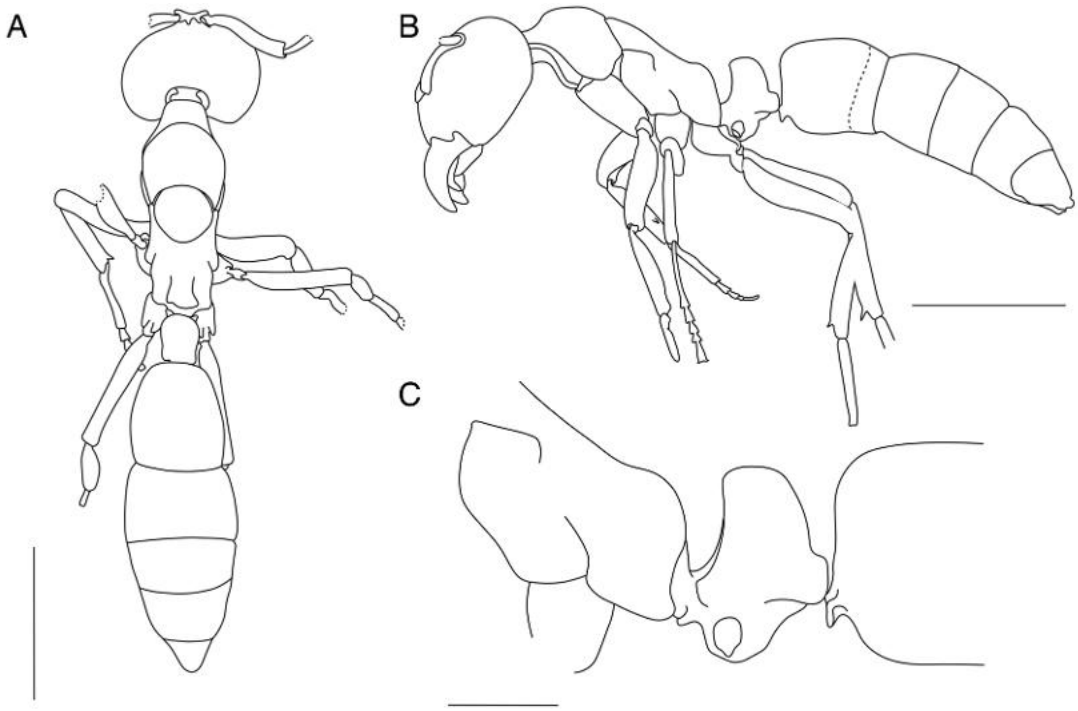


FIGURE 50. Line drawings of †*Kiskeyapone armilla* worker. **A.** Dorsal view of the body. **B.** Lateral view of the body. **C.** Close up of AI–AIII. Scale bars: A, B = 2 mm; C = 1 mm.

Type species: †*Kiskeyapone armilla* Fiorentino, Cubillos, Barden, Fernandez, and Lattke, sp. nov.

Diagnosis (worker): head subquadrate, slightly longer than wider, scape surpassing vertexal border by about two maximum scape diameters, mandible broadly triangular with 8 to 10 ill-defined teeth. Compound eye absent, clypeus with conspicuous medial tooth. Supraclypeal area deeply impressed posterior to cephalic midlength. Promesonotal suture well developed, mesonotum broadly oval, notopropodeal sulcus indistinct; ventral katepisternum with rounded gibbosity, propodeal spiracle slit-shaped. Mesotibia without "traction setae." Metatibia with one apical spur. Tarsal claws simple, arolium absent. Subpetiolar process rounded and relatively large, with prominent rounded fenestra occupying most of anterior half of process. Cuticle with shallow foveolae—irregular depressions. Hypopygium lacking teeth or stout setae.

Etymology: *Kiskeya* (or sometimes written as *quisqueya*) meaning "mother of all the land" or "great land" in Arawak, is in reference to the name given by the Taino people to the island of Hispaniola. Pone is in reference to *Ponera*, the type genus of its subfamily.

†***Kiskeyapone armilla*** Fiorentino, Cubillos, Barden, Fernández, and Lattke, sp. nov.

ZooBankLSID:urn:lsid:zoobank.org:act:C7EF798A-997B-438A-9526-C46D4965C397

Diagnosis (worker): See diagnosis for the genus.

Holotype worker measurements (in mm): HW 2.59, HL 2.64, EL –, EHT –, EHD –, EHV –, ELT –, ELA –, ELP –, MLP 1.59, SL 2.10, WL 3.97, PcL 1.58, MH 1.46, PrW 1.52, MfL 2.48, PeL 1.13, GL 5.85, TL 13.59.

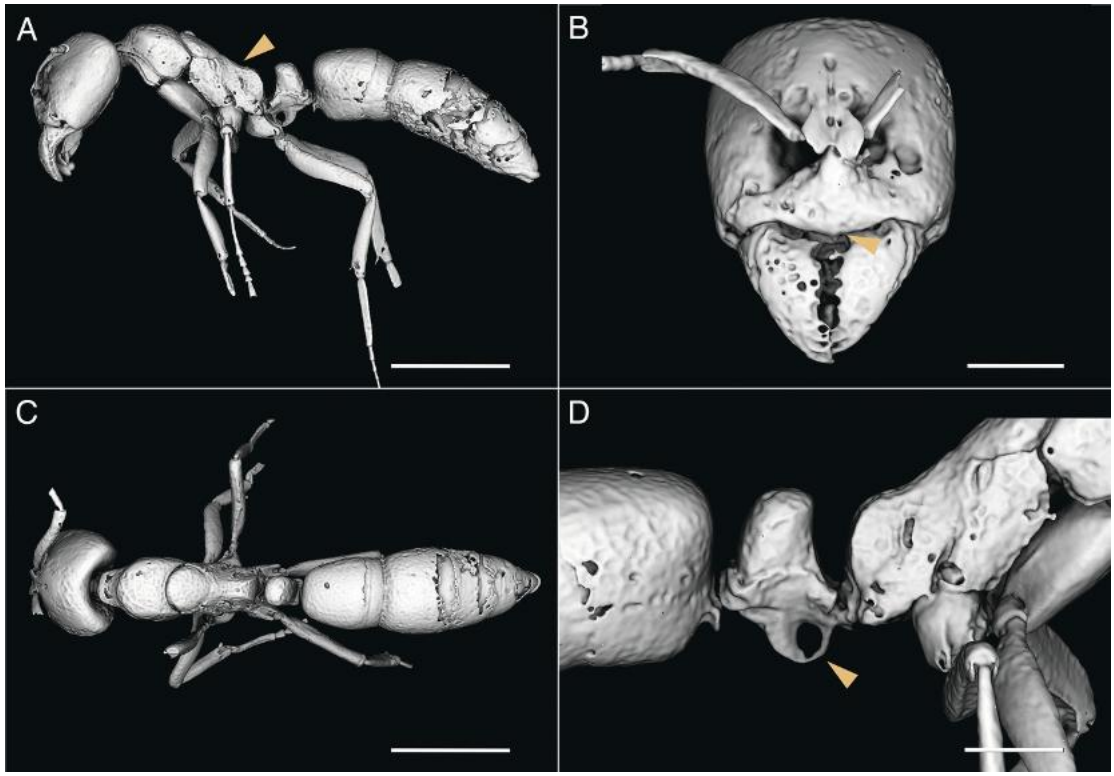


FIGURE 51. Volume renderings of †*Kiskeyapone armilla*, sp. nov. **A.** Mesosoma in lateral view, arrow indicates the notopropodeum. **B.** Head in frontal view. **C.** Mesosoma in dorsal view. **D.** Close-up of petiole in lateral view. Arrow indicates fenestrated subpetiolar process. Scale bars: A, C = 2 mm, B, D = 1 mm.

DESCRIPTION (worker): Head: Subquadrate in dorsal view, slightly longer than wide; scape surpassing vertexal border by about two maximum scape diameters. Antennal scape arched, strongly curved basally followed by broader apical curvature; scape flattened basally in lateral view, thickening apically. Medial torular lobe conceals bulbous in cephalic dorsal view, bulbous neck bent; anterior tentorial pit inconspicuous. Anterior clypeal margin medially convex with discrete median denticle and no setae. Clypeal discal area smooth, lacking carinae. Supraclypeal area deeply impressed posterior to cephalic midlength, shaped as upside-down, elongate drop. Median clypeal line deeply impressed. Clypeus forming evenly convex margin with frons in cephalic lateral view. Mandible triangular, relatively short and robust, with convex dorsal surface. Basal sulcus deeply impressed, extending along mandibular lateral edge to apex. Mandible with small erect setae along masticatory margin. Palpal formula 4, 3. Stipes with toothlike cuticular process that projects distad of palpus insertion.

Mesosoma: In dorsal view pronotum rounded, without humeral angle; promesonotal suture well marked, mesonotum broadly oval, almost circular, notopropodeal sulcus absent or faintly marked, propodeal dorsal face flattened, abruptly narrows posterior to mesonotum, modestly widening posterad to declivity. Mesosomal dorsal margin in lateral view: pronotum convex, promesonotal suture well impressed; mesonotal-propodeal margin sinuous, mesonotum weakly convex, notopropodeal sulcus indistinct; propodeum anteri-

orly with broad, shallow concavity, posteriorly convex. Small lobe or projection present on anterodorsal mesopleural margin, anapleural sulcus absent, ventral katepisternal margin with carina, mesometapleural suture shallow; propodeal spiracle slit shaped, at least 3× longer than wide. Katepisternum ventral area with rounded, distinctly defined, convex gibbosity, next to mesometapleural suture and just above mesocoxa. Propodeum unarmed, declivity laterally carinate, margins broadly convex. Metasternal process forming two broadly triangular, bluntly pointed projections. Mesotibia lacking "traction setae" on external face, internal face with preapical seta on cuticular projection; metatibia with single apical spur.

Metasoma: In lateral view petiole higher than long, subsessile, anterior node margin slightly concave, posterior node margin slightly convex. Petiolar node in dorsal view ellipsoid, wider than long. Subpetiolar process relatively large, shaped as rounded lobe: anterior margin in lateral view weakly convex, mostly vertical, anteroventral margin rounded, posteroventral margin mostly broadly concave. Large, rounded fenestra occupies most of anterior half of process. Process in ventral view shaped as longitudinal keel, widest anterad. Anterior margin of abdominal tergite 3 in lateral view mostly vertical, joining the flat to weakly convex dorsal margin through a convexity. Prora shaped as rounded lobe with flat, vertical anterior face. Cinctus well developed.

Sculpturing and setae: Dorsum of mandibles, head, mesosoma, and gaster with abundant shallow foveolae. Mesosoma with sparse erect setae.

Etymology: The specific epithet *armilla* (Latin for "bracelet, metal hoop, ring, washer") is a feminine noun. It refers to the prominent fenestra in the subpetiolar process present in this species, with semicircular shape, reminiscent of a ring or hoop.

Type material: Holotype. AMNH_JVe_781 worker, deposited in the American Museum of Natural History (figs. 49–51). Preserved within a round 20 mm × 20 mm section of dark red amber. No synclusions.

Horizon and locality: Early Miocene, Burdigalian (ca. 16 Ma; Iturralde-Vinent and MacPhee, 1996); in amber from the northern mines of the Santiago Province, Dominican Republic.

Comments: The proximity of the toruli, narrow posteromedian extension of the clypeus between the antenna, and the relatively low position of the helcium on the anterior face of abdominal tergite 3 place this ant in the subfamily Ponerinae, tribe Ponerini. The morphology seems to point toward the Ponera group of species (sensu Schmidt and Shattuck, 2014), but it does not seem to fit any genus in particular. Of special interest are the subquadrate head, clypeal tooth, lack of eyes, the single metatibial spur, the narrowed propodeal dorsal face, and the shallow cuticular depressions. Most ants in the *Ponera* group have elongate heads, but some species within these genera may have a subquadrate head, such as *Pseudoponera* stigma. In the Ponera group, a median clypeal tooth is only found in *Emeryopone* (Schmidt and Shattuck, 2014) but other ponerines may also bear a tooth such as *Simopelta* (Fernández and Guerrero, 2019) or Belonopelta (Schmidt and Shattuck, 2014). The lack of eyes, and small and closely joined frontal lobes are common in the *Ponera* group genera but may be found in other ponerines. The markedly constricted anterior propodeal dorsum is an apparent synapomorphy of *Austroponera*, *Pseudoponera*, *Wadeura*, and *Cryptopone* (Schmidt and Shattuck, 2014; Longino and Branstetter, 2020). The loss of one metatibial spur is frequent in small-bodied hypogeic ponerines. A relatively "large" fenestra is to be found in: *Ponera*, *Emeryopone*, and some *Hypoponera* (Schmidt and Shattuck, 2014), but this is relative to most other ponerines. The size of the fenestra is routinely used as a diagnostic character in keys (Schmidt and Shattuck, 2014; Esteves and Fisher, 2021) to separate the aforementioned genera, but its size in these genera pales in comparison with that of †*Kiskeyapone*. The lack of eyes strongly suggests a hypogeic lifestyle for †*Kiskeyapone*, but it lacks mesotibial traction setae, such as in the eyeless *Cryptopone*. Abundant shallow puncta

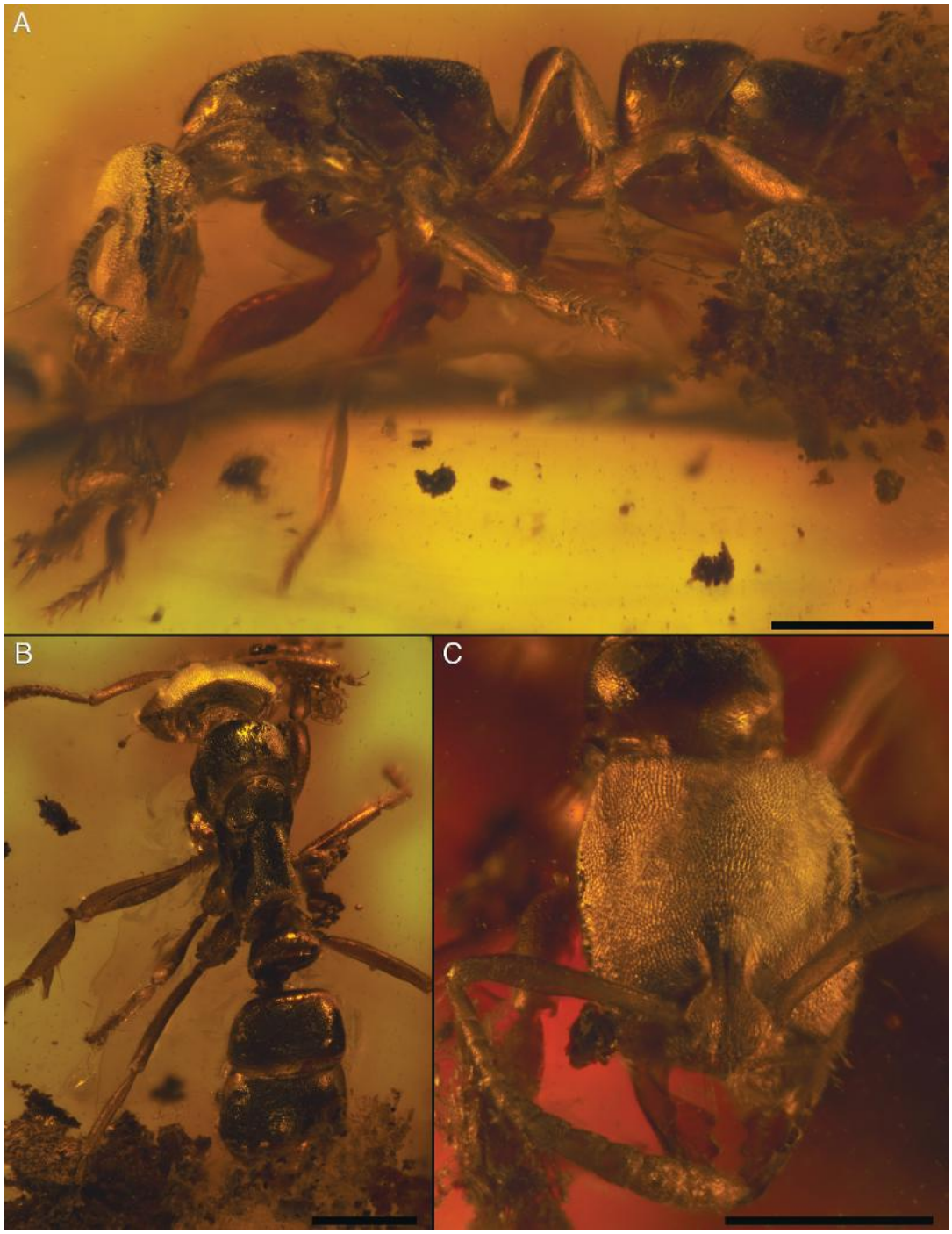


FIGURE 52. Photomicrographs of *Pseudoponera hatuey*, sp. nov. (holotype worker, AMNH_DR_14_881). **A.** Lateral view of specimen. **B.** Dorsal view of specimen. **C.** Frontal face on view of head and pronotum. Scale bars = 0.5 mm.

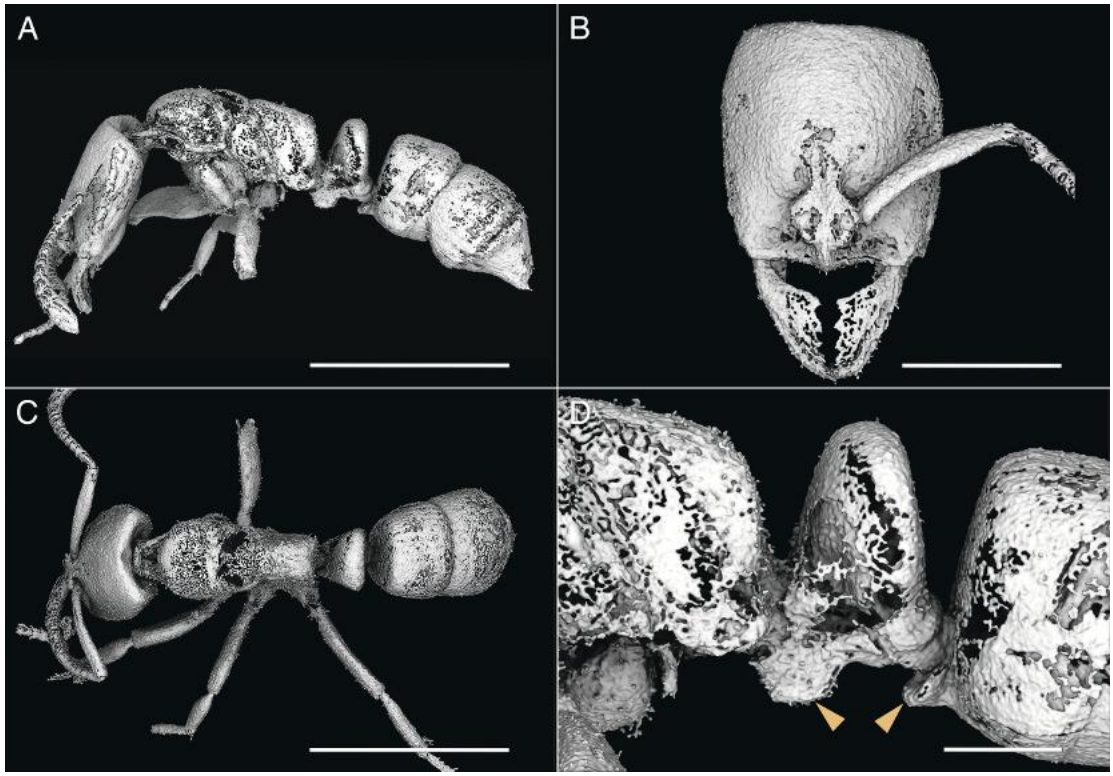


FIGURE 53. Volume renderings of *Pseudoponera hatuey*, sp. nov. **A.** Mesosoma in lateral view. **B.** Head in frontal view. **C.** Mesosoma in dorsal view. **D.** Close-up of petiole in lateral view. Arrows indicate subpetiolar projections and prora. Scale bars: A = 1 mm; B, C = 0.5 mm; D = 0.2 mm.

can be found in *Emeryopone*, but their relative size/diameter is smaller than in †*Kiskeyapone*. The rounded feature on the ventral katepisternal margin, just above the mesocoxa is present on both sides of the mesosoma is of special interest. Unfortunately, the resolution of the CT-scan reconstruction and the visibility of this feature on the specimen do not permit a detailed assessment of its morphology, but it does appear unique among ponerines. The defining apomorphies for †*Kiskeyapone* seem to be the enlarged subpetiolar process with the prominent fenestra, and the katepisternal convexity. If one were to use recent publications that include Neotropical ponerine genera, this specimen would become swamped at the couplets that separate *Ponera* from *Hypoponera* in (Schmidt and Shattuck, 2014: couplet 18; Esteves and Fisher, 2021: couplet 8).

Pseudoponera Emery, 1900

†***Pseudoponera hatuey*** Cubillos, Fernández, Lattke, and Fiorentino, sp. nov.

Figures 52, 53

ZooBank LSID: urn:lsid:zoobank.org:act:6737F0C1-170D-4778-8651-CFBEBC2238DE

Diagnosis (worker): Clypeus with median longitudinal carina and anterolateral transverse carina. Mandible with five teeth and coarsely striate dorsum. Eye reduced. Subpetiolar process in lateral view subquadrate with anteroventral facing process, anterior and posterior corners rounded.

Holotype worker measurements (in mm): HW 0.70, HL 0.75, EL 0.03, EHT 0.34, EHD 0.23, EHV 0.11, ELT 0.65, ELA 0.18, ELP 0.47,

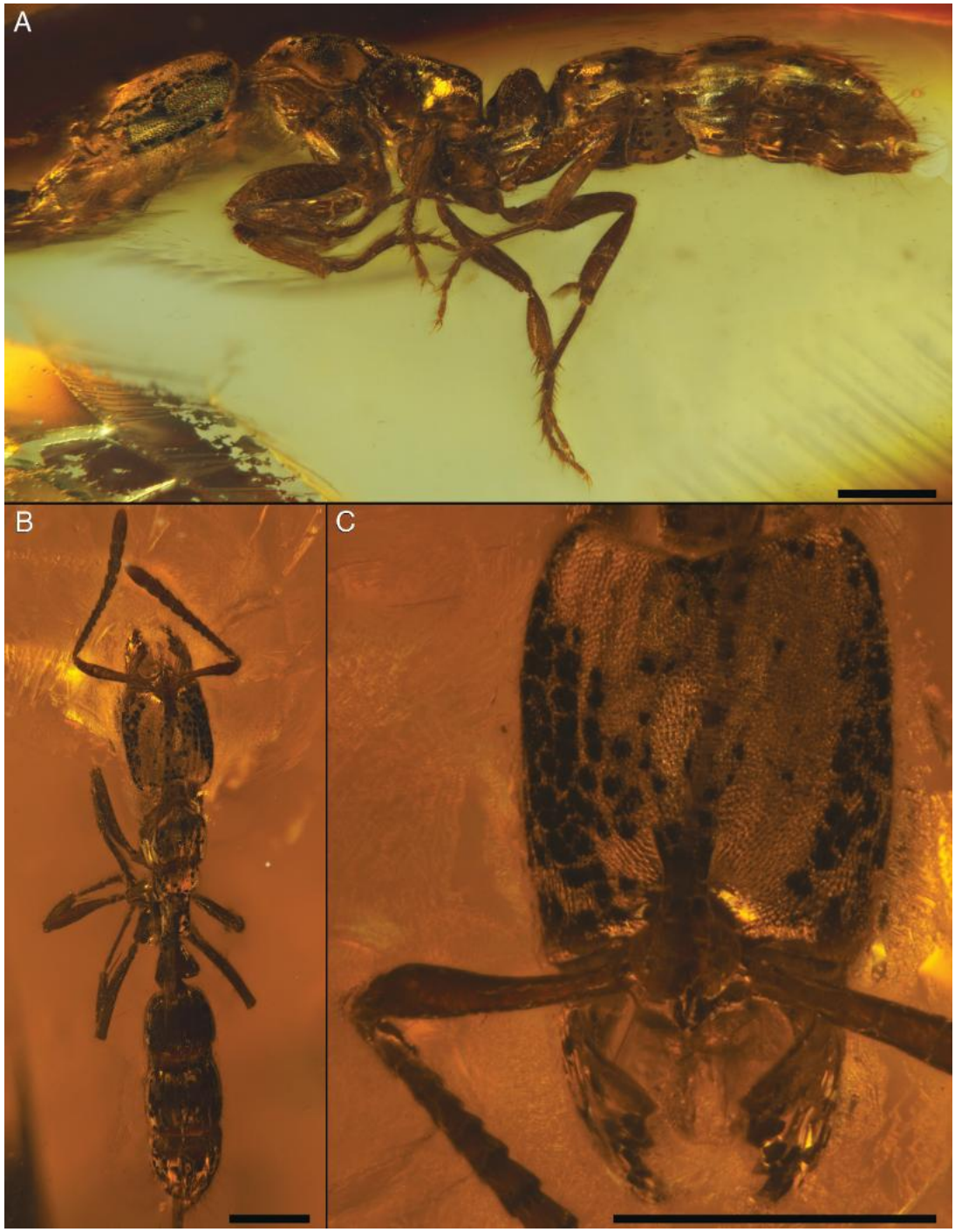


FIGURE 54. Photomicrographs of *Stenoponera petiolata*, gen. and sp. nov. (holotype worker, AMNH_DR_14_881). **A.** Lateral view of specimen. **B.** Dorsal view of specimen. **C.** Frontal face on view of head. Scale bars = 0.5 mm.

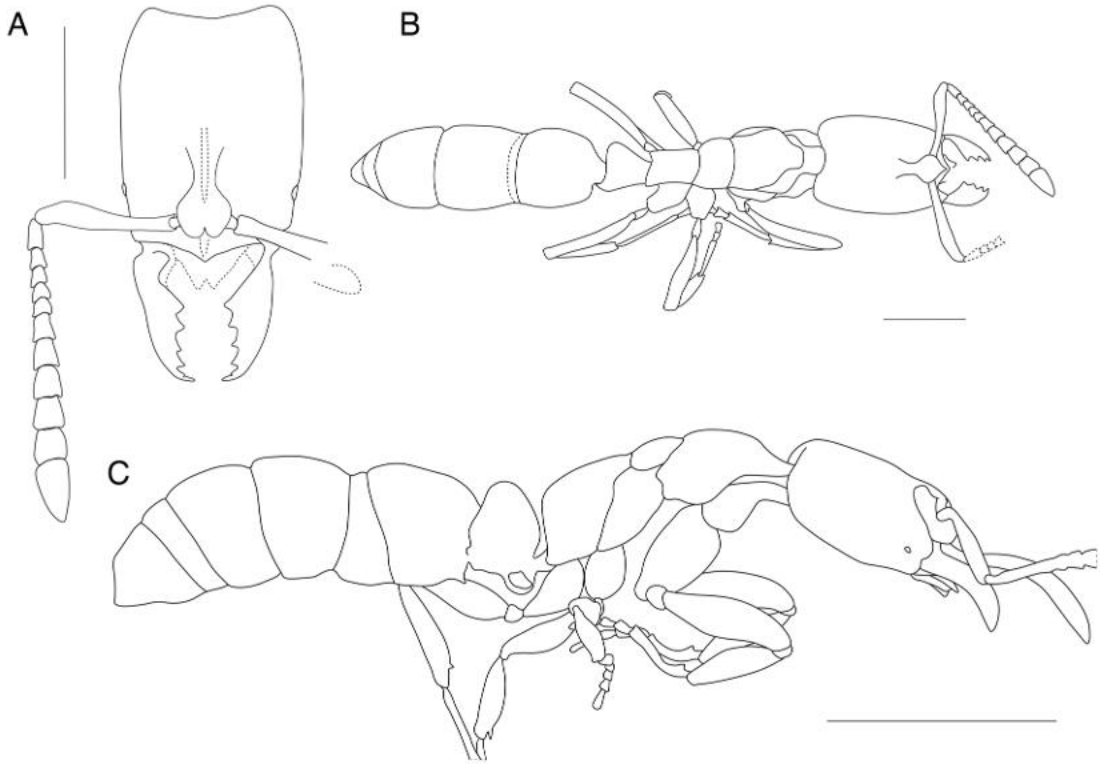


FIGURE 55. Line drawings of *Stenoponera petiolata* worker. **A.** Head in full-face view. **B.** Dorsal view of the body. **C.** Lateral view of the body. Scale bars: A, B = 0.5 mm; C = 1 mm.

MLP 0.43, SL 0.56, WL 1.01, PcL 0.30, MH 0.32, PrW 0.45, MfL 0.59, PeL 0.33, GL 1.1, TL 4.1, CI 0.92, SI 0.76 Note: average length of scapes taken from posterior cephalic view.

DESCRIPTION (worker). Head: Rectangular in dorsal view, wider posterad than anterad; posterior margin straight to feebly convex, lateral margin broadly convex, anterior clypeal margin projecting medially as broad triangle with blunt summit, laterally weakly concave. Scape surpassing posterior cephalic margin by approximately one apical width. Mandible with five large teeth, no denticles, dorsal surface coarsely striate. Eye reduced in size.

Mesosoma: Pronotal anterior margin in lateral view broadly concave, dorsal margin convex; mesonotal dorsal margin broadly convex, notopropodeal sulcus distinctly impressed; propodeal dorsal margin slightly lower than mesonotum, weakly convex, declivitous margin weakly convex. Propodeal spiracular sclerite oval, opening slit shaped; mesometapleural suture well impressed, mesopleuron with anteroventral carina ending anteriorly with rounded lobe. Mesonotum oval in dorsal view, wider than long, propodeal dorsal face elongate, wider posteriorly than anteriorly, propodeum unarmed. Metatibial apex with two spurs, claws simple, aroleum absent.

Metasoma: Petiolar node squamiform in lateral view, anterior and posterior margins straight to weakly convex, margins converging to rounded summit. Subpetiolar process subquadrate with rounded anterior and posterior corners. No fenestra observable. Node anterior margin in dorsal view convex, posterior margin concave, node 4× wider than long. Anterior margin of abdominal tergite 3 forms blunt

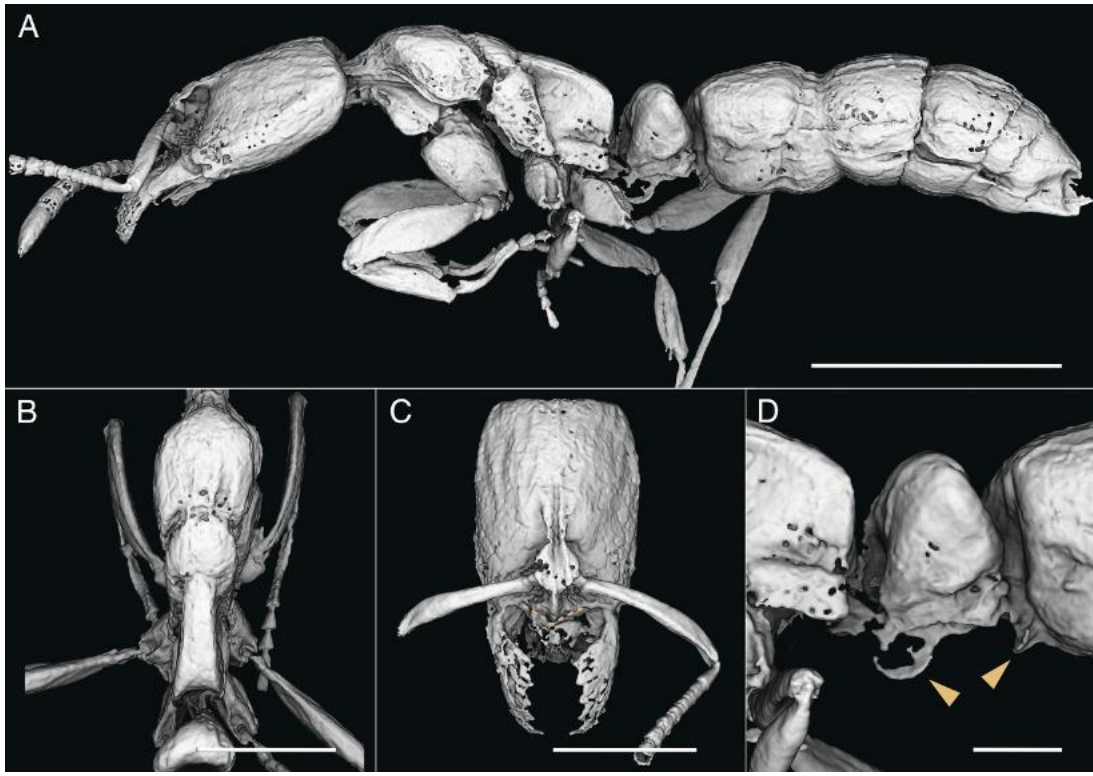


FIGURE 56. Volume renderings of *Stenoponera petiolata*, sp. nov. **A.** Mesosoma in lateral view. **B.** Mesosoma in dorsal view. **C.** Head in frontal view, dashed line outlines the triangular clypeal shelf. **D.** Close-up of petiole in lateral view. Arrows indicate subpetiolar process and prora. Scale bars: A = 1 mm; B, C = 0.5 mm; D = 0.2 mm.

right angle with dorsal margin, anterior margin straight, dorsal margin broadly convex. Prora and cinctus well developed.

Sculpturing and setae: Most sculpturing smooth with abundant, shallow and fine punctae. Body with abundant standing hairs.

Etymology: *Hatuey* refers to the Taíno leader and anticolonialist who opposed Spanish conquest in the early 16th century, becoming a powerful symbol of indigenous resistance to European colonization.

Type material: Holotype. AMNH_DR_14_881 worker, deposited in the American Museum of Natural History (figs. 52, 53). Preserved within a round 21 mm by 10 mm section of dark red amber. Synclusions include fragments of an ant head (possibly *Azteca alpha*) and a termite.

Horizon and locality: Early Miocene, Burdigalian (ca. 16 Ma; Iturralde-Vinent and MacPhee, 1996); in amber from the Northern mines of the Santiago Province, Dominican Republic.

Comments: We recognize this ant as a *Pseudoponera* because it bears the following diagnostic traits for the genus as defined in Schmidt and Shattuck (2014) and Esteves and Fisher (2021): compound eyes, basal mandibular groove, metatibial apex with two spurs, dorsal mesosomal margin fairly continuous in lateral view with shallow notopropodeal sulcus, slit-shaped spiracular opening, subpetiolar process without a fenestra, and a well-developed prora projected anteroventrally as a long, acute prominence. The gaster of the specimen presents

what is presumably an artifact in one lateral view compared with the other. With the head to the right, abdominal segments 3 and 4 in lateral appear to be divided by transverse impressions into 3 sclerites each. The tergites have a fine, but distinct longitudinal line at apparent mid-height, with the sutures separating them from the sclerites in a more ventral position than is usual, making the sclerites appear much smaller than usual. Abdominal segment 3 appears with a long and broadly convex anterior margin that curves sharply posteriorly to its midlength, and abdominal segment 4 is mostly broadly convex, sharply curving dorsally just anterad of its posterior margin. The image with the head positioned to the right, shows the tergal-sternal sutures at the expected position, and no fine, longitudinal line. The ventral sternal margins are partially obscured in this perspective.

The genus presently has six species (Bolton, 2025) and they may be separated using MacKay and MacKay (2010), which considers them as the stigma species group of the genus *Pachycondyla*. If the identification key is used, this species becomes stranded at couplet 7 because the number of mandibular teeth does not agree with any of the alternatives. The rounded corners of the subpetiolar process and the coarsely striate mandibular dorsum will quickly separate this species from the extant ones.

Stenoponera Lattke, Cubillos, Fernández, and Fiorentino, gen. nov.

ZooBank LSID: urn:lsid:zoobank.org:act:E9AE9C27-35B8-4A04-B6A8-3CFB00D84C44.

Type species: †*Stenoponera petiolata* Lattke, Cubillos, Fernández, and Fiorentino, sp. nov.

Diagnosis (worker): Eye very reduced and placed anteriorly on head. Antennal insertions placed anteriorly on head on elevated process. Frontal lobes placed next to each other, covering bulbous in dorsal view; antennal insertions exposed in lateral view. Anterior clypeal margin in dorsal head view mostly covered by triangular shelf that projects anterad from posteromedian clypeal region, overhanging anterior clypeal region and mandibles. Promesonotal suture well developed. Propodeal dorsal face elongate, dropping vertically to sides, anteriorly strongly constricted. Propodeum unarmed. Mesotibia lacking stout setae on dorsal face, apex with two apical spurs and three stout setae; metatibia with two apical spurs, one broadly pectinate, the other simple. Claws simple, no arolium. Anterior face of AT3 with median vertical keel that inserts into broad vertical concavity of posterior node face. Prora well developed. Metasoma with deep and broad longitudinal sulcus along dorsal margins of sternites, sulcus most developed in abdominal segments 5–7. Cinctus deep and wide. Posterior half of AT7 separating from AS7 in lateral view and overhanging hypopygidium, lateral gastral sulcus posteriorly forming longitudinal dorsolateral surface of AS7.

Etymology: *Stenoponera* is a name derived from the combination of the Greek word *stenos* (στενός), meaning "narrow, "close," or "small," in reference to the narrow propodeum, and *Ponera*, the type genus of the subfamily; the species name is derived from *petiole*, which is diagnostic of this genus.

†***Stenoponera petiolata*** Lattke, Cubillos, Fernández, and Fiorentino, sp. nov.

Figures 54–56

ZooBank LSID: urn:lsid:zoobank.org:act:6A9CDE64-8B93-42D5-A437-80C9B7B07154.

Diagnosis (worker): See diagnosis for the genus.

Holotype worker measurements (in mm): HW 0.58, HL 0.78, EL 0.04, EHT 0.37, EHD 0.19, EHV 0.19, ELT 0.81, ELA 0.26, ELP 0.55, MLP 0.41, SL 0.53, WL 1.08, PcL 0.41, MH 0.30,

PrW 0.36, MfL 0.67, PeW 0.28; PeL 0.3; PpeW 0.47; PpeL 0.44; GL 1.63; TL 4.17, CI 0.72; OI 0.50, SI 0.93. Note: All measurements taken using images of the fossil except for MFL, which was measured using a scaled 3D model of the ant with MeshLab; PPL was measured by assuming a hypothetical continuity of the anterolateral margins, ignoring the median keel.

DESCRIPTION (worker): Head: Longer than wide in dorsal view; posterior margin rounded, lateral margin nearly parallel. Scape fails to reach vertexal margin by 1.5–2 apical scape widths, scape widest at apical two-thirds; flagellum widening apicad, flagellomeres becoming slightly longer apicad, each flagellomere wider apically than basally. Scape with two right angles between base of shaft and bulbous. Lateral margin of frontal lobe margin convex and higher than internal margin, longitudinal groove extends posterad from between lobes to cephalic midlength, posteromedian cephalic region, close to vertex with longitudinal low carina along same axis as anterior groove. Anterior clypeal margin broadly convex in cephalic dorsal view, but margin mostly covered by triangular shelf; shelf with longitudinal median ridge, dorsal margin of ridge convex in lateral view. Labium elongate in cephalic ventral view, with apical half roughly rectangular and more than twice as wide as base; lateral margin of stipes forms blunt extremely obtuse angle, widest at midlength, internal margin weakly concave and raised as perpendicular, thick carina. Hypostomal teeth well developed, triangular, bluntly pointed. Dorsal cephalic surface with 8–10 shallow and broad longitudinal sulci. Mandible semitriangular, basal sulcus well developed, dorsum roughly striate with about seven coarse teeth, no denticles. Eye small, with less than 10 ommatidia, placed anteriorly, closer to mandibular base than to cephalic midlength.

Mesosoma: In lateral view with dorsal margin relatively uniform, anterior pronotal margin straight to feebly concave, dorsal margin weakly convex; promesonotal suture shallow, but distinct; mesonotum weakly convex; notopropodeal sulcus weakly impressed; propodeal dorsal margin broadly convex, separated from straight declivitous margin by convexity, dorsal and declivitous margins forming weakly obtuse angle, almost right-angled. Anterodorsal margin of propodeal lateral face rounded and overhanging most of lateral face, overhang diminishing posterad. Lateral pronotal face with sulcus and carina along ventral margin; mesometanotal suture developed as distinct ridge, anteroventral margin of mesopleuron carinate, anapleural sulcus absent. Metapleuron mostly forming longitudinal swelling. Mesosoma widest at anterior pronotum in dorsal view, mesonotum anteriorly convex, widest posterior to midlength, notopropodeal sulcus shallow, dorsal propodeal face elongate and semiparallel, anterior margin less than half as wide as mesonotal width, lateral margins weakly diverging posterad. Mesonotal lateral margin overhanging anterior anepisternum and posterior pronotal side. Declivitous propodeal face concave and laterally bound by broad carina. Propodeal spiracle circular, placed just ventrad of propodeal midheight, anterior to metapleural gland opening. Propleuron well developed, its height in lateral view similar to that of pronotum at pronotal midlength; prosternal process prominent, V-shaped. Metasternal process shaped as gibbosity with two teeth; mesosternal process bidentate, teeth on gibbosity, anterior mesosternal face with longitudinal median crest that joins gibbosity. Posterior protibial face at midlength with low keel along internal margin. Arch of protarsal base, opposite strigil, with 10 slender setae; protarsomeres with very stout and long apical setae. Claws simple, elongate; arolia absent.

Metasoma: Petiolar node in lateral view dome shaped, anterior margin broadly convex, node highest just posterad of petiolar midlength, posterior margin broadly convex; node widest posterad in dorsal view; posterior node face with broad and deep, median, vertical sulcus. Subpetiolar process well developed, subquadrate, anterior margin weakly sinuous, ventral margin convex, posterior margin weekly concave. Gaster elongate in lateral view, ventral margin of tergites

overhang sternites. Constriction between the abdominal segments 4 and 5 well developed, not as strongly as cinctus. Anterolateral margin of abdominal tergite 3 vertical, weakly concave; anteromedian face with vertical, quadrilateral keel that slopes anteroventrally from anterodorsal margin of tergite and projects anteriorly into posterior sulcus of node, anterior margin of keel straight and vertical. Keel in triangular in dorsal view. AS3 ventral margin mostly convex; prora projects anteriorly as oval cup, anterior margin vertical in lateral view; dorsomedian area with anteriorly projecting bifurcate vertical carina. abdominal tergite 7 (pygidium) ending in blunt point.

Sculpturing and setae: Mandibular dorsum longitudinally coarsely striate; head dorsum densely punctate with narrow longitudinal smooth strip extending from between frontal carinae to vertex. Dorsolateral head surface with two or three broad, shallow, longitudinal sulci. Mesosoma and gaster mostly densely punctate; posterior pronotal margin and anterior mesonotal margin strongly scrobiculate. Mesosoma and gastral tergites with broad and shallow longitudinal sulci

Etymology: The specific epithet petiolata is derived from the Latin *petiolus*, "having a petiole." It refers to the distinct petiolar morphology present in this species.

Type material: Holotype. AMNH_DR_14_897 worker, deposited in the American Museum of Natural History (figs. 54–56). Preserved within a 11 mm by 7 mm section of orange amber. No synclusions.

Horizon and locality: Early Miocene, Burdigalian (ca. 16 Ma; Iturralde-Vinent and MacPhee, 1996); in amber from the northern mines of the Santiago Province, Dominican Republic.

Comments: *Stenoponera* stands out among Ponerines, and all other ants in general, with an unusual morphology that cannot be confused with any other genus in the subfamily: anteriorly placed antennae, a keel that projects from the anterior abdominal tergite 3 face into a broad sulcus on the posterior node face, the broad longitudinal sulci of the head, mesosoma, and gaster, and the deep groove on the gastral side. The helcium seems to be positioned more ventrally on the anterior gastral face, and the frontal lobes are closely fused to each other, permitting a thin, posterior sliver of the clypeus to project posteriorly, characters that suggest an affinity to Ponerini. Beyond that, it is difficult to relate it with any other known ponerine due to the highly derived nature of its morphology.

The antennae are positioned along the anterior clypeal margin, well anterad of the eye in a way reminiscent of Proceratinae and Dorylinae, but the antennal insertions are well covered by the frontal lobes and the lateral clypeus is not narrowed as in dorylines (Bolton, 2003; Borowiec, 2016). The posterior elevation of the clypeus that projects anteriorly as a shelf that overhangs the rest of the clypeus and the mandibles is reminiscent of morphologies in proceratiines (Bolton, 2003), but the ponerine traits of *Stenoponera* strongly imply convergence. The narrow and elongate propodeum is found in several ponerine genera, such as *Hagensia*, *Mesoponera*, and *Hypoponera* (Schmidt and Shattuck, 2014), but again the strong apomorphies of *Stenoponera* suggest that these are homoplastic.

The slot and tab configuration of the posterior node face with the anterior face of abdominal tergite 3 suggests a functional role in bracing the gaster during behavior of importance. Given the presence of a sting and the usual predatory behavior of ponerines, it could be assumed this is associated with hunting, such as subduing prey. However, ponerines usually bend their gaster beneath their body to facilitate stinging their prey. This implies arching the gaster ventrally and then thrusting anteriorly, a movement that would increase the distance between the faces of abdominal tergite 3 and the petiolar node. In an alternative hunting scenario, the ant could be on top of its prey, eliminating the necessity for anterior thrusting. The deep lateral sulcus along the whole gastral length is also unknown among ants in general, including its role with the posterior

rooflike separation of abdominal tergite 7 from abdominal sternite 7. Some features of the specimen are probably taphonomic artifacts, such as the conspicuous dark spots on the cephalic dorsum or what seem to be longitudinal raised carinae on the cephalic and mesosomal dorsum. These features are not registered in the scans. Other possible artifacts may be the stronger than usual constriction between abdominal segments 4 and 5, the general elongation of the body and body parts, the apparent partial collapse of the lateral propodeum and metapleuron. Nevertheless, this may not be the case, given the uniform nature of these morphologies on both sides of the ant body. The exoskeleton of this ant also appears to be quite sclerotized. The unique morphology of this extraordinary ant suggests a highly specialized natural history.

ACKNOWLEDGMENTS

We would like to thank David Grimaldi and Agnieszka Pierwola for their help with the specimens at the American Museum of Natural History, as well as for insightful comments on early drafts of this work. We also thank Pheobu Fu of the AMNH and Julian Katzke and Christine Sosiak of the Okinawa Institute of Science and Technology for their assistance with CT scanning and reconstruction. For their creative input on the project, we thank Gabriel de los Santos and America Sanchez of the Museo Nacional de Historia Natural "Prof. Eugenio de Jesús Marcano," along with Celaine Yens and Kendy Arias of the Universidad Autónoma de Santo Domingo. Many thanks to Brandon S. Arredondo for the illustrations of the †*Chimerodous alpha* habitus and Kristina Camia for the illustrations of †*Kiskeyapone* and †*Stenoponera*. We would also like to thank the three reviewers of this work for providing insightful and important feedback that greatly improved the quality and cohesiveness of this monograph. Funding: G.F. received funding from the Theodore Roosevelt Memorial Fund. T.R.S. and J.S.-C. received funding from the National Science Foundation (NSF grant DEB-1927161). G.P.C. is supported by the São Paulo Research Foundation (FAPESP grant 2023/12809-0). J.P.C. is supported by the Coordination for the Improvement of Higher Education Personnel (CAPES grant 88887.132404/2025-00). R.J.G. is supported by Minciencias under contract 2021–2029 (Universidad del Magdalena and ICETEX). D.C. is supported by the National Council for Scientific and Technological Development (CNPq grant 142556/2025-4). B.B.B. was supported by the Museum für Naturkunde, Berlin, and the National Science Foundation (NSF grant DEB-2019431). R.S.P. is supported by a Postdoctoral Fellowship from the College of Science at the University of Utah. P.B. and G.F. are supported by an NSF CAREER grant (DEB-2144915). Imaging on Zeiss Xradia Versa 630 partially supported by NSF MRI grant no. 2320473. J.E.L. received support from CNPq Grant 4508306043/2023-8. R.M.F. is supported the National Council for Scientific and Technological Development (CNPq grant 304012/2023-8).

REFERENCES

Antropov, A., et al. 2014. The wasps, bees and ants (Insecta: Vespida=Hymenoptera) from the Insect Limestone (Late Eocene) of the Isle of Wight, UK. Earth and Environmental Science Transactions of the Royal Society of Edinburgh 104: 335–446.

Archibald, S., S. Cover, and C. Moreau. 2006. Bulldog ants of the Eocene Okanagan Highlands and history of the subfamily (Hymenoptera: Formicidae: Myrmeciinae). Annals of the Entomological Society of America 99: 487–523.

Aria, C., V. Perrichot, and A. Nel. 2011. Fossil Ponerinae (Hymenoptera: Formicidae) in Early Eocene amber of France. Zootaxa 2870: 53–62.

Bai, F., H. Liang, and H. Qu. 2019. Structural evolution of Burmese amber during petrifaction based on a comparison of the spectral characteristics of amber, copal, and rosin. Journal of Spectroscopy 2019: 6904541.

Barden, P. 2017. Fossil ants (Hymenoptera: Formicidae): ancient diversity and the rise of modern lineages. Myrmecological News 24: 1–30.

Barden, P., B.E. Boudinot, and A. Lucky. 2017. Where fossils dare and males matter: combined morphological and molecular analysis untangles the evolutionary history of the spider ant genus *Leptomyrmex* Mayr (Hymenoptera: Dolichoderinae). Invertebrate Systematics 31: 765–780.

Baroni Urbani, C. 1980a. First description of fossil gardening ants. (Amber Collection Stuttgart and Natural History Museum Basel; Hymenoptera: Formicidae. I: Attini). Stuttgarter Beiträge zur Naturkunde B, Geologie und Paläontologie: 54: 1–13.

Baroni Urbani, C. 1980b. *Anochetus corayi* n. sp., the first fossil Odontomachiti ant. (Amber Collection Stuttgart: Hymenoptera, Formicidae. II: Odontomachiti). Stuttgarter Beiträge zur Naturkunde B, Geologie und Paläontologie 55: 1–6.

Baroni Urbani, C. 1980c. The first fossil species of the Australian ant genus *Leptomyrmex* in amber from the Dominican Republic. Stuttgarter Beiträge zur Naturkunde B, Geologie und Paläontologie 62: 1–10.

Baroni Urbani, C. 1994a. The identity of the Dominican *Paraponera* [Amber Collection Stuttgart: Hymenoptera, Formicidae. V: Ponerinae, partim]. Stuttgarter Beiträge zur Naturkunde B, Geologie und Paläontologie 197: 1–9.

Baroni Urbani, C. 1994b. [Untitled. *Acanthognathus poinari* n. sp.]. *In* C. Baroni Urbani and M.L. De Andrade (editors), First description of fossil Dacetini ants with a critical analysis of the current classification of the tribe. Stuttgarter Beiträge zur Naturkunde B, Geologie und Paläontologie 198: 41–44.

Baroni Urbani, C. 1995. Invasion and extinction in the West Indian ant fauna revisited: the example of *Pheidole* [Amber Collection Stuttgart: Hymenoptera, Formicidae. VIII: Myrmicinae, partim]. Stuttgarter Beiträge zur Naturkunde. Serie B (Geologie und Paläontologie) 222: 1–12.

Baroni Urbani, C., and M.L. De Andrade. 1994. First description of fossil Dacetini ants with a critical analysis of the current classification of the tribe [Amber Collection Stuttgart: Hymenoptera, Formicidae. VI: Dacetini]. Stuttgarter Beiträge zur Naturkunde B, Geologie und Paläontologie 198: 1–65.

Baroni Urbani, C., and M.L. de Andrade. 2003. The ant genus *Proceratium* in the extant and fossil record (Hymenoptera: Formicidae). Museo Regionale di Scienze Naturali, Monografie 36: 1–492.

Baroni Urbani, C., and E.O. Wilson. 1987. The fossil members of the ant tribe Leptomyrmecini (Hymenoptera: Formicidae). Psyche (Cambridge) 94: 1–8.

Baroni Urbani, C., and M.L. De Andrade. 2007. The ant tribe Dacetini: limits and constituent genera, with descriptions of new species. Annali del Museo Civico di Storia Naturale Giacomo Doria (Genova) 99: 1–191.

Bisulca, C., P.C. Nascimbene, L. Elkin, and D.A. Grimaldi. 2012. Variation in the deterioration of fossil resins and implications for the conservation of fossils in amber. American Museum Novitates 3734: 1–19.

Blaimer, B.B. 2012. A subgeneric revision of *Crematogaster* and discussion of regional species-groups (Hymenoptera: Formicidae). Zootaxa 3482 (1): 47–67.

Bolton, B. 1994. Identification guide to the ant genera of the world. Cambridge, MA: Harvard University Press.

Bolton, B. 2003. Synopsis and classification of Formicidae (Memoirs of the American Entomological Institute 71). Gainesville, FL: American Entomological Institute.

Bolton, B. 2007. Taxonomy of the dolichoderine ant genus *Technomyrmex* Mayr (Hymenoptera: Formicidae) based on the worker caste. Contributions of the American Entomological Institute 35 (1): 1–150.

Bolton, B. 2025. An online catalog of the ants of the world. Online resource (https://antcat.org/), accessed June 28, 2025.

Bolton, B., and B.L. Fisher. 2016. Ants of the world. Ants of Africa and Madagascar: a guide to the genera. Berkeley, CA: University of California Press.

Borowiec, M.L. 2016. Generic revision of the ant subfamily Dorylinae (Hymenoptera, Formicidae). ZooKeys 608: 1–280.

Borowiec, M.L., et al. 2025. Evaluating UCE data adequacy and integrating uncertainty in a comprehensive phylogeny of ants. Systematic Biology 74 (5): 700–722.

Boudinot, B.E. 2019. Capítulo 15. Clave para las subfamilias y géneros. *In* F. Fernández, R.J. Guerrero, and T. Delsinne (editors), Hormigas de Colombia: 487–500. Bogotá: Universidad Nacional de Colombia.

Boudinot, B.E., R.S. Probst, C.R.F. Brandão, R.M. Feitosa, and P.S. Ward. 2016. Out of the Neotropics: newly discovered relictual species sheds light on the biogeographical history of spider ants (*Leptomyrmex*, Dolichoderinae, Formicidae). Systematic Entomology 41: 658–671.

Boudinot, B.E., et al. 2024. Et latet et lucet: Discoveries from the Phyletisches Museum amber and copal collection in Jena, Germany. Deutsche Entomologische Zeitschrift 711, 111–176

Bouju, V., et al. 2026. The myrmicine thief ants Solenopsis (Hymenoptera: Formicidae) in Dominican amber: first fossil record of the genus in fossilized resin. Fossil Record 29 (2): 499–517.

Brache L. 2025. Parachute science in paleontology as distributive epistemic injustice. Philosophy of Science 92 (5): 1076–1085.

Braga, J.C., et al. 2012. Pliocene-Lower Pleistocene shallow-water mixed siliciclastics and carbonates (Yanigua and Los Haitises formations) in eastern Hispaniola (Dominican Republic). Sedimentary Geology 265–266: 182–194.

Brandão, C.R.F., C. Baroni Urbani, J. Wagensberg, and C.I.Yamamoto. 1999 ("1998"). New *Technomyrmex* in Dominican amber (Hymenoptera: Formicidae), with a reappraisal of Dolichoderinae phylogeny. Entomologica Scandinavica 29: 411–428.

Brandão, C.R.F., R.G. Martins-Neto, and M.A. Vulcano. 1989. The earliest known fossil ant (first Southern Hemisphere Mesozoic record) (Hymenoptera: Formicidae: Myrmeciinae). Psyche 93 (3/4): 195–208.

Brody, R.H., H.G. Edwards, and A.M. Pollard. 2001. A study of amber and copal samples using FT-Raman spectroscopy. Spectrochimica Acta A, Molecular and Biomolecular Spectroscopy 57: 1325–1338.

Brown, W. L. 1960. Contributions toward a reclassification of the Formicidae. III. Tribe Amblyoponini (Hymenoptera). Bulletin of the Museum of Comparative Zoology, 122, 143–230.

Brown, W.L., Jr. 1973. A comparison of the Hylean and Congo–West African rain forest ant faunas. *In* Tropical forest ecosystems in Africa and South America: a comparative review: 161–185. Washington, DC: Smithsonian Institution Press.

Casadei-Ferreira, A., J.C.M. Chaul, and R.M. Feitosa. 2019. A new species of *Pheidole* (Formicidae, Myrmicinae) from Dominican amber with a review of the fossil records for the genus. ZooKeys 866: 117–125.

Cisneros, J.C., et al. 2022. Digging deeper into colonial palaeontological practices in modern day Mexico and Brazil. Royal Society Open Science 9 (3): 210898.

Cuezzo, F., and R.J. Guerrero. 2012. The ant genus *Dorymyrmex* Mayr (Hymenoptera: Formicidae: Dolichoderinae) in Colombia. Psyche 2012: 1–24.

Currie, S.J.A. 1997. A study of New Zealand Kauri copal. Journal of Gemology 25: 408–416.

De Andrade, M.L. 1992. First fossil "true *Macromischa*" in amber from the Dominican Republic (Hymenoptera, Formicidae). Mitteilungen der Schweizerischen Entomologischen Gesellschaft 65: 341–351.

De Andrade, M.L. 1994. Fossil Odontomachiti ants from the Dominican Republic [Amber Collection Stuttgart: Hymenoptera, Formicidae. VII: Odontomachiti]. Stuttgarter Beiträge zur Naturkunde B, Geologie und Paläontologie 199: 3–11.

De Andrade, M.L. 1995. The ant genus *Aphaenogaster* in Dominican and Mexican amber (Amber Collection Stuttgart: Hymenoptera, Formicidae. IX: Pheidolini). Stuttgarter Beiträge zur Naturkunde B, Geologie und Paläontologie 223: 1–11.

De Andrade, M.L. 1998a. First description of fossil *Acanthostichus* from Dominican amber (Hymenoptera: Formicidae). Mitteilungen der Schweizerischen Entomologischen Gesellschaft 71: 269–274.

De Andrade, M.L. 1998b. Fossil and extant species of *Cylindromyrmex* (Hymenoptera: Formicidae). Revue Suisse de Zoologie 105: 581–664.

De Andrade, M.L. 1998c. First fossil records of the ant genus *Discothyrea* in Dominican and Mexican amber (Hymenoptera, Formicidae). Fragmenta Entomologica 30: 210–214.

De Andrade, M.L. 2001. A remarkable Dominican amber species of *Cylindromyrmex* with Brazilian affinities and additions to the generic revision (Hymenoptera: Formicidae). Beiträge zur Entomologie 51: 51–63.

De Andrade, M.L. 2003. First descriptions of two new amber species of *Cyphomyrmex* from Mexico and the Dominican Republic (Hymenoptera: Formicidae). Beiträge zur Entomologie 53: 131–139.

De Andrade, M.L. 2004. A new species of *Platythyrea* from Dominican amber and description of a new extant species from Honduras (Hymenoptera: Formicidae). Revue Suisse de Zoologie 111: 643–655.

De Andrade, M.L., and C. Baroni Urbani. 1999. Diversity and adaptation in the ant genus *Cephalotes*, past and present. Stuttgarter Beiträge zur Naturkunde B, Geologie und Paläontologie 271: 1–889.

De Andrade, M.L., C. Baroni Urbani, C.R.F. Brandão, and J. Wagensberg. 1999. Two new species of Leptothorax "*Nesomyrmex*" fossils in Dominican amber (Hymenoptera: Formicidae). Beiträge zur Entomologie 49: 133–140.

Dlussky, G.M. 1981. Miocene ants (Hymenoptera, Formicidae) of the USSR. *In* V.N. Vishnyakova, G.M.

Dlussky, and L.N. Pritykina (editors), New fossil insects from the territories of the USSR (Trudy Paleontologicheskogo Instituta 183): 64–83. Moscow: Akademiya Nauk SSSR.

Dlussky, G.M. 1999. New ants (Hymenoptera, Formicidae) from Canadian amber. Paleontological Journal 33: 409–412.

Dlussky, G.M. 2009. The ant subfamilies Ponerinae, Cerapachyinae and Pseudomyrmecinae (Hymenoptera, Formicidae) in the Late Eocene ambers of Europe. Paleontological Journal 43: 1043–1086.

Dlussky, G.M., and A.P. Rasnitsyn. 2002. Ants (Hymenoptera: Formicidae) of formation Green River and some other Middle Eocene deposits of North America. Russian Entomological Journal 11: 411–436.

Dlussky, G.M., and S. Wedmann. 2012. The poneromorph ants (Hymenoptera, Formicidae: Amblyoponinae, Ectatomminae, Ponerinae) of Grube Messel, Germany: high biodiversity in the Eocene. Journal of Systematic Palaeontology 10: 725–753.

Dlussky, G., D. Brothers, and A. Rasnitsyn, A. 2004. The first Late Cretaceous ants (Hymenoptera: Formicidae) from southern Africa, with comments on the origin of the Myrmicinae. Insect Systematics and Evolution 35: 1–13.

Dlussky, G.M., A.P. Rasnitsyn, and K.S. Perfilieva. 2015. The ants (Hymenoptera: Formicidae) of Bol'shaya Svetlovodnaya (Late Eocene of Sikhote-Alin, Russian Far East). Caucasian Entomological Bulletin 11 (1): 131–152.

Doré, M., et al. 2025. Evolutionary history of ponerine ants highlights how the timing of dispersal events shapes modern biodiversity. Nature Communications 16: 8297.

Dos Santos, C.D.A., J.C.M. Chaul, and J.E. Serrão. 2025. Taxonomic contributions to *Mycetomoellerius* Solomon et al., 2019 (Hymenoptera: Formicidae: Myrmicinae): description of two new species and a key for the genus. Zootaxa 5569 (1): 93–118.

Economo, E.P., N. Narula, N.R. Friedman, M.D. Weiser, and B. Guénard. 2018. Macroecology and macroevolution of the latitudinal diversity gradient in ants. Nature Communications 9: 1778.

Edwards, H.G., and D.W. Farwell. 1996. Fourier transform–Raman spectroscopy of amber. Spectrochimica Acta A, Molecular and Biomolecular Spectroscopy 52: 1119–1125.

Esteves, F.A., and B.L. Fisher. 2021. *Corrieopone nouragues* gen. nov., sp. nov., a new Ponerinae from French Guiana (Hymenoptera, Formicidae). ZooKeys 1074: 83–173.

Feitosa, R.M., and A.M. Dias. 2024. An illustrated guide for the identification of ant subfamilies and genera in Brazil. Insect Systematics and Evolution: 1–121.

Fernández, F., and R.J. Guerrero. 2008. *Technomyrmex* (Formicidae: Dolichoderinae) in the New World: synopsis and description of a new species. Revista Colombiana de Entomología 34: 110–115.

Fernández, F., and R.J. Guerrero. 2019. Subfamilia Ponerinae. *In* F. Fernández, R.J. Guerrero, and T. Delsinne, (editors), Hormigas de Colombia: 509–553. Bogotá, Colombia: Universidad Nacional de Colombia.

Fernández, F., and E.E. Palacio. 1997. Clave para las *Pogonomyrmex* (Hymenoptera: Formicidae) del Norte de Suramérica, con la descripción de una nueva especie. Revista de Biología Tropical 45 (4): 1649–1661.

Fernández, F., R.M. Feitosa, and J. Lattke. 2014. *Kempfidris*, a new genus of myrmicine ants from the Neotropical region (Hymenoptera: Formicidae). European Journal of Taxonomy 85: 1–10.

Fernández, F., R.J. Guerrero, and A.F. Sanchez-Restrepo. 2021. Systematics and diversity of Neotropical ants. Revista Colombiana de Entomología 47 (1): 20 pp.

Ferrer, E., and D.I. Matos Cobas. 2022. Claves para la identificación de las subfamilias, géneros y especies de hormigas (Hymenoptera: Formicidae) de Cuba. Boletín de la Sociedad Entomológica Aragonesa 70: 237–334.

Fiorentino, G., et al. 2023. Deep time extinction of largest insular ant predators and the first fossil *Neoponera* (Formicidae: Ponerinae) from Miocene age Dominican amber. BMC Biology 21: article 26.

Fiorentino, G., R. Probst, A. Richter, E.P. Economo, and P. Barden. 2025. A fossil-informed pattern of body size increase and local extinction in *Basiceros* dirt ants (Hymenoptera: Formicidae). Proceedings of the Royal Society of London B, Biological Sciences 292 (2045): 20242171 (11 pp.).

Fiorentino, G., V. Bouju, D. Sosa, S. Navarro, and P. Barden. 2026. The ant genus *Hypoponera* (Hymenoptera: Formicidae) in Dominican amber. Journal of Paleontology 2026: 1–5.

Fisher, B.L., et al. 2025. A genus-level classification of the ant subfamily Ponerinae (Hymenoptera, Formicidae). ZooKeys 1264: 281–349.

França, E., and L. Gomes. 2025. Fast mandibles, sharp eyes: a new fossil species of *Odontomachus* (Latreille, 1804) gr. *cornutus* (Formicidae: Ponerinae) from Mexican amber formation. Paleoentomology 8 (4): 439–446.

Fontenla, J.L. 1997. Lista preliminar de las hormigas de Cuba (Hymenoptera: Formicidae). Cocuyo 6: 18–21.

Fontenla J.L., and J. Alfonso-Simonetti. 2018. Classification of Cuban ants (Hymenoptera: Formicidae) into functional groups. Poeyana Revista Cubana de Zoologia 506: 21–30.

Grimaldi, D.A., 2019. Amber. Current Biology 29: R861–R862.

Grimaldi, D.A., and M.S. Engel. 2005. Evolution of the insects. New York: Cambridge University Press.

Grimaldi, D.A., A. Shedrinsky, A. Ross, and N.S. Baer. 1994. Forgeries of fossils in "amber": history, identification and case studies. Curator 37: 251–274.

Grimaldi, D., D. Agosti, and J.M. Carpenter. 1997. New and rediscovered primitive ants (Hymenoptera: Formicidae) in Cretaceous amber from New Jersey, and their phylogenetic relationships. American Museum Novitates 3208: 1–43.

Guénard, B., V. Perrichot, and E.P. Economo. 2015. Integration of global fossil and modern biodiversity data reveals dynamism and stasis in ant macroecological patterns. Journal of Biogeography 42 (12): 2302–2312.

Hanson, B. 2025. ChemoSpec: exploratory chemometrics for spectroscopy. R package version 6.3.0.

Harris, R. 1979. A glossary of surface sculpturing. Occasional Papers in Entomology 28. Sacramento, CA: State of California, Dept. of Food and Agriculture, Division of Plant Industry, Laboratory Services.

Heer, O. 1849. Die Insektenfauna der Tertiärgebilde von Oeningen und von Radoboj in Croatien. Zweiter Theil: Heuschrecken, Florfliegen, Aderflüger, Schmetterlinge und Fliegen. Leipzig: W. Engelmann.

Heinrichs, J., et al. 2013. The moss *Macromitrium richardii* (Orthotrichaceae) with sporophyte and calyptra enclosed in Hymenaea resin from the Dominican Republic. Polish Botanical Journal 58: 221–230.

Herrera, M.S., and G. Maharaj. 2025. Promoting equity between the global north and global south in entomological research. Current Opinion in Insect Science 69: 101357.

Iturralde-Vinent, M.A., and R.D. MacPhee. 1996. Age and paleogeographical origin of Dominican amber. Science 273: 1850–1852.

Iturralde-Vinent, M.A., and R.D. MacPhee. 2019. Remarks on the age of Dominican amber. Palaeoentomology 2: 236–240.

Jacintho, G. de F., J.C.M. Chaul, G.A. Teixeira, L.A.C. Barros, and J.E. Serrão. 2025. A morphological and cytogenetic study of two *Fulakora* Mann, 1919 (Hymenoptera: Formicidae), with the description of a new species. Zootaxa 5588 (1): 77–104.

Jaffe, K., and J. Lattke. 1994. Ant fauna of the French and Venezuelan islands in the Caribbean. *In* D.F. Williams (editor), Exotic ants, biology, impact and control of introduced species: 181–190. Boulder, CO: Westview Press.

Ješovnik, A., and T.R. Schultz. 2017. Revision of the fungus-farming ant genus *Sericomyrmex* Mayr (Hymenoptera, Formicidae, Myrmicinae). ZooKeys 670: 1–109.

Johnson, R.A., and S.P. Cover. 2015. A taxonomic revision of the seed-harvester ant genus *Pogonomyrmex* (Hymenoptera: Formicidae) on Hispaniola. Zootaxa 3972 (2): 231–249.

Kass, J.M., et al. 2022. The global distribution of known and undiscovered ant biodiversity. Science Advances 8.

Keller, R.A. 2011. A phylogenetic analysis of ant morphology (Hymenoptera: Formicidae) with special reference to the poneromorph subfamilies. Bulletin of the American Museum of Natural History 355: 1–90.

Khalaim, A. I. 2008. Two New Species of the Genus Diaparsis Förster from Southern China (Hymenoptera: Ichneumonidae: Tersilochinae). Zoosystematica Rossica 17 (1): 89–92.

Kugler, C. 1977 ("1976"). A new species of *Platythyrea* (Hymenoptera, Formicidae) from Costa Rica. Psyche (Cambridge) 83: 216–221.

Kugler, C. 1994. A revision of the ant genus *Rogeria* with description of the sting apparatus (Hymenoptera: Formicidae). Journal of Hymenoptera Research 3: 17–89.

Ladino, N., and R.M. Feitosa. 2020. Taxonomic revision of the genus *Prionopelta* Mayr, 1866 (Formicidae: Amblyoponinae) for the Neotropical region. Zootaxa 4821 (2): 201–249.

LaPolla, J.S. 2005. Ancient trophophoresy: a fossil *Acropyga* (Hymenoptera: Formicidae) from Dominican amber. Transactions of the American Entomological Society 131: 21–28.

LaPolla, J.S., and G.M. Dlussky. 2010. Review of fossil *Prenolepis* genus-group species (Hymenoptera: Formicidae). Proceedings of the Entomological Society of Washington 112 (2): 258–273.

LaPolla, J. S., R.J. Kallal, and S.G. Brady. 2012. A new ant genus from the Greater Antilles and Central America, *Zatania* (Hymenoptera: Formicidae), exemplifies the utility of male and molecular character systems. Systematic Entomology 37: 200–214.

LaPolla, J.S., G.M. Dlussky, and V. Perrichot. 2013. Ants and the fossil record. Annual Review of Entomology 58: 609–630.

LaPolla, J.S. and R.J. Kallal. 2019. *Nylanderia* of the world, part III: *Nylanderia* in the West Indies. Zootaxa 4658 (3): 401–451.

Lapolla, J.S., and D.E. Greenwalt. 2015. Fossil ants (Hymenoptera: Formicidae) of the Middle Eocene Kishenehn Formation. Sociobiology 62 (2): 163–174.

Lattke, J.E. 2002. Nuevas especies de *Gnamptogenys* Roger, 1863 de América (Hymenoptera: Formicidae: Ponerinae).

Lattke, J.E. 2003. The genus *Platythyrea* Roger, 1863 in Dominican Amber (Hymenoptera: Formicidae: Ponerinae). Entomotropica 18 (2): 107–111.

Laza, J.H. 1982. Signos de actividad atribuibles a *Atta* (Myrmicidae, Hymenoptera) en el Mioceno de la provincia de La Pampa, República Argentina. Ameghiniana 19: 109–124.

Lepeco, A., O.M. Meira, D.M. Matielo, C.R. Brandão, and G.P. Camacho. 2025. A hell ant from the Lower Cretaceous of Brazil. Current Biology 35 (9): 2146–2153.

Longino, J.T. 2013. A review of the Central American and Caribbean species of the ant genus *Eurhopalothrix* Brown and Kempf, 1961 (Hymenoptera, Formicidae), with a key to New World species. Zootaxa 3693: 101–151

Longino, J.T., and B.E. Boudinot. 2013. New species of Central American *Rhopalothrix* Mayr, 1870 (Hymenoptera, Formicidae). Zootaxa 3616: 301–324.

Longino, J.T., and M.G. Branstetter. 2020. Phylogenomic species delimitation, taxonomy, and "bird guide" identification of the Neotropical ant genus Rasopone (Hymenoptera: Formicidae). Insect Systematics and Diversity 4 (2): 1–33.

Longino, J.T., and F. Fernández. 2007. Taxonomic review of the genus *Wasmannia*. Memoirs of the American Entomological Institute 80: 271–289.

Lubertazzi, D. (2019). The ants of Hispaniola. Bulletin of the Museum of Comparative Zoology 162 (2): 59–210.

Lucky, A., and P.S. Ward. 2010. Taxonomic revision of the ant genus *Leptomyrmex* Mayr (Hymenoptera: Formicidae). Zootaxa 2688: 1–67.

MacKay, W. 1991. *Anochetus brevidentatus*, new species, a second fossil Odontomachiti ant (Hymenoptera: Formicidae). Journal of the New York Entomological Society 99: 138–140.

MacKay, W.P. 1993. A review of the New World ants of the genus *Dolichoderus* (Hymenoptera: Formicidae). Sociobiology 22: 1–148.

MacKay, W.P., and E. MacKay. 2010. The systematics and biology of the New World ants of the genus *Pachycondyla* (Hymenoptera: Formicidae). Lewiston, NY: Edwin Mellen Press.

Marcineiro, F., and J. Lattke. 2024. Review of ant genus *Pachycondyla* Smith, 1858 in Brazil (Hymenoptera: Formicidae). Zootaxa 5461 (1): 1–62.

McKellar, R.C, J.R.N. Glasier, and M.S. Engel. 2013. New ants (Hymenoptera: Formicidae: Dolichoderinae) from Canadian Late Cretaceous amber. Bulletin of Geosciences 88: 583–594.

Mertz, D.F., and P.R. Renne. 2005. A numerical age for the Messel fossil deposit (UNESCO World Heritage Site derived from dating on a basaltic rock fragment. Courier-Forschungsinstitut Senckenberg 255: 67.

Monarrez, P.M., et al. 2022. Our past creates our present: a brief overview of racism and colonialism in Western paleontology. Paleobiology 48 (2): 173–185.

Moreau, C.S., and C.D. Bell. 2013 Testing the museum versus cradle tropical biological diversity hypothesis: phylogeny, diversification, and ancestral biogeographic range evolution of the ants. Evolution: International Journal of Organic Evolution 67 (8): 2240–2257.

Moreau, C.S., C.D. Bell, R. Vila, S.B. Archibald, and N.E. Pierce. 2006. Phylogeny of the ants: diversification in the age of angiosperms. Science 312: 101–104.

Nakamura G, et al. 2025. The hidden biodiversity knowledge split in biological collections. Proceedings of the Royal Society of London B, Biological Sciences: 292 (2058): 20251045.

Ngô-Muller, V., et al. 2021. The first representative of the trap-jaw ant genus *Anochetus* Mayr, 1861 in Neogene amber from Sumatra (Hymenoptera: Formicidae). Comptes Rendus Palevol 20 (2): 21–27.

Ortiz, C.M., and F. Fernández. 2014. *Brachymyrmex* species with tumuliform metathoracic spiracles description of three new species and discussion of dimorphism in the genus (Hymenoptera, Formicidae). ZooKeys 371: 13–33.

Ortiz-Sepulveda, C.M., B. Van Bocxlaer, A.D. Meneses, and F. Fernández. 2019. Molecular and morphological recognition of species boundaries in the neglected ant genus *Brachymyrmex* (Hymenoptera: Formicidae): toward a taxonomic revision. Organisms Diversity and Evolution: 19 (3): 447–542.

Pagliano, G., and P. Scaramozzino. 1990 ("1989"). Elenco dei generi di Hymenoptera del mondo. Memorie della Società Entomologica Italiana 68: 1–210.

Penney, D. 2010. Dominican amber. *In* D. Penney (editor), Biodiversity of fossils in amber from the major world deposits: 22–41. Manchester, UK: Siri Scientific Press.

Perez-Gelabert, D.E. 2020. Checklist, bibliography and quantitative data of the arthropods of Hispaniola. Zootaxa 4749 (1): 1–668.

Perrichot, V. 2022. The first fossil occurrence of *Odontoponera* (Formicidae: Ponerinae), from Middle Miocene Zhangpu amber. Palaeoworld 32: 693–698.

Perrichot, V., R. Salas-Gismondi, and P.-O. Antoine. 2019. The ant genus *Tapinoma* Förster (Formicidae: Dolichoderinae) in Miocene amber of Peru. Palaeoentomology 2: 585–590.

Prebus, M., and D. Lubertazzi. 2016. A new species of the ant genus *Bothriomyrmex* Emery, 1869 (Hymenoptera: Formicidae) from the Caribbean region. European Journal of Taxonomy 0 (211).

Prebus, M.M. 2021. Taxonomic revision of the *Temnothorax salvini* clade (Hymenoptera: Formicidae), with a key to the clades of New World *Temnothorax*. PeerJ 9: e11514.

Radchenko, A.G. 2023. A new ant genus (Hymenoptera, Formicidae) from the Late Eocene Rovno amber. Zoodiversity 57 (4): 323–336.

Radchenko, A., and M. Khomych. 2025. The oldest known *Cardiocondyla* ant (Hymenoptera, Formicidae) from the late Eocene Rovno amber (Ukraine). Palaeoentomology 8 (3): 307–315.

Raja, N.B., et al. 2022. Colonial history and global economics distort our understanding of deep-time biodiversity. Nature Ecology and Evolution 6 (2): 145–154.

Rao, Z., et al. 2013. Natural amber, copal resin and colophony investigated by UV-VIS, infrared and Raman spectrum. Science China Physics, Mechanics and Astronomy 56: 1598–1602.

Raven, P.H., et al. 2020. The distribution of biodiversity richness in the tropics. Science Advances 6 (37): eabc6228 (5 pp.).

Roghi, G., E. Ragazzi, and P. Gianolla. 2006. Triassic Amber of the Southern Alps (Italy). Palaios 21: 143–154.

Saitta, E.T., and T.G. Kaye. 2025. Experimental maturation of pine resin in sediment to investigate the formation of synthetic copal and amber. Scientific Reports 15: 7627.

Sánchez Herrera, M., et al. 2024. Systematic challenges and opportunities in insect monitoring: a Global South perspective. Philosophical Transactions of the Royal Society B 379 (1904): 20230102.

Sarnat, E.M., N.R. Friedman, G. Fischer, B. Lecroq-Bennet, and E.P. Economo. 2017. Rise of the spiny ants: diversification, ecology and function of extreme traits in the hyperdiverse genus *Pheidole* (Hymenoptera: Formicidae). Biological Journal of the Linnean Society 122 (3): 514–538.

Sawh, I., et al. 2023. The first fossil replete ant worker establishes living food storage in the Eocene. Myrmecological News 33: 133–147.

Schmidt, C.A., and S.O. Shattuck. 2014. The higher classification of the ant subfamily Ponerinae (Hymenoptera: Formicidae), with a review of ponerine ecology and behavior. Zootaxa 3817 (1): 1–242.

Schultz, T.R. 2007. The fungus-growing ant genus *Apterostigma* in Dominican amber. Memoirs of American Entomological Institute 80: 425–436

Seyfullah, L.J., et al. 2018. Production and preservation of resins–past and present. Biological Reviews 93: 1684–1714.

Shattuck, S.O. 1992a. Review of the dolichoderine ant genus *Iridomyrmex* Mayr with descriptions of three new genera (Hymenoptera: Formicidae). Journal of the Australian Entomological Society 31: 13–18.

Shattuck, S.O. 1992b. Generic revision of the ant subfamily Dolichoderinae (Hymenoptera: Formicidae). Sociobiology 21: 1–181.

Seifert, B. 2002. The ant genus *Cardiocondyla* (Insecta: Hymenoptera: Formicidae) - a taxonomic revision of the *C. elegans*, *C. bulgarica*, *C. batesii*, *C. nuda*, *C. shuckardi*, C. *stambuloffii*, *C. wroughtonii*, *C. emeryi*, and *C. minutior* species groups. Annalen des Naturhistorischen Museums in Wien, Serie B für Botanik und Zoologie 104: 203–338.

Seifert, B. 2023. The ant genus *Cardiocondyla* (Hymenoptera: Formicidae): the species groups with Oriental and Australasian origin. Diversity 15 (1): 25–56.

Seifert, B. 2024. A taxonomic revision of the ants of the *Cardiocondyla wroughtonii* group (Hymenoptera: Formicidae) with a checklist of the *Cardiocondyla* species of the world. Soil Organisms 96 (2): 113–144.

Solomon, S.E., et al. 2019. The molecular phylogenetics of *Trachymyrmex* Forel ants and their fungal cultivars provide insights into the origin and coevolutionary history of 'higher-attine' ant agriculture. Systematic Entomology 44 (4): 939–956.

Solórzano Kraemer, M.M., A.S. Kraemer, F. Stebner, D.J. Bickel, and J. Rust. 2015. Entrapment bias of arthropods in Miocene amber revealed by trapping experiments in a tropical forest in Chiapas, Mexico. PLoS One 10: e0118820.

Solórzano Kraemer, M.M., et al. 2018. Arthropods in modern resins reveal if amber accurately recorded forest arthropod communities. Proceedings of the National Academy of Sciences of the United States of America 115: 6739–6744.

Solórzano-Kraemer, M.M., X. Delclòs, M.S. Engel, and E. Peñalver. 2020. A revised definition for copal and its significance for palaeontological and Anthropocene biodiversity-loss studies. Scientific Reports 10: 19904.

Sosiak, C.E., and P. Barden. 2021. Multidimensional trait morphology predicts ecology across ant lineages. Functional Ecology 35 (1): 139–152.

Sosiak, C.E., M.L. Borowiec, and P. Barden. 2022 (retracted). An Eocene army ant. Biology Letters 18: 20220398.

Tay, T.S., Z.X. Shen, and S.I. Yee. 1998. On the identification of amber and its imitations using Raman spectroscopy: preliminary results. Australian Gemmologist 20 (3): 114–123.

Tozetto, L., J.C. Chaul, B.W. Boudinot, and J.E. Lattke. 2022. Review of the *Leptogenys unistimulosa* species group (Hymenoptera: Formicidae) with the description of a new Amazonian species. Revista Brasileira de Entomologia 66 (3): e20220045.

Varela-Hernández, F., and Riquelme, F. 2024. *Pheidole praehistorica* sp. nov., a new addition to spiny ants of the genus *Pheidole* Westwood, 1839 (Formicidae, Myrmicinae) from Oligo-Miocene Mexican amber. European Journal of Taxonomy 968 (1): 86–97.

Varela-Hernández, F., F. Riquelme, R.J. Guerrero, and C.M. Vázquez-Franco. 2022 ("2023"). New ant species *Schismiscapus exstinctum* gen. et sp. nov. (Formicidae: Dolichoderinae) from Miocene Mexican amber. Historical Biology 35 (7): 1209–1215.

Varela-Hernández, F., F. Riquelme, and R.J. Guerrero. 2023. A Miocene ant species of the genus *Forelius* Emery, 1888 (Hymenoptera: Formicidae: Dolichoderinae) from Mexico. Palaeontologia Electronica 26 (3): a36.

Varela-Hernández, F., F. Riquelme, and R.J. Guerrero. 2024 ("2025"). New genus and species of ponerine ant (Hymenoptera: Formicidae) from Mexican amber. Historical Biology 37 (5): 1134–1140.

Vierbergen, G., and J. Scheven. 1995. Nine new species and a new genus of Dominican amber ants of the tribe Cephalotini (Hymenoptera: Formicidae). Creation Research Society Quarterly 32 (3): 158–170.

Wagner-Wysiecka, E., 2018. Mid-infrared spectroscopy for characterization of Baltic amber (succinite). Spectrochimica Acta A, Molecular and Biomolecular Spectroscopy 196: 418–431.

Wang, B., et al. 2021. The mid-Miocene Zhangpu biota reveals an outstandingly rich rainforest biome in East Asia. Science Advances 7 (18): eabg0625.

Ward, P.S. 1992. Ants of the genus *Pseudomyrmex* (Hymenoptera: Formicidae) from Dominican amber, with a synopsis of the extant Antillean species. Psyche 99: 55–85.

Ward, P.S., and B.L. Fisher. 2016. Tales of dracula ants: the evolutionary history of the ant subfamily Amblyoponinae (Hymenoptera: Formicidae). Systematic Entomology 41 (3): 683–693.

Ward, P.S., S.G. Brady, B.L. Fisher, and T.R. Schultz. 2010. Phylogeny and biogeography of dolichoderine ants: effects of data partitioning and relict taxa on historical inference. Systematic Biology 59: 342–362.

Ward, P.S., B.B. Blaimer, and B.L. Fisher. 2016. A revised phylogenetic classification of the ant subfamily Formicinae (Hymenoptera: Formicidae), with resurrection of the genera *Colobopsis* and *Dinomyrmex*. Zootaxa 4072: 343–357.

Ward, P.S., B.L.Fisher, J.J. Wernegreen, and B.B. Blaimer. 2025. Evolutionary history, novel lineages and symbiont coevolution in the ant tribe Camponotini (Hymenoptera: Formicidae). Systematic Entomology 50 (3): 646–676.

Wheeler, W.M. 1915 ("1914"). The ants of the Baltic Amber. Schriften der Physikalisch-Ökonomischen Gesellschaft zu Königsberg 55: 1–142.

Wild, A.L. 2007. Taxonomic revision of the ant genus *Linepithema* (Hymenoptera: Formicidae). University of California Publications in Entomology 126: 1–151.

Wild, A.L., and F. Cuezzo. 2006. Rediscovery of a fossil dolichoderine ant lineage (Hymenoptera: Formicidae: Dolichoderinae) and a description of a new genus from South America. Zootaxa 1142: 57–68.

Wilson, E.O. 1985a. Invasion and extinction in the West Indian ant fauna: evidence from the Dominican amber. Science 229: 265–267.

Wilson, E.O. 1985b. Ants of the Dominican amber (Hymenoptera: Formicidae). 1. Two new myrmicine genera and an aberrant *Pheidole*. Psyche (Cambridge) 92: 1–9.

Wilson, E.O. 1985c. Ants of the Dominican amber (Hymenoptera: Formicidae). 3. The subfamily Dolichoderinae. Psyche (Cambridge) 92: 17–37.

Wilson, E.O. 1985d. Ants of the Dominican amber (Hymenoptera: Formicidae). 2. The first fossil army ants. Psyche (Cambridge) 92: 11–16.

Wilson, E.O. 1985e. Ants from the Cretaceous and Eocene amber of North America. Psyche 92 (2–3), 205–216.

Wilson, E.O. 1986 ("1985"). Ants of the Dominican amber (Hymenoptera: Formicidae). 4. A giant ponerine in the genus *Paraponera*. Israel Journal of Entomology 19: 197–200.

Wilson, E.O. 1988. The biogeography of the West Indian Ants (Hymenoptera: Formicidae). *In* J.K. Liebher (editor). Zoogeography of Caribbean insects: 214–230. Ithaca, NY: Cornell University Press.

Winkler, W., E.C. Kirchner, M. Musso, and A. Asenbau. 1998. Untersuchungen an fossilen und rezenten Har-

zen mittels Raman-Spektroskopie. Mitteilungen der Österreichischen Mineralogischen Gesellschaft 143: 398401.

Winkler, W., E.C. Kirchner, A. Asenbaum, and M. Musso. 2001. A Raman spectroscopic approach to the maturation process of fossil resins. Journal of Raman Spectroscopy 32 (1): 59–63.

Zhang, J. 1989. Fossil insects from Shanwang, Shandong, China. Jinan, China: Shandong Science and Technology Publishing House.

APPENDIX 1

List of Recorded Ponerinae Genera from the Fossil Record, Ordered Alphabetically

Columns: **No.**, total number of Ponerine genera known from the fossil record. **Extant,** number of extant genera. **Extinct,** number of extinct genera; Spp., number of speciesknown for the genus in that deposit. Since a genus maybe found in more than one deposit, only the first mention is taken into account and scored a value of one. **Age** refers to the geologic period or epoch for each deposit. **Eocene ssp., Oligocene ssp.,** and **Miocene ssp.** refer respectively to the number of species known from each epoch. **Carbonate** and **Amber** refer to the type of fossil. The remaining columns tally the number of fossil species known from the labelled regions, with **Global South** encompassing Central and South America, Africa, and most of Asia with the exception of China.

Genus	No. g	Extant	Extinct	Spp.	Age	Eocene ssp.	Oligocene ssp.	Miocene ssp.	Deposit	Carbonate	Amber	Global S.	N. America	Europe	Asia	DR	Oceania
Afropone	1		1	2	Cretaceous				Botswana	2		2					
Anochetus	1			8	Miocene			8	DR		8	8				8	
Anochetus		1		1	Miocene			1	Sumatra, Indonesia		1	1					
Archiponera	1		1	1	L Eocene	1			Florissant, CO	1			1				
Austroponera	1			1	Miocene			1	Foulden Maar, NZ	1							1
Brachyponera	1	1		1	Miocene			1	DR		1	1				1	
Cayrapone	1	1		1	Miocene			1	DR		1	1				1	
Cephalopone	1	1	1	2	Eocene	2			Messel, Germany	2				2			
Cryptopone	1			1	Eocene	1			Baltic		1			1			
Cyrtopone	1	1	1	4	Eocene	4			Messel, Germany	4				4			
Desyopone	1		1	1	Miocene			1	Ethiopia		1	1					

APPENDIX 1 *continued*

Genus	No. g	Extant	Extinct	Spp.	Age	Eocene ssp.	Oligocene ssp.	Miocene ssp.	Deposit	Carbonate	Amber	Global S.	N. America	Europe	Asia	DR	Oceania
Eogorgites	1		1	1	Eocene	1			Fushun, China	1					1		
Eoponerites	1		1	1	Eocene	1			Fushun, China	1					1		
Furcisutura	1		1	1	Eocene	1			Fushun, China	1					1		
Hypoponera	1			1	Eocene	1			Baltic		1			1			
Leptogenys	1	1		1	Miocene			1	Shandong, China	1					1		
Leptogenys		1		1	Miocene			1	DR		1	1				1	
Longecapitia	1		1	1	Eocene	1			Fushun, China	1					1		
Mayaponera	1			1	Miocene			1	DR		1	1				1	
Messelepone	1	1	1	1	Eocene	1			Messel, Germany	1				1			
Mixoponera	1		1	1	Miocene			1	DR		1	1				1	
Neoponera	1			1	Miocene			1	DR		1	1				1	
Odontomachus	1	1		2	Miocene			2	DR		2	2				2	
Odontomachus				1	Miocene			1	Czech Republic	1				1			

APPENDIX 1 *continued*

Genus	No. g	Extant	Extinct	Spp.	Age	Eocene ssp.	Oligocene ssp.	Miocene ssp.	Deposit	Carbonate	Amber	Global S.	N. America	Europe	Asia	DR	Oceania
Odontomachus				1	Miocene			1	Chiapas, Mexico		1	1					
Odontoponera	1			1	Miocene			1	Zhangpu, China	1					1		
Pachycondyla	1	1		7	Eocene	7			Europe	7					7		
Pachycondyla		1		4	Eocene	4			Europe		4			4			
Pachycondyla				3	Oligocene		1		Germany	3				3			
Pachycondyla				1	Eocene	1	3		United States	1			1				
Pachycondyla				2	Miocene			2	China	2					2		
Platythyrea	1			4	Miocene			4	DR		4	4				4	
Platythyrea		1		1	Eocene	1			Oise, France		1			1			
Platythyrea				1	Eocene	1			Baltic		1			1			
Ponera	1			1	Oligocene		1		Europe		1			1			
Ponera		1		1	Oligocene		1		Europe	1				1			
Ponera				3	Eocene	3			Europe		3			3			
Ponerites	1		1	10	Eocene—Mio	1	1	1	Europe	10				10			

APPENDIX 1 *continued*

Genus	No. g	Extant	Extinct	Spp.	Age	Eocene ssp.	Oligocene ssp.	Miocene ssp.	Deposit	Carbonate	Amber	Global S.	N. America	Europe	Asia	DR	Oceania
Ponerites				5	Eocene	5			Kishenehn, MT	5			5				
Protopone	1		1	6	Eocene	6			Messel, Germany	6				6			
Protopone				1	Eocene	1			Sakhalin, Russia		1			1			
Pseudoponera	1			1	Miocene			1	DR		1	1				1	
Siinikaponera	1	1	1	1	Oligo-Miocene		1		Chiapas, Mexico		1	1					
Stenoponera	1		1	1	Miocene			1	DR		1	1				1	
Taphopone	1		1	6	Miocene			6	Europe	6				6			
Totals	**31**	**14**	**16**	**98**		**44**	**8**	**38**		**59**	**39**	**28**	**7**	**47**	**15**	**22**	**1**

APPENDIX 2

Fourier Transform Raman (FTR) Spectroscopy
FTR replicates of peak ratio for each specimen tested in this study.

Species	Specimen	Peak ratio
-	Colombian copal	1.039
-	AMNH Dominican Copal #1	0.937
-	AMNH Dominican Copal #2	0.913
Fulakora lata	AMNH DR 99 24	1.068
		1.099
		1.101
		1.334
Prionopelta ambigua	MNHNSD FOS 18.117	0.764
		0.825
		0.823
		1.060
Chimerodous alpha	AMNH DR 10 165	0.904
		0.908
		0.949
		1.028
Schismiscapus hispaniolae	AMNH DR 10 240	1.122
		1.003
		1.024
Poneracantha minima	MNHNSD FOS 18.120	0.828
		0.828
		0.806
		0.777
Brachymyrmex atrapada	MNHNSD FOS 18.121	0.807
		0.817
		0.782
		0.769
Camponotus matunai	MNHNSD FOS 18.122	0.917
		0.914
		0.932
		0.911
Acromyrmex yuca	AMNH DR 99 416	0.696
		0.697
Cardiocondyla larimar	AMNH DR 14 278	0.700
		0.749
		0.957
		0.883
		1.105
		0.924
Crematogaster diunota	MNHNSD FOS 18.123	0.854
		0.851
		0.851
		0.831
Eurhopalothrix electrina	AMNH DR 14 907	0.873
		0.871
		0.765
		0.766
Kempfidris priminatus	AMNH DR rp 519	0.818
		0.820
		0.734
		0.927
Mycetamoellerius yucahu	AMNH DR 15 48	0.987
		1.044
		0.968
		0.961
Paratrachymyrmex primaevus	AMNH DR rp 359	0.765
		0.764
		0.942
		0.946
Pogonomyrmex tempopogo	pale 44137	0.947
		0.817
		0.792
		0.808

APPENDIX 2 *continued*

Species	Specimen	Peak ratio
Rhopalothrix macorixia	AMNH DR 14 935	0.975
		1.071
		0.952
		0.923
Rogeria primaeva	MNHNSD FOS 18.124	0.859
		0.859
		0.898
		0.777
Allomerus bi	AMNH DR 11735	0.822
		0.823
		0.815
		0.821
Brachyponera mamajuanis	AMNH DR 14 945	0.936
		1.007
		1.124
		1.110
Cayrapone hupia	AMNH DR 14 51	0.911
		0.912
		0.934
		0.982
Leptogenys intacta	AMNH DR 10 239	0.770
		0.769
		1.015
		0.939
Kiskeyapone armilla	AMNH DR rp 781	0.989
		0.939
		0.928
		0.935
Mayaponera bachata	AMNH DR 14 930	0.825
		0.826
		0.832
		0.820
Pseudoponera hatuey	AMNH DR 14 881	1.163
		1.162
		1.063
		1.059
Stenoponera petiolata	AMNH DR 14 897	0.992
		0.832
		0.861
		0.878

Scientific Publications of the American Museum of Natural History

American Museum Novitates
Bulletin of the American Museum of Natural History
Anthropological Papers of the American Museum of Natural History

Publications Committee
Lorenzo Prendini, Chair

Board of Editors
Jin Meng, Paleontology
Lorenzo Prendini, Invertebrate Zoology
John S. Sparks, Vertebrate Zoology
Peter M. Whiteley, Anthropology

Managing Editor
Mary Knight

Submission procedures can be found at http://research.amnh.org/scipubs

All issues of *Novitates* and *Bulletin* are available on the web (https://digitallibrary.amnh.org/handle/2246/5). Order printed copies on the web from:
https://shop.amnh.org/books/scientific-publications.html

or via standard mail from:
American Museum of Natural History—Scientific Publications
Central Park West at 79th Street
New York, NY 10024

♾ This paper meets the requirements of ANSI/NISO Z39.48-1992 (permanence of paper).

On the cover: A worker ant, *Schimiscapus hispaniolae*, preserved as an inclusion within Miocene Dominican amber.